POLITECNICO
MILANO 1863

SCUOLA DI INGEGNERIA INDUSTRIALE
E DELL'INFORMAZIONE

Sustainability of Wind Energy in Italy: Life Cycle Assessment of the Iurefalco Wind Farm

TESI DI LAUREA MAGISTRALE IN
ENERGY ENGINEERING
INGEGNERIA ENERGETICA

Author: **Guglielmo Cantisani**

Student ID: 995116
Advisor: Prof. Paolo Silva
Co-advisor: Ing. Francesca Pippione
Academic Year: 2023-24

Abstract

The present study is devoted to the evaluation of the environmental sustainability of an onshore Italian wind farm featuring 6 G114 – 2.5 MW wind turbines, with a focus on its effects towards the global energy balance and carbon footprint. The analysis was conducted by applying the LCA methodology "from-cradle-to-grave" according to the ISO 14040 and 14044 regulating frameworks.

The goal of the assessment is outlining the eco-profile of the generation of 1 GWh of electricity. The interpretation of the results allowed to emphasize the most critical stages of the system's life cycle, as well as the evaluation of the environmental performance expressed through the Energy Payback Time (EPBT) and Carbon Payback Time (CPBT) indexes.

As expected, the raw materials acquisition phase turned out to determine the highest fraction of the impacts, accounting for 69% of the life cycle primary energy consumption and 72% of the damage generated by the greenhouse gas emissions. Wind turbines represented the major contributors, mostly due to the large amount of steel required for the construction of the tower and the energy-intensive composite for the blades. The EPBT of the system was found equal to 1.52 years, while its CPBT to 0.86 years. Compared to the reviewed studies, these values resulted to be above average. This outcome was justified as consequence of the lower wind resource characterizing the site and the use of different methodological approaches, especially related to the end-of-life modeling. Moreover, the availability of primary data concerning the plant's civil works granted an in-depth evaluation of the impacts associated to many processes typically neglected.

Further considerations have been made by assessing the sensitivity of the most uncertain parameters of the system. Specifically, it was demonstrated that the system's useful life and capacity factor can significantly influence the environmental performance of the system, while the turbines' reliability determines a more limited effect.

Keywords: life cycle assessment; LCA; wind power plant; sustainability; renewable energy; wind energy

Abstract in italiano

Il presente studio è volto alla valutazione della sostenibilità ambientale di un impianto eolico onshore italiano costituito da 6 turbine modello G114 – 2.5 MW, focalizzando l'attenzione sui suoi effetti verso il bilancio energetico globale e l'impronta carbonica. L'analisi è stata svolta mediante l'applicazione della metodologia LCA "dalla culla alla tomba" nel rispetto delle norme ISO 14040 e 14044.

L'obiettivo del lavoro è definire l'eco-profilo per la generazione di 1 GWh di elettricità. L'interpretazione dei risultati ha permesso di evidenziare le fasi più critiche del ciclo di vita del sistema e la valutazione delle performance ambientali tramite l'uso degli indici di payback relativi all'energia primaria investita ed i gas serra emessi.

Come atteso, la fase di acquisizione delle materie prime ha dimostrato determinare la maggiore frazione degli impatti, pari al 69% dell'energia primaria complessivamente impiegata nel ciclo di vita ed il 72% del danno generato dalle emissioni di gas serra. I maggiori contributori sono le turbine, in larga parte a causa dell'ingente quantità di acciaio richiesta per la costruzione della torre e del materiale composito per la costruzione delle pale. L'indice di payback sull'energia investita è risultato pari a 1.52 anni, mentre quello sulle emissioni pari a 0.86 anni. Confrontando tali valori con la letteratura, essi si sono rivelati essere al di sopra della media. Tale esito è stato giustificato come conseguenza della più bassa risorsa ventosa riguardante il sito e l'utilizzo di differenti approcci metodologici, in particolare la modellizzazione del fine vita. Inoltre, la disponibilità di dati primari inerenti ai lavori civili eseguiti durante la costruzione dell'impianto ha consentito una valutazione approfondita degli impatti relativi a diversi processi solitamente trascurati.

Ulteriori considerazioni sono state effettuate mediante l'analisi della sensibilità dei parametri più incerti del sistema. Nel dettaglio, è stato dimostrato che la vita utile dell'impianto e il suo capacity factor possono influenzare notevolmente le performance ambientali del sistema, mentre l'affidabilità delle turbine gioca un ruolo minore.

Parole chiave: valutazione del ciclo di vita; LCA; impianto eolico; sostenibilità; energia rinnovabile; energia eolica

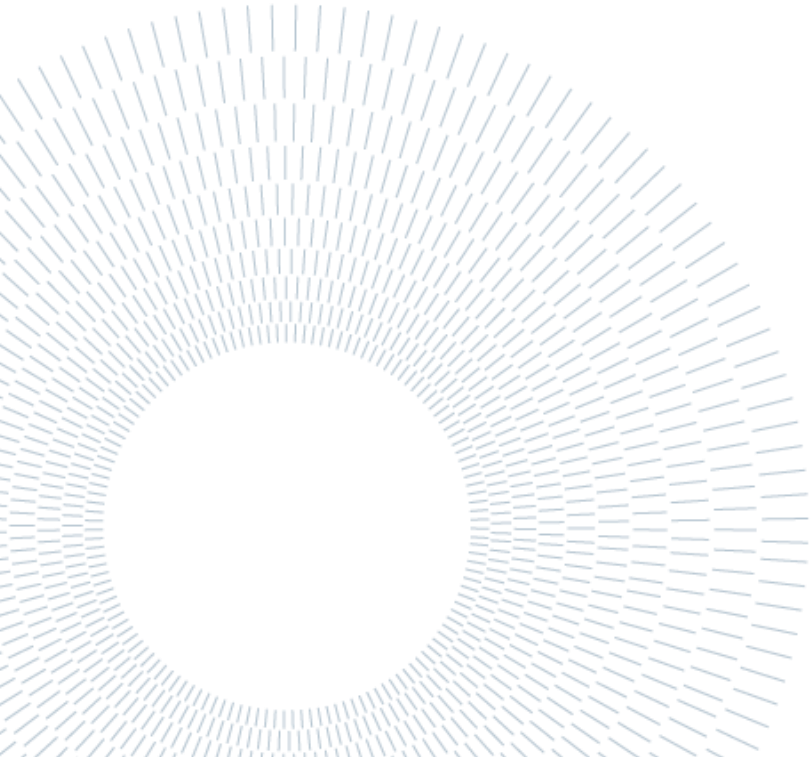

Contents

Abstract ..... **i**

Abstract in italiano ..... **iii**

Contents ..... **v**

1 Introduction **2**

2 Brief overview of renewable electricity market in Europe **7**

3 Case study description **11**

4 LCA methodology **23**

5 Literature review **31**

5.1. Life cycle phases assumptions and main results 40

5.1.1. Manufacturing phase 40

5.1.2. Transportation phase 42

5.1.3. Installation phase 43

5.1.4. Operation and Maintenance phase 44

5.1.5. End-of-life phase 46

6 Goal and scope definition, data collection and life cycle inventory **51**

6.1. Goal and scope definition 51

6.1.1. Product system, functional unit and allocation procedures definition 51

6.1.2. Choice of the impact assessments methods 55

6.1.3. End-of-life modeling 57

6.1.4. Data quality 59

6.2. Life cycle inventory 60

6.2.1. Introduction 60

6.2.2. Raw materials acquisition 60

6.2.3. Components manufacturing 99

6.2.4. Components assembly and installation 113

6.2.5. Operation and maintenance (O&M) 124

6.2.6. Decommissioning 127

6.2.7. End-of-life 133

7 LCIA and results interpretation **145**

7.1. LCA results: life cycle phases 146

7.1.1. Raw materials acquisition 149

7.1.2. Components manufacturing 162

7.1.3. Operation and Maintenance 165

7.1.4. End-of-life 166
7.2. Environmental indexes calculation and comparisons with other studies 170
7.3. Interpretation of CED category indicators' results 177
7.4. Sensitivity analyzes 180
7.4.1. Wind power plant useful life 180
7.4.2. Wind turbine's components replacement rates 182
7.4.3. Annual energy yield 184
8 Conclusions, limitations, and recommendations 197
References 203
A Appendix A 213
A.1. Tables 214
List of Figures 217
List of Tables 221
Acknowledgements 227

1 Introduction

The recent disruptions due to the energy crisis started in Europe in 2022 and the effects on earth's climate caused by the growing anthropogenic emissions of greenhouse gases (GHGs) are bringing the attention like never before on the necessity of implementing a decisive prosecution of energy-climatic policies in favor of the energy transition. During the 20th century, the increasing energy requirements caused by an unprecedented growth of the population and the global economic boom made fossil fuels the primary energy source for the development of almost any industrial sector. The main reasons that led to such a widespread diffusion of fossil fuels were related to their high energy density compared to other energy sources and the high level of programmability that they offer in energy generation. Besides these evident advantages, it's now clear that the overall amount of GHGs on earth has been sharply increasing due to the intensive exploitation of fossil sources of energy concentrated in a very small amount of time compared to the one needed to generate them, and it's very likely that the climatic change is related to the same reason (IPCC, 2021). It's obvious that, if this is really the case, the factor that can modify the course of the ongoing climatic change is how each political institution will behave in order to limit as much as possible fossil fuels consumption in every economical field.

The EU, in comparison to other world nations, has always given more importance to these topics. Starting from the Kyoto Protocol in 2005, which was the first world-scale agreement with the aim of limiting the effects of the global warming on the climate and to which 191 nations joined (Europe included), even after the end of its effects in 2012 the EU continued to follow the same guidelines, defining more strict objectives and acting primarily on 3 fields: electrification, energy efficiency and renewable energy sources, in particular non-programmable ones. The motivations that led towards this type of program were not limited to the climatic issue, but also to the purpose of reducing the energy dependence of Europe against other nations. Fossil fuels in fact, which were and still are nowadays the main primary energy source for mankind, are unevenly distributed around the world, therefore relying uniquely on them could determine serious implications, including economic disparities and geopolitical tensions between governments. Renewable energies, instead, especially wind and solar, have a much uniform density around the globe, while also providing clean power source. These 3 points of action planned by the EU are closely related to each other: typically, the most used energy carrier dedicated to the energy conversion

from renewable sources is the electric one, and such carrier strongly contributes in raising the energy efficiency level of a nation since the technologies for final use that exploit electrical energy are often the most advanced, whatever their purpose is. It's also evident that pushing towards electrification could be one of the most effective ways to reduce both resource consumption and environmental impact, even more since the consumption itself of electrical energy does not have any effect on GHGs emissions. The energy conversion process takes an important role in this context: while the conversion processes of traditional thermoelectric plants powered by fossil fuels constitutes not only something not sustainable energetically speaking as previously stated, but they also involve the emission of large quantities of GHGs, renewable power plants produce electric power by the exploitation of practically unlimited sources of energy while emitting no GHG.

The EU is trying to manage all of this operating at a community level through the definition of directives and regulations which establish the global objectives, while each member state is called to set the means with which it will achieve them. In a bit more than thirty years, by following the type of policies just mentioned, the EU decreased its GHG emissions by 31% compared to 1990 and its primary energy consumption by 16% compared to 2005 (EEA, 2023a). The biggest contribution comes with no doubt from the energy supply sector (Figure 1.1), which has historically been the most impactful in relation to the climatic change (EEA, 2023a). The main factors that led to this result are essentially two:

1. The reduction of the energy intensity by means of a stronger energy efficiency (EEA, 2023a).

2. The reduction of the carbon intensity by choosing a primary energy mix that replaced part of the fossil sources with renewable sources of energy, mainly driven by the outbreak of wind and solar power technologies, which led to a total share of renewables of 22.5% in 2022 (EEA, 2023a).

It's already clear that these two technologies will have a huge influence on the actions taken by Europe to mitigate climate change and its energy dependence on foreign countries, since wind and solar energies still have a very promising potential compared to other renewables (EEA, 2023a).

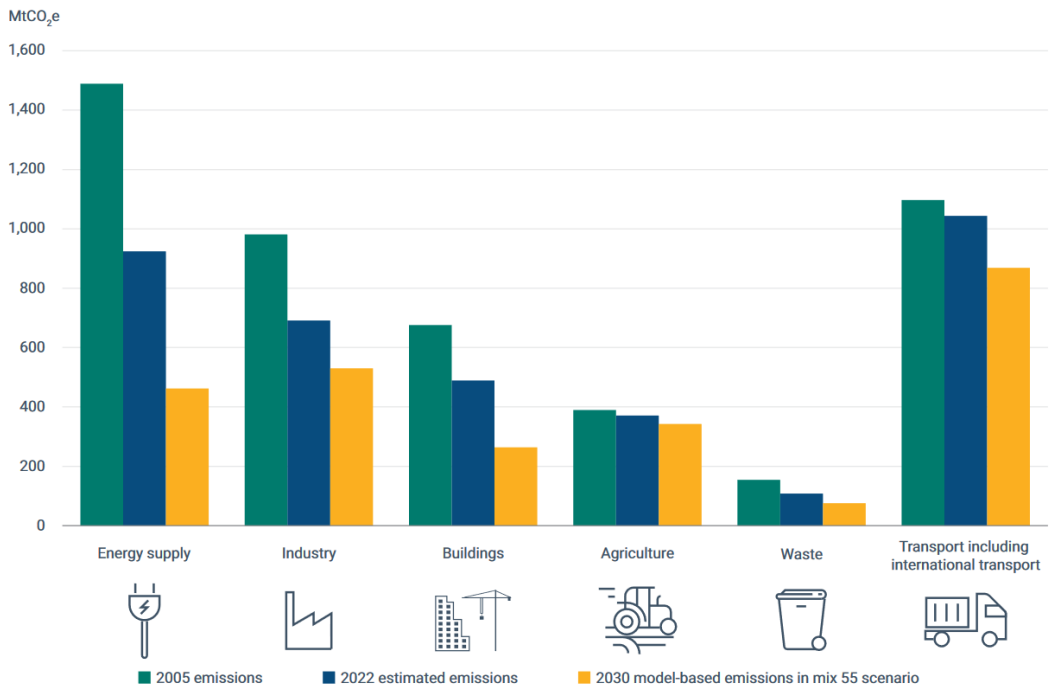

Figure 1.1: GHG emissions reduction over time by sector (EEA, 2023a).

The new international agreements on climate change are setting very challenging goals. As a result of the Paris Agreement held in 2015, which involved for the first time all world's nations due to the rising sensitivity on the topic, it was established that everyone should have taken actions in order to limit global warming to 1.5 °C by 2050. The commitments that Europe plans to sustain to contribute for this goal are specified in the European Green Deal, introduced in 2019. Specifically, it was decided that the EU as community will have to reduce the overall GHG emissions by at least 55% in respect to the 1990 amount, with the aim of becoming the first carbon neutral region by 2050 (EEA, 2023a). This includes also reaching a target of 42.5% renewable energy share by 2030 and a reduction by 11.7% of the energy final consumption in respect to the value predicted in 2020 for 2030 (EEA, 2023a). By following the current rate of advancement, it's certain that each state will have to be in a much higher level of commitment to be sure of accomplishing these goals, since in 2023 only 6 European nations are expecting to have by 2030 GHGs emissions lower than their target (EEA, 2023a). Improvements need to be made especially in those sectors that are struggling more, such as transports, buildings and agriculture. On top of that, it's not completely sure that relying on the renewable technologies currently available will end in the meeting of the targets set for 2050. As with every type of technology, also renewable ones present some issues:

1. Low energy density compared to fossil-driven technologies. This means that to obtain a certain power output it will be necessary to have a bigger plant layout compared to the one used in traditional fossil fuel technologies.

2. The energy production from renewable sources is often characterized by non-programmability. This applies especially to wind and solar technologies, which are also the ones in which Europe is investing way more than others. The energy per unit time that is made available typically has an unsteady behavior and, most importantly, not fully predictable. This generates issues in the management of the grid balance, that get worse with growing non-programmable renewable power plant share in the grid.

3. Even though the power conversion from renewable sources of energy is obtained through GHGs emissions-free processes, the whole life cycle of renewable power plants is characterized by the inevitable necessity of using fossil fuels to make this conversion possible, which makes them, after all, not net-zero-impact. This is an extremely important aspect heading towards carbon neutrality, since the relevance of these emissions is directly related to the type of technology chosen and its application, therefore it's crucial to make careful assessments before investing.

The last point just discussed represents the central topic of the present work. Specifically, the attention will be brought on the wind technology and its points of strength/weakness compared to other renewables, with the aim of outlining its level of sustainability not only from the carbon footprint point of view, but also towards the use of primary energy resources. The research will be carried out by assessing the environmental performance of an existing onshore wind farm installed in Italy, including in the evaluation all the stages in which the system is involved, from the *raw materials acquisition* to the *end-of-life*. From the interpretation of the results, the main goal will be clarifying if the wind technology can actually contribute in reaching the climate targets and overcoming energy dependance, while also highlighting which are its most critical aspects and how to possibly improve them in order to limit as much as possible the impacts on the environment.

2 Brief overview of renewable electricity market in Europe

In 2023, the new global installations of renewable electric capacity were almost 50% higher than the previous year, reaching 507 GW (IEA, 2023). This significative jump was possible especially thanks to the massive investments made by China regarding wind and solar PV (IEA, 2023). It's expected that, following this trend, wind and solar global electrical renewable generation will overcome coal-fired power generation by 2025, becoming the biggest energy sources for electricity production (IEA, 2023). Nevertheless, this unprecedented growth of variable renewables technologies in China is hiding the slower progress in the remaining countries, including Europe (IEA, 2023). The reasons that made the building-up of this gap are multiple:

- The rising inflation due to the higher interest rates (from 1% to nearly 5%) defined by the European Central Bank, in concomitance with a cut of the interests from China. This led to higher equipment costs for both offshore and onshore wind and solar PV (IEA, 2023).

- The uncertainty developed in investors after the governments interventions in the energy markets to safeguard the consumers from the rising energy cost as a result of the energy crisis (IEA, 2023).

- Slower progresses in defining targets and incentives for renewables in developing countries (IEA, 2023).

- The insufficient investment in grid infrastructure for both developing and advanced countries, which caused the queuing of a lot of renewable power plants projects even almost completed (> 3 TW) (IEA, 2023).

- Together with the grid investments, the extended time to obtain the permissions for the installation of the power plants is further delaying the advancements to reach the set targets (IEA, 2023).

If the scenario remains just as it is now in terms of policies and market conditions, the IEA forecasts that the global renewable capacity will reach around 7300 GW by 2028

(IEA, 2023). Considering the same trend for the following 2 years, this value will stop around 2.5 times its level in 2022, failing to reach the tripling target (IEA, 2023). By overcoming these challenges in the short term, instead, it's estimated that the total renewable capacity will touch 8130 GW by 2028, projected to 3 times its level in 2022 by 2030 (IEA, 2023).

Despite all the difficulties of the last few years, the risk of energy supply outages determined by the geopolitical tensions resulting from the conflict between Russia and Ukraine brought both the solar PV and wind EU market towards new records in additional capacity installations in 2023 (SPE, 2023). As already remarked, these two technologies are expected to cover the most important role in the EU energy transition.

For the third year in a row, the solar PV market is expected to grow more than 40% compared to the previous one, attesting new installations counting up to 55.9 GW across the 27 Member States (SPE, 2023). The cumulative capacity has already grown by 27%, reaching 263 GW vs 207 GW in 2022 (SPE, 2023). Germany, Spain and Italy resulted to be the largest expanding markets, considering that almost 50% of the total new capacity was driven by them. Interestingly, the main drivers that led to such growth were different in each case (SPE, 2023). The German expansion took advantage from the upwards revisions of the feed-in tariffs for the new rooftop installations until the end of 2024 compared to what was established back in July 2022 in the Renewable Energy Sources Act, together with a further reduction of taxes for solar systems (SPE, 2023). The Spanish one, instead, still focused on the ground-mounted PV parks, in which the country is still one of the major global leaders, due to the relatively very young solar rooftop sector (SPE, 2023). On the other hand, the Italian scenario based its growth on the residential and C&I applications, which accounts respectively for 40 and 43% of the new power installed (SPE, 2023). Similar differences among the Member States clearly depends on the type of political support and the targets assessed towards the meeting of the 2030 solar targets. Nevertheless, the general trend resulting from the recent inflationary environment was able to determine an overall rooftop capacity increase from 60 (2022) to 66% of the total PV share, while utility-scale plants faced the opposite fate lowering from 40 to 34% (SPE, 2023). On a long term perspective, rooftop solar is still expected to prevail on utility-scale plants, even though the gap between the two applications will reduce a bit (Figure 2.1) (SPE, 2023).

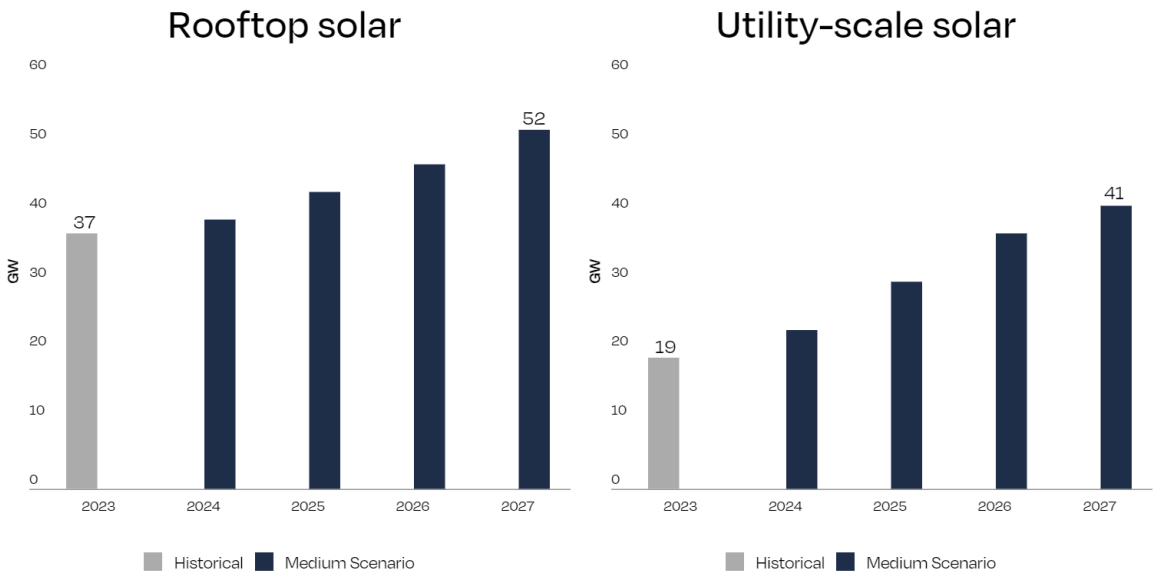

Figure 2.1: Rooftop and utility-scale solar capacity trend forecast in Europe up to 2027 (SPE, 2023).

In 2023, the EU-27 installed 16.2 MW of wind capacity, the highest amount ever recorded (WindEurope, 2023). The total capacity installed reached 220 GW, of which 201 GW belong to onshore installations, while 19 GW to offshore installations (WindEurope, 2023). The new European permitting rules are allowing a faster and more consistent plants construction: it's expected that, at this rate, the 2024-2030 period will bring the installed power to 393 GW (Figure 2.2), almost reaching the 425 GW target set by the European Commission (WindEurope, 2023). Offshore plants deployments forecasts suggests that by 2030 new wind power plants installations will overcome for the first time onshore installations (WindEurope, 2023). The relevance of this event is crucial, since up to now the unexploited offshore potential is still massive due to the relatively low technology maturity compared to the onshore one. Due to the progressive developments of the sector, bigger and more powerful machines have been introduced in the market (WindEurope, 2023). However, this is not only a consequence of technological improvements, but it's also a strategic decision. A large part of the most profitable onshore sites has in fact already been occupied by older projects, hence new models of turbines installed for recent applications require to compensate the reduced mean wind speed with bigger rotors (WindEurope, 2023). The superimposition of these two effects generated a continuous increasing of the turbines' diameter over time, as well as hub height (Figure 2.3).

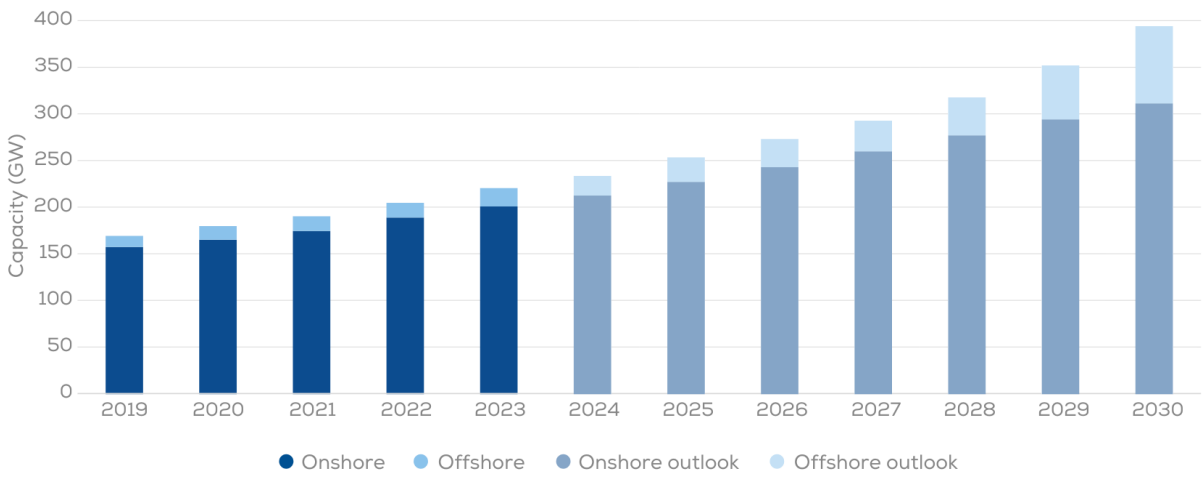

Figure 2.2: Total installed wind capacity trend forecast in EU up to 2030 (WindEurope, 2023).

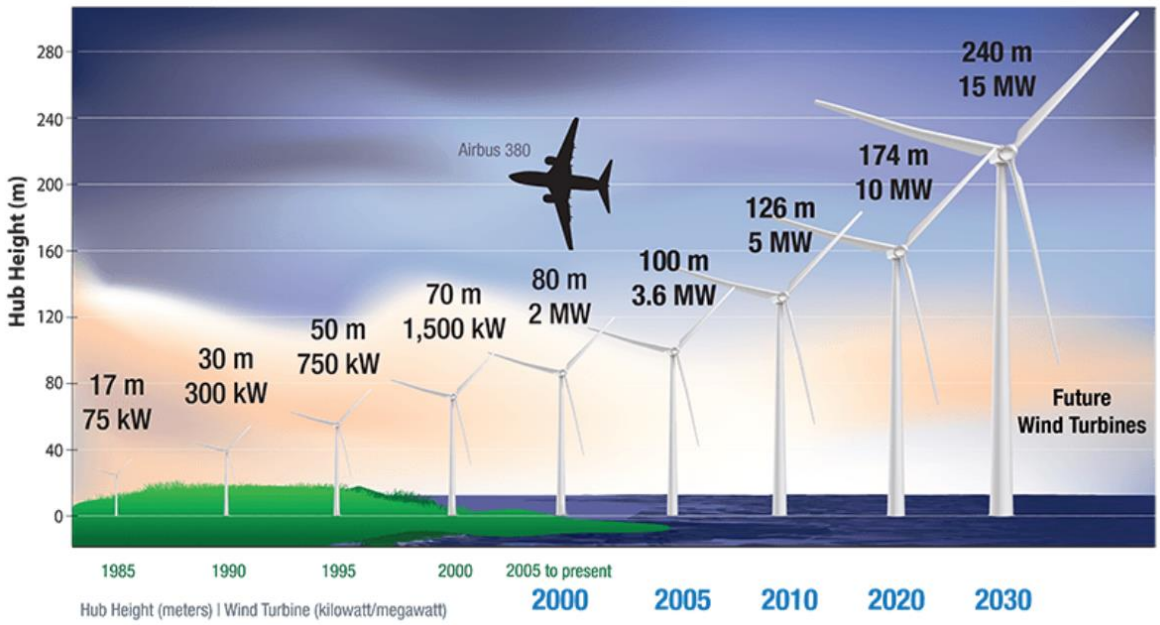

Figure 2.3: Evolution of wind turbines' size and nominal power over time (NREL, 2020).

3 Case study description

The onshore wind power plant object of the study denominated "Iurefalco" is located in Puglia region, Italy, specifically in Sannicandro di Bari municipality. The area interested by the power plant extends for approximately 150 ha, while its mean altitude is around 300 m. The power plant features 6 G114-2.5 MW wind turbines that generate electric power at medium voltage (20 kV). The produced electric power is delivered through a MV cable duct transmission system towards a transformer substation, in order to raise its voltage to a value compatible with the one of the grid. Since the grid segment to which the power plant's electric system is connected presents a voltage of 150 kV, the transformer type used is 150/20 kV. The link between the transformer substation and the national transmission grid is represented by the primary station managed by the TSO (TERNA), with which the transformer substation is connected through a HV cable duct transmission system. The complete layout of the power plant is depicted in Figure 3.1.

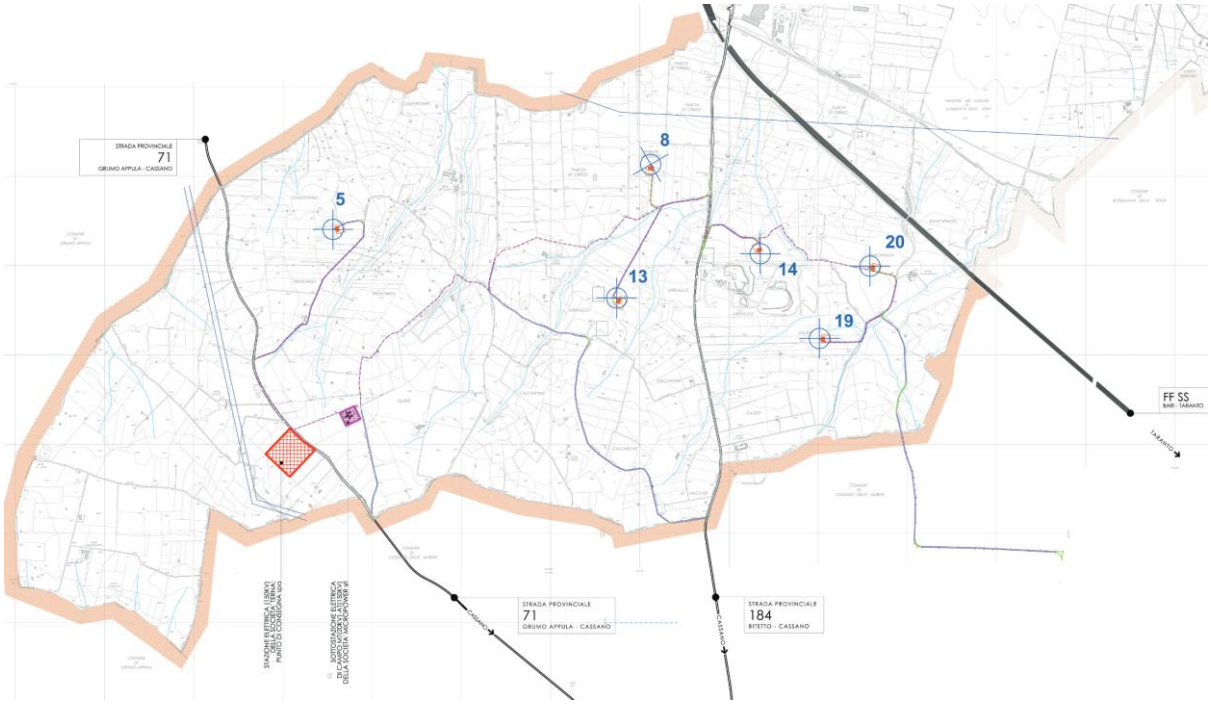

Figure 3.1: layout of the wind power plant. In blue the location of the 6 WTGs; in purple hatched lines the path followed by the MV and HV cables. The filled regions in purple and red represent respectively the transformer substation and primary substation (adapted from Project documentation).

The area occupied by the power plant belongs to the territory of the *Media Murgia*, a region known for its high presence of limestone deposits and dry landscape. The region is characterized by minor slopes and a limited presence of vegetation, especially forests, whose place has been replaced by cultivated zones. The calcareous areas that typically can be found in the region have a very old origin, dating back to 130 million years ago. In the course of thousands of years, rainwater and other meteorological phenomena shaped the rocks forming valleys of various and complex geometries, caves and chasms.

The power plant site develops in a low urbanized region. The few buildings that are present refer to farmhouses or other agricultural activities, with some of them even inhabited and abandoned. Regarding infrastructures, instead, the region is served by a dense system of public roads, among them it's worth to mention the SP 236 Bari – Cassano delle Murge, SP 71 Grumo Appula – Cassano delle Murge (depicted in Figure 3.1) and the SP 184 Grumo Appula – Cassano delle Murge (depicted in Figure 3.1). These roads, together with those internal to the site, allow to reach the position of each installed wind turbines. Around the area of the power plant, towards north-east, it is located the railway station of Sannicandro di Bari, which belongs to the Bari-Taranto railway route. Moreover, internally to the site, it is present an open-air limestone cave whose resources have been extracted to cover the demand of inert materials needed for the plant civil works. The cave, visible in the scheme depicted in Figure 3.1, lies a

few tens of meters away from WTG[1] 14. WTG 14 is the only wind turbine in the site whose surroundings are uncultivated. WTG 05, 08, 13 and 19, instead, are partly surrounded by olive and almond trees. WTG 20 surroundings are constituted by arable land. Overall, although the orography of the site is characterized by extended plains with small slopes (< 2%), the presence of trees can affect both the vertical and horizontal wind distribution, thus the power production of the wind turbines. Relying on the data provided by the plant's EPC Contractor, in its first year of operation (10/2022 – 10/2023) the power plant generated about 36,266 MWh, equal to 2417 equivalent hours of operation. This electricity production could potentially replace about 2,923 TOE/y (tons of oil equivalent per year), considering a conversion factor of 0,0806 TOE/MWh.

The synthetic data regarding the main features of the wind turbines and power plant producibility are summarized in Table 3.1.

Table 3.1: Main features of the power plant.

Wind power plant nominal power	15 MW
Lifetime	25 y
Number of turbines	6
Turbine model	Gamesa G114 - 2.5MW
Rotor diameter	114 m
Hub height	93 m
Net electricity production[2]	36.266 GWh/y
Net equivalent hours	2417 h
CF	0.276

Each wind turbine can be schematized in 3 main components (Figure 3.2):

- *Tower*: the tower is a vertical tubular structure that has 2 main roles: the first is supporting the weight of every other component contained in the wind turbine. Shape, thickness and material of the tower are the main parameters that allow a proper and safe execution of this duty. For example, using larger thicknesses of the tubular structure or more resistant materials can help in supporting heavier elements. The second role is related to the elevation of the energy conversion mechanism that transforms the kinetic energy of the wind into electrical energy. The height required by the wind turbine project can depend on several factors, including the nominal power of the wind turbine, the typical wind profile of the site and the power curve of the turbine. In general, the tower is made of several conical tubes that mounted one on the top of the other allow

[1] Wind Turbine Generator.

[2] Based on the plant's first year of operation, from 10/2022 to 10/2023.

to reach the desired altitude in respect to the terrain. The more the required height, the bigger and/or more numerous are the conical segments. At the bottom of the tower is located an access door that allows through the use of a ladder the inspection of the components mounted on its top.

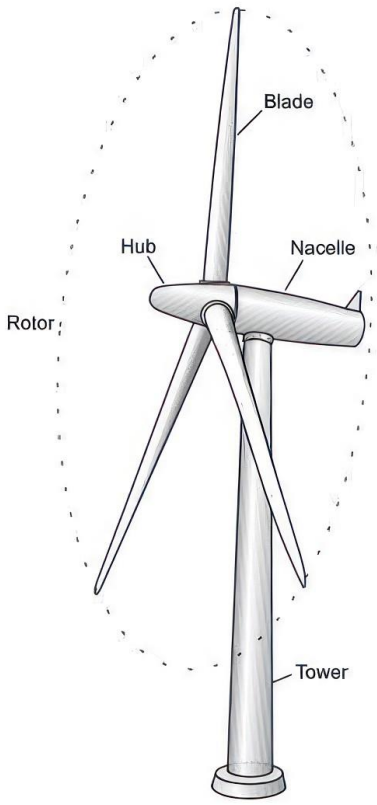

Figure 3.2: Wind turbine's main components (Gode, 2020).

- *Rotor*: the rotor is made of 2 main components, the blades (3) and the hub, joint together to rotate around a rotation axis. The aim of a wind turbine is converting the kinetic energy of the wind stream intercepted by the blades swept area in electrical energy by performing 2 types of conversion. The first one transforms the kinetic energy of the wind into mechanical energy by means of the blades' aerodynamic profiles. These profiles interact with the wind in such a way that the impact between the blades and the stream generates a force on each blade able to determine a torque on the rotor axis. The torque triggers the rotation of the assembly and generates a mechanical power given by the product between the torque itself and the rotational speed. This conversion has a certain efficiency, called aerodynamic efficiency (η_{aero}), whose entity depends on several factors, including the speed of the wind, the shape of the blades' profile and the rotational speed of the rotor. Defining as:

$$P\ [W] = \frac{1}{2}\dot{m}v^2 = \frac{1}{2}\rho A v^3 \tag{3.1}$$

the power associated with the kinetic energy of the wind, where $\dot{m}\ \left[\frac{Kg}{s}\right]$ is equal to the mass flow rate of the wind stream passing through the rotor area, $\rho\ \left[\frac{Kg}{m^3}\right]$ is the air density, $A\ [m^2]$ is the rotor area and $v\ \left[\frac{m}{s}\right]$ is wind speed at hub height, the power extracted by the rotor may be written as:

$$P_{mec}\ [W] = \eta_{aero} \cdot P = \frac{1}{2}\eta_{aero}\rho A v^3 \tag{3.2}$$

The mechanical energy exiting from this system will be submitted to the second conversion process that takes place in the nacelle of the turbine.

- *Nacelle*: the nacelle contains all the remaining components of the wind turbine (Figure 3.3). These components can be classified depending on the functions performed in the system:

  - *Structural/protective components*: cover and frame. The cover of the nacelle has the role of protecting the components inside the nacelle from exposure to meteorological events and environmental conditions. This component presents a series of accesses that allow operators to perform inspections of the internal area of the nacelle. Typically, these accesses are located between the top of the tower and the bottom of the cover and between the hub and the front of the cover. The frame is a structural element that supports the nacelle's components and transmits the loads to the tower. Since the loads resulting from the power conversion system are generally cyclic, this component must be able to bear significative fatigue stresses for prolonged periods to be suitable for its application.

  - *Drive train components*: main shaft, gearbox, generator. These components are the ones that are necessary to convert the mechanical energy in input from the rotor into electric energy. The main shaft is the element that delivers the torque produced by the wind to the gearbox. The shaft is joined to the hub through a bolted flange and it is supported by a couple of bearings that are linked to the frame. Since the rotational

speed of the rotor (which is equal to that of the main shaft) is too slow to be compatible with the one required to produce electrical energy with the generator, the main shaft speed needs to be raised by adding another component to the transmission, i.e. the above-mentioned gearbox. Therefore, the gearbox has 2 main roles: transmitting the torque produced by the wind to the generator and raising the rotational speed of the outlet shaft compared to the one of the inlet. This is achieved by employing several gears in parallel and series configuration.

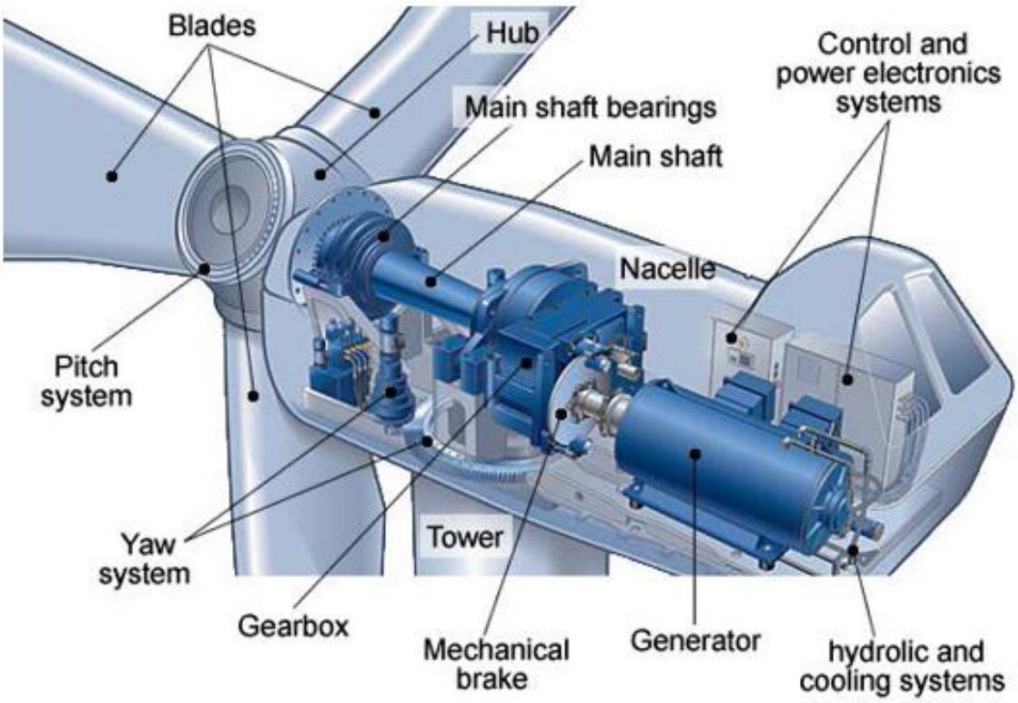

Figure 3.3: Overview of Nacelle's main components (Tchakoua et al., 2013).

The addition of the gearbox to the energy conversion system is not burden-free, since a part of the energy will be lost in heat due to the dissipative phenomena related to friction between each component that take place during the gearbox operation. The efficiency of the transmission depends on several factors, including the number and type of components involved in the mechanism, the effectiveness of the lubrication system, the maintenance frequency but also on the specific operating mode of the gearbox in terms of rotational speed and torque. Given the value of this efficiency, called mechanical efficiency (η_{mec}), the mechanical power exiting from the gearbox can be expressed as:

$$P_{mec,out}\ [W] = P_{mec,in} \cdot \eta_{mec} = P_{mec} \cdot \eta_{mec} = \frac{1}{2}\eta_{aero}\eta_{mec}\rho A v^3 \qquad (3.3)$$

where $P_{mec,in}$ is the mechanical power calculated with eq. 3.2.

The generator is the component that converts the mechanical energy leaving the gearbox into electrical energy. When coupled with a gearbox, the generator is typically a doubly-fed asynchronous machine having 4 poles in the case of frequency of the electricity generated equal to 50 Hz or 6 poles when it's equal to 60 Hz. The doubly-fed asynchronous generator, unlike the traditional synchronous generator, allows the machine to operate at variable speed since its working frequency is not constrained to the one of the grid. This is an advantage for technologies that, likewise the wind turbine, work very frequently at non-uniform rotational speed. Nevertheless, also in this case the energy conversion process is interested by energy losses due to different mechanical and electrical phenomena. To the first category belong the windage losses and friction losses, while to the second the joule effect losses, eddy currents losses, and hysteresis losses. Defining an overall efficiency of the energy conversion process that happens in the generator, called electrical efficiency (η_{el}), the electric power output of the entire conversion process of the wind turbine can be expressed as:

$$P_{el}\ [W] = P_{mec,out} \cdot \eta_{el} = \frac{1}{2}\eta_{aero}\eta_{mec}\eta_{el}\rho A v^3 = \frac{1}{2}c_p\rho A v^3 \qquad (3.4)$$

Where c_p, also known as power coefficient, is the product between all the efficiencies discussed. It's worth noting that the value of c_p, which expresses the ratio between the electrical power produced by the wind turbine and the kinetic power of the wind, can't in any case exceed the value of $c_p = \frac{16}{27} = 0.593$ due to the existence of a theoretical limit demonstrated by the engineer Albert Betz. This means that real wind turbines will be capable of converting only a fraction of the wind kinetic power that is always lower than 60%. Moreover, in real applications, the c_p is never constant but depends on the operating conditions and the design of each machine.

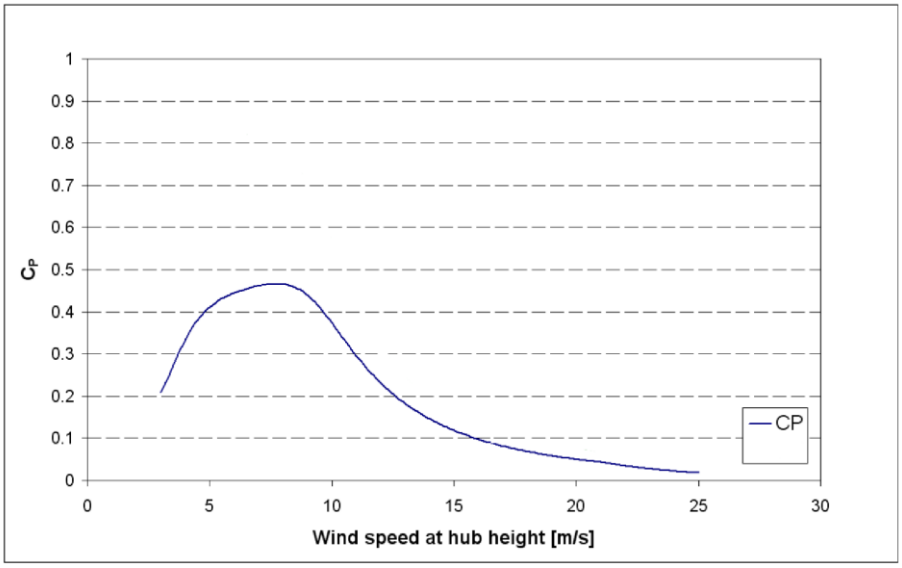

(a) cp curve

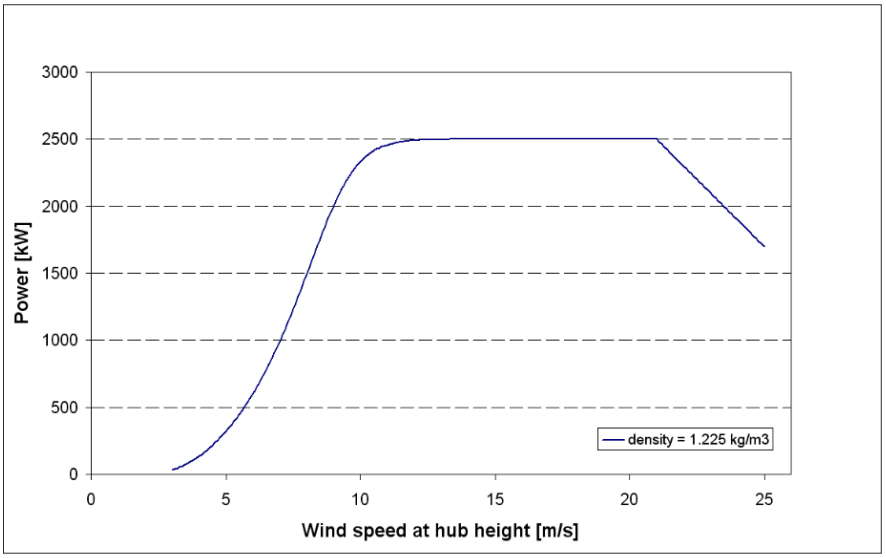

(b) Power curve

Figure 3.4: G114-2.5 MW power and cp curve (adapted from Project documentation).

The curve that outlines the behavior of c_p in function of the wind speed for a specific machine is obtainable dividing the electric power produced by the machine with the kinetic power of the wind at corresponding speeds for the entire operative range. The power produced by the machine is described for every model of wind turbine using a power curve. The power curve that refers to the G114-2.5 MW wind turbine is reported in Figure 3.4, together with its c_p curve. Generally, wind turbines are designed to not produce electrical power when the wind speed is lower than a certain value, called cut-in speed. In the case of the G114-2.5 MW, this speed is equal to 3 $\frac{m}{s}$. Since the power is zero, also the

c_p results to be equal to zero in this range (eq. 3.4). For wind speeds higher than the cut-in speed, instead, wind turbines are generally designed to produce as much power as possible, hence the goal is to have always the maximum possible c_p. However, the c_p can't assume a constant value since, as introduced before, the power losses in the rotor and in the drive train depend on operative condition of the wind turbine. Typically, the c_p tends to increase steeply for wind speeds slightly higher than the cut-in speed before stabilizing around a maximum value. When the wind speed approaches the rated speed (14 $\frac{m}{s}$ in the case of the G114-2.5 MW turbine), i.e. the speed for which the power produced by the wind turbine is equal to the nominal one, the c_p start to decrease since otherwise the turbine would produce a power greater than what the generator can convert. This reduction is not caused by the natural effects of the operating conditions on the turbine's components, but it's the designed regulation system that does it on purpose to limit the power output and avoid damage to the structure. For wind speeds greater than the rated one, the c_p keeps decreasing for the same reason, until the stresses on the blades caused by the impact of the wind start to be such that the reduction of rotational speed and ultimately the stoppage of the turbine is required to preserve their integrity. In the case of the G114-2.5 MW wind turbine, 21 $\frac{m}{s}$ is the speed above which the rotational speed is reduced, while above 25 $\frac{m}{s}$ the turbine is stopped.

- *Other mechanical devices*: yaw system, brake system, pitch system. These devices are mechanical units triggered by the turbine control system depending on the data collected by the anemometer and the wind vane installed on top of the nacelle. The yaw system allows the rotation of the nacelle around the axis of the tower to face the wind always perpendicularly and upwind in respect to the rotor surface. The brake system, instead, acts on the gearbox outlet shaft (high speed shaft) when the turbine is already stopped to maintain the stationary condition in safety. In fact, the wind turbine rotor is always stopped using aerodynamic solutions which involve the blades, not the brake system. The pitch system allows the blades to rotate around their axis. In most wind turbines, this rotation is used to control aerodynamically the operation of the machine, for example limiting the power produced to not exceed the rated one or, as said before, stopping aerodynamically the turbine when the wind speed reaches the cut-off value.

- *Other electrical components*: transformer and control system. The nacelle integrated transformer performs a first increase of the voltage of the

current produced by the generator. Depending on the specific design criteria of the power plant, the output voltage can vary from a few thousands volts to few tens of thousands. This is done in order to prevent electrical losses due to the length of the transmission system leading up to the transformer substation. The control system, instead, consists in a group of electrical cabinets responsible for monitoring and handling several types of units of the wind turbine: mechanical units, such as the above mentioned blades' pitch angle control mechanism, the yaw angle control mechanism and the brake mechanism; electrical units, in particular the frequency converter, which is responsible for the power management and the connection/disconnection of the doubly-fed asynchronous generator to/from the grid; auxiliary units, in particular the heating and cooling systems of the nacelle; the hydraulic system.

– *Hydraulic system*: the hydraulic system is managed by the control system through the transmission of electric signals. Its main purpose is supplying pressurized fluid to several mechanical units, including the pitch control actuators, the brake system of the transmission of the wind turbine and the brake of the yaw system. Since many of these units are very important in terms of safety of the wind turbine, the hydraulic system always includes a fail-safe activation system in case the control system is not working due to electrical issues.

Each wind turbine, given the weight of its components, is installed on a proper foundation that gives stability to the structure and prevents sinking in the terrain. Moreover, in front of each turbine, it's always needed a platform that allows the passage and the operations of the building machines, as well as the storage of the turbine's main components while performing its erection. The surface extension, the construction materials and their thickness employed to build the platforms have been chosen by the manufacturer of the turbines based on the site orography and the equipment used, since the manufacturer himself managed the turbines installation. It's worth noting that the use of the platforms is limited only to the construction phase of the wind power plant, therefore, after the end of the required civil works, a portion of the platforms has been removed to make possible the recultivation of the soil. The remaining part has been left unchanged since it will still be needed for maintenance activities concerning the wind turbine's components.

To allow access to each wind turbine, several internal roads have been built according to the turbines' manufacturer prescriptions. These roads must ensure the safe passage of the lorries that perform the special transports associated with the major wind turbine's component, i.e. the tower segments, the blades and the nacelle. Hence, likewise the platforms, the surface of these roads must be characterized by very small slopes and be as regular as possible, besides having sufficient resistance to the loads

imposed by the vehicles. The layout of the site has been defined granting good compatibility with the existent internal and external viability, avoiding the construction of new roads and performing only minor adjustment, such as road enlargements, traffic sings removals, sidewalks removal and so on. After the transport phase of the turbines' components, the original state of the modified locations was restored in a few weeks.

Most of the components used in the G114-2.5 MW turbines are manufactured by Siemens Gamesa factories in Spain. Those components that are instead purchased by SG from other countries suppliers are imported to Spain for the assembling and then delivered by road and ship transport to the customers (Siemens Gamesa Renewable Energy, 2017). In the case of Iurefalco wind power plant, the tower segments are produced and transported in Italy, while all the other components are either produced or imported in Spain and then delivered via ship to Italy (Siemens Gamesa Renewable Energy, 2017).

The electric power transmission system of the power plant, as introduced before, is composed of 2 main units: the MV and the HV cable ducts. Their construction includes the excavation of a trench in which the cables that deliver the electric power produced by the wind turbines are placed and then covered with compacted inert materials up to ground level. It's worth noting that the cables are not directly buried in the ground, but they are inserted in corrugated pipes with proper diameter. Together with the cables, it's also placed in the trenches an optical fiber network that connects the control room placed in the transformer substation with the WTGs. Similarly to the cables, the optic fiber is also inserted in corrugated pipes. Moreover, the HV cable trench features a copper rope for the grounding of the HV transmission line. Both trenches mostly follow the path of the internal roads of the power plant, but when required they also cross the topsoil or the public roads that pass through the site (i.e. SP 71 and SP 184, see Figure 3.1).

The transformer substation is defined by an open-air rectangular square delimited by a concrete wall. The internal area can be divided into 2 sections: the first one contains all the electromechanical components needed for the voltage increase of the electricity coming from the MV cable ducts. This section is paired with a rainwater drainage system due to the absence of a rooftop. Moreover, a lighting system provides the required illumination in the evening and night hours. The second section is composed by a couple of metallic shelters that contain the electronic system used for the control and management of the wind turbines (SCADA system). The 2 shelters come with several other auxiliary systems to allow their proper functionality: electrical system, lighting system, anti-intrusion system, HVAC system, fire-fighting system and a diesel power generation unit.

4 LCA methodology

The Life Cycle Assessment is a tool used by companies or public administrations able to identify opportunities to make better the environmental performance of a product, seen as a tangible object or as a service, considering all the stages included in its life cycle (ISO 14040:2006). LCA methodology aims to give a clear and complete idea on the interactions that exist between the system under investigation and the environment, underlining the consequences of each activity involved and providing the managers and directors sufficient pieces of information to make decisions in favor of sustainability. The approach followed by the LCA methodology is systematic, but the techniques, the depth of the study, and the requirements are often case dependent, in accordance with the intended application selected by the organization (ISO 14040:2006).

The ISO (International Organization for Standardization) committee contributed during the years in the standardization of the LCA methodology by publishing the standard series 14040, implemented and updated also in Italy as UNI standards (2006). The regulatory framework includes the UNI EN ISO 14040:2006 and the UNI EN ISO 14044:2006, which replace the old UNI EN ISO 14040:1998, UNI EN ISO 14041: 1999, UNI EN ISO 14042: 2001 and UNI EN ISO 14043: 2001. These standards can be applied to any type of product regardless of its nature or application field.

According to the ISO 14040:2006 standard, an LCA study consists in 4 phases that are strictly connected to each other (Figure 4.1):

- *Goal and scope definition*: in this phase it's required to define the intended application of the LCA, the motivations that led to the study implementation, the intended audience and whether the results are intended to be used in comparative assertions disclosed to the public (ISO 14040:2006). The central purpose of this process is identifying the main features of the analysis to have clear in mind which are the most suitable approaches to carry it out. Thus, the key aspects that need to be defined are related to the extension of the system to be analyzed, the functional unit of the study, the allocations procedures, which impact categories are worth to be considered, the required data and the assumptions/limitations (ISO 14040:2006). The system boundaries may involve different life cycle phases depending on how the goal and scope of the study are defined. In particular, the analysis may involve only a single phase of the product life cycle ("gate-to-gate" assessment), a portion ("cradle-to-gate" or

"gate-to-grave" assessment), or the entire life cycle ("cradle-to-grave" assessment).

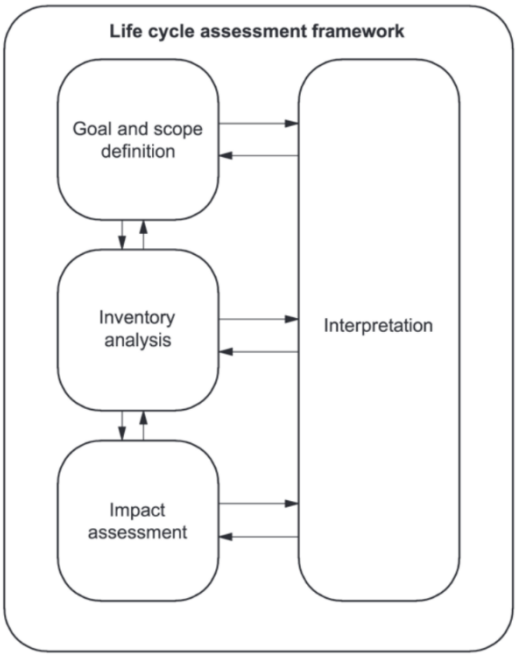

Figure 4.1: LCA framework (modified from ISO 14040:2006)

Each unit process belonging to each phase in the system is characterized by energy or material exchanges with other processes or with other systems (not included in the boundaries). The inputs and outputs involved constitute the main objects of study for the selected impact categories to be evaluated, since they carry all the interactions between the system and the environment.

In this context, the functional unit represents a reference unit of measurement to which associate each input and output flow (ISO 14040:2006). This reference is fundamental to allow the comparability of different LCA results, especially when the systems analyzed are different, since otherwise there would be no common basis to make comparisons (ISO 14040:2006). Thus, all the data regarding material and energy flux should always be referred to the functional unit. The data themselves should also satisfy, depending on the goal and scope of the assessment, requirements related to their temporal and spatial background, to their precision and completeness, but most importantly to the reliability of their source. Data can in fact be classified in 3 categories:

- *Primary data*: these data are derived from direct measurements, which are typically the most reliable source. However, data acquisition from

direct measurements often has the drawback of being challenging and time-consuming.

- *Secondary data*: these data are derived from literature sources or national/international databases. They represent a good compromise between reliability and ease of acquisition.

- *Tertiary data*: these data are derived from estimates or assumptions based on mean values. Although their acquisition is typically faster and easier compared to the other two, their reliability is often small, therefore the use of tertiary data should be limited as much as possible.

- *Inventory analysis*: this phase represents the core of the entire LCA, since it involves the entire data collection and the quantification regarding all the relevant inputs and outputs in the system (Figure 4.2) (ISO 14040:2006). One of the most important features of the inventory analysis, also known as life cycle inventory analysis (LCI), is that the processes of collection and quantification are iterative due to their nature. In fact, collecting data also means learning more about the system, which often results in the definition of new data requirements compared to the ones defined at the start (ISO 14040:2006).

  Inputs and outputs can be classified not only in relation to their physical interpretation (material flows, energy flows), but also to the role they assume or the transformations they underwent prior incoming to or after exiting from a unit process. For example, as "elementary flow" is defined a material or energy flow that enters the system (leaves the system) without previous human transformations (without subsequent human transformations) (ISO 14040:2006). As "ancillary input" is instead defined a material input that has been used in a process to produce the product but it does not represent a part of the product itself (ISO 14040:2006). Given the variety of the possible inputs and outputs, it's evident that the LCI can be a quite expensive and time-consuming phase in an LCA study. For this reason, it is fundamental setting constraints on data collection, typically called "cut-off criteria", which specifies the amount (usually in terms of percentage of the total) of material or energy flows referred to a single process or to the entire system that can be excluded from the study (ISO 14040:2006). Eventually, the same thing can also be done with the level of environmental significance (ISO 14040:2006).

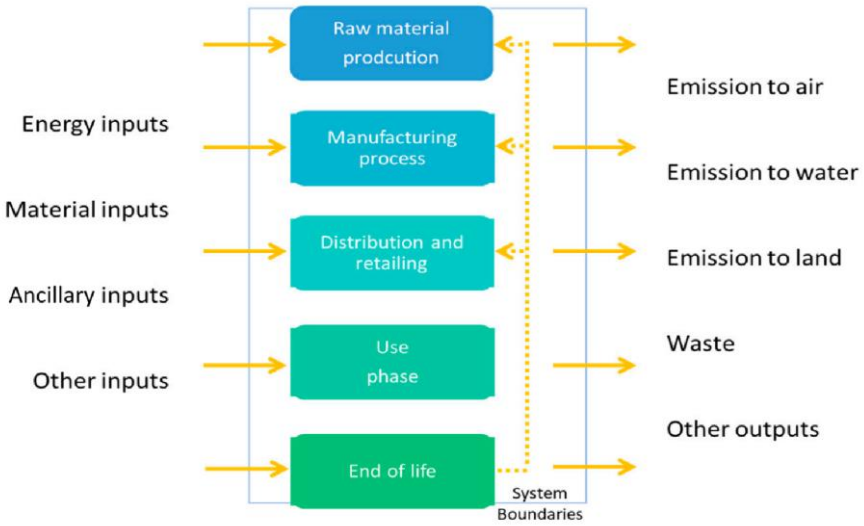

Figure 4.2: Schematic representation of a generic system interested by input and output flows (Köck et al., 2023).

The cut-off specifications, considering how they are defined, clearly depends on the goal and scope of the analysis. When dealing with a system that generates more than one product, a new problem arises regarding the assignment of the material and energy flows to each of them to be able to evaluate the respective environmental impacts. As anticipated before in the goal and scope section, an allocation procedure should be defined to solve this issue. Different types of allocation procedures exist, but the most used are related to the mass of the products, their economic value or area/volume. Whatever the chosen criterion, the allocation is then performed according to the fraction of the selected aspect represented by each product. To sum up, the LCI phase should consists in the following activities:

- Outlining a graphical representation of the system broken down in its unit processes. Each process should be described emphasizing those aspects that are related to the determination of the relevant inputs and outputs (ISO 14044:2006).

- Describing the data collection and calculation techniques, their classification and units of measurement used (ISO 14044:2006).

- Calculating the data following the assumptions and techniques established in the previous step (ISO 14044:2006).

- Validating the data: this includes, for example, the verification of the mass and energy balance related to each unit process (ISO 14044:2006).

  - Associating the data to the functional unit (ISO 14044:2006).

  - Applying the allocation procedure if the system presents more than one product (ISO 14044:2006).

- *Impact assessment*: the impact assessment phase, also known as LCIA (life cycle impact assessment), consists in the evaluation of the environmental impacts determined by the material and energy flows involved in the system (ISO 14040:2006). This phase should be carried out according to the goal and scope of the study, but also based on what has been obtained at the end of the LCI phase. In particular, it should be checked if the quality of the LCI data and results is suitable to proceed with the LCIA phase while meeting the requirements established in the goal and scope, as well as in the cut-off criteria (ISO 14044:2006). In general, this phase consists in mandatory elements and optional elements (ISO 14044:2006):

  - *Mandatory elements*: they include the selection of the impact categories, category indicators and characterization models; the attribution of the LCI results to the chosen impact categories, also called *classification*; the calculation of the category indicator results, also called *characterization* (ISO 14044:2006). Impact categories, likewise the category indicators and characterization models, should be consistent with the goal and scope of the study and be internationally accepted (ISO 14044:2006). Impact categories can be classified in *input-related* and *output-related* categories. The former refer to the impacts associated to the use of those materials that are employed as input to the system, e.g. minerals, fuels, water. The latter, instead, refer to the impacts associated with the environmental emissions of various toxic or non-toxic substances, such as carbon dioxide, nitrogen oxides, and so on. The category indicators are the elements that represent each impact category. For example, considering the Climate Change (CC) impact category, which refers to the impacts of the system emissions to the greenhouse effect (i.e. output-related category), a possible category indicator could be the infrared radiative forcing, measured in $\frac{W}{m^2}$, but many others can be used in function of the goal of the analysis (ISO 14044:2006). The characterization model represents the link between the LCI results and the category indicator used for the impact category (ISO 14044:2006), therefore it's a fundamental element in the classification phase. During the characterization phase it's performed the final translation in quantitative terms of what obtained in the previous phases, using category indicators: the characterization factors (inherent to the specific characterization model) are used to multiply each input or output in

order to obtain the overall impact related to the category considered. In Figure 4.3 is depicted an example taken from the ISO 14044:2006 standard that covers all the aspects just discussed.

Term	Example
Impact category	Climate change
LCI results	Amount of a greenhouse gas per functional unit
Characterization model	Baseline model of 100 years of the Intergovernmental Panel on Climate Change
Category indicator	Infrared radiative forcing (W/m^2)
Characterization factor	Global warming potential (GWP_{100}) for each greenhouse gas (kg CO_2-equivalents/kg gas)
Category indicator result	Kilograms of CO_2-equivalents per functional unit
Category endpoints	Coral reefs, forests, crops
Environmental relevance	Infrared radiative forcing is a proxy for potential effects on the climate, depending on the integrated atmospheric heat adsorption caused by emissions and the distribution over time of the heat absorption

Figure 4.3: Definition of the mandatory elements concerning the evaluation of the system's carbon footprint (ISO 14044:2006).

– *Optional elements*: they include normalization procedures; grouping procedures; weighting procedures; data quality analysis (ISO 14044:2006). These elements can be used along with the mandatory ones depending on the goal and scope of the analysis, since they may add some useful information to better understand and interpret the results of the LCIA (ISO 14044:2006). In the *normalization* phase, the numerical values obtained through the category indicators are divided by a selected reference value, for example the average value of inputs and outputs related to a given area (e.g. global) and temporal scale (ISO 14044). In *grouping*, instead, impact categories are either sorted on a nominal basis or ranked according to individual hierarchy preferences in order to make additional evaluations and interpretations of the results (ISO 14044:2006). In *weighting*, the numerical results are weighted using factors based on individual choices (ISO 14044:2006). Each company/organization may have different preferences depending on the context and goals, therefore these aspects must be clarified (ISO 14044:2006). Additional data quality analysis may be conducted to (i) determine how variations in data and methodological choices influence the results of the study (*sensitivity analysis*) and (ii) how uncertainties in data and assumptions evolve during the calculations and how they influence the reliability of the results (*uncertainty analysis*) (ISO 14044:2006).

- *Interpretation*: in the interpretation phase, the results obtained during the LCIA phase are considered together to make findings and elaborate conclusions that are coherent with the goal and scope of the LCA (ISO 14040:2006). In particular, this phase should provide suggestions for the improvement of the system looking at its eco-profile and sustainability. For example, after the identification of the hotspots related to the selected impact categories, different scenarios that may represent a solution to the highlighted issues can be discussed and compared to present a new improved version of the system. Each conclusion and recommendation should be in any case verified through completeness and consistency checks to be sure that all relevant information and data needed for the interpretation phase are available and complete (*completeness check*) and consistent with the goal and scope (*consistency check*) (ISO 14044:2006). Moreover, likewise the LCIA phase, a sensitivity check may be used to evaluate the reliability of the conclusions by making different assumptions, using different methods, indicators and so on.

5 Literature review

In this section, a review of selected paper works regarding LCA of wind power plants will be conducted to inform about the general context in which this type of technology is called to operate and most importantly which are the hotspots and their impact in relation to the energy balance of the system and its carbon footprint. It's worth noting that, as anticipated in Chapter 4, in LCA studies, even following the same regulatory framework, each phase can be characterized by non-uniform assumptions and methodologies depending on which are the goal and scope of the analysis, making direct comparisons of LCI datasets quite difficult. Moreover, significant variability may involve the configurations and the operating conditions of the systems analyzed, determining further issues in the comparisons (Dolan and Heath, 2012). For these reasons, depending on the specific technology employed for electricity production, a series of harmonization techniques have been introduced which cover both technical and methodological aspects of the analysis, in order to reduce the variability of the compared results (Turconi et al., 2013). In the case of wind energy, these harmonization techniques are reported for the estimation of the Global Warming Potential (see Figure 4.3) in Dolan and Heath (2012), including: type of technology (e.g. onshore, offshore), type of Global Warming Potential, the operating lifetime, the capacity factor, the system boundaries (Turconi et al., 2013). A similar approach may be followed for the energy balance as well (Dolan and Heath, 2012). Typically, very few LCA studies perform in their literature review harmonization operations, due to the amount of data required on each work that is often not available. While also in the case of the present study harmonization wasn't possible, it was highlighted when feasible the possible influence of parameters, assumptions or methodologies over the disparities between the results related to the different works.

The reviewed LCA studies are reported in Table A.1. Studies published prior to 2008 were not considered to avoid the comparison of too old technologies with the newer. Both onshore and offshore types of power plant have been analyzed, as well as wind farms and single turbine configurations. As said before, to make fair comparisons, only technologies with the same configuration and type should be considered, but it's very interesting in any case analyzing which are the factors that lead to certain gaps of values for the estimated indicator results to understand more about the technology and its weaknesses from an environmental point of view. It should be noted that not every LCA included in this review assesses both primary energy consumption and carbon footprint, but in some cases only one of these was addressed by the authors.

The main parameters and results of the reviewed studies, as well as the characterization models used for the evaluation of the impacts, are reported in Table A.1, A.2.

All the power plants discussed in the reviewed studies except one present an expected lifetime of 20 years, while the rated power of the turbines ranges from 0.66 to 6 MW. When possible, data concerning the turbines' dimensions and the wind characteristics were included in the tables. The capacity factor of each turbine, when not specified in the studies, was calculated using the information on the annual energy yield of the power plant, assuming that each turbine produces the same amount of energy (assumption used by all the authors who dealt with wind farms). The indicator's results related to the primary energy consumption and carbon footprint of each plant have been expressed in terms of unit per kWh of electric energy delivered to the grid for all the studies, in order to have uniform units of measurement. When presented in this way, these indicator results are called *energy intensity* and *GHG intensity*. Overall, their values range from 0.020 to 0.162 $\frac{kWhp}{kWhel}$ in the case of the primary energy consumption, while from 4.65 to 18.00 $\frac{gCO2\ eq}{kWhel}$ in the case of the carbon footprint. Additionally, environmental indexes have been used by all the authors to give a synthetic interpretation on the level of sustainability concerning the results energy balance and carbon footprint. Specifically, the Energy Payback Time (EPBT) defined as:

$$EPBT\ [year] = \frac{E_{prim,tot}\ [GWh]}{AEY\ \left[\frac{GWh}{year}\right]} \tag{5.1}$$

where $E_{prim,tot}$ is the total primary energy consumption and AEY is the mean annual energy yield of the power plant, represents the time expressed in years that is necessary for the power plant to deliver to the grid an amount of electric energy equal to the primary energy that has been used over its entire life cycle. In general, the lower the EPBT, the lower is the primary energy consumed compared to the one produced by the power plant, hence the lower is the amount of primary energy resources consumed, both fossil and renewable. In the reviewed studies, this index ranges from 0.4 to 3.23 years, corresponding to 4.8 and 38.8 months. This index is often used together with the Energy Return On Investment (EROI), which is another index that instead gives a quantitative idea on how much is the total electric energy delivered to the grid over the plant lifetime compared to the primary energy consumed. The EROI is defined as:

$$EROI\ [-] = \frac{AEY\left[\frac{GWh}{year}\right] \cdot plant\ lifetime\ [years]}{E_{prim,tot}\ [GWh]} \tag{5.2}$$

In this case, the higher the EROI, the higher is the energy delivered to the grid from the power plant compared to the primary energy consumed during its life cycle, hence the higher is the level of sustainability towards the energy resources exploitation. In the reviewed studies, the EROI ranges from 6.2 to 50. Only few authors included in their studies additional indexes regarding carbon footprint. Specifically, the most used resulted to be the Carbon Payback Time (CPBT) that, similarly to the EPBT, represents the time expressed in years that is necessary for the power plant to compensate its GHGs emissions during its entire lifetime. The CPBT is defined as:

$$CPBT\ [year] = \frac{e_{tot}[KgCO2eq]}{e_{saved,year}\left[\frac{KgCO2eq}{year}\right]} \tag{5.3}$$

where e_{tot} is the amount of GHG emitted during the plant life cycle (expressed for example by the GWP index) and $e_{saved,year}$ is the amount of the annual savings of GHG emissions in respect to a reference non-renewable electricity generation technology. From the evaluation of the reviewed studies, it has been possible to point out the main parameters, assumptions and methodologies that affect the results of the assessments:

1. LCI data acquisition approaches. To carry out an LCA study, retrieving data according to the goals of the study with the aim of making a complete LCI is fundamental. Typically, two approaches can be used during this phase: *process chain analysis* (PCA) and *input-output analysis* (IOA). PCA is a bottom-up approach that utilizes input data related to the specific processes often taken directly from the power plant (Turconi et al., 2013). This is an expensive method compared to the other, but generally more precise (Turconi et al., 2013). In PCA, due to its complexity, a cut-off criterion is frequently used to neglect minor influences on the system, leading to an incomplete boundary which often underestimates the impacts (Turconi et al., 2013). On the other hand, IOA is a top-down approach that is based on monetary data related to each economic sector, in which the inputs are not the ones related to the specific application but those coming from other sectors are included as well (Turconi et al., 2013). Compared to PCA, IOA presents larger system boundaries since no cut-off criteria are used, but at the same time it's less case-dependent and less precise, often overestimating the impacts (Turconi et al., 2013).

To mitigate the issues related to each approach, hybrid methods that use both have been developed over the years, but they are rarely used in literature. In this literature review only one LCA study that utilizes a hybrid method was included (Crawford, 2009). Another interesting work made by White (2007) could not be included since it doesn't use a proper hybrid method but only one of the two depending on the quality of the available data for the specific life cycle phase, while also crossing the time threshold set before (< 2008). Nevertheless, given the importance of the differences with the other studies, whose authors always preferred to use process chain analysis whichever the phase considered, the key results taken from the three wind farm analyzed by White (2007) were retrieved from another LCA review made by Davidsson et al. (2012). According to the authors of the review, White (2007) estimated the primary energy used by each power plant by using PCA when the quality of the data related to the phase considered was acceptable, while IOA when data were considered lacking (Davidsson et al., 2012). Specifically, IOA was used for the *operation and maintenance* phase in all the three studies, which accounts for 34%, 16% and 11% of the total primary energy used, respectively (Davidsson et al., 2012).

These numbers are in high contrast with the results obtained by the other studies, as will be shown, since the total contribution associated to the operational phase of wind turbine power plants accounts on average for 4% of the total primary energy consumption. Crawford (2009), on the other hand, using a hybrid method, concluded that the total embodied energy in the system may count a contribution up to 78% coming from Input-Output data, while the rest from process data, therefore stating that embodied energy analysis methods of wind power plants based on PCA may be up to 78% incomplete (Crawford, 2009). The use of PCA most likely underestimates energy consumption, but it's possible as well that IOA overestimates this aspect too much (Davidsson et al., 2012). That's why the use of both methodologies should be chosen in this type of study to make further analysis and consider all the possible scenarios (Davidsson et al., 2012).

2. Type of power plant. The systems that characterize onshore and offshore plants, although satisfying the same requirements, such as production, transformation and transmission of the electric power, are structured by components whose impacts in terms of primary energy consumption and GHGs emissions differ a lot with each other. Typically, offshore systems have the advantage of exploiting higher wind resource at the same height compared to onshore system thanks to the orography of the locations, while also experiencing more regular wind speeds during the day. These two aspects generally make the capacity factor of offshore plants substantially higher than onshore plants, determining for the same installed capacity and similar boundary conditions of the system a higher annual energy yield. However, these advantages are counterbalanced by the higher energy demand, as well as GHGs emissions, over the entire life cycle of the offshore plant (Kaldellis and Apostolou, 2017), which typically

make greater global energy intensity and GHGs intensity of the system compared to the onshore plants. A more detailed explanation about the major contributing factors to these aspects will be reported in the next paragraphs related to the discussion of the specific life cycle phases of the wind power plants.

3. Expected life. All the authors except Bonou et al. (2016) (for one of the two offshore monopile plants analyzed) assumed that the expected life of the wind power plant would be 20 years (25 years in the case of Bonou et al. (2016)). Since the total energy delivered to the grid by the power plant is proportional to its operation period, it's clear that the specific environmental impact (and the revenues) could benefit from having a higher lifetime than expected.

Alsaleh and Sattler (2019) conducted a sensitivity analysis on the extension of the turbine life span for an onshore wind farm located in Texas (US). The authors evaluated the environmental impacts for an expected life of 20, 25 and 30 years. Compared to the baseline case of 20 years, although additional years of operation involve higher energy yield and revenues, it's also true that more maintenance than usual is needed due to the faster deterioration over time of the wind turbine components (Alsaleh and Sattler, 2019). However, the negative effects of the additional maintenance were demonstrated to be more than counterbalanced by the additional energy production: while in 20 years the ratio between the AEY and the yearly cumulative energy demand was 3.2, in the case of 25 and 30 years this ratio was 4.2 and 5.1, respectively (Alsaleh and Sattler, 2019). A similar evaluation could be done also for the carbon footprint of the system, most likely getting similar results. Since the advantages in extending the power plant life span strongly prevail over the disadvantages in terms of environmental impacts, it can be concluded that this represents a big step forward in improving the sustainability of this type of technology.

4. Capacity factor (CF). CF by definition is equal to the ratio between the net electric energy produced in a given period by the wind turbine and the electric energy that the turbine would have produced if running constantly at its rated power in the same period, thus the annual energy yield of a wind power plant is closely related to the CF. The mean AEY over the plant lifetime is generally one of the most uncertain parameters in a LCA, as confirmed by several of the reviewed studies, and it's probably the most critical since the energy produced represents the product of the system, hence all the impacts associated to the life cycle of the plant are allocated to this quantity. The uncertainty of CF is related to the fact that, depending directly on the AEY, it depends also on several factors whose nature is typically statistical, such as wind speed, turbulence, drive train degradation, other than design characteristics as the location of the plant, the power curve of the turbine and more.

Oebels and Pacca (2013) conducted a sensitivity analysis on the average CF of the wind power plant located in Brazil for the estimation of the specific global GHGs emissions. Compared to the baseline case with CF=34.25%, two new cases were analyzed, respectively with CF=22.18% (worst case) and CF=51.9% (best case) (Oebels and Pacca, 2013). The variation of the impacts was evaluated for the most GHGs-intensive production processes, i.e. steel and reinforced concrete production (Oebels and Pacca, 2013). The sensitivity analysis showed that upon the reduction of the CF from 34.25% to 22.18%, the mean specific emissions of these critical processes grew by more than 50% in respect to the previous value (Oebels and Pacca, 2013). On the other hand, upon the increase of the CF to 51.9% the mean specific emissions decreased by 33% (Oebels and Pacca, 2013). The results show how much is important using an accurate estimation of the CF, since its variation clearly reveals significant deviations from the initial outcome (Oebels and Pacca, 2013).

5. Electricity mix. The impacts related to the use of electric energy over the wind power plant life cycle mainly depend on which technology is employed to convert the primary energy resources into electricity. In the case of thermoelectric power plants or, more in general, power plants that use fossil or renewable fuels (e.g. coal-fired, gas-fired, biomass-fired, nuclear power plants), the primary energy consumption concerning the exploitation of a unit of electric energy is computed starting from the total heating value of the respective fuel. On the other hand, for renewable plants that don't use fuels (e.g. wind, hydro, PV power plant) the primary energy consumption is computed starting directly from the electricity output using a conventional conversion factor. Regarding the carbon footprint of the energy conversion, instead, the GHGs emissions are always evaluated by direct measurements.

Since regional and national electricity generation mixes can be widely different and electricity usage pays an important role in the energy balance and carbon footprint of a wind power plant life cycle, it's clear that this aspect has significant influence in a LCA study. To give an idea of the possible differences that can be found worldwide, the electricity generation mix used in the works of Ardente et al. (2008) and Oebels and Pacca (2013) have been compared from the carbon footprint point of view. Both studies considered as reference for the calculations the national electricity generation mix, in particular the Italian and the Brazilian one, respectively. The mean GHGs emissions generated by the Italian mix, according to the sources used by Ardente et al. (2008), were equal to 0.167 $\frac{Kg\ CO2}{MJel}$, compared to only 0.018 $\frac{Kg\ CO2}{MJel}$ generated by the Brazilian mix. This means that with the same electric energy consumption, the contribution to the carbon footprint given by the Italian wind power plant would be more than 9 times higher. Oebels and Pacca themselves in their results discussion stated that one of the most probable causes for which the carbon footprint of the Brazilian power plant is so low (7.1 $\frac{gCO2\ eq}{kWhel}$) compared to the other studies reviewed could be the national

electricity generation mix, whose specific emissions were almost 8 times lower than the global standard (Oebels and Pacca, 2013).

6. Scale effects. Several of the reviewed studies tried to put in evidence the possible presence of scale effects regarding the primary energy consumption and carbon footprint of a wind power plant. Tremeac and Meunier (2009) analyzed two single turbine systems with nominal capacity 4.5 MW and 250 W by evaluating their carbon footprint, concluding that the impacts for the smaller turbine are much higher in terms of GHGs intensity due to the smaller amount of electricity produced compared to its nominal power (Tremeac and Meunier, 2009). This issue was attributed to the unoptimized aerodynamic profile of the 250 W turbine, designed primarily to accommodate robustness requirements for end users on isolated sites (Tremeac and Meunier, 2009). Crawford (2009) analyzed two single turbine systems with nominal capacity 3 MW and 0.85 MW by evaluating the embodied energy during their life cycle. He concluded that despite the higher EROI given by the larger 3 MW turbine, its value represents only a small increment compared to the one given by the 0.85 MW turbine, since the two differ only by 11% (23 vs 21). Thus, the size of the turbines seems not to be an important parameter when optimizing the energy balance of a wind power system (Crawford, 2009). Chipindula et al. (2018) assessed the carbon footprint of 3 onshore and 4 offshore (2 monopile and 2 semi-submersible floating) wind farms installed in Texas (US), whose main features are shown in Table 5.1.

Table 5.1: Main characteristics and environmental impacts concerning the 7 wind farm analyzed by Chipindula et al. (2018).

Configuration	Type	Turbine rated power (MW)	GHG intensity (gCO2eq/kWhel)
Wind farm	Onshore	1	7.35
Wind farm	Onshore	2	7.09
Wind farm	Onshore	2.3	5.84
Wind farm	Offshore (monopile)	2	9.49
Wind farm	Offshore (monopile)	2.3	6.49
Wind farm	Offshore (semi-submersible)	2.3	7.89
Wind farm	Offshore (semi-submersible)	5	7.28

The GHGs intensity characterizing each type of power plant turned out to decrease with increasing turbines' rated power, indicating a possible scale effect for the carbon footprint. Nevertheless, it's not completely clear if scale effects are present for this technology when dealing with both primary energy consumption and carbon footprint. Bhandari et al. (2020) tried to put in evidence using a linear regression model

if a correlation exists between the GWP of the system and the size of the turbines, starting from data obtained by LCA studies published in the previous 20 years. They discovered that a negative linear correlation exists for increasing turbines' rated power, but the significance was quite low (Bhandari et al., 2020). Kaldellis and Apostolou (2017) outlined a possible behavior of the specific embodied energy with increasing turbines' rated power in single turbine systems and wind farm systems by reviewing several LCA studies on onshore and offshore wind power plants. The authors obtained that, for both the plant's type, the range between 0 and 0.5 MW is characterized by a strong economy of scale effect, hence with specific embodied energy (MWhpr/kW) highly decreasing with the nominal power. However, for higher nominal power this trend tends to revert, until a minimum in the specific embodied energy is reached (Kaldellis and Apostolou, 2017). Thus, for turbine's nominal power greater than 1.5-2 MW, the specific embodied energy starts to increase (Figure 5.1). According to the authors, this behavior could be explained due to the presence of technological barriers that prevent reaching a plateau for the specific embodied energy (Kaldellis and Apostolou, 2017). All in all, the effective presence of economy of scale effects in wind power plant technology regarding the primary energy consumption and GHGs emissions is still vague, since the parameters that can affect these aspects are manifold. The simple choice of the site of the plant can affect a high number of variables such as capacity factor, transportation impacts, installation impacts, logistics issues and so on, therefore the problem in reality is probably way more complex than considering only the rated power of the single turbines.

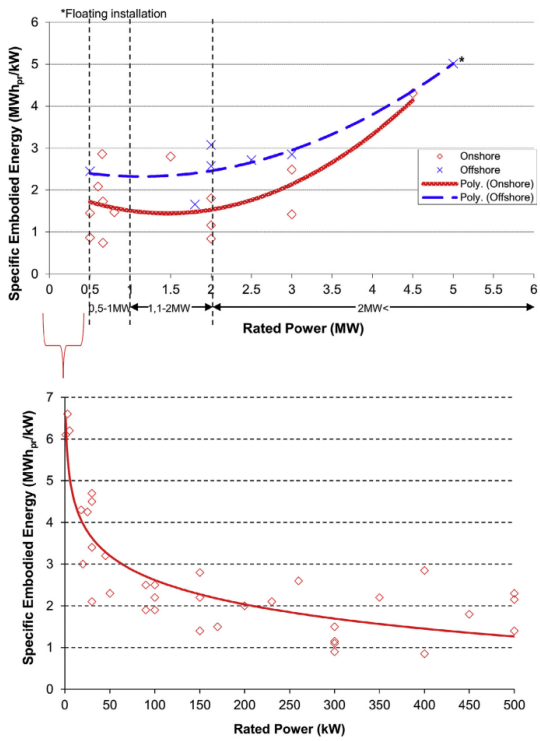

Figure 5.1: Specific embodied energy evolution with turbine rated power (Kaldellis and Apostolou, 2017).

7. Drive train type. The impacts of the wind turbine's drive train type have been investigated by the reviewed studies for single turbine systems. In general, drive trains can be classified in 2 categories: geared and gearless. While in geared turbines, as discussed in Chapter 3, the rotational speed of the rotor is significantly lower than the one of the generator, in the case of gearless turbines the rotor is directly connected to the generator, since it's composed by a higher number of magnetic poles than the doubly-fed asynchronous. The absence of the gearbox determines a series of possible advantages: higher reliability of the transmission system, higher efficiency, less frequent maintenance, lower noise. However, especially in turbines with higher rated power, the lower rotational speed of the generator determines a much higher torque, therefore the dimensions and weight of the generator usually are much larger than the one required by doubly-fed asynchronous ones. Gearless turbines may feature 2 types of generators: electrically excited synchronous generators and permanent magnet generators. In the former, the magnetic field is produced by an electric circuit fed with direct current, while in the latter it's produced by a rotating permanent magnet.

Schreiber et al. (2019) conducted a study that compares three 3 MW onshore wind turbines installed in the same site which feature all the discussed drive train types, i.e. geared (DFIG), gearless with electrically excited synchronous generator (DDSG) and gearless with permanent magnet generator (DDPMSG). The production of the three turbines is expected to be influenced only by the efficiency of and the reliability of the drive train components. Specifically, both gearless wind turbines are expected to have higher efficiencies thanks to the absence of the gearbox, as well as higher flexibility in part-load operations (Schreiber et al., 2019). Moreover, the amount of resources required for scheduled and unscheduled maintenance activities is higher for the geared turbine due to the presence of an additional component (the gearbox) and the need of lubrication (Schreiber et al., 2019). About manufacturing, the 3 turbines present similar rotor and tower both in terms of weight and material composition, but the weight of the foundations is different probably due to the variable weights of the nacelles. Specifically, the foundations weight for the DFIG, DDPMSG and DDSG wind turbines is 860 t, 1244 t and 1747 t, respectively (Schreiber et al., 2019). The results of the assessment showed that among the 3 systems, the most impactful for both the primary energy consumption and carbon footprint was the DDSG, as reported in Table 5.2. In fact, assuming the same rated power, the DDSG is typically bigger compared to DDPMSG, overtaking at the same time also the weight of the entire drive train mechanism characterizing the DFIG. Additionally, the impact of the substitution of one generator in the case of DDSG is the highest for the same reason (Schreiber et al., 2019).

All in all, although the gearless configurations have several advantages compared to the geared one, especially when dealing with bigger turbines the dimensions of the generators and the consequences that they determine can be worse than the presence of an additional component in the transmission, at least when considering the

environmental burdens related to the energy balance of the system and its carbon footprint.

Table 5.2: Main characteristics and environmental impacts concerning the 3 single turbine wind power plants analyzed by Schreiber et al. (2019).

Configuration	Turbine rated power (MW)	Drive train type	EPBT (years)	GHG intensity (gCO2eq/kWhel)
Single turbine	3	DFIG	0.5	12.43
Single turbine	3	DDSG	0.28	7.25
Single turbine	3	DDPMSG	0.28	7.25

5.1. Life cycle phases assumptions and main results

All the reviewed studies dealt with cradle-to-grave life cycle assessments. The specific definition of the boundaries referring to each life cycle phase depends on the goal and scope of the analysis, as well as on the data constraints and cut-off criteria (ISO 14040:2006). However, most of the authors subdivided the life cycle in: *manufacturing* phase, *transportation* phase, *installation* phase, *operation and maintenance* phase, *end-of-life* phase.

5.1.1. Manufacturing phase

The *manufacturing* phase always represents the most impactful phase in a wind power plant life cycle. Typically, in the manufacturing stage are included the processes of (i) acquisition of raw materials (ii) materials transformation (refining) (iii) components production and assembly. These processes refer not only to the wind turbines but also to any other material or auxiliary material that is used to complete the wind power plant construction, which usually involves the building of the turbines foundations, the transformer substation, the cable ducts, the platforms, the internal and external roads and the electric power transmission system. Regarding the first of the three processes, especially in relation to the turbines, all the authors referred to the mass of the raw materials using the one of the corresponding refined materials. This problem is very common in wind power plant LCA studies, as discussed by Davidsson et al. (2012), since the real numbers concerning the unprocessed materials then used in the manufacturing processes characterizing the wind turbines components are often unknown due to confidentiality. Considering that each manufacturing process has its own material efficiency, the raw materials mass is always higher than the refined one and involves a primary energy consumption and GHGs emissions that are bigger than expected. To examine the effects of this issue, Xu et al. (2018) performed a sensitivity analysis on the mass of raw materials, discovering that the carbon footprint (expressed

in terms of Global Warming Potential) and the fossil primary energy consumption are not sensibly influenced by these variations, if not in large percentage amounts (Xu et al., 2018).

Another problem encountered during the comparison of various studies is represented by the lack of transparency in reporting the type of some materials contained in the LCI, especially steels. Since the impact of the production of these materials is strongly dependent on the type of alloy used, results can be a lot affected by the choice of the database that refers to that specific alloy, hence clarifying this aspect is quite important. This issue may also be caused by the difficulties in retrieving or showing to the public data regarding the materials used in the power plant considering that, as said before, confidentiality often covers them.

One last observation about the raw materials acquisition is that, apart from the turbines' foundations, only a few of the reviewed studies accounted for the materials and auxiliary materials used in the wind power plant other than those used in wind turbines. Even though this simplifies a lot the analysis, it has been proven by other authors (and by the present study, as it will be shown) that their contribute is not negligible when assessing the carbon footprint and the primary energy consumption of the system. More in details, Bonou et al. (2016), Ardente et al. (2008) and Alsaleh and Sattler (2019) were the only ones that included in some ways in their studies the impacts of the extraction and consequently the transformation of the materials used for the plant's civil works, as well as for the electric power transmission. Ardente et al. (2008) pointed out that 30% of the total primary energy consumption of the system has been employed for the building works, which included the platforms, roads and paths, foundations, cable trenches, power cables and the transformer room (Ardente et al., 2018). Taking out the foundations, which represent almost 50% of this 30%, the remaining 15% refers to all the other civil works activities and the electric power transmission system. Subtracting the fuel consumption of the building machines, which usually accounts for a small percentage as will be shown in the present study, it can be stated that around 10% of the total primary energy consumption derives from the materials and their transformation before installation, value whose neglection can't be done with ease.

Evaluating the impacts of the transformation of each material, most of the authors agree on the fact that the process used to produce the material which constitutes the wind turbine blades (usually *prepreg*) is the most energy intensive one, as well as for the GHGs emissions, on specific basis. On total basis, instead, the impact of the material is obviously also dependent on its mass percentage in each wind power plant's component. In all the considered studies except one (Martínez et al. (2009)), steel, cast iron and stainless steel were the most impactful in relation to the indicators of GWP and cumulative energy demand (*prepreg* for Martínez et al. (2009)). This result is supported by the fact that the heaviest parts of the turbines, i.e. the tower and the nacelle, present a high share of ferrous materials.

In offshore power plants, compared to onshore ones, a large amount of steel is also used for the turbines' foundations, the power cables and the offshore transformer stations (OTM), which normally determines higher environmental impacts compared to onshore plants. While for onshore plants the component whose production determines the highest impact in every study reviewed except one is the turbine's tower (the blades in the case of Martínez et al. (2009)), for the offshore plants its place is taken by the turbines' foundations, due to the huge amounts of steel required to build them. Kaldellis and Apostolou (2017) in their review of 26 onshore and offshore wind power plants highlighted that, although the contribution of the wind turbines on the total impacts is the largest for onshore plants, accounting on average for 70% of the overall impacts, in offshore plants this contribution is reduced to 25-40%, since the foundations alone typically account for 25-45% (Kaldellis and Apostolou, 2017). Moreover, the construction of the electric power transmission (undersea cables and offshore transformer modules) is way more expensive compared to the onshore one (Kaldellis and Apostolou, 2017). A clear example of the differences between these two types of systems is underlined by Bonou et al. (2016), whose work compares 2 onshore and 2 offshore monopile wind power plants. On average, the contribution to the Climate Change indicator represented by the foundations' materials for the offshore plants is greater than the one determined by the tower for the onshore plants (29% vs 25%), while the tower itself for the offshore plants accounts for only 10% (Bonou et al., 2016).

5.1.2. Transportation phase

The *transportation* phase, on the other hand, provides way less uniform results among each study. This is caused by the high variability of scenarios in which the supply chain for a wind power plant can operate. Specifically, it was possible to highlight that the impact of transportation depends mainly on 3 factors: (i) distances between the wind turbines components' manufacturers and the wind power plant (ii) the type of mean of transport (iii) the weight of the components/materials transported.

Oebels and Pacca (2013) compared the environmental burdens of the transportation phase concerning a Brazilian power plant with the one related to the wind farm assessed by Vestas for the 2-MW V80 wind turbine product. Despite the distances covered by components, materials and equipment were significantly different, the transportation impacts towards the system's GWP resulted be far from behaving in a proportional way. For the Brazilian power plant, the total distance covered was 125,000 Km, with more than 70,000 Km of road transports, while in the comparison study it was only 700 km covered by trucks and trains (Oebels and Pacca, 2013). According to the authors, this inconsistency is caused by the technology of the transportation processes used by Vestas, which appears to be less efficient. Moreover, a significant fraction of the transports for the Brazilian plant was made by boat, which has been shown to be more efficient by several authors.

Alsaleh and Sattler (2019), for example, showed that the GWP of US trucks used to cover 656 Km of road transport was higher than the one related to the transoceanic ship transport, used to cover 8325 Km (Alsaleh and Sattler, 2019). Tremeac and Meunier (2009) also suggest that boat or train transport are preferred to truck transport for efficiency reasons (Tremeac and Meunier, 2009). Overall, it's not so rare that even though the distances involved in the transportation phase are significantly lower in one case compared to another, the impacts associated are still higher, therefore much attention should be put also in the choice of the type of mean of transport in addition to the minimization of the distances.

5.1.3. Installation phase

The *installation* phase of a wind power plant normally includes (i) the civil works inside the site, including the construction of the turbines' foundations, the platforms, cable trenches, internal roads and the transformer substation, (ii) the civil works outside the site, usually modifications to the external viability to make feasible the transport of the wind turbines parts (iii) the erection of the wind turbines and the electric power transmission system to the grid.

This phase, although included in most of the reviewed LCAs, is often characterized by incompleteness and assumptions, especially regarding the civil works. Some studies considered only the construction of the turbines foundations and only from a manufacturing point of view (Guezuraga et al. (2012), Al-Behadili and El-Osta (2015), Zhuo et al. (2023), Martínez et al. (2009)), without including any equipment or fuel used by building machines, therefore ignoring the installations burdens. More in details, Bonou et al. (2016), Ardente et al. (2008) and Alsaleh and Sattler (2019) were the only ones that included in their studies both the materials (manufacturing stage) and equipment + fuel use (installation stage) about all the civil works associated to the wind plant construction and turbines installation, relying on primary data given by suppliers, operators and engineers. Gomaa et al. (2019), Chipindula et al. (2018) (for the onshore installations) and Schreiber et al. (2019) estimated the fuel consumption of the building machines, therefore accounting for the installation phase, but excluding the acquisition and transport of the materials required by many of the civil works activities. Tremeac and Meunier (2009) estimated the installation's impacts using literature data. All the other authors included in their studies just the inventory concerning the turbines' foundations manufacturing, sometimes even without considering the fuel consumption of the building machines needed for their construction.

Overall, it's not so easy to put in evidence a mean contribution of the installation phase, since a lot of authors merged the impacts of this phase with the one of the manufacturing phase. However, relying on the data available, it's possible to outline the main trends for the different systems: first, offshore power plants seem to have the biggest contribution for the installation phase compared to onshore ones. Bonou et al.

(2016) obtained that this phase can count up to 11% of the total climate change contribution, while for the onshore this fraction is limited to a bit more than 5% (Bonou et al., 2016). This difference is due to the higher energy required to perform the foundation setting and cables laying, which leads to higher GHGs emissions, but also to the use of vessels, not required in onshore plants (Bonou et al., 2016). A similar conclusion can be obtained using the work of Chipindula et al. (2018) by comparing the total fuel consumption used in the construction of the onshore and offshore plants analyzed. In the case of the 2 offshore plants, the energy required by the boats in terms of liters of fuel is the dominant, especially for the shallow-water power plant, counting alone more than 10 times the one required by all the building machines for the onshore plant investigated by the authors (Chipindula et al., 2018).

5.1.4. Operation and Maintenance phase

The *Operation and Maintenance (O&M)* phase for a wind power plant covers the longest fraction of its life cycle and it's associated to the actual use of the system for producing electrical power. The "Operation" part is related to the execution of those activities that are planned day by day, such as personnel arrangements, turbine monitoring, responding to failure occurrences and so on. The "Maintenance" part, instead, divides in two typologies: (i) Scheduled maintenance: includes those activities that have the objective of restoring or improving the operational state of the components or systems that normally have defined useful life, typically much lower than the expected life of the turbine/power plant (Walford, 2006). Some examples includes periodic inspections or substitutions of components, lubricant oils replacements and sensors tuning (Walford, 2006). (ii) Unscheduled maintenance: includes the repairing or the substitution of components/systems whose failure wasn't previously expected (Walford, 2006).

In the reviewed LCA studies, some authors omitted completely or partially this phase, assuming that its influence on the environmental impacts would have been negligible or simply because there were no data available. Regarding those who accounted for the O&M phase, since typically the turbines monitoring and operation (starting, stopping, regulation, resetting) are managed through the SCADA (Supervisory Control and Data Acquisition) system, which is fully automated and operates from a central station (Walford, 2006), it was common the assumption of neglecting this contribution or in alternative considering its effect reducing by a small percentage the net energy output produced by the wind turbines, which represents the consumption of the SCADA system itself.

The biggest contributions of this phase are related to the maintenance part. Scheduled maintenance activities generally determine more limited impacts compared to the unscheduled ones, given that in all the cases turbine dismounting is not required and the materials used, together with the energy consumption of the activities, are more limited. Moreover, the mean time to recovery after the interruption (if there is any) of

the production is also shorter, hence the loss of energy production associated with the maintenance is lower.

On the contrary, unscheduled maintenance typically involves more time and resources to be performed, depending on the occurrence. This type of interventions often implies turbines stoppage for longer time and, in the worst cases, even the turbines disassembly, especially when major components or systems need to be replaced after an unexpected failure. Replacing major components of the wind turbines represents a critical event in terms of environmental impacts (and cost), since the largest contribution in the primary energy consumption and carbon footprint during the wind power plant life cycle comes from their production. In addition, if these components aren't produced by local manufacturers, i.e. transport is relevant, the burdens are even higher and the mean time to recovery may be a lot more extended. Regarding unscheduled maintenance, all the authors, given the importance of the just discussed issue, included in their study the impacts of major components critical failures, whose frequencies have been estimated either through statistical databases or other literature sources consultation. Specifically, the assumptions in relation to scheduled and unscheduled maintenance for each reviewed LCA study are reported in Table A.3.

Since each power plant has to work in different operating conditions depending on its location and each model of turbine has also different requirement in terms of recommended periodical maintenance activities, the scheduled maintenance modeling has been done in unique ways. Nevertheless, regular inspections and lubricants and oils substitutions were included by almost all the authors, even though in different amounts. Many of them also included the distances covered by the personnel or the materials to reach the power plant location, as well as the vehicle used.

For unscheduled maintenance, instead, the differences were much bigger. In general, it was supposed that gearless turbines present lower failure rates compared to geared turbines, since the gearbox is typically a critical component in terms of reliability given that it contains several mechanical parts subjected to continuous wear and high loads. For this reason, many LCA studies included in the unscheduled maintenance activities the substitution of part or the entire gearbox after a certain number of years. About the other major turbine's components, instead, a wide spectrum of approaches has been highlighted, more or less conservative. For the turbine's blades, while some authors assumed no substitution during the lifetime of the plant, others supposed a number up to 3 per turbine (Zhuo et al., 2023). For the generator, instead, the range goes from zero to an entire component substitution per turbine (Martínez et al., 2009). For the other nacelle's components, when accounted for, typically it has been assumed the substitution of 15% of them. Only Alsaleh and Sattler (2019) assumed the replacement of the brake system and the control system, every 5 and 10 years, respectively (Alsaleh and Sattler, 2019). Although the exact numerical contribution of the O&M phase wasn't available in several LCA studies regarding the primary energy consumption and/or the carbon footprint, it has been possible to underline that an important role is

covered by the number and the type of major turbine components that will effectively be replaced during the lifetime of the power plant. As also demonstrated by this study, the supply of additional turbine's components is much more impactful than what is normally done during the scheduled maintenance or the operations, since typically they are very heavy and made of material whose production is highly energy intensive. This is most likely the reason for which in the work of Zhuo et al. (2023) the O&M phase accounts for more than 15% of the total Global Warming Potential, while in the others it usually stays around values lower than a half of this one (Zhuo et al., 2023). In fact, Zhuo et al. assumed the highest replacement rate of the wind turbine's major components among all the LCA studies reviewed.

Since the real evolution of the unscheduled maintenance activities is strongly dependent on statistical phenomena which are related to the manufacturing techniques used to produce the turbine's components, their operative conditions and how their degradation is delayed (also through scheduled maintenance activities), it's clear that the impacts estimated by each author for this life cycle stage will always have a certain degree of uncertainty, therefore a proper sensitivity analysis should be conducted to be sure of the consistency of the results.

5.1.5. End-of-life phase

In 2022 Europe decommissioned 454 MW of wind capacity, while it's estimated that about 5.6 GW will be decommissioned in the 5 years following (WindEurope, 2023). The number of turbines reaching their end-of-life stage is expected to increase a lot in the future (Gennitsaris et al., 2023). Given the established regulatory framework in Europe aimed to achieve the challenging objectives for the safeguard of the environment, finding clean and efficient ways to manage wind turbine's decommissioning is essential.

It's widely accepted that the recycling rate of a wind turbine, excluding its foundation, ranges between 80 and 90% (Gennitsaris et al., 2023). Such high values are possible due to the large presence of metallic materials in the wind turbines components, such as steel, cast iron, copper, aluminium and others. The efficiency of the recycling processes of metals typically is in the order of 90%, while the remaining 10% is disposed in landfill. These materials are very easy to separate and in general they get new life through casting processes after undergoing certain mechanical pre-treatments like sorting, grinding and so on.

Although metals can be considered very close to circularity, the same can't be said for the turbine's foundation, which represents a high fraction of the total mass of the turbine. Nowadays, 3 possible scenarios are followed when decommissioning a wind power plant regarding the turbines foundations: (i) they are left in situ (ii) disposed in landfills (iii) recovered to be transformed in secondary raw material, in particular inert aggregates which can be used in replacement of new mined resources. According to

literature, the recovery of the foundations can reduce not only resource depletion (then contributing to circularity) but also non-renewable energy consumption, as well as GHGs emissions. The main issues that make complex concrete recovery are related to the fact that the environmental impacts associated to transportation of waste concrete to the recovery centers are typically high due to the long distances between them and the site, but also for a matter of costs: the production cost of concrete starting from virgin materials is normally low, hence the interest in recycling waste concrete is not so high even if in general the employed technologies are not expensive (Gennitsaris et al., 2023). Moreover, the recycling rate of the mechanical process used to transform the waste concrete in aggregates depends on the type of process and the type of concrete. The inert aggregates used in concrete production need to meet proper particle size dimensions, but the recycling process always produces a certain fraction of powder, which is not suitable to be used in aggregates. The amount of powder generated is related to the 2 factors just mentioned. Due to this issue, the recycling rate of waste concrete is usually lower than the one achievable by metals recycling (De Brito and Agrela, 2019).

The hardest challenge that characterizes the end-of-life environmental footprint of a wind turbine is for sure how to manage the blades' waste material. Typically, a wind turbine blade can be made of several materials that together form a composite, including thermoplastic coatings, glass fibers, carbon fibers, balsa wood, adhesives (Mishnaevsky, 2021). Right now, the most common ways to manage the blades end-of-life is through landfill disposal or incineration. Nevertheless, it's expected that landfill disposal of composite materials will be severely reduced or banned in the next years by the EU, in order to reach the goals set for the circular economy by 2030. On top of that, blades incineration also determines negative environmental effects, not only due to GHGs emissions but also ash formation (Gennitsaris et al., 2023). The amount of blade waste is forecasted to reach 325,000 tons in 2050 (Lichtenegger et al., 2020), therefore it's crucial to follow new guidelines with the aim of reducing as much as possible the use of landfills and incineration while promoting material recycling and recovery through eco-compatible solutions.

Several possibilities have been discussed in the last years. The first one, which is the simplest, consists in delaying the degradation of the blades in order to increase their lifetime, hence delaying also the production of the waste (Mishnaevsky, 2021). This can be done through approaches which include reparations, better maintenance, refurbishment and reuse (Mishnaevsky, 2021). It's important to say that reusing the blades is not limited to the same application as before. Other types of applications suggested are for architecture purposes, bus shelters, city benches and more, but obviously in these cases additional requirements and testing are needed (Mishnaevsky, 2021).

Speaking about recycling processes, they can be classified as mechanical, thermal or chemical. Mechanical processes are performed by using only mechanical stresses on

the material. The most used mechanical processes nowadays involve shredding, crushing, or milling the composite material (Mishnaevsky, 2021). By using these processes, the material is transformed into small pieces - whose dimensions depend on the process chosen - which can be used as reinforcement material in a lot of applications, for example in cement production (Mishnaevsky, 2021). Mechanical recycling processes are typically cheap, but in general can't easily allow material separation, which is done instead by thermal and chemical processes (Mishnaevsky, 2021).

Thermal recycling processes involve material's transformation using heat. Conventional pyrolysis and microwave pyrolysis are the most applied thermal recycling processes (Gennitsaris et al., 2023). Pyrolysis is conducted by heating the material to temperatures in the range of 450-700 °C in an oxygen-free environment. In these conditions, the matrix of the composite material is transformed into gas, oil and char (with different fractions), while the fibers are not subjected to any reaction and can be separated at the end of the process (Mishnaevsky, 2021). The products of the pyrolysis reactions have a high energy content that can be exploited for heating applications or even to feed the process itself, since it's endothermic. Their heating values range from 13.9 to 37.7 $\frac{MJ}{m^3}$ for pyrolytic gas and 33.6 to 37 $\frac{MJ}{m^3}$ for pyrolytic oil, depending on the reactor typology and process conditions used (Gennitsaris et al., 2023). Gennitsaris et al. (2023) showed that while conventional pyrolysis results to be quite inefficient due to its high energy requirements estimated at 30 $\frac{MJ}{Kg}$, microwave pyrolysis could determine large reductions in fossil and nuclear fuels consumption as well as moderate reduction in GHGs emissions requiring only 10 $\frac{MJ}{Kg}$, assuming that the avoided energy consumption for both technologies would be equal to the energy needed for the production of virgin glass fiber reinforced polymer (22.5 $\frac{MJ}{Kg}$) (Gennitsaris et al., 2023).

Chemical recycling processes are able to obtain the separation between matrix and fibers by using specific chemical solutions, e.g. supercritical fluids, benzyl alcohol, catalytic solutions, which decompose the polymer maintaining the physical properties of the fibers (Mishnaevsky, 2021). These processes can achieve cleaner and stronger fibers compared to thermal processes due to the lower temperatures involved, therefore resulting in being more promising (Mishnaevsky, 2021). Recycled fibers can be used, analogously to crushed composites through mechanical processes, in concrete production applications, particleboard, as reinforcement in multilayer panels and more (Mishnaevsky, 2021).

Despite the potential of the just described recycling solutions, it's undeniable that they have some drawbacks, not only caused by the variability of quality, size and resistance of the produced fibers, but also for the high cost of the processes themselves, causing slow progresses in the implementation of fibers recycling processes (Mishnaevsky,

2021). A definitive solution in blade waste management could be the development of fully recyclable and sustainable blades to be implemented in the next generation wind turbines. Several options have been already tested by using thermoplastic polymers instead of thermosets (typically epoxy or polyesters, which are non-recyclable materials) as matrix that are easy to remove from the composite, allowing also to reuse the fibers (Mishnaevsky, 2021). On the other hand, bio-based composites made of natural components have been used for small and medium-sized turbines, but for now they don't seem to be suitable for large scale applications, due to their poor mechanical properties (Mishnaevsky, 2021).

In such complex and uncertain context, it should not be surprising that the end-of-life stage of a wind power plant often is the most incomplete or omitted part in an LCA study. Considering the reviewed works, 4 out of 14 didn't include the end-of-life phase, as shown in Table A.2. Among the studies that included this stage, it was possible to highlight some common trends:

1. The assumed recycling rates for waste metallic materials coming from the wind power plants are very high, typically equal or greater than 85%. Plastic materials, instead, are mainly expected to be disposed in landfill.

2. The waste concrete deriving from the turbines' foundations and other civil works performed in the plant is expected either to be left in situ or disposed in landfill. Only Bonou et al. (2016) assumed recycling, but for only 50% of the total mass (Bonou et al., 2016).

3. The waste blades are expected either to be incinerated or disposed in landfill. Only Tremeac and Meunier (2009) and Ardente et al. (2008) assumed recycling for 98% and 20% of the mass, respectively, but without specifying the type of recycling process used.

4. The dismantling phase of the power plant has been modeled similarly to the installation phase.

5. The incineration and the recycling of waste materials have been treated as credit for the system by almost all the authors. Only Ardente et al. (2008) and Schreiber et al. (2019) didn't give any credit to the system as result of the end-of-life phase.

When a waste material is recycled or incinerated, it can be converted into secondary raw material or into heat/energy, respectively. These useful effects generated by waste management can be modeled in different ways when dealing with an LCA study. Generally, the problem to solve in this case is how to assign the credit resulting from the recovery of the materials. The two most used approaches in literature are the 100-0 approach (also known as "cut-off") and the 0-100 approach (also known as "substitution approach"). When using the 100-0 approach, the main target is promoting the use of a recycled material that otherwise would be treated as waste (Tagliabue, 2015). For this reason, the credit resulting from the reuse of the material is

allocated entirely to the system that will effectively use the material, while no credit is given to the system upstream (Tagliabue, 2015). When using the 0-100 approach, instead, the emphasis is put on avoiding the input of additional virgin material on the market, therefore it's rewarded the system that generates the secondary raw material but not the utilizer (Tagliabue, 2015). The entity of the credit itself will then depend on what is going to be the avoided product after the recycling. Therefore, the choice of the first or the latter is not only determined by the goal of the LCA study, but also on which aspect of the recycling the author wants to value (Tagliabue, 2015).

When giving to the system analyzed recycling credits, it has been demonstrated by the reviewed studies that the results concerning its environmental impacts can change significantly. This is true especially thanks to the effect of metals recycling, in particular steel, since they represent the most impactful resource employed in any wind power plant due to the combination of their mass fraction and the energy intensity of their manufacturing processes. Moreover, the higher the recycling rate of the materials, the higher is the benefit for the system. As a result of the end-of-life phase for the wind power plants analyzed, all the related impacts regarding the primary energy consumption and the GHGs emissions were moderately or considerably negative when assigning credits to the system, thus reducing both energy intensity and GHG intensity. This aspect should not be underestimated when comparing two LCA studies of the same type of product but with different end-of-life approaches since the reduction of the impacts due to the effects of the credits can be even higher than 30-40% of the total.

6 Goal and scope definition, data collection and life cycle inventory

The life cycle assessment of the Iurefalco wind power plant has been conducted according to the ISO 14040:2006 and ISO 14044:2006 methodological framework, hence the process flow of the entire study follows the approach described in the above-mentioned standards, as illustrated in Chapter 4.

6.1. Goal and scope definition

The goal of the study is evaluating the environmental sustainability of a renewable power plant for electricity generation installed in Italy, specifically an onshore wind farm, focusing on its effects on the global energy balance and carbon footprint. The main purpose of renewable power plants is generating power without the exploitation of fossil sources of energy with the aim of promoting energy independence, lowering GHGs emissions, enhancing public health and meeting climate targets. However, to make this generation possible, their entire life cycle is characterized by the unavoidable need for fossil resources, which determines in any case a non-null environmental impact. For this reason, the study aims to give a quantitative estimation of these impacts to effectively understand the entity of the advantages that this technology is capable to give compared to the traditional fossil fuel-based ones while achieving the same output. Moreover, a further investigation will be conducted to highlight the most critical elements of the plant life cycle from the environmental point of view in order to discuss possible issues and potential improvements that may be made in the future.

6.1.1. Product system, functional unit and allocation procedures definition

The main components that characterize the physical system of the wind power plant consist of:

- wind turbines (and their foundations),
- platforms,

- internal roads,
- cable trenches,
- electric power transmission system and
- transformer substation.

All these elements have been preliminarily described along with the role they assume in Chapter 3. Wind power plants use the kinetic energy extracted from the wind to produce electricity, which represents the only product of the system. Since the aim of this study is comparing the impacts associated to the plant's production of electricity with other technologies (renewable or traditional) that have the same type of output, the functional unit of the assessment has been chosen as "the delivery of 1 GWh of electricity to the national grid". This means that the impacts related to all the power plants included in the comparison will be referred to the production of the same amount of energy exiting the system (i.e. 1 GWhel). For the main scenario, calculations will be done supposing that the wind power plant will deliver to the grid, over each year of its expected life, an amount of electricity equal to net production occurred in the first year of operation - corresponding to 36.2656 GWhel - for a total of 906.6407 GWhel.

As already explained in Chapter 5, this type of functional unit is the most diffused among LCAs that deal with electricity generation technologies. However, although this choice allows relatively simple comparison procedures between them, it should be always clear that non-programmable renewable and traditional technologies can hardly be considered as delivering the exact same type of service, since they are normally used to cover different roles in the management of the grid balance. Specifically, traditional power plants, which are programmable by definition, usually cover the energy demand only when non-programmable renewables like solar and wind power plants aren't able to do it due to the unavailability of the power source or when the renewable production alone is not sufficient to completely satisfy it. Non-programmable renewables, instead, usually cover the demand whenever they can if allowed by the grid load, therefore they are limited only by the actual source availability (Turconi et al., 2013). This behavior is more evident with increasing share of non-programmable renewables in a certain region.

The system object of the LCA includes all the phases related to the wind power plant life cycle starting from the raw materials acquisition to its end-of-life (i.e. "cradle-to-grave" assessment), since with the goal of the study it's planned to obtain a complete eco-profile of the plant to evaluate its actual impact on the environment without neglecting any contribution. A schematic representation of the system is depicted in Figure 6.1. It's important to note that each phase may involve not only the 6 main

components making up the physical system of the power plant, but also many other auxiliary components/systems affected by the plant life cycle. More in details:

- In *row materials acquisition* are included all the unit processes that refer to the row materials extraction, processing and transport to the place where they will be transformed into semi-finished products or finished products. This applies for example to the wind turbines, the transformer substation, as well as the other main components of the power plant, but also to those auxiliary materials that are required to make possible the special transport of the major parts of the wind turbine (e.g. the blades) to the site location, in particular the inert materials required for the road enlargements substrates, the asphalt, the concrete used to rebuild the dismantled curbs and so on.

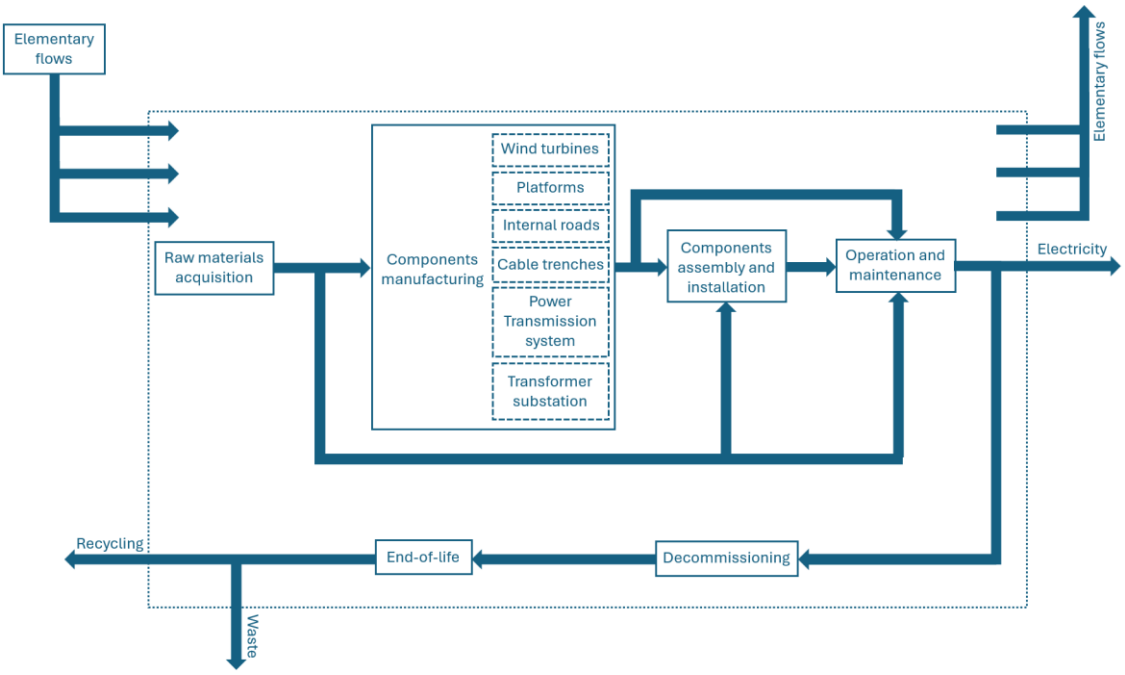

Figure 6.1: Product system of the LCA.

- In *components manufacturing* are included all the unit processes that refer to the transformation of raw materials into finished products, together with their transport to the place where they will be employed. Several components used in the power plant, including all the turbines components except the tower segments, are produced in regions outside of Italy. For this reason, both road transport and sea transport have been included.

- In *components assembly and installation* are included all the unit processes that refer to the assembly of the components transported to the power plant site, as well as their installation. This applies for example to the civil works that involve

the building of the turbines foundations, the construction of the transformer substation, the excavation and the refill of the cable trenches, but also the works required for the external roads adjustments. The equipment and the hours worked by each building machine during this phase have been obtained through the consultation of the daily reports written during the construction phase of the power plant.

- In *operation and maintenance (O&M)* are included all the unit processes that refer to the period of time that goes from the first start-up of the wind power plant to its decommissioning phase. The plant's expected life in the case of the present study has been set to 25 years. During the plant operation, periodical inspections as well as other scheduled maintenance activities for the wind turbines will be carried out, but clearly a certain number of unscheduled maintenance activities must be predicted, especially regarding critical failures of major turbines components. For this purpose, typical failure rates estimated for the major components of a large group of European wind turbines have been retrieved from literature sources and then linked to the turbines involved in the power plant object of the study. Considering that this topic is quite uncertain, further evaluations will be conducted through sensitivity analysis to highlight the reliability of the results.

- In the *decommissioning* phase, wind turbines are expected to be dismantled together with the power transmission system (MV and HV cables), the electro-mechanical system of the transformer substation and part of its sub-systems (mainly composed of electronic components). The turbines foundations, instead, are expected to be left on site. Moreover, a large part of the site will be restored to its natural condition.

- In the *end-of-life* phase, waste materials deriving from the decommissioning phase are expected to be either landfilled, incinerated or recycled depending on the type of material, its application and status after 25 years of operation. The analysis conducted in the present study focused on the forecasted materials' destinations contained in the available documentation of the power plant.

All the life cycle phases just presented with the respective unit processes are characterized by material and energy flows in input and output that will be collected in the LCI of the assessment and then evaluated in terms of environmental impacts using the selected LCIA methodologies. Since the system is single product, the allocation method simply consists in the attribution of all the material and energy fluxes to the production of electricity, normalized using the above-mentioned functional unit.

6.1.2. Choice of the impact assessments methods

The choice of the impact assessment methods, as well as the environmental indicators, has been made according to the goal of the study related to a better understanding of the impacts involved between the system and the environment concerning energy balance and carbon footprint. Specifically, it is addressed the level of renewability and sustainability that characterize both aspects. For the energy balance, the main targets are:

1. The evaluation of the fraction represented by the primary energy consumption over the entire life cycle of the wind power plant in respect to the total electric energy delivered to the national grid.

2. The evaluation of the time required by the wind power plant to fully compensate, with the delivered electric energy, the primary energy required during its life cycle.

3. The evaluation of the share of total primary energy consumption represented by fossil and renewable resources, respectively.

On the other hand, for carbon footprint, the main targets are:

1. The evaluation of the kilograms of CO2-equivalent emitted over the wind power plant life cycle per kWh of electric energy delivered to the grid that would cause the same environmental damage in terms of global warming of the total mass of the real GHGs emitted.

2. The evaluation of the time required by the wind power plant to fully compensate, with the delivered electric energy, the kilograms of CO2-equivalent otherwise emitted by a representative fossil-fired technology providing the same type of service.

The calculation of the impacts related to each category has been performed using the LCA software SimaPro V9.2. In SimaPro, it's possible to define a virtual model of the system's life cycle phases relying on the processes contained in the databases available on the platform or by defining custom processes based on the known data. Since each process consists in several unit processes based on the exchange of energy and/or material flows with the environment, SimaPro evaluates the relative impacts depending on the specific impact assessment methods selected. For the present study, the Ecoinvent V3.7.1 database was used to define most of the processes involved in the system. The software offers a certain number of impact assessment methods that can be used to reach the targets defining the goal of the study. Specifically, for the energy balance and carbon footprint, the most interesting result to be the Cumulative Energy Demand (CED) and the Intergovernmental Panel on Climate Change (IPCC) 2021 methods.

The CED method evaluates the primary energy consumption related to 5 impact categories (PRé Sustainability, 2022):

- Non renewable, fossil;
- Non renewable, nuclear;
- Renewable, biomass;
- Renewable, wind, solar, geothermal;
- Renewable, water.

The primary energy consumption related to the use of fuels (fossil or renewable) is calculated considering the energy content based on their heating value. In the CED standard, the type of heating value employed in the calculations is the HHV, but SimaPro also offer a version of the CED that uses the LHV (PRé Sustainability, 2022). Overall, this method allows both the estimation of the total primary energy consumption and how it is shared between each energy source. By knowing also the annual production of the power plant, it's possible to achieve all the target set for the energy balance impact assessment. Specifically, the first and the second target will be met through the calculation of the EPBT and EROI indexes, given the total primary energy consumption and the annual/total electricity production, while the third target will be met computing the share of the 5 impact categories results of the CED in respect to the total primary consumption.

The IPCC 2021 method evaluates the damage caused by the carbon footprint of the system by using 2 characterization factors: the Global Warming Potential (GWP) or the Global Temperature Potential (GTP). The GWP quantifies how much the GHGs emitted in the atmosphere over the system life cycle heat the environment. This is done comparing the infrared radiative forcing of the total mass of each GHG with the equivalent mass of CO2 that would cause the same effect over a certain time horizon (PRé Sustainability, 2022). Similarly, the GTP quantifies the temperature variation caused by the emission of these GHGs with the equivalent effect caused by a certain mass of CO2 (PRé Sustainability, 2022). The impacts resulting from these two evaluations are, for these reasons, expressed in form of kg of CO2 equivalent. Moreover, the total mass of CO2 equivalent can be shown as subdivided 3 impact categories (PRé Sustainability, 2022):

- Fossil emissions;
- Biogenic emissions;
- Land transformation emissions.

While the choice between the 2 characterization factors has small relevance in the achievement of the targets set for the carbon footprint of the system, given that both

GWP and GTP assess the effects of the system on the global warming (although in different ways), for the present study the GWP was the preferred one considering that it gives the highest potential of comparison with other LCAs concerning electricity generation technologies, in which this characterization factor is the most diffused when dealing with global warming impacts. Moreover, since during the LCI phase will be included data from other LCAs regarding elements of the transformer substation whose inventory wasn't possible to be retrieved, the choice has been also driven by the fact that these data are expressed in terms of GWP in all the cases. A similar evaluation was done also for the CED: the data concerning the primary energy consumption included in these LCAs refer to the LHV deriving from renewable and fossil resources, therefore the CED LHV version should be the preferred one. However, given that the majority of the LCA studies dealing with electricity generation technologies use the standard CED (based on the HHV), results will be expressed with both versions by properly adjusting the contribution associated with the LHV data.

About the temporal extension of the GWP, in SimaPro are included horizons of 20, 100 and 500 years (PRé Sustainability, 2022). Usually, 100 years is the preferred version since GWP100 is the recommended factor in the Global Guidance for Life Cycle Impact Assessment Indicators and Methods (GLAM) (PRé Sustainability, 2022), not to mention that the GWP100 is also the most used factor among the comparison studies and in all the LCAs used in the inventory phase. Lastly, in a similar way compared to the case of the energy balance, the second target concerning the carbon footprint of the system will be met through the calculation of the CPBT index once the overall damage caused by the GHGs emission is known from the IPCC GWP100 method.

6.1.3. End-of-life modeling

One of the major points of discussion in the LCA methodology is how to deal with the end-of-life of the waste materials generated by the system. In general, waste can be managed through landfill disposal, incineration, reusing or recycling. While in the case of landfill disposal the waste loses any possible residual value, in all the other cases it can represent a resource. For example, when incinerating a waste, the heat released by the combustion may be used for various purposes, including energy generation, district heating, and much more. When reusing or recycling waste materials or components, instead, the impacts related to the introduction of new virgin materials and possibly the energy consumption related to given manufacturing processes is avoided, since these items already embedded those impacts on the environment.

The main problem is then how to manage the value generated to an item that otherwise would be worthless. As introduced in Chapter 5, this problem is typically solved using two methodologies, the 100-0 and the 0-100 approach, depending on which aspect the emphasis of the recycling or reuse of the material is put on. Eventually, a hybrid 50-50 approach can also be used in case equal importance is given in crediting both the

upstream and downstream systems that deal with the recovered item. Currently, a standard approach suggested for any LCA study does not exist, since the decision depends mostly on the goal and scope of the analysis. Moreover, each method has pros and cons when compared to the other. In the case of the present study, the 100-0 approach was chosen as end-of-life modeling approach, hence the recycling credit will be assigned entirely to the downstream system that recycles the material after its first use. This choice was justified considering that the 100-0 approach:

- Allows a more conservative, simple, direct estimation of environmental impacts associated with the product's life cycle (Ekvall et al., 2020).

- Doesn't depend on the specific context, hence determines generalizable results (Ekvall et al., 2020).

- Includes all stages of the product life cycle without risk of burdens double counting and ensuring symmetry of material flows (Ekvall et al., 2020).

- It's structured in a way such that its parameters can be influenced by decisions made by policymakers dealing with the product life cycle (Ekvall et al., 2020).

It's worth noting that just like waste recycling does not determine any benefit for the system that generates the waste itself, for the same reason if this system uses recycled products, they will be available burden-free as result of the effects of the recycling credit. That's why this approach is often referred to as "cut-off" approach.

The main challenge concerning the 100-0 approach is defining the boundaries between the upstream and downstream system, since they determine which processes should be included for the computation of the environmental impacts. In this case, the approach suggested by the General Programme Instructions (GPI) for the International EPD System was used, which states that *"waste processing shall be assigned to the product system that generates the waste until the end-of-waste state is reached"* (EPD International, 2021). The end-of-waste state is fulfilled when:

- The recovered item can be employed for specific applications (EPD International, 2021).

- The recovered item has a positive economic value and can be placed in an existing market (EPD International, 2021).

- The recovered item properties meet the standards set by the legislation (EPD International, 2021).

- Using the recovered item does not determine detrimental effects on the environment and on human health (EPD International, 2021).

This principle applies differently in function of the type of waste disposal. When the waste item is incinerated with energy recovery (e.g. for steam generation), the end-of-waste state is fulfilled after the incineration of the waste itself, therefore the corresponding environmental burdens should be entirely accounted for the system that generated the waste, from the transport to the facility to the combustion and consequent disposal of the slurry (EPD International, 2021). When the waste item is incinerated to be used as secondary fuel (e.g. by co-incinerators), instead, the end-of-waste state is fulfilled before the incineration of the waste itself, hence the environmental burdens deriving from the transformations that the waste undergoes after the transport to the incinerator should be excluded from the system (EPD International, 2021). When the waste item is landfilled or incinerated without energy recovery, the end-of-waste state is never reached during the entire waste disposal process, hence the environmental impacts should be entirely accounted for the system that generated the waste (EPD International, 2021). Recycled or reused items will affect the upstream system only for those processes needed for the preparation of the waste to the actual recycling/reusing operations. Specifically, sorting procedures, pre-treatments and transport requirements prior reaching the recycling facility gate should be considered. The benefits associated with reuse, recycling and eventually with the energy recovery deriving from incineration should be credited in any case to the downstream system, according to what has been outlined about the 100-0 approach (EPD International, 2021).

6.1.4. Data quality

Data concerning each stage of the wind power plant life cycle have been retrieved, whenever possible, from the available documentation dealing with the design phase of the plant provided by the EPC Contractor, which represents the most reliable and accurate source used for the inventory definition. Scientific literature works and, more rarely, estimation based on average data were used, instead, in case the above-mentioned documentation resulted insufficient to cover the aspects required by the goal and scope of the analysis. The Ecoinvent database represented the primary source used to derive, link and compute all the material and energy flows that are necessary to evaluate the environmental impacts associated with processes and activities emerging from the documentation. Since each process contained in the database is normally defined for several geographical areas, the more relevant version concerning the actual geographic context involved in the execution of the activities has been selected. Moreover, the idea behind the application of the 100-0 approach promoting the use of burden-free recycled products has been integrated to each dataset using the "cut-off by classification" model available in Ecoinvent.

6.2. Life cycle inventory

6.2.1. Introduction

In this section will be described the methodology adopted for the data collection concerning material and energy flows for each life cycle phase of the wind power plant. Particular attention will be given to the data sources type and their reliability, as well as the models and assumptions used for the inventory building. The single unit processes will be illustrated outlining their main interrelationships and the most important factors that affect input and output flows.

6.2.2. Raw materials acquisition

The *raw materials acquisition* phase represents the starting point of the wind power plant life cycle. As anticipated in the goal and scope definition, in this phase are included all the unit processes that refer to the row materials extraction, processing and their transport to the place where they will be transformed into semi-finished products and finished products. These unit processes refer to all the physical components present in the power plant (wind turbines, platforms, internal roads, cable trenches, power transmission system and transformer substation), but also to the building works required for the transportation of the major components of the wind turbines. The procedures carried out during the data collection regarding the amount of raw materials needed for each item will be described individually.

For the estimation of the inventory data related to the transport of these materials, the *market* and *transformation* datasets contained in the Ecoinvent database were used. The first type of dataset is recommended when specific information regarding the location of the supplier and the consumer of the product/service selected is not known (PRé Sustainability, 2023). The *market* dataset, in fact, provides the missing transport data by using average values deriving from the market or industry sector calculated for a selected geographical area (PRé Sustainability, 2023). The *transformation* dataset, instead, does not include any information concerning the supplying of the product/service, expecting that the user will select or define other processes to account for it. When the *transformation* dataset was used in the present study, transport requirements have been considered using the *market for transport* dataset in Ecoinvent, which contains the inventory data required for the delivery of the service of transportation of 1 ton of goods for a distance of 1 km using a certain type of means of transport (selected by the user). Specifically, the process *Transport, freight, lorry, unspecified {RER}| transport, freight, lorry, all sizes, EURO4 to generic market for transport, freight, lorry, unspecified | Cut-off, U* was selected when dealing with any type of road transport involved in the plant life cycle. This choice is based on the assumption that EURO 4 lorries (vehicles registered between 2006 and 2009) have been used along any trip connecting the suppliers and the consumer belonging to the system analyzed.

Since the capacity of the vehicles used wasn't available, the "unspecified capacity" version of the dataset was selected. The reference geographical area for this process was chosen to match the region where the transport operations took place.

Unless differently specified, the distances involved in all the road trips were computed through the Google maps software giving as input the location of suppliers and consumers. Given that sea transport resulted to be more case-specific, the process chosen to model the inventory data related to each trip will be discussed individually in the next paragraphs. In any case, unless differently specified, the distances involved in all the sea trips were computed using the software SeaRates, developed by DP World, giving as input the starting and ending harbor involved.

Wind turbines

The evaluation of the amount of raw materials needed for the manufacturing of the six G114 – 2.5 MW wind turbines has been done according to the following procedure:

1. Determination of the masses of the wind turbine's major components (tower, rotor, nacelle).

2. Determination of the masses concerning the sub-components that make up the major components of the turbine.

3. Determination of the materials mass fractions related to each sub-component.

The masses of the turbine's major components can vary depending on several factors, first among all its rated power. Generally, higher rated powers mean also bigger turbines, as demonstrated by eq. 3.4, which is now recalled:

$$P_{el}\,[W] = P_{mec,out} \cdot \eta_{el} = \frac{1}{2}\eta_{aero}\eta_{mec}\eta_{el}\rho A v^3 = \frac{1}{2}c_p \rho A v^3 \qquad (3.4)$$

For example, when having a bigger rotor, the blades' swept area A increases, hence the electric power increases linearly. Instead, when raising the turbine hub height with the same vertical wind profile, the wind speed v that crosses the rotor gets higher thanks to the effect of the boundary layer that characterizes the interaction between the wind stream and the soil, therefore the rated power will increase with its cubic power.

However, additional factors may influence the turbine's weight. First, the turbine's wind class. The wind class is related to specific wind parameters that characterize the installation site of the turbine, i.e. the mean wind speed and turbulence intensity. Each wind class is defined according to the IEC 61400-1 standard (Figure 6.2). In general, when the site features higher mean wind speed and turbulence intensity (hence, the wind class goes towards the IA+ class), the wind turbine structure needs to withstand stronger stresses coming from the wind, therefore its major components are designed

to be more robust and heavier. At the same time, to achieve the same power, if the site presents a better wind resource it's also true that the dimensions of the rotor and the tower may be reduced thanks to the effect of the higher mean wind speed at the same height shown by eq. 3.4. Overall, the final result on the wind turbine weight will be given by the superimposition of these two opposing effects.

Other parameters that can affect the wind turbine weight are related to the specific design of each structural and functional component of the wind turbine. The choice of different materials, for example, can affect both density and resistance (i.e. the thickness) of each item, as well as the same function achieved by a certain component may be done using different configurations that reduce or increase the overall weight. An emblematic example has been already shown in the literature review of the present study when dealing with the drive train types: gearless configurations that use direct-drive synchronous generators are characterized by heavier generators than those which use direct-drive permanent magnet synchronous generators, considering that in the first case the generator is typically bigger (especially in turbines with high rated power).

Wind turbine class		I	II	III	S
V_{ave}	(m/s)	10	8,5	7,5	Values specified by the designer
V_{ref}	(m/s)	50	42,5	37,5	
	Tropical (m/s) $V_{ref,T}$	57	57	57	
A+	I_{ref} (-)	0,18			
A	I_{ref} (-)	0,16			
B	I_{ref} (-)	0,14			
C	I_{ref} (-)	0,12			

The parameter values apply at hub height and

V_{ave} is the annual average wind speed;

V_{ref} is the reference wind speed average over 10 min;

$V_{ref,T}$ is the reference wind speed average over 10 min applicable for areas subject to tropical cyclones;

A+ designates the category for very high turbulence characteristics;

A designates the category for higher turbulence characteristics;

B designates the category for medium turbulence characteristics;

C designates the category for lower turbulence characteristics; and

I_{ref} is a reference value of the turbulence intensity (see 6.3.2.3).

Figure 6.2: Wind classes definition according to the IEC 61400-1 standard (IEC 61400-1:2019).

For the specific case of the power plant object of the study, data regarding the weight of the turbine's major components have been retrieved from the technical documentation available based on the information given by the manufacturer. The weight of each component is reported in Table 6.1.

The tower is the heaviest major component of the wind turbine, accounting for more than half of the total mass. The G114 – 2.5 MW features a 4-segment tubular tower to reach a hub height of 93 m. The nacelle and the rotor, instead, represents almost a third

and a fifth, respectively, of the total mass. The rotor is equipped with blades 56 m long, that together with the hub define a rotor diameter of 114 m.

Table 6.1: Weight of the major turbine's components.

Component	Weight (t)	Mass fraction (%)
Tower	185.90	52.44
Nacelle	101.35	28.59
Rotor	67.27	18.97
Total	354.52	100

For the determination of the mass of each sub-components that make up the tower, nacelle and rotor, both manufacturer data (primary data) and literature data (secondary data) have been used, since the only data available provided by Siemens Gamesa were not sufficient to obtain a complete inventory. From the technical report referring to the G114 – 2.5 MW wind turbine, it was possible to obtain that:

- The tower does not include any sub-component (neglecting the 4 segments architecture, which is irrelevant since they are composed of the same materials in the same mass fraction).

- The nacelle includes the sub-components shown in Table 6.2.

- The rotor is subdivided into hub, blades (3) and cone, which protects the hub from interaction with the atmosphere.

Table 6.2: Nacelle sub-components of the G114 – 2.5 MW wind turbine.

Number	Sub-component
1	Cover
2	Frame
3	Main shaft
4	Gearbox
5	Yaw system
6	Mechanical brake
7	Hydraulic unit
8	Generator
9	Transformer
10	Electrical cabinets
11	Service crane
12	Cables

From the technical documentation available based on the information given by the manufacturer, it was possible to retrieve the mass of the blades and that of the sum of hub and cone. The values are reported in Table 6.3.

Table 6.3: Weight of the G114 – 2.5 MW rotor's sub-components.

Component	Sub-component	Weight (t)
Rotor	**Hub and cone**	26.80
	Blades (3)	40.47
	Total	67.27

No information was available, instead, for the weight of the nacelle sub-components besides the total weight of the drive train (main shaft, gearbox and generator), equal to 45.90 t. For this reason, the determination of the missing data was done by referring to literature LCA studies. The reference works have been chosen following several criteria:

- The type of turbine used in the reference studies should have had a similar rated power (max. 0.5 MW of difference) to avoid as much as possible the presence of scale effects when transferring the mass fraction of each sub-components of the reference turbine's nacelle to those of the G114 – 2.5 MW.

- The reference turbines whose manufacturer coincides with the one of the G114 – 2.5 MW (Siemens Gamesa) were preferred on the others.

- Since the weight of the sub-components is closely correlated also to the type of materials used, the turbines whose materials or main materials coincide with those employed in the nacelle's sub-components of the G114 – 2.5 MW are preferred on the others. About this criterion, in Table 6.4 are gathered all the main materials that were possible to retrieve from the turbine's technical report referred to each sub-component, not only of the nacelle but also of the rotor and tower.

- Only turbines having the same type of drive train as the G114 – 2.5 MW should have been considered. Specifically, as described in Chapter 3, the G114 – 2.5 MW is a geared turbine, hence only reference turbines with a gearbox were considered. This criterion was included especially because as previously stated, the weight of the generator can vary a lot depending on the type of drivetrain, not to mention the obvious absence of the gearbox if the drive train is gearless type.

Table 6.4: Main materials of all the turbine's sub-components retrieved from the G114 – 2.5 MW technical report.

Component	Sub-component	Main materials
Tower	**4 sections**	Structural carbon steel (painted)
Nacelle	**Cover**	Fiberglass and epoxy resin
	Frame	Iron
	Main shaft	Steel (not specified)
	Gearbox	-
	Yaw system	-
	Mechanical brake	-
	Hydraulic unit	-
	Generator	-
	Transformer	-
	Electrical cabinets	-
	Service crane	-
	Cables	-
Rotor	**Blades**	Fiberglass and epoxy resin
	Hub	Cast iron
	Cone	Fiberglass and epoxy resin

Among all the LCA studies reviewed for this purpose, the work of Martínez et al. (2009) was the only one that met every selection criterion just described. Martínez et al. conducted a life cycle assessment "from-cradle-to-grave" on the Munilla onshore wind farm, located in Spain (Martínez et al., 2009). The turbine model installed in this power plant is the G8X – 2 MW, manufactured by Siemens Gamesa (Martínez et al., 2009). The G8X – 2 MW presents a diameter of 80 m and a hub height of 70 m. The weight of each sub-component of the turbine, as well as the materials used, are contained in Table 6.5. It has been possible to observe that:

- The rated power of the turbine, as well as its manufacturer, satisfy the first and second selection criterion.

- The materials of the G114 – 2.5 MW wind turbine referring to its sub-components retrieved from the technical report are equal[3] to those of the G8X – 2 MW.

- The G114 – 2.5 MW and the G8X – 2 MW have the same drive train type (geared).

[3] The steel alloy contained in the main shaft of the G114 and G8X wind turbines was assumed to be identical.

Table 6.5: Weights and mass fractions and material fractions of sub-components for the G8X – 2 MW wind turbine (Martínez et al., 2009).

Component	Sub-component	Weight (t)	Sub-component mass fraction (%)	Material weight (t)	Material	Material fraction for sub-component (%)
Tower	**3 sections**	143	100.00	143	Steel	100.00
Nacelle	**Frame**	10.5	22.78	10.5	Iron	100.00
	Main shaft	6.1	13.23	6.1	Steel	100.00
	Transformer	5	10.85	0.149	Silica	3.00
				1.5	Copper	30.00
				3.3	Steel	66.00
	Generator	6.5	14.10	0.195	Silica	3.00
				2	Copper	31.00
				4.29	Steel	66.00
	Gearbox	16	34.71	8	Iron	50.00
				8	Steel	50.00
	Cover	2	4.34	0.8	Fibre glass	40.00
				1.2	Resin	60.00
	Total	46.1	100.00			
Rotor	**Hub**	14	41.41	14	Cast iron	100.00
	Nose-cone	0.31	0.92	0.124	Fibre glass	40.00
				0.186	Resin	60.00
	3 blades	19.5	57.68	11.7	Resin	60.00
				7.8	Fibre glass	40.00
	Total	33.81	100.00			

Therefore, the use of the data related to the weight of the G8X – 2 MW sub-components has been evaluated as acceptable for the computation of the respective sub-components weight in the G114 – 2.5 MW.

Nevertheless, the subdivision of the nacelle's mass in its sub-components made by Martínez et al. (2009) is still not sufficient to cover all the items reported in Table 6.4. Specifically, data regarding the yaw system, mechanical brake, hydraulic unit, electrical cabinets, service crane and the cables are still unknown. Martínez et al. (2009) stated that the mass of the nacelle they accounted for represents 85 % of the total (Martínez et al., 2009), therefore, the residual 15 % has been attributed to the remaining components whose reference data still need to be found. Since for these components no additional information about the main materials used is present in the documentation, the choice of the reference turbine has been done ignoring the third selection criterion, possibly excluding also the second in the case no other alternatives had been found.

Reference data for the remaining components were retrieved from Crawford (2009). Crawford studied the impacts related to the primary energy consumption for 2 types of turbines with nominal power 0.85 MW and 3 MW, respectively (Crawford, 2009). The inventory data related to the 3 MW turbine were considered (Table 6.6). Given that Crawford didn't include for this type of turbine information regarding the electrical cabinets and hydraulic unit and no better sources were found, the 15% residual mass of the nacelle was attributed entirely to the other sub-components.

Table 6.6: Inventory data for the 3MW wind turbine reported by Crawford (2009).

Component	Sub-component	Weight (t)	Sub-component mass fraction (%)	Material weight (t)	Material	Material fraction for sub-component (%)
Tower	**Painted steel**	160	100.00	158.76	Steel	99.23
				1.24	Paint	0.78
Nacelle	**Bedplate/frame**	13	19.12	13	Steel	100.00
	Cover	9.33	13.72	9.33	Steel	100.00
	Generator	7.14	10.50	5.71	Steel	79.97
				1.43	Copper	20.03
	Brake system	1.02	1.50	1.02	Steel	100.00
	Gearbox	24.06	35.38	23.58	Steel	98.00
				0.241	Copper	1.00
				0.241	Aluminium	1.00
	Cables	1.63	2.40	0.69	Aluminium	42.33
				0.94	Copper	57.67
	Yaw system	3.87	5.69	3.87	Steel	100.00
	Crane	1.02	1.50	1.02	Steel	100.00
	Transformer/sensors	6.93	10.19	3.47	Steel	50.07
				1.38	Copper	19.91
				1.38	Aluminium	19.91
				0.7	Plastic	10.10
	Total	68	100.00			
Rotor	**Hub**	19.2	48.00	19.2	Steel	100.00
	Blades	20.07	50.18	12.04	Fibre glass	59.99
				8.03	Epoxy	40.01
	Bolts	0.73	1.83	0.73	Steel	100.00
	Total	40	100			

This assumption was used since typically the mass of the hydraulic unit and the electrical cabinets together represents a small percentage of the total mass of the nacelle, which anyways will be entirely accounted. Therefore, the only effect of this choice is related to the overall materials fraction of this 15% of the nacelle's mass (since the other sub-components have different material composition), but considering what just said it's expected to be negligible.

The computed mass fractions of the remaining sub-components obtained through Crawford (2009) are contained in Table 6.7. These fractions will be applied directly to the 15% of the total mass of the G114 – 2.5 MW nacelle and then the results will be linked to the respective sub-components. The mass fractions referring to the nacelle's components included in Martínez et al. (2009), instead, will be recomputed - starting from Table 6.5 data - for the drive train components and the rest of the nacelle (together assumed to represent the remaining 85% of the nacelle's mass), since the drive train mass is known from the G114 – 2.5 MW technical report. These two calculations are reported in Table 6.8, 6.9. Finally, the resulting mass fractions will be applied to the mass of the drive train (45.90 t) and that of the nacelle needed to reach 85% of the total (equal to 86.15 t).

Table 6.7: Mass fraction of the missing nacelle's sub-components (Crawford, 2009).

Sub-component	Weight (t)	Mass fraction (%)
Brake system	1.02	13.53
Cables	1.63	21.62
Yaw system	3.87	51.33
Crane	1.02	13.53
Total	7.54	100

Table 6.8: Mass fraction of the drive train's components (Martínez et al., 2009).

Sub-component	Weight (t)	Mass fraction (%)
Main shaft	6.1	21.33
Gearbox	16	55.94
Generator	6.5	22.73
Total	28.6	100

Table 6.9: Mass fraction of the remaining sub-components making up 85 % of the nacelle's mass (Martínez et al., 2009).

Sub-component	Weight (t)	Mass fraction (%)
Frame	10.5	60.00
Transformer	5	28.57
Cover	2	11.43
Total	17.5	100

The material fractions of the sub-components whose composition hasn't been possible to retrieve from the technical report of the G114 – 2.5 MW will be determined depending on the data source used for the computation of the mass fraction just

described. Hence, the components whose mass fraction was computed starting from Martínez et al. (2009) inventory data will present the material fractions for the corresponding items, otherwise the material fractions will be the ones contained in Crawford's inventory data. To consider the contribution of the paint coating the steel of the tower, the same material fraction used by Crawford (2009) was included in the G114 – 2.5 MW inventory data. The contribution of the cone, instead, was separated by the one of the hub using the mass and material fractions contained in Martínez et al. (2009) (Table 6.10).

Table 6.10: Mass fractions hub (Martínez et al., 2009).

Sub-component	Weight (t)	Mass fraction (%)
Hub	14	97.83
Cone	0.31	2.17
Total	14.31	100.00

Putting together all the pieces, the final inventory data regarding the single wind turbine are reported in Table 6.11.

For each major component and sub-component, assemblies and sub-assemblies, respectively, have been defined in SimaPro. The processes related to the acquisition of each material used in the turbine have been defined in SimaPro as reported in Table 6.12. All the processes belong to the *market* dataset, since in any case specific information regarding the transport between the supplier and the consumer (in this case, the company that will manufacture the components starting from the materials selected) of the materials are not known.

Table 6.11: Inventory data for the raw materials used in a single G114 – 2.5 MW turbine.

Component	Sub-component	Weight (t)	Sub-component mass fraction (%)	Material weight (t)	Material	Material fraction for sub-component (%)
Tower	**Painted steel**	185.90	100	184.46	Steel	99.23
				1.44	Paint	0.78
Nacelle	**Frame**	24.15	23.83	24.15	Iron	100.00
	Main shaft	9.79	9.66	9.79	Steel	100.00
	Transformer	11.50	11.35	0.46	Silica	4.00
				3.45	Copper	30.00
				7.59	Steel	66.00
	Generator	10.43	10.29	0.31	Silica	3.00
				3.23	Copper	31.00
				6.89	Steel	66.00
	Gearbox	25.68	25.34	12.84	Iron	50.00
				12.84	Steel	50.00
	Cover	4.60	4.54	1.84	Fibre glass	40.00
				2.76	Epoxy	60.00
	Brake system	2.06	2.03	2.06	Steel	100.00
	Cables	3.29	3.24	1.39	Aluminium	42.33
				1.90	Copper	57.67
	Revolving system	7.80	7.70	7.80	Steel	100.00
	Crane	2.06	2.03	2.06	Steel	100.00
	Total	101.35	100			
Rotor	**hub**	26.22	38.98	26.22	Cast iron	100.00
	Cone	0.58	0.86	0.35	Epoxy	60.00
				0.23	Fibre glass	40.00
	blades (3)	40.47	60.16	24.28	Epoxy	60.00
				16.19	Fibre glass	40.00
	Total	67.27	100			

Table 6.12: Definition of the Ecoinvent processes for each material used in the wind turbine.

Component	Material	Mass per turbine (t)	Mass per wind farm (t)	Mass per wind farm/FU (t/GWh)	SimaPro process (Ecoinvent database)
Tower	Steel	184.46	1,106.76	1.22	Steel, low-alloyed {GLO}| market for steel, low-alloyed | Cut-off, U
	Paint	1.44	8.64	0.01	Alkyd paint, white, without water, in 60% solution state {RER}| market for alkyd paint, white, without water, in 60% solution state | Cut-off, U
Nacelle	Steel	49.02	294.12	0.32	Steel, low-alloyed {GLO}| market for steel, low-alloyed | Cut-off, U
	Iron	36.99	221.93	0.24	Ferrite {GLO}| market for ferrite | Cut-off, U
	Silica	0.77	4.64	0.01	Silica sand {GLO}| market for silica sand | Cut-off, U
	Aluminium	1.39	8.35	0.01	Aluminium, primary, ingot {IAI Area, EU27 & EFTA}| market for aluminium, primary, ingot | Cut-off, U
	Copper	8.58	51.47	0.06	Copper, cathode {GLO}| market for copper, cathode | Cut-off, U
	Epoxy	2.76	16.56	0.02	Epoxy resin, liquid {RER}| market for epoxy resin, liquid | Cut-off, U
	Fibre glass	1.84	11.04	0.01	Glass fibre reinforced plastic, polyamide, injection moulded {GLO}| market for glass fibre reinforced plastic, polyamide, injection moulded | Cut-off, U
Rotor	Cast iron	26.22	157.32	0.17	Cast iron {GLO}| market for cast iron | Cut-off, U
	Epoxy	24.63	147.79	0.16	Epoxy resin, liquid {RER}| market for epoxy resin, liquid | Cut-off, U
	Fibre glass	16.42	98.51	0.11	Glass fibre reinforced plastic, polyamide, injection moulded {GLO}| market for glass fibre reinforced plastic, polyamide, injection moulded | Cut-off, U

Wind turbines foundations

Each wind turbine installed in the wind farm is anchored to a reinforced concrete foundation buried in the ground. Foundations have a fundamental role in the turbines operation. The loads generated by the turbine weight and the impact of the wind on the structure are sent to the base of the tower. The goal of the foundation is to receive these loads and transmit them to the ground while maintaining the stability of the structure. Since the stresses involved are very high due to the dimensions and the weight of the single wind turbine, its foundation is typically quite massive. The design of the foundations depends not only on the loads intensity but also on the type of terrain and its topography. Specifically, the loads transmitted to the ground need to be such that, even in the worst case, no dangerous soil collapses or instabilities are triggered.

In the Iurefalco power plant 2 types of foundations are used, named *foundation 1* and *foundation 2*, used by 4 and 2 turbines, respectively. The foundation plinth is placed in both cases on a circular base with a diameter of approximately 20 m, as shown in Figure 6.3. On the top of the plinth is located the collar on which the wind turbine will be anchored. The base, plinth and collar are made of different types of concrete, whose resistance classes have been retrieved from the component's technical drawings. The reinforcing bars are made of B450C steel. The additional steel required for the grouting is low-alloyed (structural steel). The installation of the foundation requires the excavation of a cylindrical pit 3.5 m deep (on average) and with a diameter of 22 m. The foundation is then buried with inert materials, specifically limestone gravel, properly compacted to reach the desired height. From the balance of the excavated soils and rocks along the entire site, it has been possible to assume that the inert materials needed for the refill of the pit were entirely derived from the excavation of the cable trenches and the pits themselves, therefore no further virgin materials were used.

The foundation presents a certain number of holes required to allow the passage of the MV cables coming from the nacelle of the tower, the copper ropes used for the grounding of the electrical system and the optic fiber strands. The amount of copper used for the ropes was included in the assembly of each foundation. The MV cables and optic fiber materials, instead, will be part of the power transmission system assembly.

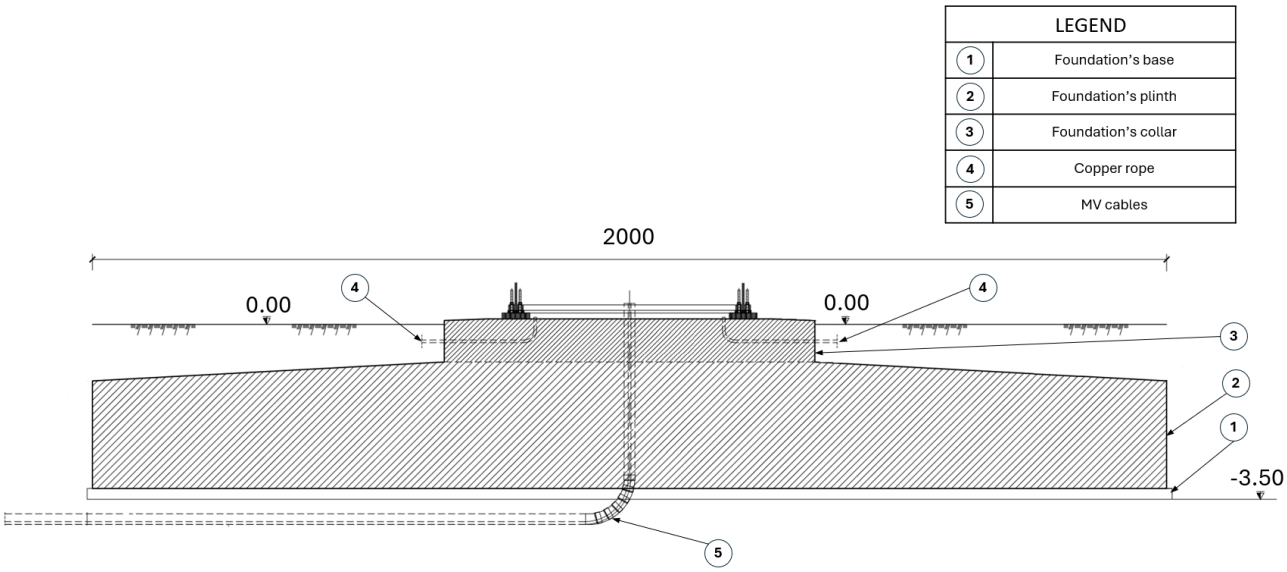

(a) Longitudinal section of the wind turbines' foundations.

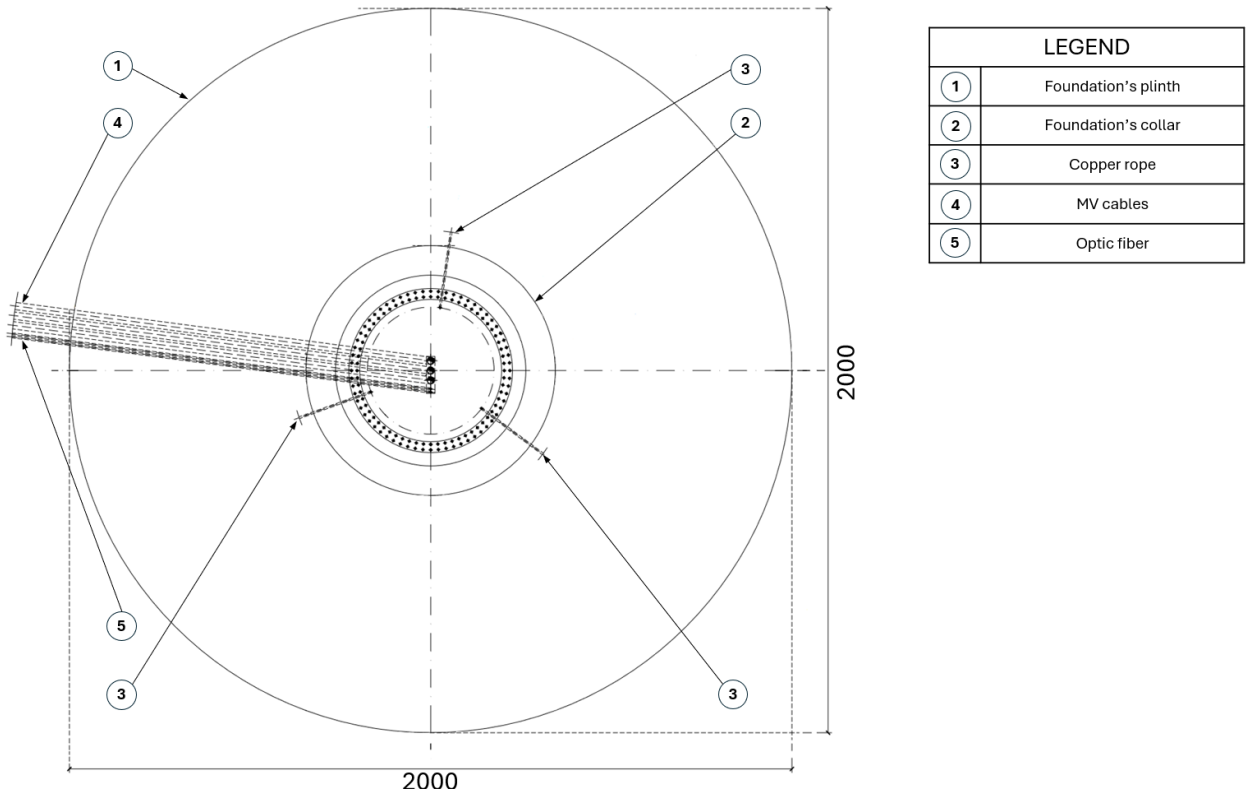

(b) Top view of the wind turbines' foundations

Figure 6.3: Wind turbines' foundations design details (adapted from Project documentation).

All the quantities of the mentioned materials referring to the respective sub-components of each foundation were retrieved either from the bill of quantities documentation or technical drafts (Table 6.13).

It's important to note that, in the case of concrete used for these components, the most suitable Ecoinvent processes related to its production allocate the material and energy flows to each cubic meter of concrete and not to each kilogram. This could be a problem for the estimation of the impacts related to the concrete end-of-life since SimaPro manages only mass-based recycling/waste scenarios and not volume-based ones. However, since the turbines' foundations are expected to be left in situ, these components will not be included in the end-of-life phase.

A last clarification is related to the use of *transformation* datasets and not *market* for the concrete the steel (low-alloyed and reinforcing). This was done since in both cases the production facilities used to generate these components were known from the technical documentation of the power plant, therefore the contribution of the transport was evaluated separately with higher precision. To assess the weight of the concrete used, only for the transportation sake, the sum of the volumes reported in Table 6.13 was conservatively multiplied by a reference density of 2,400 $\frac{Kg}{m^3}$ even if SimaPro suggests slightly lower densities for each concrete type. Since both concrete and reinforcing steel are assumed to not undergo additional refinement processes and the low-alloyed steel components are manufactured in the same facility where the steel is produced, these items are transported directly to the power plant site without requiring any intermediate trip. For this reason, their transport inventory will be included in the components manufacturing phase, as specified in the goal and scope section.

Table 6.13: Inventory data concerning the raw materials employed in the two types of foundations.

Component	Material	Volume per turbine (m^3)	Mass per turbine (t)	Mass per wind farm (t)	Mass per wind farm/FU (t/GWh)	SimaPro process (Ecoinvent database)
Foundation 1	**Concrete 50 MPa**	30.00	72.00	288.00	0.32	Concrete, 50MPa {GLO}| concrete production, 50MPa, with cement, CEM II/B | Cut-off, U
	Concrete 40 MPa	682.00	1636.80	6547.20	7.22	Concrete, 40MPa {GLO}| concrete production, 40MPa, for building construction, with cement, CEM III/A | Cut-off, U
	Concrete 20 MPa	64.00	153.60	614.40	0.68	Concrete, 20MPa {GLO}| concrete production, 20MPa, with cement, CEM II/B | Cut-off, U
	Reinforcing steel (B450C)	-	90.19	360.77	0.40	Reinforcing steel {Europe without Austria}| reinforcing steel production | Cut-off, U
	Steel	-	2.99	11.94	0.01	Steel, low-alloyed {Europe without Switzerland and Austria}| steel production, electric, low-alloyed | Cut-off, U
	Copper	-	8.28	33.12	0.04	Copper, cathode {GLO}| market for copper, cathode | Cut-off, U
Foundation 2	**Concrete 50 MPa**	30.00	72.00	144.00	0.16	Concrete, 50MPa {GLO}| concrete production, 50MPa, with cement, CEM II/B | Cut-off, U
	Concrete 40 MPa	548.10	1315.44	2630.88	2.90	Concrete, 40MPa {GLO}| concrete production, 40MPa, for building construction, with cement, CEM III/A | Cut-off, U
	Concrete 20 MPa	68.60	164.64	329.28	0.36	Concrete, 20MPa {GLO}| concrete production, 20MPa, with cement, CEM II/B | Cut-off, U
	Reinforcing steel (B450C)	-	97.89	195.78	0.22	Reinforcing steel {Europe without Austria}| reinforcing steel production | Cut-off, U
	Steel	-	6.99	13.97	0.02	Steel, low-alloyed {Europe without Switzerland and Austria}| steel production, electric, low-alloyed | Cut-off, U
	Copper	-	8.28	16.56	0.02	Copper, cathode {GLO}| market for copper, cathode | Cut-off, U

Wind turbines platforms

In front of each wind turbine is located a service platform used as working area for vehicles, cranes and building machines. A portion of the platform is dedicated for the storage of the wind turbine components waiting to be installed. The access to each platform is provided by the roads internal to the site.

Wind turbine platforms have to withstand high stresses caused by the passage and operations of very heavy machines, as well as the weight of the components themselves. For these reasons, the dimensions, the construction materials and the thickness of each platform are designed to manage all of this in safety. It's worth noting that these parameters depend also on the site orography and on the type of soil on which platforms are built, since their stability is strictly related to the mean slope and soil resistance.

Most of the design features of the wind turbine platforms have been established by the wind turbine manufacturer, which managed all the activities related to the turbines' installation (Figure 6.4). Each platform required the excavation of a mean area of approximately 3000 m^2 for a depth included between 0.3 and 0.4 m. The excavated volume has been filled with several layers of limestone gravel with variable granulometry, properly compacted to reach the desired height in respect to the ground. The total (apparent) volume of limestone gravel used has been retrieved from the bill of quantities. This volume has been then converted into mass using a mean density of 1,700 $\frac{Kg}{m^3}$ based on the data retrieved from the civil works report of the site.

From the balance of the excavated soils and rocks along the entire site, it has been possible to conclude that part of the limestone gravel was derived from the material excavated during the construction of other elements of the power plant such as the cable trenches and the foundations pits, therefore only a fraction of the total mass has been extracted from limestone quarries. As anticipated in the case study description, the limestone quarry used for all the civil works internal to the site is located near WTG 14. The fraction of limestone gravel extracted from the quarry represents the only contribution of virgin material used for the platform construction, whose mass is reported in Table 6.14. In this case, the *transformation* dataset was chosen to evaluate the contribution of the transport with higher precision. Since limestone gravel is assumed to not undergo additional refinement processes, it's transported directly to the use location. For this reason, its transport inventory will be included in the components manufacturing phase, as specified in the goal and scope section.

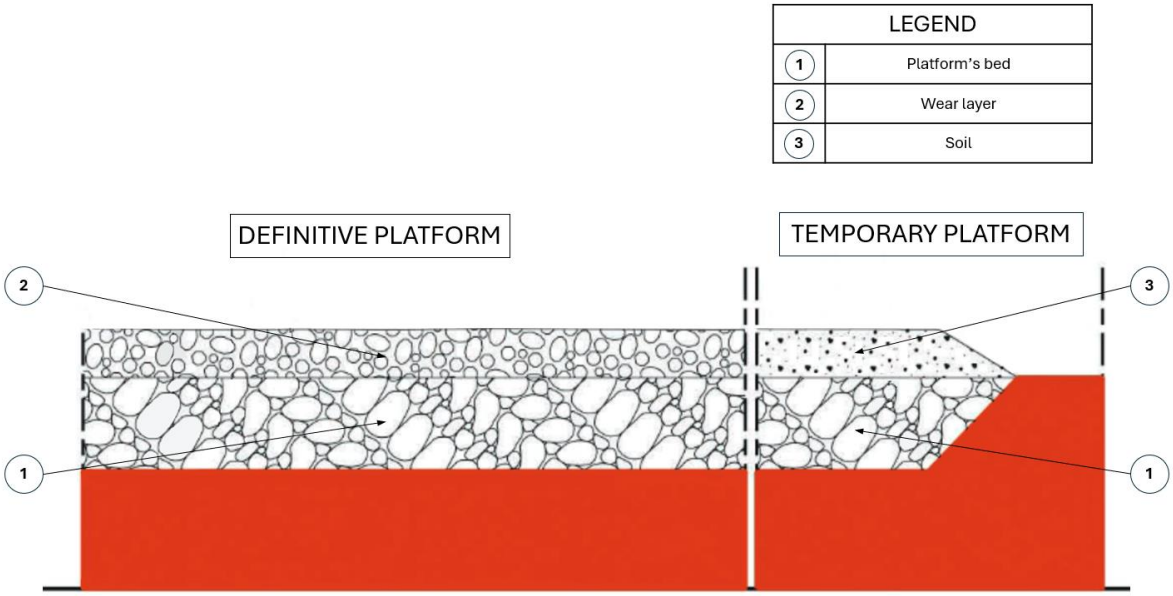

(a) Longitudinal section of definitive and temporary platforms (after renaturation).

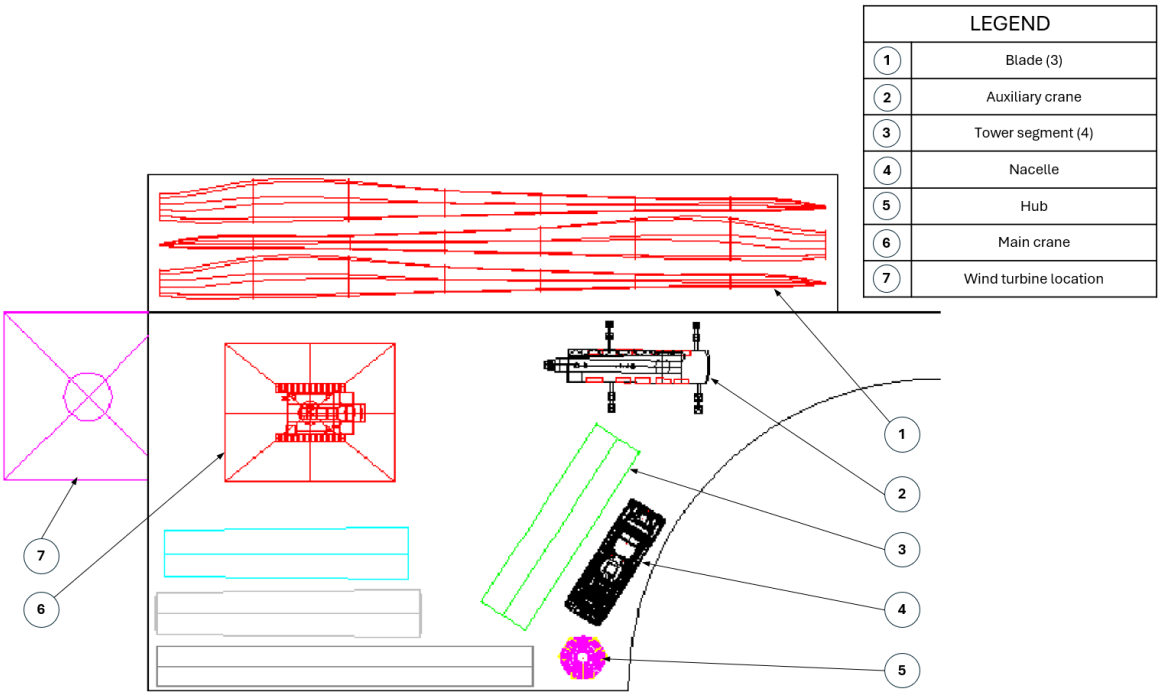

(b) Typical disposition of the turbine's components and cranes on the platform at the start of the assembly phase.

Figure 6.4: Wind turbines' platforms design details (adapted from Project documentation).

Table 6.14: Inventory data related to the raw materials used for the platforms construction.

Component	Material	Mass per wind farm (t)	Mass per wind farm/FU (t/GWh)	SimaPro process (Ecoinvent database)
Platforms	Limestone gravel	13969.44	15.41	Limestone, crushed, for mill {RoW}| limestone production, crushed, for mill | Cut-off, U

Internal roads

The internal roads of the power plants lead vehicles, cranes and building machines to the location of the six wind turbines starting from the existent viability external to the site. Several paths already used for the passage of agricultural machinery have been adjusted to make them suitable for the construction phase. Eventually, new paths have been built to link the existent paths with the wind turbines' platforms.

The internal roads, likewise the platforms, are built to withstand the high stresses transferred to the ground by the passage of heavy machines, carrying in this case not only the turbines' components but also the construction materials that are used throughout the entire site. The width of the roads, the profile of the turns, the roads' structure and all the other design parameters have been determined according to the prescriptions given by the turbines' manufacturer. On average, each internal road requires the excavation for its entire length of a volume 4.5 m wide and 0.3 m deep, as shown in Figure 6.5. Similarly to the platforms, this volume is filled using several layers of limestone gravel with variable granulometry, compacted to reach the ground level. Due to the presence of dry-stone walls following the roads path, these walls have been demolished and then rebuilt using limestone bricks coming from the quarry internal to the site. The demolished material, as well as the excavated, has been reused throughout the site. The limestone gravel used to refill the excavated volume, similarly to the walls, has been extracted from the local quarry, therefore, all the limestone needed for the internal roads is derived from virgin material.

The total volumes of limestone gravel and limestone bricks were retrieved from the bill of quantities. These volumes have been converted in masses using a density of 1,700 $\frac{Kg}{m^3}$ (as in the case of the platforms) for the limestone gravel and a conservative density of 2,400 $\frac{Kg}{m^3}$, equal to the one of the material, for the limestone rocks, since in this last case the void percentage between each rock is expected to be lower than in the case of the compacted limestone gravel, but no further information was possible to be retrieved from the plant documentation. All the values concerning this part are reported in Table 6.15. Since limestone gravel and bricks are assumed to not undergo additional refinement processes, they are transported directly to the use location. For this reason, their transport inventory will be included in the components manufacturing phase, as specified in the goal and scope section.

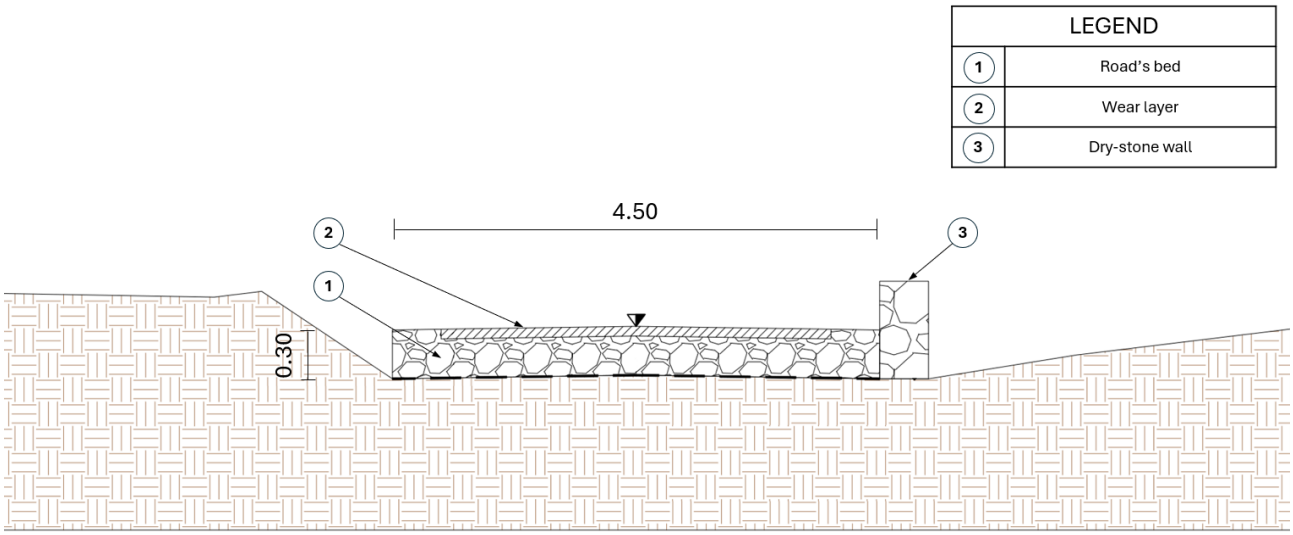

Figure 6.5: Longitudinal section of a typical internal road (adapted from Project documentation).

Table 6.15: Inventory data related to the raw materials used for the internal roads construction.

Component	Sub-component	Material	Mass per wind farm (t)	Mass per wind farm/FU (t/GWh)	SimaPro Process (Ecoinvent database)
Internal roads	**Roads**	Limestone gravel	12,748.05	14.06	Limestone, crushed, for mill {RoW}| limestone production, crushed, for mill | Cut-off, U
	Walls	Limestone bricks	1,548.00	1.71	Limestone, unprocessed {RoW}| limestone quarry operation | Cut-off, U

External roads

Considering that the blades used in the G114 – 2.5 MW wind turbine are 56 m long and the nacelle alone weights more than 100 tons, it's clear that the roads travelled by those vehicles that have to transport such challenging loads must have specific requirements to make the transportations possible. Specifically, it's required that:

- The slope of each road must be included in the admissible range.
- The radius of the turns must be compatible with the size of the vehicle, the component transported and the type of maneuver to be performed.
- The intersections must be free from any obstacle that can damage the components or the vehicles during the roads crossing.

- The roads surface must be free from potholes and bumps while also having sufficient resistance to the loads transferred to the ground by the vehicles.

The site of the power plant, as anticipated in the case study description, is located in an area well served by public roads. Since the internal viability was designed to maximize the compatibility with such roads, there was no need for the construction of new routes. The civil works, instead, were limited to minor road adjustments (with consequent restoration) wherever the existing road conditions didn't meet the 4 requirements just presented.

Overall, the external roads adjustments involved 15 locations spread along the tracks covered by the blades, the hub, the tower segments and the nacelle. The main activities performed include:

- Trees and bushes removal,
- Traffic signs removal and restoration,
- Curbs, sidewalks and roundabouts removal and reconstruction,
- Roads enlargements construction,
- Dry-stone walls demolition and reconstruction.

Curbs, sidewalks and roundabouts are mainly made of concrete blocks. The volume removed to allow the special transports is equal to the volume reconstructed right after. For the roads enlargements and substrates reconstruction, limestone gravel extracted from local quarries was used, properly compacted to reach the desired stiffness and stability. The reconstruction of the dry-stone walls was instead carried out using limestone bricks.

The volume of materials required for each activity was retrieved from the bill of quantities referring to the external roads civil works. These volumes have been converted in masses using specific densities for each material involved:

- For concrete, a reference density of 2,400 $\frac{Kg}{m^3}$ was chosen.
- For limestone gravel and limestone bricks, similarly to the case of the civil works internal to the site, a density of 1,700 $\frac{Kg}{m^3}$ and 2,400 $\frac{Kg}{m^3}$, respectively, was chosen.

The total amounts are reported in Table 6.16. In this case, for both limestone and concrete, the *market* dataset of Ecoinvent was selected since it wasn't possible to retrieve the location of the suppliers.

Table 6.16: Inventory data related to the raw materials used for the external roads adjustments.

Component	Sub-component	Material	Mass per wind farm (t)	Mass per wind farm/FU (t/GWh)	SimaPro Process (Ecoinvent database)
External roads	**Roads enlargements**	Limestone gravel	620.06	0.68	Limestone, crushed, for mill {RoW}| market for limestone, crushed, for mill | Cut-off, U
	Walls	Limestone bricks	115.20	0.13	Limestone, unprocessed {RoW}| market for limestone, unprocessed | Cut-off, U
	Curbs	Concrete	8.63	0.01	Concrete block {RoW}| market for concrete block | Cut-off, U
	Sidewalks	Concrete	109.75	0.12	Concrete block {RoW}| market for concrete block | Cut-off, U
	Roundabouts	Concrete	351.84	0.39	Concrete block {RoW}| market for concrete block | Cut-off, U

Cable trenches and power transmission system

MV trench

The electric power produced by the wind turbines, after the first voltage increase from 690 V to 20 kV occurred in the nacelle's transformer, is delivered through the MV cable transmission system towards the 150/20 kV transformer substation. These cables are placed on the bottom of a trench that follows for the most part the internal roads of the site. In some sections, the site's topsoil and the public roads are crossed. The trench is filled, depending on the location, with several layers of inert materials. The cables are not directly buried, but they are first inserted in corrugated pipes with proper diameter. The optic fibre network that links the control room located in the transformer substation with each wind turbine is also placed in the MV cable trench.

The civil works for the trench building require the excavation of a pit, along the entire trench length, with different dimensions depending on the trench segment:

- For the segments that cross the soil, a pit 1.2 m deep and 0.5 m wide is required, as shown in Figure 6.6a. After the laying of the corrugated pipes, these segments will be filled for 0.4 m with sand derived from limestone rocks and for 0.8 m with limestone gravel, both properly compacted to reach the ground level.

- For the segments that cross the public roads, instead, a pit 1.3 m deep and 0.6 m wide is required, as shown in Figure 6.6b. After the laying of the corrugated

pipes, these segments will be filled for 0.4 m with sand derived from limestone rocks and for approximately 0.85 m with concrete. The remaining depth will be covered with a bituminous conglomerate. To perform the excavation activities, it was necessary the complete demolition of the road surface (approx. 0.15 m deep) along the entire length of the trench segments. After the end of the pit construction, this surface was restored to its original condition.

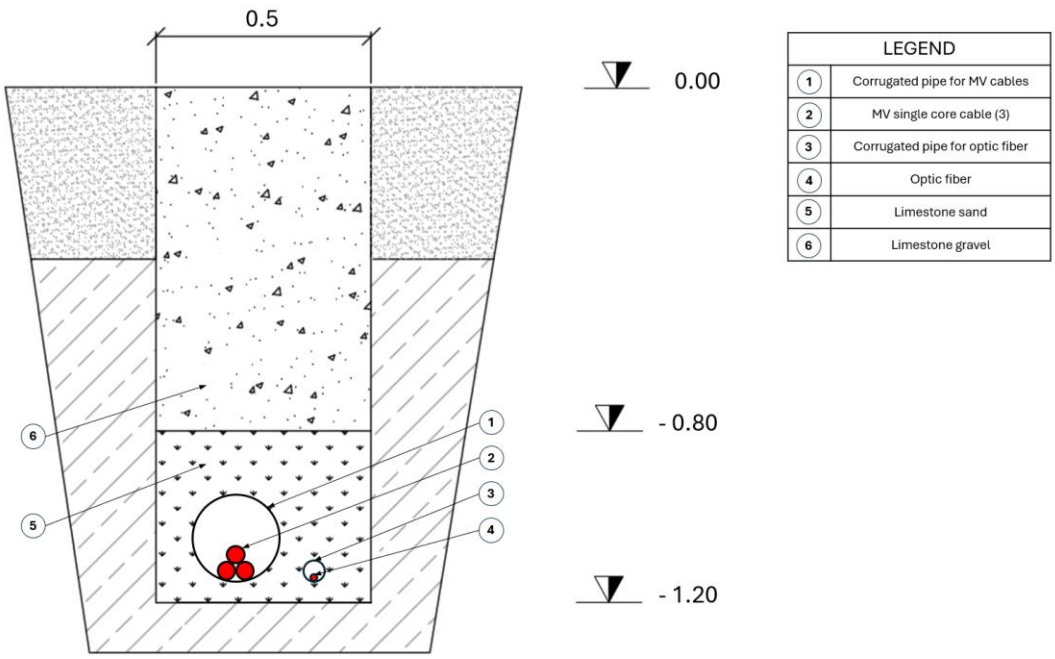

(a) Longitudinal section of soil-crossing trench segments.

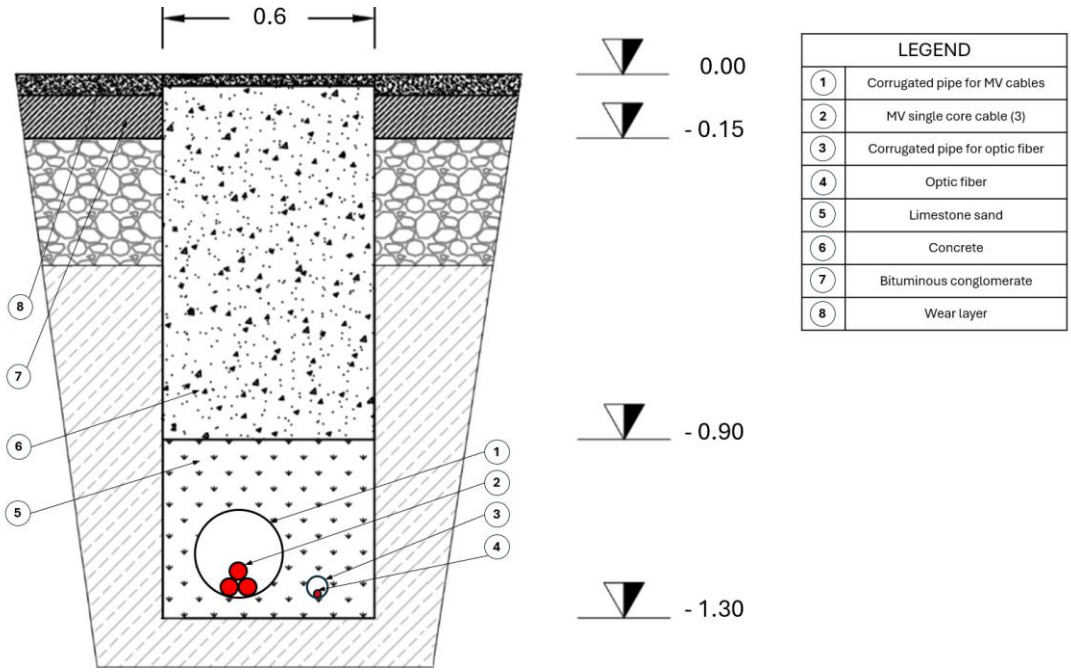

(b) Longitudinal section of road-crossing trench segments.

Figure 6.6: MV trench design details (adapted from Project documentation).

Since part of the path followed by the MV trench was occupied by dry-stone walls, these walls have been demolished and then rebuilt after the completion of the work.

The volume of the materials used was retrieved from the bill of quantities related to the plant civil works. From the balance of the excavated soils and rocks, it has been possible to conclude that all the limestone gravel required was derived from the excavation activities, hence further extractions of virgin limestone from the quarry internal to the site were performed only to obtain the sand and the limestone bricks for the walls reconstruction. A density of 1,900 $\frac{Kg}{m^3}$ after compaction was estimated for the limestone sand, while 2,400 $\frac{Kg}{m^3}$ was assumed for the limestone bricks (similarly to the other sections). For the concrete and the asphalt used in the public roads sections, instead, a density of 2,400 $\frac{Kg}{m^3}$ and 2,100 $\frac{Kg}{m^3}$, respectively, was used. Except for the asphalt, whose supplier was not reported in the available documentation, for all the other materials the *transformation* dataset of Ecoinvent was used. Since these materials are assumed to not undergo additional refinement processes, they are transported directly to the use location. For this reason, their transport inventory will be included in the components manufacturing section, as specified in the goal and scope section.

HV trench

The electric power leaving the transformer substation is delivered to the primary substation (excluded from the system of this study) that connects the plant to the national grid. This is done, similarly to the MV section, through the construction of an underground HV cable transmission system. Also in this case, the HV cables and the optic fibre that links the transformer substation and the primary substation are placed in corrugated pipes buried under inert materials up to the ground level. Additionally, in the HV section, it's also present a copper rope that extends for the entire length of the trench to grant the grounding of the electric system.

The civil works for the HV trench building require the excavation of a pit 1.5 m deep and 0.5 m wide along its entire length, as shown in Figure 6.7. After the laying of the corrugated pipes, the trench has been filled for 0.5 m with sand derived from limestone rocks, for another 0.5 m with limestone gravel and for the last 0.5 m with concrete.

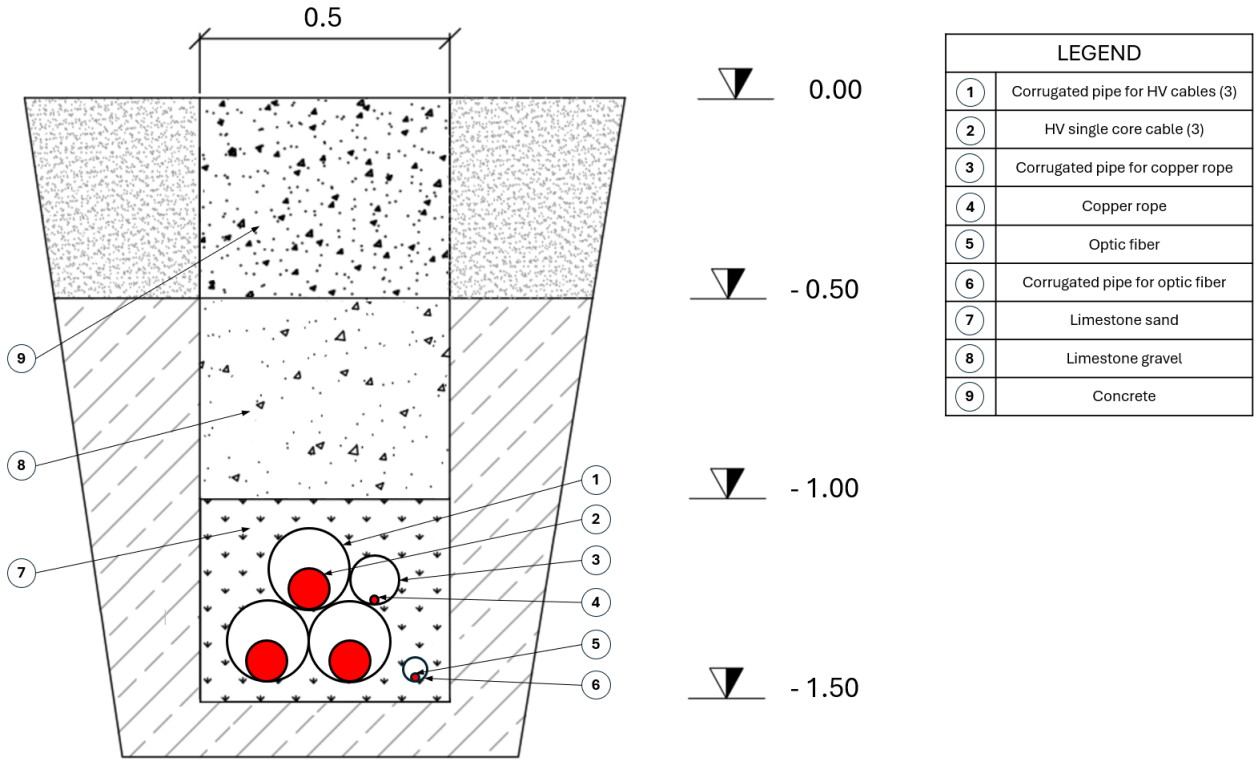

Figure 6.7: HV trench design details (adapted from Project documentation).

The volume of the materials used was retrieved from the bill of quantities related to the plant civil works. Regarding the use of limestone and concrete, the same comments made for the MV trench apply also in this case (densities, virgin material usages, transports). The complete inventory for the cable trenches is reported in Table 6.17. Again, as in the case of wind turbine foundations, the process chosen for concrete production allocates the data on each cubic meter of concrete instead of to each kilogram, possibly causing problems for the end-of-life modeling. However, since the corrugated pipes are not expected to be extracted from the trench, its inert materials won't be in any case included in the end-of-life phase.

Table 6.17: Inventory data related to the raw materials used for the MV and HV trench construction.

Component	Sub-component	Material	Volume (m^3)	Mass per wind farm (t)	Mass per wind farm/FU (t/GWh)	SimaPro process (Ecoinvent database)
Cable trenches	**HV and MV trenches**	Limestone sand	1867.90	3549.01	3.91	Limestone, crushed, for mill {RoW}| limestone production, crushed, for mill | Cut-off, U
		Asphalt	602.81	1265.89	1.40	Mastic asphalt {GLO}| market for mastic asphalt | Cut-off, U
		Concrete 30 Mpa	563.47	1352.33	1.49	Concrete, 30MPa {GLO}| concrete production, 30MPa, for building construction, with cement, CEM III/A | Cut-off, U
	Walls	Limestone bricks	30.00	72.00	0.08	Limestone, unprocessed {RoW}| limestone quarry operation | Cut-off, U

MV and HV cables

In the Iurefalco wind power plant, single core cables are used for both MV and HV transmission systems. In general, single core MV electric cables are composed of 6 main layers (Figure 6.8) (Saveri, 2010):

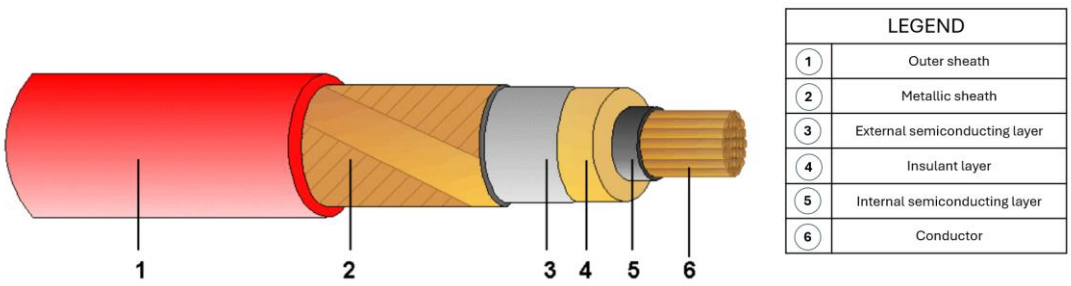

Figure 6.8: graphical representation of the 6 main layers of a single core MV cable (adapted from Saveri, 2010).

- Conductor. The conductor is a metallic unit whose purpose is carrying the current. It's composed of several strands whose number depends on current characteristics and on the type of material used, typically copper or aluminium.

- Internal semiconducting layer. This semiconducting layer is located between the conductor and the insulant layer of the cable. Its main goal is to evenly distribute the electric field generated by the current passing through the conductor avoiding the direct contact between the conductor and the insulant, since this condition typically can cause electric field concentration in specific points able to break the insulant material. Common materials used for the semiconducting layer are conductive polymers.

- Insulant layer. The insulant layer is used to confine the current in the conductor to prevent possible leakage in the other conductive elements of the cable, which could lead to dangerous conditions threatening the integrity of the cable itself. The most used insulant materials are XLPE (Cross-Linked polyethylene), HDPE (High Density Polyethylene) and HEPR (Hard Ethylene-Propylene Rubber).

- External semiconducting layer: This semiconducting layer is located between the insulant layer and the metallic sheath. The purpose of this layer is to further decrease the risk of electric field concentrations in certain points of the insulant layer. It's usually made of the same material used for the internal layer (conductive polymer).

- Metallic sheath. The metallic sheath has the role of protecting the internal layers of the cable from the introduction of moisture coming from the environment, especially when the cables are buried. It can be made up of a layer of metallic strands or metallic tape, usually aluminium or copper.

- Outer sheath. The outer sheath is used to protect and increase the stiffness of the cable. It's typically made of polymeric materials, e.g. PVC (polyvinyl chloride) or HEPR.

HV single core cables are composed of the same typology of layers just discussed for the MV cables. However, due to the higher operating voltage, they usually have more and bigger conductive strands, as well as more and thicker insulant layers, metallic sheaths and semiconductive layers. In the case of the present study, two types of MV cables and one type of HV cable are used.

The first type of MV cable is employed for the connection between the wind turbines and the transformer substation. This cable has a single core aluminium conductor with XLPE insulation. The metallic sheath consists of aluminium tape longitudinally applied to the cable surface. The semiconducting layers, due to the lack of data, are

supposed to be made of semiconducting XLPE. Polyester non-woven tape is used as water blocking layer. The outer sheath is composed of polyethylene (PE).

The second type of MV cable is employed internally to the transformer substation. This cable has a single core copper conductor with HEPR insulation. The metallic sheath consists of a layer of copper strands applied on the cable surface. The semiconducting layers, due to the lack of data, are supposed to be made of semiconducting HEPR. The outer sheath is composed of PVC.

HV cables have a single core aluminium conductor with XLPE insulation. Two metallic sheaths are present in this case: one consists of a layer of aluminium strands applied on the cable surface, the other consists of aluminium/polyethylene tape longitudinally applied. The semiconductive layers, due to the lack of data, are supposed to be made of semiconducting XLPE. Polyester non-woven tape is used as water blocking layer. The outer sheath is composed of HDPE.

Since the cables are single core, three cables per line have been used. The mass of each material used has been estimated knowing the total length of the cables from the power plant technical documentation, the nominal thickness of each layer and the cable weight per meter from the cables' datasheets (Table 6.18, 6.19). For the implementation of the inventory data in SimaPro several assumptions have been made, due to the lack of suitable processes:

- XLPE and HEPR have been modeled as HDPE.

- For the AL/PE tape (applied longitudinally), a process that involves the allocation of data on the length of the tape instead of the mass has been used. The calculation of the total length was based on the ratio between the reference width of the tape used by the process and the total perimeter of the cylindrical surface to cover: the entire length of the cable, if the tape is not wide enough, must be covered a number of times equal to this ratio (rounded up to the next integer). Using this process, the end-of-life of such material had to be ignored due to the same problem discussed for the turbines' foundations. This simplification was considered acceptable since the mass of the AL/PE tape represents a very small percentage of the HV cable mass, hence the impact associated is expected to be just as small.

- The semiconducting XLPE and HEPR have been modeled as HDPE.

All the processes refer to the *market* dataset.

Table 6.18: Inventory data related to the raw materials used for the HV cables.

Component	Sub-component	Material	Mass per wind farm (t)	Mass per wind farm/FU (t/GWh)	SimaPro process (Ecoinvent database)
Power transmission system	**HV cables**	Aluminium	2.67786	0.00295	Aluminium, primary, ingot {IAI Area, EU27 & EFTA}| market for aluminium, primary, ingot | Cut-off, U
		Semiconducting XLPE	0.66703	0.00074	Polyethylene, high density, granulate {GLO}| market for polyethylene, high density, granulate | Cut-off, U
		XLPE	4.05976	0.00448	Polyethylene, high density, granulate {GLO}| market for polyethylene, high density, granulate | Cut-off, U
		AL/PE	0.02633	0.00003	Sealing tape, aluminium/PE, 50 mm wide {GLO}| market for sealing tape, aluminium/PE, 50 mm wide | Cut-off, U
		Polyester non-woven	0.06974	0.00008	Textile, nonwoven polyester {GLO}| market for textile, nonwoven polyester | Cut-off, U

Table 6.19: Inventory data related to the raw materials used for the MV cables.

Component	Sub-component	Material	Mass per wind farm (t)	Mass per wind farm/FU (t/GWh)	SimaPro process (Ecoinvent database)
Power transmission system	**MV cables (Wind turbines)**	Aluminium	18.32743	0.02021	Aluminium, primary, ingot {IAI Area, EU27 & EFTA}| market for aluminium, primary, ingot | Cut-off, U
		Semiconducting XLPE	4.19318	0.00462	Polyethylene, high density, granulate {GLO}| market for polyethylene, high density, granulate | Cut-off, U
		XLPE	8.30390	0.00916	Polyethylene, high density, granulate {GLO}| market for polyethylene, high density, granulate | Cut-off, U
		HDPE	5.82857	0.00643	Polyethylene, high density, granulate {GLO}| market for polyethylene, high density, granulate | Cut-off, U
		Polyester non-woven	0.46788	0.00052	Textile, nonwoven polyester {GLO}| market for textile, nonwoven polyester | Cut-off, U
	MV cables (Transformer substation)	Copper	0.66125	0.00073	Copper, cathode {GLO}| market for copper, cathode | Cut-off, U
		Semiconducting HEPR	0.06038	0.00007	Polyethylene, high density, granulate {GLO}| market for polyethylene, high density, granulate | Cut-off, U
		HEPR	0.15842	0.00017	Polyethylene, high density, granulate {GLO}| market for polyethylene, high density, granulate | Cut-off, U
		PVC	0.10810	0.00012	Polyvinylchloride, bulk polymerized {GLO}| market for polyvinylchloride, bulk polymerized | Cut-off, U

Copper rope, optic fiber and corrugated pipes

The copper rope used in the HV trenches has a nominal section of 70 mm^2 and it extends for the entire length of the trench. The total mass of copper was obtained multiplying the volume (section · length) for the density, assumed equal to 8960 $\frac{kg}{m^3}$ (pure copper). The mass of the optic fibre, instead, was obtained by multiplying its mass per meter retrieved from the datasheet for the total length between the transformer substation and the wind turbines (MV network) plus the distance between the transformer substation and the primary substation (HV network).

The corrugated pipes used for each single core MV and HV cable present an external diameter of 200 and 160 mm, respectively. As already shown in Figure 6.6, 6.7, the MV cables are placed in a single corrugated pipe, while each HV cable is placed in a separate one. The corrugated pipes used for the optic fibre and copper rope, instead, have an external diameter of 50 and 110 mm, respectively. All the pipes are made of HDPE. The mass per meter of each model of pipe has been retrieved from SolPreA.

Overall, the inventory data used for these 3 items are reported in Table 6.20. Here, due to the lack of data on the optic fibre composition, glass fibre was assumed to be the dominant material. All the processes refer to the *market* dataset.

Table 6.20: Inventory data related to the raw materials used for the copper rope, optic fiber and corrugated pipes.

Component	Sub-component	Material	Mass per wind farm (t)	Mass per wind farm/FU (t/GWh)	SimaPro process (Ecoinvent database)
Power transmission system	**Corrugated pipes**	HDPE	15.00750	0.01655	Polyethylene, high density, granulate {GLO}| market for polyethylene, high density, granulate | Cut-off, U
	Optic fibre	Glass fibre	1.08000	0.00119	Glass fibre {GLO}| market for glass fibre | Cut-off, U
	Copper rope	Copper	0.36000	0.00040	Copper, cathode {GLO}| market for copper, cathode | Cut-off, U

Transformer substation

The transformer substation of the wind power plant is dedicated to the execution of several important functions:

- MV/HV voltage conversion of the electric power produced by the wind turbines. This is done to deliver the power to the primary substation with a voltage compatible with the one of the national grid.

- Connection to the grid. Besides the transformer used for the voltage increase, the substation also contains all the electromechanical components needed for the connection and disconnection to the grid.

- Wind turbines control and monitoring. The substation is equipped with electronic systems that allow through the optic fibre network the management of the turbines' operations in real time based on the data received on the grid, on the turbines' production and on the wind conditions.

As anticipated in the case study description, the internal area of the substation can be divided into 2 sections, as shown in Figure 6.9a. The first one (Section A), paved with limestone gravel, contains the electromechanical components used for the connection to the grid and the voltage conversion. These components include (see Figure 6.9b):

- N. 1 power transformer 16/20 MVA,

- N. 1 headframe,

- N. 3 HV cable terminals,

- N. 6 surge arresters 170 kV,

- N. 1 three-pole disconnector,

- N. 3 voltage transformers 170 kV,

- N. 3 current transformers 170 kV,

- N.1 three-pole switch 170 kV,

- N. 1 neutral cable terminal,

- N. 3 surge arresters 24 kV,

- N. 9 insulators 24 kV.

Each component is supported by galvanized steel beams and it's installed on reinforced concrete foundations.

The second section (Section B), paved with asphalt, contains the two metallic shelters that protect the electronic equipment used for the wind turbines control and monitoring. The shelters, similarly to the electromechanical components, are installed on reinforced concrete foundations.

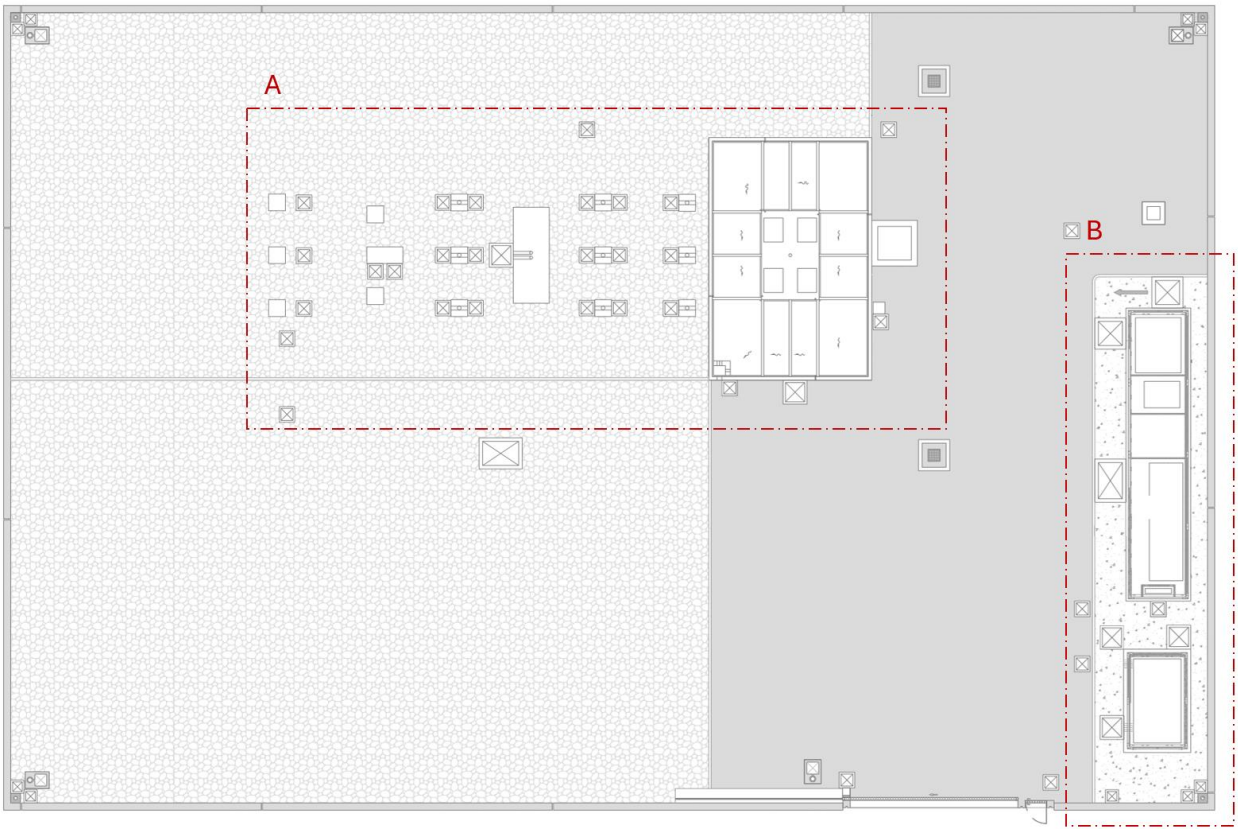

(a) Top view of the transformer substation.

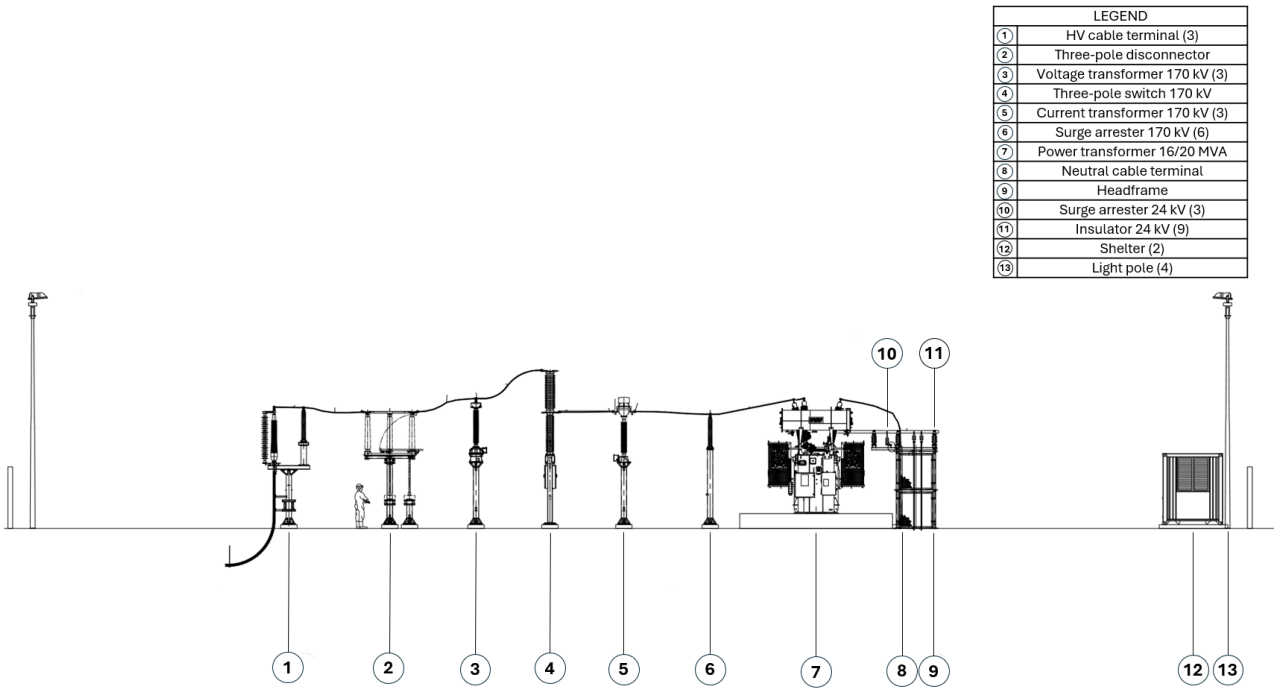

(b) Longitudinal section of the transformer substation.

Figure 6.9: Transformer substation design details (adapted from Project documentation).

Several auxiliary systems allow the proper and safe functioning of the transformer substation. A rainwater drainage system is required to dispose the water built-up in the internal area of the substation (which is open-air). The lighting system, instead, provides the required illumination in the evening and night hours. The 2 shelters also present specific auxiliary systems that have already been mentioned in the case study description (Chapter 3). The internal surface of the transformer substation is delimited by a reinforced concrete wall, while access to the structure is provided by an electric gate.

The transformer substation is the component on which the lowest amount of data was available from the plant documentation. Specifically, the material inventory concerning the electronic equipment in the shelters, the electric gate and all the auxiliary systems of the substation has been impossible to retrieve. For the other items, instead, the inventory was obtained by doing some assumptions, when needed:

- All the volumes of materials required for the civil works of the transformer substation except for the electromechanical components foundations, obtained instead through the bill of quantities concerning these items, was computed starting from the technical drawings available from the plant documentation, including the amount of limestone gravel mined from the quarry internal to the site, the asphalt for the pavement, the concrete used for curbs, platforms and the external walls. The amount of copper used for the grounding of the electric system was known.

- The weight of each electromechanical component, except for the three-pole switch, was given, but insufficient data regarding the material composition were available. For the transformer and the three-pole switch, it was possible to use the data reported in two LCAs dealing with similar products. Specifically, the EPD focused on Tamini's transformer TR 18EN084 25/25/8 MVA and Hitachi's COMPASS I TPO 170 kV three-pole switch were used (Tamini, 2020; Hitachi, 2021). Both EPDs consists in LCA studies "from-cradle-to-grave". Among the impact categories assessed, the carbon footprint and the primary energy consumption were included. In both EPDs the characterization factors used for the carbon footprint was the GWP100 (equal to the case of the present study). For the primary energy consumption, instead, the energy values were expressed per source type (fossil or renewable) using the fuels LHV. When evaluating the CED standard, fuels HHVs are required. According to Frischknecht et al. (2015), the maximum systematic deviation in CED when using fossil fuels and biomass LHV or HHV is 10% (Frischknecht et al., 2015). For this reason, the energy values reported in both EPDs (fossil and renewables) have been conservatively increased by a 10% factor to compute the CED standard.

In each EPD, the impacts related to the Upstream, Core and Downstream phase of the product life cycle are reported. The Upstream phase includes those unit processes that characterize the raw materials acquisition, manufacturing and the transport of components to the assembly facilities (Tamini, 2020). In the Core phase are included the product assembly, testing and disassembly to transport the parts in site (Tamini, 2020). In the Downstream phase is included, instead, the distribution (transport in site), use and end-of-life (Tamini, 2020).

According to the transformer EPD, the use phase is responsible for more than 90% of the total impacts related to the GWP and primary energy consumption (Tamini, 2020). These impacts are associated to the energy losses of the transformer, which need to be balanced by the average electricity mix production. Since the effect of the energy losses of the transformer is already included in the net electric production of the power plant, the relative impacts should be ignored in the case of the present study. Moreover, considering that the use phase impacts accounts as practically the entire Downstream phase, the only phases that appeared to be relevant were the Upstream and Core. The LCA results are reported in the EPD using a reference unit of 25 MVA (nominal power of the transformer) for 1 year of operation (Table 6.21). To use them in the case of the transformer of the present study, whose nominal power and expected life are, respectively, 16 MVA and 25 years, the results need to be multiplied by a factor equal to $\frac{16\,MVA \cdot 25\,y}{25\,MVA \cdot 1\,y} = 16$ (Table 6.22). Following this procedure, the impacts related to the carbon footprint and primary energy consumption for the transformer are accounted for its entire life cycle, as shown in Table 6.23.

Table 6.21: LCIA output for Tamini's transformer. FU=25 MVA, 1 year. Numbers in parenthesis refer to the real contributions used in the present study with the neglection of the use phase (Tamini, 2020).

Impact category		MU	Upstream	Core	Downstream	Total
Global Warming Potential (GWP)	**Fossil CO2eq**	Kg CO2eq	6593	1070	278435 (0)	286098 (7663)
	Biogenic CO2eq	Kg CO2eq	414	58.3	10434 (0)	10906.3 (472.3)
	Land transformation CO2eq	Kg CO2eq	6.49	0.25	21.9 (0)	28.64 (6.74)
	Total CO2eq	Kg CO2eq	6590	1111	280739 (0)	288440 (7701)
Use of primary resources	**Primary energy resources - Renewable**	MJ	11988.1	374	149141.9 (0)	161504 (12362.1)
	Primary energy resources - Non-Renewable	MJ	115676.3	16217.5	4015940.2 (0)	4147834 (131893.8)

Table 6.22: LCIA output for Tamini's transformer referred to the Iurefalco's 16 MVA transformer.

Impact category		MU	Upstream	Core	Downstream	Total
Global Warming Potential (GWP)	**Fossil CO2eq**	Kg CO2eq	105488	17120	0	122608
	Biogenic CO2eq	Kg CO2eq	6624	932.8	0	7556.8
	Land transformation CO2eq	Kg CO2eq	103.84	4	0	107.84
	Total CO2eq	Kg CO2eq	105440	17776	0	123216
Use of primary resources	**Primary energy resources - Renewable**	MJ	191809.6	5984	0	197793.6
	Primary energy resources - Non-Renewable	MJ	1850820.8	259480	0	2110300.8

Table 6.23: Life cycle impacts for the 16 MVA transformer.

Impact category		MU	Upstream	Core	Downstream	Total
Global Warming Potential (GWP)	**Fossil CO2eq**	Kg CO2eq/GWh	116.35039	18.88289	0	135.23328
	Biogenic CO2eq	Kg CO2eq/GWh	7.30609	1.02885	0	8.33494
	Land transformation CO2eq	Kg CO2eq/GWh	0.11453	0.00441	0	0.11894
	Total CO2eq	Kg CO2eq/GWh	116.29745	19.60644	0	135.90389
Use of primary resources	**Primary energy resources - Renewable**	MJ/GWh	211.56076	6.60019	0	218.16095
	Primary energy resources - Non-Renewable	MJ/GWh	2041.40488	286.19937	0	2327.60424

A similar discussion applies for the three-pole switch. According to the EPD, the impacts related to the use phase represent more than 80% of the total GWP and primary energy consumption (Hitachi, 2021). Electric losses account for the entire primary energy consumption of the use phase, while for 60% of the GWP. The remaining 40% of the GWP is represented by the SF6 gas losses (used as insulant in the switch). Following the same reasoning done with the transformer, only the impacts related to SF6 losses during the use phase have been considered. Upstream and Core impacts, instead, have been fully considered. In the case of the three-pole switch, the total impacts for the single component were taken, since it's expected that a similar item has been installed also in the power plant object of the study (Table 6.24 - 6.26).

Table 6.24: LCIA output for Hitachi's three-pole switch. Numbers in parenthesis refer to the real contributions used in the present study with the neglection of the electric losses (Hitachi, 2021).

Impact category		MU	Upstream	Core	Downstream	Total
Global Warming Potential (GWP)	**Fossil CO2eq**	Kg CO2eq	16800	317	35700 (14280)	52817 (31397)
	Biogenic CO2eq	Kg CO2eq	135	1.5	276 (110.4)	412.5 (246.9)
	Land transformation CO2eq	Kg CO2eq	19.8	0.933	3.16 (1.3)	23.893 (22.033)
	Total CO2eq	Kg CO2eq	16954.8	319.433	35979.16 (14391.7)	53253.393 (31665.933)
Use of primary resources	**Primary energy resources - Renewable**	MJ	25000	25700	73100 (0)	123800 (50700)
	Primary energy resources - Non-Renewable	MJ	156000	4820	307000 (0)	467820 (160820)

Table 6.25: LCIA output for Hitachi's three-pole switch referred to the one used in the Iurefalco power plant.

Impact category		MU	Upstream	Core	Downstream	Total
Global Warming Potential (GWP)	**Fossil CO2eq**	Kg CO2eq	16800	317	14280	31397
	Biogenic CO2eq	Kg CO2eq	135	1.5	110.4	246.9
	Land transformation CO2eq	Kg CO2eq	19.8	0.933	1.3	22.033
	Total CO2eq	Kg CO2eq	16954.8	319.433	14391.7	31665.933
Use of primary resources	**Primary energy resources - Renewable**	MJ	25000	25700	0	50700
	Primary energy resources - Non-Renewable	MJ	156000	4820	0	160820

Table 6.26: Life cycle impacts for the three-pole switch.

Impact category		MU	Upstream	Core	Downstream	Total
Global Warming Potential (GWP)	**Fossil CO2eq**	Kg CO2eq/GWh	18.52994	0.34964	15.75045	34.63003
	Biogenic CO2eq	Kg CO2eq/GWh	0.14890	0.00165	0.12177	0.27232
	Land transformation CO2eq	Kg CO2eq/GWh	0.02184	0.00103	0.00143	0.02430
	Total CO2eq	Kg CO2eq/GWh	18.70068	0.35233	15.87365	34.92666
Use of primary resources	**Primary energy resources - Renewable**	MJ/GWh	27.57432	28.34640	0.00000	55.92072
	Primary energy resources - Non-Renewable	MJ/GWh	172.06375	5.31633	0.00000	177.38008

For the other electromechanical components, the material composition was roughly estimated based on the information reported in each component's datasheets. In general, the typologies of insulator used are made of porcelain or glass fibre and silicone, while the metal support is usually in aluminium.

- The mass of the shelters has been assumed to be composed of steel only.

Overall, the inventory data for the considered subcomponents are reported in Table 6.27.

Table 6.27: Inventory data referred to the raw materials used for the transformer substation civil works and electromechanical components (Shelters included).

Component	Sub-component	Material	Mass per wind farm (t)	Mass per wind farm/FU (t/GWh)	SimaPro Process (Ecoinvent database)
Transformer substation	**Civil works**	Concrete	678.32119	0.74817	Concrete block {RoW}| market for concrete block | Cut-off, U
		Reinforcing steel (B450C)	21.98646	0.02425	Reinforcing steel {Europe without Austria}| reinforcing steel production | Cut-off, U
		Asphalt	99.31320	0.10954	Mastic asphalt {GLO}| market for mastic asphalt | Cut-off, U
		Limestone gravel	748.00000	0.82502	Limestone, crushed, for mill {RoW}| limestone production, crushed, for mill | Cut-off, U
		Copper	0.07644	0.00008	Copper, cathode {GLO}| market for copper, cathode | Cut-off, U
	Electromechanical components	Steel	10.00353	0.01103	Steel, low-alloyed {GLO}| market for steel, low-alloyed | Cut-off, U
		Aluminium	1.28440	0.00142	Aluminium, primary, ingot {RoW}| market for aluminium, primary, ingot | Cut-off, U
		Silicone	0.27637	0.00030	Silicone product {RoW}| market for silicone product | Cut-off, U
		Glass fibre	0.13955	0.00015	Glass fibre {GLO}| market for glass fibre | Cut-off, U
		Porcelain	1.06950	0.00118	Ceramic tile {GLO}| market for ceramic tile | Cut-off, U

6.2.3. Components manufacturing

At the end of the *raw materials acquisition* phase, raw materials are ready to be transformed into finished products. In the *components manufacturing* phase, the processes included will deal with all the operations that occur starting from the reception of the raw materials by the first manufacturer to the delivery of the finished products to the location of use. Similarly to the previous life cycle phase, each

procedure carried out for the data collection will be discussed separately for the single main components that characterize the physical system of the wind power plant. It's important to note that each material may undergo multiple manufacturing processes until achieving the desired product, even performed in different locations. For this reason, both production and transport activities must be tracked. In this context, *market* and *transformation* datasets present in Ecoinvent can still be used to properly model the relations between the supplier and the consumer of each product/service.

Wind turbines

Wind turbines manufacturing is quite a complex topic. Components and sub-components undergo several mechanical, thermal and chemical treatments depending on their physical and functional nature. Moreover, given the variability of the possible configurations in terms of materials used (e.g. concrete or steel in the tower, carbon fiber or glass fiber composites in the blades), size (eg. small-scale and large-scale turbines) and applications (e.g. onshore or offshore, higher or lower wind class), the scenario is even more complicated. Finding specific inventory data on manufacturing for the wind turbine model used in the Iurefalco power plant wasn't possible, since typically these are confidential pieces of information managed by the turbine's manufacturer. For this reason, data for this LCI phase were derived from literature sources.

One of the most common approaches used in literature to account for the manufacturing efforts related to wind turbines is based on the data contained in the wind energy section of the Ecoinvent database. In this section, manufacturing processes are assumed on a material basis, as shown in Table 6.28. For each process, it was possible to compute the material efficiency by evaluating the fraction of additional material reported in the Ecoinvent processes required to produce 1 kg of product. According to Ecoinvent, iron and cast iron are the only materials for which no relevant manufacturing processes are required other than the production of the materials themselves. Glass fiber, instead, is expected to be injection moulded. This process has been already included when selecting the material process for glass fiber used in wind turbines (*Glass fibre reinforced plastic, polyamide, injection moulded {GLO}| market for glass fibre reinforced plastic, polyamide, injection moulded | Cut-off, U)*, therefore it was neglected to avoid double counting. Regarding silica, which is used as insulant material in the transformer and generator, due to the lack of information in the Ecoinvent database, only the melting of silica sand required to obtain the desired shape was considered, since it is expected to be the most energy intensive operation. Melting has been assumed to be performed using a gas-fired oven with a thermal efficiency of 90%. The total heat required was computed with:

$$Q\ [MJ] = m\left[\frac{c_p\left(T_f - T_0\right)}{\eta_{th}\cdot 10^6} + \Delta H_{fus}\right] \tag{6.1}$$

Table 6.28: Manufacturing processes used in the wind energy section of the Ecoinvent database.

Material	Manufacturing process	Ecoinvent process	Material efficiency (%)
Steel	Sheet rolling	Sheet rolling, steel {RER}| processing | Cut-off, U	92.1
Cast iron	-	-	-
Iron	-	-	-
Aluminium	Sheet rolling	Sheet rolling, aluminium {RER}| processing | Cut-off, U	98.8
Copper	Wire drawing	Wire drawing, copper {RER}| processing | Cut-off, U	96.2
Fibre glass	Injection moulding	Injection moulding {RER}| processing | Cut-off, U	95

Where m [Kg] is the total mass of silica to melt, $c_p \left[\frac{J}{Kg \cdot K}\right]$ is the mean specific heat of silica sand during heating, assumed to be equal to 710 $\frac{J}{Kg \cdot K}$; T_f [°C] is the melting point of silica, assumed to be equal to 1,710 °C; T_0 [°C] the ambient temperature, assumed to be equal to 25 °C; $\Delta H_{fus} \left[\frac{MJ}{Kg}\right]$ is the latent heat of fusion for silica, assumed to be equal to 1.7 $\frac{MJ}{Kg}$; η_{th} is the thermal efficiency of the oven. Applying eq. 6.1 to the mass of silica contained in the turbine's transformer (459.97 kg) and generator (312.95 kg), a total heat of 1393.38123 MJ and 948.02625 MJ is obtained, respectively.

According to the Ecoinvent processes referring to wind energy, an electric consumption of 0.5 $\frac{kWh}{Kg}$ has been assumed for the assembly of the individual turbine's parts, for a total of 177,260 kWh per turbine. Since the assembly of the nacelle and rotor parts is carried out in Siemens Gamesa factories in Spain, the dataset referring to the Spanish electricity mix (*Electricity, medium voltage {ES}| market for electricity, medium voltage | Cut-off, U*) was used for the respective assemblies. On the other hand, since the tower segments are manufactured in Italy, the dataset referring to the Italian electricity mix (*Electricity, medium voltage {IT}| market for electricity, medium voltage | Cut-off, U*) was used. Moreover, for the steel tower, given the importance of its size, welding was also included in the inventory since typically each segment is made of several rolled steel slabs welded longitudinally and then circumferentially (Figure 6.10).

Figure 6.10: Manufacturing processes for the steel tower (Hyundai Welding, 2023).

The overall welding seams length is estimated to be equal to 3.8 times the tower height (Schreiber et al., 2019), i.e. 93 m in the case of the G114 – 2.5 MW wind turbine. The Ecoinvent process chosen for welding of the steel parts is *Welding, arc, steel {RER}| welding, arc, steel | Cut-off, U*, which require the total length of the seams to allocate the inventory data (353.4 m per turbine). The complete inventory concerning materials and components manufacturing processes is shown in Table 6.29, 6.30.

Table 6.29: Inventory data concerning the material manufacturing processes used for the production of the turbines' components.

Material	Mass per turbine (t)	Mass per wind farm (t)	Mass per wind farm/FU (t/GWh)	SimaPro Process (Ecoinvent database)
Steel	233.48	1,400.88	1.55	Sheet rolling, steel {RER}| processing | Cut-off, U
Cast iron	26.22	157.32	0.17	-
Iron	36.99	221.93	0.24	-
Aluminium	1.39	8.35	0.01	Sheet rolling, aluminium {RER}| processing | Cut-off, U
Copper	8.58	51.47	0.06	Wire drawing, copper {RER}| processing | Cut-off, U
Fibre glass	18.26	109.55	0.12	-

Table 6.30: Inventory data concerning the turbine's components manufacturing processes.

Component	Manufacturing process	Allocation quantity	Value per turbine	Value per wind farm	Value per wind farm/FU	SimaPro Process (Ecoinvent database)
Nacelle and rotor components	Assembly of sub-components	Electric energy (KWh)	84,310	505,860	557.950	Electricity, medium voltage {ES}| market for electricity, medium voltage | Cut-off, U
Tower	Assembly of sub-components	Electric energy (KWh)	92,950	557,700	615.128	Electricity, medium voltage {IT}| market for electricity, medium voltage | Cut-off, U
	Welding	Welding seam length (m)	353.4	2,120.4	2.339	Welding, arc, steel {RER}| welding, arc, steel | Cut-off, U
Transformer	Silica melting	Total fuel heating value (MJ)	1,393.381	8,360.287	9.221	Heat, district or industrial, natural gas {RER}| market group for heat, district or industrial, natural gas | Cut-off, U
Generator	Silica melting	Total fuel heating value (MJ)	948.026	5,688.158	6.274	Heat, district or industrial, natural gas {RER}| market group for heat, district or industrial, natural gas | Cut-off, U

Information on road and sea trips followed by each wind turbine component was retrieved partly from the EPD of the G114 – 2.5 MW wind turbine published by

Siemens Gamesa (Siemens Gamesa Renewable Energy, 2017) and partly from the available plant documentation. In the EPD, the environmental impact related to the life cycle of a hypothetical wind farm composed of 9 G114 – 2.5 MW wind turbines installed in an average European location is assessed (Siemens Gamesa Renewable Energy, 2017). In the "Wind turbine generator manufacturing" section are reported the locations of the manufacturing plants involved in the production of each rotor and nacelle sub-component (see Table 6.31). Since for the nacelle frame and rotor hub no explicit data are present, in the case of these 2 components the *market* dataset of Ecoinvent was used. Specifically, the dataset still refers to the iron and cast iron making processes (described in the *raw materials acquisition* section), since, as already mentioned, no additional manufacturing processes are considered for iron and cast iron parts. Considering that all the components are assembled in the Gamesa Ágreda manufacturing plant, it's assumed that the *market* dataset accounts for all the trips before reaching this location. In Ágreda, the delivery of the turbine's components is organized in: Nacelle, hub and cone, single blades. To the weight of the single components, the one of the equipment that will used in site must be added. These components arrive in Italy via ship. Since no information was available on the harbor of departure, the Barcelona harbor was selected as possible alternative, considering that it's located in the most favorable location to arrive in Italy via ship. The arrival harbor in Italy is located in Taranto. The length of the trip Taranto – Site was known from the power plant documentation. The tower segments are produced in Italy. The corresponding length of the road trip was retrieved from the plant documentation.

As already discussed in the *raw materials acquisition* section, for each road transport whose inventory data weren't computed using the *market* dataset, the Ecoinvent process *Transport, freight, lorry, unspecified {RER}| transport, freight, lorry, all sizes, EURO4 to generic market for transport, freight, lorry, unspecified | Cut-off, U* was selected. The process chosen for the sea transport was, instead, *Transport, freight, sea, container ship {GLO}| market for transport, freight, sea, container ship | Cut-off, U*. Overall, the inventory data concerning the wind turbines transport to the site are shown in Table 6.31, 6.32. The allocation unit used by the *market for transport* datasets in Ecoinvent is tons (of goods) per kilometer, hence all the data are expressed in this way.

Table 6.31: Inventory data related to the wind turbines' components and sub-components transport requirements from the suppliers to the site's location. Note: Trip [r] = road trip. Trip [s] = sea trip.

Component	Sub-component	Trip	Length (Km)	Item weight (t)	t*km
	Frame	(market)	(market)	(market)	(market)
	Main shaft	Vitkovice - Gamesa Ágreda [r]	2,359	9.79	23,094.28
	Cover	INPRE - Gamesa Ágreda [r]	68	4.60	313.24
	Generator	Gamesa Cantarey - Gamesa Ágreda [r]	331	10.43	3,452.93
	Brake system	KTR - Gamesa Ágreda [r]	268	2.06	551.16
	Gearbox	GET ECHESA Asteasu - GET TRELSA Lerma [r]	236	25.68	6,060.08
		GET TRELSA Lerma - Gamesa Ágreda [r]	217	25.68	5,572.20
	Cables	ABB - Gamesa Ágreda [r]	261	3.29	857.77
	Revolving system	Reducel - Gamesa Ágreda [r]	114	7.80	889.53
	Crane	Vicinay - Gamesa Ágreda [r]	261	2.06	536.77
	Transformer	ABB - Gamesa Ágreda [r]	261	11.50	3,001.31
Nacelle		Gamesa Ágreda - Barcellona Port [r]	418	112.14	46,874.10
		Barcellona Port - Taranto Port [s]	1,613	112.14	180,880.21
		Taranto Port - Site [r]	84	112.14	9,400.05
	Hub	(market)	(market)	(market)	(market)
	Cone	INPRE - Gamesa Ágreda [r]	83.8	0.58	39.51
Hub + Cone		Gamesa Ágreda - Barcellona Port [r]	418	30.26	12,648.26
		Barcellona Port - Taranto Port [s]	1,613	30.26	48,807.77
		Taranto Port - Site [r]	84	30.26	2,536.46
Blade (1)		Fiberblade As Somozas - Gamesa Ágreda [r]	663	13.49	8,943.87
		Gamesa Ágreda - Barcellona Port [r]	418	16.85	7,043.30
		Barcellona Port - Taranto Port [s]	1,613	16.85	27,179.05
		Taranto Port - Site [r]	84	16.85	1,412.45
	Tower T1	Italy - Site [r]	312	59.79	18,667.93
	Tower T2	Italy - Site [r]	312	45.01	14,053.25
	Tower T3	Italy - Site [r]	312	38.79	12,111.21
	Tower T4	Italy - Site [r]	312	42.31	13,210.24

Table 6.32: Inventory data related to the wind turbines' components and sub-components transport requirements from the suppliers to the site's location (grouped).

Component	t*km per turbine	t*km per wind farm	t*km per wind farm/FU (t*km/GWh)
Nacelle	281,483.17	1,688,899.03	1,862.81
Hub + cone	64,032.00	384,191.99	423.75
Blades	133,736.01	802,416.08	885.04
Tower	58,042.63	348,255.77	384.12

Wind turbines foundations

The manufacturing processes concerning wind turbines foundations are related to the transformation of copper into copper rope and low-alloyed steel into grouting components, since, as anticipated in the *row materials acquisition* phase, all the other transformation processes are already included in the material processes used for both concrete and reinforcing steel. In Table 6.33 it's illustrated how this was implemented in SimaPro. The manufacturing processes were selected according to what has been discussed in the wind turbines' manufacturing section. The choice of the *market* dataset for copper wire drawing is related to the fact that the supplier of the copper rope is unknown. Regarding the transport of concrete, reinforcing steel and grouting components, instead, the suppliers were known from the plant documentation, therefore the inventory data have been calculated in the same way illustrated in the previous paragraph. The complete inventory data are contained in Table 6.34.

Table 6.33: Inventory data concerning the manufacturing processes used for the production of the copper rope and grouting components used in the turbines' foundations.

Component	Sub-component	Material	Mass per wind farm/FU (t/GWh)	SimaPro Process (Ecoinvent database)
Foundation 1	Copper rope	Copper	0.04	Wire drawing, copper {GLO}| market for wire drawing, copper | Cut-off, U
	Grouting components	Steel	0.01	Sheet rolling, steel {RER}| processing | Cut-off, U
Foundation 2	Copper rope	Copper	0.02	Wire drawing, copper {GLO}| market for wire drawing, copper | Cut-off, U
	Grouting components	Steel	0.02	Sheet rolling, steel {RER}| processing | Cut-off, U

Table 6.34: Inventory data related to the transport requirements characterizing the concrete, reinforcing steel and grouting components used in the turbines' foundations, from the suppliers to the site's location.

Component	Material/Sub-component	Transport type	Length (Km)	Mass per wind farm/FU (t/GWh)	t*km per wind farm/FU (t*km/GWh)
Foundation 1	Concrete 50 MPa	Road	15.2	0.32	4.83
	Concrete 40 MPa	Road	15.2	7.22	109.77
	Concrete 20 MPa	Road	15.2	0.68	10.30
	Reinforcing steel (B450C)	Road	108.8	0.41	44.73
	Grouting components	Road	108.8	0.01	1.43
Foundation 2	Concrete 50 MPa	Road	15.2	0.16	2.41
	Concrete 40 MPa	Road	15.2	2.90	44.11
	Concrete 20 MPa	Road	15.2	0.36	5.52
	Reinforcing steel (B450C)	Road	108.8	0.22	23.49
	Grouting components	Road	108.8	0.02	1.68

Wind turbines platforms

As anticipated in the *row materials acquisition* phase, the materials used in the wind turbines platforms don't need further transformations to be employed, therefore the inventory related to this section is empty. Regarding transport, instead, even if the limestone quarry used for the extraction activities is located internally to the site, since the weight of the limestone extracted is very high, its contribution has been accounted by assuming a mean transport distance equal to the one between the quarry and the 4 accesses to the site, equal to 2.1 km, as shown in Table 6.35.

Table 6.35: Inventory data related to the transport requirements characterizing each material used in the turbines' platforms, from the suppliers to the site's location.

Component	Material	Transport type	Length (Km)	Mass per wind farm/FU (t/GWh)	t*km per wind farm/FU (t*km/GWh)
Platforms	Limestone gravel	Road	2.1	15.41	32.36

Internal roads

Similarly to the case of wind turbines platforms, the materials used in the internal roads of the site don't need further transformations to be employed, therefore the

inventory related to this section is empty. The calculations regarding transport have also been done in the same way (Table 6.36).

Table 6.36: Inventory data related to the transport requirements characterizing each material used in the internal roads, from the suppliers to the site's location.

Component	Material	Transport type	Length (Km)	Mass per wind farm/FU (t/GWh)	t*km per wind farm/FU (t*km/GWh)
Internal roads	Limestone gravel	Road	2.1	14.06	29.53
	Limestone bricks	Road	2.1	1.71	3.59

External Roads

The processes used for the acquisition of the materials employed in the external roads construction already contain all the transformations needed to obtain the finished products, therefore the inventory related to this section is empty. Moreover, since the materials are directly used for the construction activities, the *market* dataset used in the *raw materials acquisition* phase already accounts for the transport inventory requirements.

Cable trenches and power transmission system

Also in this case, the processes used for the acquisition of the materials employed in the HV and MV trenches construction already contain all the transformations required to obtain the finished products, therefore the inventory related to this section is empty. For the transport activities, while the supplier of the asphalt was unknown (hence, the *market* dataset has been used), the others were known from the plant documentation. The same assumptions used for limestone transportation in the wind turbines platforms section were applied also here. The data regarding this part are contained in Table 6.37.

Table 6.37: Inventory data related to the transport requirements characterizing each material used in the cable trenches, from the suppliers to the site's location.

Component	Sub-component	Material	Transport type	Length (Km)	Mass per wind farm/FU (t/GWh)	t*km per wind farm/FU (t*km/GWh)
Cable trenches	**HV and MV trenches**	Limestone sand	Road	2.1	3.91	8.22
		Asphalt	(market)	(market)	(market)	(market)
		Concrete 30 Mpa	Road	15.2	1.49	22.67
	Walls	Limestone bricks	Road	2.1	0.08	0.17

The manufacturing processes concerning the materials used in cables are mainly related to the transformation of metals in strands and polymers in pipes, therefore, processes dealing with wire drawing and pipe extrusion have been selected in Ecoinvent (Table 6.38). For aluminium, copper wire drawing was chosen as proxy transformation since processes referring specifically to aluminium were not available. All the processes belong to the *transformation* dataset of Ecoinvent, since the locations of the manufacturers were known from the plant documentation.

Transport from manufacturers to site of the HV cables and the MV cables used in the transformer substation involved both sea and road transport. The MV cables used for the turbines, instead, were transported only by road. The transport requirements are contained in Table 6.39. In this case, for sea transport, the process *Transport, freight, sea, ferry {GLO}| market for transport, freight, sea, ferry | Cut-off, U* has been used.

Table 6.38: Inventory data concerning the manufacturing processes used for the production of the MV and HV cables.

Material	Manufacturing process	Ecoinvent process	Mass per wind farm/FU (t/GWh)
Aluminium Copper	Wire drawing	Wire drawing, copper {RER}| wire drawing, copper | Cut-off, U	0.024
Semiconducting XLPE XLPE HDPE Semiconducting HEPR HEPR PVC	Pipe extrusion	Extrusion, plastic pipes {RER}| extrusion, plastic pipes | Cut-off, U	0.026

Table 6.39: Inventory data related to the transport requirements characterizing the MV and HV cables used in the power transmission system, from the suppliers to the site's location.

Component	Sub-component	Transport type	t*km per wind farm	t*km per wind farm/FU (t*km/GWh)
Power transmission system	**MV cables (Wind turbines)**	Road	6923.06	7.64
	MV cables (Transformer substation)	Road	522.14	0.58
		Sea	6.42	0.01
	HV cables	Road	10527.7	11.61
		Sea	2393.92	2.64

The materials used to produce the corrugated pipes and the copper rope, similarly to the cables, are mainly involved in pipe extruding and wire drawing operations, respectively. The glass fibre used in the optic fiber, instead, is expected to not undergo any additional process. The inventory data concerning this part are contained in Table 6.40. The *market* dataset was used for wire drawing since the supplier of the copper rope and optic fibre is unknown. For the optic fibre, instead, due to what has been just discussed, the *market* dataset belonging to the glass fibre material process is expected

to account for all the transport requirements up to the delivery of the product to the site's location, i.e. the location of the consumer.

Table 6.40: Inventory data concerning the manufacturing processes used for the production of the corrugated pipes and the copper rope used in the power transmission system.

Component	Sub-component	Material	Manufacturing process	Ecoinvent process	Mass per wind farm/FU (t/GWh)
Power transmission system	**Corrugated pipes**	HDPE	Pipe extrusion	Extrusion, plastic pipes {RER}| extrusion, plastic pipes | Cut-off, U	0.0165
	Copper rope	Copper	Wire drawing	Wire drawing, copper {GLO}| market for wire drawing, copper | Cut-off, U	0.0004

For the corrugated pipes, instead, the supplier was retrieved from the plant documentation. The transport requirements are reported in Table 6.41.

Table 6.41: Inventory data related to the transport requirements characterizing the corrugated pipes used in the power transmission system, from the suppliers to the site's location.

Component	Sub-component	Transport type	Length (Km)	Mass per wind farm/FU (t/GWh)	t*km per wind farm/FU (t*km/GWh)
Power transmission system	**Corrugated pipes**	Road	590	0.02	9.77

Transformer substation

The processes used for the acquisition of the materials employed in the transformer substation civil works already own the required transformations to obtain the finished products, therefore also in this case the inventory related to this section is empty. Transport has been accounted for all the materials except limestone using the *market* dataset, since the suppliers were unknown. The inventory data regarding limestone transport requirements are contained in Table 6.42.

Table 6.42: Inventory data related to the transport requirements characterizing the limestone gravel used in the transformer substation, from the suppliers to the site's location.

Component	Sub-component	Material	Transport type	Length (Km)	Mass per wind farm/FU (t/GWh)	t*km per wind farm/FU (t*km/GWh)
Transformer substation	**Civil works**	Limestone gravel	Road	2.1	0.83	1.73

Considering the type of material processes selected for the electromechanical components, the only relevant manufacturing processes worth considering involve the amount of steel and aluminium used. As first approximation, the same manufacturing processes used for the wind turbines were used. The *transformation* dataset has been selected since the supplier of each component was known from the plant documentation (Table 6.43).

Table 6.43: Inventory data concerning the manufacturing processes used for the production of the electromechanical components employed in the transformer substation.

Component	Sub-component	Material	Manufacturing process	Ecoinvent process	Mass per wind farm/FU (t/GWh)
Transformer substation	**Electromechanical components**	Steel	Sheet rolling	Sheet rolling, steel {RER}| sheet rolling, steel | Cut-off, U	0.011
		Aluminium	Sheet rolling	Sheet rolling, aluminium {RoW}| sheet rolling, aluminium | Cut-off, U	0.001

The transport requirements of the electromechanical components have been aggregated, as done with the MV and HV cables, in road and sea transport, as shown in Table 6.44. In this case, the process used for the sea transport is *Transport, freight, sea, container ship {GLO}\| market for transport, freight, sea, container ship \| Cut-off, U.*

Table 6.44: Inventory data related to the transport requirements characterizing the electromechanical components employed in the transformer substation, from the suppliers to the site's location.

Component	Sub-component	Type of transport	t*km per wind farm	t*km per wind farm/FU (t*km/GWh)
Transformer substation	**Electromechanical components**	Road	7395.20	8.16
		Sea	15495.53	17.09

6.2.4. Components assembly and installation

When all the components, equipment and materials arrive at the construction site, building works are required for the installation of each main item of the wind power plant. Specifically, in the *components assembly and installation* phase, the attention is focused on the energy demand related to the building machinery employed in the site and in those external areas that require adjustments to make the special transports possible.

The construction activities started on 01.03.2021 and ended on 15.11.2022. From the power plant documentation, it was possible to retrieve the daily reports concerning the activities performed from the first to the last working day. Each report contains the type of activity performed, building machinery used and hours worked. To obtain the inventory data related to the total energy consumption and the corresponding GHG emissions, the methodology suggested in the "Air pollutant emission inventory guidebook 2023" by the European Environment Agency (EEA) for the European Monitoring and Evaluation Programme (EMEP) was followed (EEA, 2023b). In Part B section 1.A.4, this document provides guidance for the estimation of combustion and evaporative emissions driven by the operation of non-road mobile machinery (NRMM) (EEA, 2023b). The EEA suggests 3 possible methods depending on the type of available data concerning the equipment used, as shown in Figure 6.11.

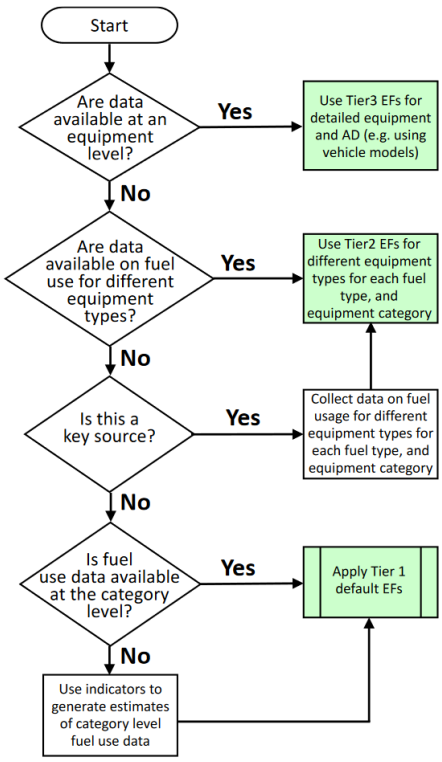

Figure 6.11: Procedure used to select the most appropriate method for the estimation of the pollutant emissions from NRMM (EEA, 2023b).

If the level of detail of the information is high, more accurate methodologies are suggested (EEA, 2023b). Since in the case of the present study data were available at an equipment level, i.e. including operational data and size of the engine, the tier 3 methodology was used (EEA, 2023b). The tier 3 methodology evaluates the mass of emissions of the generic pollutant "i" caused by NRMM activities as (EEA, 2023b):

$$E\ [g] = N \cdot H \cdot P \cdot (1 + DFA) \cdot LFA \cdot EF \tag{6.2}$$

where E is the mass of the emissions related to the "i" pollutant, N is the number of engines, H is the number of hours worked by each machine, P [kW] is the power of the engine, DFA is the deterioration factor adjustment, LFA is the load factor adjustment and $EF\ \left[\frac{g}{kWh}\right]$ is the base emission factor for the "i" pollutant (EEA, 2023b). The base emission factors depend on several aspects, including the fuel (e.g. diesel or gasoline) and the technology level of the engine (EEA, 2023b). Since diesel is the type of fuel used by all the NRMM in the construction site, EFs for diesel machinery have been considered. The EFs contained in the guidebook refer to the following technology levels: < 1981, 1981–1990, 1991–Stage I, Stage I, II, IIIA, IIIB, IV and V. The Stages from I to V are associated to specific limitations on pollutant emissions established by the European Commission for diesel NRMM starting from machinery registered in 1999 (Stage I) to 2019 and beyond (Stage V), as shown in Figure 6.12 (EEA, 2023b). It's worth noting that these limitations don't depend exclusively on the technology but also on the engine rated power, since typically more powerful engines are also more efficient.

For the purpose of the present study, given that the exact technology level of each machine wasn't known, the use of NRMM belonging to Stage V was conservatively excluded, while it was assumed that every machine used in the construction site should have had an engine whose emissions at nominal load are consistent with the technology level right before the most recent one. This technology level depends on the specific rated power of the engine, since, as shown in Figure 6.12, Stages requirements don't apply for any power class but only for those to which the EU Directive explicitly refers. Therefore, for the power classes to which belongs the NRMM used in the construction site, the technology levels assumed are reported in Table 6.45.

Table 2-3 Overview of EU directive requirements relevant for emissions control from diesel-fuelled non-road machinery

Stage	Engine size	CO	VOC	NO_x	$VOC+NO_x$	PM	Diesel machinery			Tractors	
							EU Directive	Implement. date Transient	Implement. date Constant	EU Directive	Implement. Date
	[kW]			[g/kWh]							
Stage I											
A	130<=P<560	5	1.3	9.2	-	0.54	97/68	1/1 1999	-	2000/25	1/7 2001
B	75<=P<130	5	1.3	9.2	-	0.7		1/1 1999	-		1/7 2001
C	37<=P<75	6.5	1.3	9.2	-	0.85		1/4 1999	-		1/7 2001
Stage II											
E	130<=P<560	3.5	1	6	-	0.2	97/68	1/1 2002	1/1 2007	2000/25	1/7 2002
F	75<=P<130	5	1	6	-	0.3		1/1 2003	1/1 2007		1/7 2003
G	37<=P<75	5	1.3	7	-	0.4		1/1 2004	1/1 2007		1/1 2004
D	18<=P<37	5.5	1.5	8	-	0.8		1/1 2001	1/1 2007		1/1 2002
Stage IIIA											
H	130<=P<560	3.5	-	-	4	0.2	2004/26	1/1 2006	1/1 2011	2005/13	1/1 2006
I	75<=P<130	5	-	-	4	0.3		1/1 2007	1/1 2011		1/1 2007
J	37<=P<75	5	-	-	4.7	0.4		1/1 2008	1/1 2012		1/1 2008
K	19<=P<37	5.5	-	-	7.5	0.6		1/1 2007	1/1 2011		1/1 2007
Stage IIIB											
L	130<=P<560	3.5	0.19	2	-	0.025	2004/26	1/1 2011	-	2005/13	1/1 2011
M	75<=P<130	5	0.19	3.3	-	0.025		1/1 2012	-		1/1 2012
N	56<=P<75	5	0.19	3.3	-	0.025		1/1 2012	-		1/1 2012
P	37<=P<56	5	-	-	4.7	0.025		1/1 2013	-		1/1 2013
Stage IV											
Q	130<=P<560	3.5	0.19	0.4	-	0.025	2004/26	1/1 2014	1/1 2014	2005/13	1/1 2014
R	56<=P<130	5	0.19	0.4	-	0.025		1/10 2014	1/10 2014		1/10 2014
Stage V[A]											
NRE-v/c-7	P>560	3.5	0.19	3.5		0.045	2016/1628		2019		2019
NRE-v/c-6	130≤P≤560	3.5	0.19	0.4		0.015			2019		2019
NRE-v/c-5	56≤P<130	5.0	0.19	0.4		0.015			2020		2020
NRE-v/c-4	37≤P<56	5.0			4.7	0.015			2019		2019
NRE-v/c-3	19≤P<37	5.0			4.7	0.015			2019		2019
NRE-v/c-2	8≤P<19	6.6			7.5	0.4			2019		2019
NRE-v/c-1	P<8	8.0			7.5	0.4			2019		2019
Generators	P>560	0.67	0.19	3.5		0.035			2019		2019

A = For selected machinery types, Stage V includes emission limit values for particle number.

Figure 6.12: Overview of the Stages concerning the limitations on pollutants emissions for NRMM imposed by the European Commission (EEA, 2023b).

Table 6.45: Technology levels chosen for the power classes involved in the construction site.

Power [kW] / Technology level	8≤P<19	19≤P<37	37≤P<56	56≤P<75	75≤P<130	130≤P<560
Stage	V	IIIA	IIIB	IV	IV	IV

Machines with power included between 8 and 19 kW still presents a technology level consistent with the Stage V prescriptions, but only for the reason that the previous regulation concerning this type of machines refers to machines registered between 1991 and 1999 (Stage I), which was considered too much detrimental for the analysis.

The *EFs* are gathered in Figure 6.13 depending on the engine power and technology level for the main pollutants deriving from diesel combustion: NOx, VOC, CH4, CO,

N2O, NH3, PM, PM10, PM2.5, BC (Black Carbon)[4]. Particular attention is also given to CO2 and SO2, even though the estimation of the emissions deriving from these two pollutants will be done in a different way starting from the fuel consumption of the NRMM, since, as reported in the guidebook, they can be considered as independent from the engine technology and size (EEA, 2023b).

Table 3-6 Baseline emission factors and fuel consumption (FC) for diesel NRMM [g/kWh]

Engine Power (kW)	Technology Level	NO_x	VOC	CH_4	CO	N_2O	NH_3	PM	PM_{10}	$PM_{2.5}$	BC	FC
P<8	<1981	12.00	5.00	0.120	7.00	0.035	0.002	2.800	2.800	2.800	1.540	300
P<8	1981-1990	11.50	3.80	0.091	6.00	0.035	0.002	2.300	2.300	2.300	1.265	285
P<8	1991-Stage I	11.20	2.50	0.060	5.00	0.035	0.002	1.600	1.600	1.600	0.880	270
P<8	Stage V	6.08	0.68	0.016	4.80	0.035	0.002	0.400	0.400	0.400	0.320	270
8<=P<19	<1981	12.00	5.00	0.120	7.00	0.035	0.002	2.800	2.800	2.800	1.540	300
8<=P<19	1981-1990	11.50	3.80	0.091	6.00	0.035	0.002	2.300	2.300	2.300	1.265	285
8<=P<19	1991-Stage I	11.20	2.50	0.060	5.00	0.035	0.002	1.600	1.600	1.600	0.880	270
8<=P<19	Stage V	6.08	0.68	0.016	3.96	0.035	0.002	0.400	0.400	0.400	0.320	270
19<=P<37	<1981	18.00	2.50	0.060	6.50	0.035	0.002	2.000	2.000	2.000	1.100	300
19<=P<37	1981-1990	18.00	2.20	0.053	5.50	0.035	0.002	1.400	1.400	1.400	0.770	281
19<=P<37	1991-Stage I	9.80	1.80	0.043	4.50	0.035	0.002	1.400	1.400	1.400	0.770	262
19<=P<37	Stage II	6.50	0.60	0.014	2.20	0.035	0.002	0.400	0.400	0.400	0.320	262
19<=P<37	Stage IIIA	6.08	0.60	0.014	2.20	0.035	0.002	0.400	0.400	0.400	0.320	262
19<=P<37	Stage V	3.81	0.42	0.010	2.20	0.035	0.002	0.015	0.015	0.015	0.002	262
37<=P<56	<1981	7.70	2.40	0.058	6.00	0.035	0.002	1.800	1.800	1.800	0.990	290
37<=P<56	1981-1990	8.60	2.00	0.048	5.30	0.035	0.002	1.200	1.200	1.200	0.660	275
37<=P<56	1991-Stage I	11.50	1.50	0.036	4.50	0.035	0.002	0.800	0.800	0.800	0.440	260
37<=P<56	Stage I	7.70	0.60	0.014	2.20	0.035	0.002	0.400	0.400	0.400	0.320	260
37<=P<56	Stage II	5.50	0.40	0.010	2.20	0.035	0.002	0.200	0.200	0.200	0.160	260
37<=P<56	Stage IIIA	3.81	0.40	0.010	2.20	0.035	0.002	0.200	0.200	0.200	0.160	260
37<=P<56	Stage IIIB	3.81	0.28	0.007	2.20	0.035	0.002	0.025	0.025	0.025	0.020	260
37<=P<56	Stage V	3.81	0.28	0.007	2.20	0.035	0.002	0.015	0.015	0.015	0.002	260
56<=P<75	<1981	7.70	2.40	0.058	6.00	0.035	0.002	1.800	1.800	1.800	0.990	290
56<=P<75	1981-1990	8.60	2.00	0.048	5.30	0.035	0.002	1.200	1.200	1.200	0.660	275
56<=P<75	1991-Stage I	11.50	1.50	0.036	4.50	0.035	0.002	0.800	0.800	0.800	0.440	260
56<=P<75	Stage I	7.70	0.60	0.014	2.20	0.035	0.002	0.400	0.400	0.400	0.320	260
56<=P<75	Stage II	5.50	0.40	0.010	2.20	0.035	0.002	0.200	0.200	0.200	0.160	260
56<=P<75	Stage IIIA	3.81	0.40	0.010	2.20	0.035	0.002	0.200	0.200	0.200	0.160	260
56<=P<75	Stage IIIB	2.97	0.28	0.007	2.20	0.035	0.002	0.025	0.025	0.025	0.020	260
56<=P<75	Stage IV	0.40	0.28	0.007	2.20	0.035	0.002	0.025	0.025	0.025	0.020	260
56<=P<75	Stage V	0.40	0.13	0.003	2.20	0.035	0.002	0.015	0.015	0.015	0.002	260
75<=P<130	<1981	10.50	2.00	0.048	5.00	0.035	0.002	1.400	1.400	1.400	0.770	280
75<=P<130	1981-1990	11.80	1.60	0.038	4.30	0.035	0.002	1.000	1.000	1.000	0.550	268
75<=P<130	1991-Stage I	13.30	1.20	0.029	3.50	0.035	0.002	0.400	0.400	0.400	0.220	255
75<=P<130	Stage I	8.10	0.40	0.010	1.50	0.035	0.002	0.200	0.200	0.200	0.160	255
75<=P<130	Stage II	5.20	0.30	0.007	1.50	0.035	0.002	0.200	0.200	0.200	0.160	255
75<=P<130	Stage IIIA	3.24	0.30	0.007	1.50	0.035	0.002	0.200	0.200	0.200	0.160	255
75<=P<130	Stage IIIB	2.97	0.13	0.003	1.50	0.035	0.002	0.025	0.025	0.025	0.020	255
75<=P<130	Stage IV	0.40	0.13	0.003	1.50	0.035	0.002	0.025	0.025	0.025	0.020	255
75<=P<130	Stage V	0.40	0.13	0.003	1.50	0.035	0.002	0.015	0.015	0.015	0.002	255
130<=P<560	<1981	17.80	1.50	0.036	2.50	0.035	0.002	0.900	0.900	0.900	0.450	270
130<=P<560	1981-1990	12.40	1.00	0.024	2.50	0.035	0.002	0.800	0.800	0.800	0.400	260
130<=P<560	1991-Stage I	11.20	0.50	0.012	2.50	0.035	0.002	0.400	0.400	0.400	0.200	250
130<=P<560	Stage I	7.60	0.30	0.007	1.50	0.035	0.002	0.200	0.200	0.200	0.140	250
130<=P<560	Stage II	5.20	0.30	0.007	1.50	0.035	0.002	0.100	0.100	0.100	0.070	250
130<=P<560	Stage IIIA	3.24	0.30	0.007	1.50	0.035	0.002	0.100	0.100	0.100	0.070	250
130<=P<560	Stage IIIB	1.80	0.13	0.003	1.50	0.035	0.002	0.025	0.025	0.025	0.018	250
130<=P<560	Stage IV	0.40	0.13	0.003	1.50	0.035	0.002	0.025	0.025	0.025	0.018	250
130<=P<560	Stage V	0.40	0.13	0.003	1.50	0.035	0.002	0.015	0.015	0.015	0.002	250
P>560	Stage V	3.50	0.13	0.003	1.50	0.035	0.002	0.045	0.045	0.045	0.002	250

Figure 6.13: Emission factors for diesel NRMM (EEA, 2023b).

[4] Particulate emissions (PM, PM10, PM2.5, BC) have been included in the inventory only for the sake of completeness, since their effect on the global warming is not considered by the IPCC 2021 GWP100 method (IPCC).

Fuel consumption is estimated using a separate coefficient which is managed in the same way as the emission factor. Just like them, in fact, the fuel consumption coefficient (FC) is expressed in $\frac{g}{kWh}$, therefore, using eq. 6.2, it was possible to evaluate not only the pollutants emissions but also the total amount of diesel fuel consumed during the construction activities.

The load factor and the deterioration factor adjustments depend on the specific pollutant considered. Since in real applications NRMM doesn't work constantly at rated power, the load factor expresses the fraction represented by the mean operating power in respect to the rated one $\left(LF = \frac{P_{mean}}{P_{rated}}\right)$. The power to use as P in eq. 6.2 is in fact equal to $P = P_{rated} \cdot LF = P_{mean}$. To conservatively account for this phenomenon, a LF equal to 0.67 was chosen for every machine used. The corresponding load factor adjustments for the affected pollutants in function of the engine technology level are contained in Figure 6.14. Considering the technology levels and the load factor chosen, it's evident that the EFs that will be affected by the LFA will be only those related to the 19≤P<37 power class (Stage IIIA), since all the other EFs refers to power classes whose technology level is IIIB or higher. Moreover, as shown in Figure 6.14, also the fuel consumption of the 19≤P<37 class will be slightly affected.

Table 3-14 Transient operation adjustment factors for diesel engines

Technology Level	Load	Load factor	NO_x	VOC	CO	TSP	FC
Stage II and prior	High	>0.45	0.95	1.05	1.53	1.23	1.01
Stage IIIA	High	>0.45	1.04	1.05	1.53	1.47	1.01
Stage IIIB-V	High	>0.45	1	1	1	1	1
Stage II and prior	Middle	0.25≤LF≤0.45	1.025	1.67	2.05	1.6	1.095
Stage IIIA	Middle	0.25≤ LF≤0.45	1.125	1.67	2.05	1.92	1.095
Stage IIIB-V	Middle	0.25≤ LF≤0.45	1	1	1	1	1
Stage II and prior	Low	<0.25	1.1	2.29	2.57	1.97	1.18
Stage IIIA	Low	<0.25	1.21	2.29	2.57	2.37	1.18
Stage IIIB-V	Low	<0.25	1	1	1	1	1

Figure 6.14*: Load factor adjustments for the affected pollutants. Note: TSP = Total Suspended Particles = PM (Particulate matter with diameter > 10 μm) (EEA, 2023b).*

The deterioration factor is calculated as (EEA, 2023b):

$$DF = \frac{K}{LT} \cdot DF \tag{6.3}$$

Where DF is the deterioration factor, K is the engine age expressed with a number between 0 and the average machine lifetime (in years), LT is the average machine lifetime (in years) and DF is the maximum deterioration factor for the affected pollutants, reported in Figure 6.15 (EEA, 2023b).

Table 3-11 Deterioration factors for diesel machinery relative to average engine life time

Emission Level	NO_x	VOC	CO	TSP
Before Stage I	0.024	0.047	0.185	0.473
Stage I	0.024	0.036	0.101	0.473
Stage II	0.009	0.034	0.101	0.473
Stage IIIA, IIIB, IV, V	0.008	0.027	0.151	0.473

Figure 6.15: Maximum deterioration factors corresponding to the average engine lifetime for diesel NRMM (EEA, 2023b).

Supposing an intermediate engine age between the "as new" condition and its average lifetime for all the machines $\left(\frac{K}{LT} = 0.5\right)$, the DFs become as shown in Table 6.46.

Table 6.46: Deterioration factors related to an intermediate engine age.

Emission Level	NOx	VOC	CO	TSP
Before Stage I	0.012	0.0235	0.0925	0.2365
Stage I	0.012	0.018	0.0505	0.2365
Stage II	0.0045	0.017	0.0505	0.2365
Stage IIIA, IIIB, IV, V	0.004	0.0135	0.0755	0.2365

Given the technology levels selected for the NRMM employed in the construction site (Table 6.45), the DFs used in eq. 6.2 belong exclusively to the last row of Table 6.46.

The model, the rated power and the hours worked by each NRMM were retrieved from the daily reports of the construction activities found in the available plant documentation. It was possible to subdivide the activities into 4 groups: wind turbines erection and platforms construction, cable trenches and internal roads construction, external roads adjustments and transformer substation construction. In Table 6.47 are shown the total number of hours worked by each type of machine ($N \cdot H$ in eq. 6.2) for the specific activity group, together with their rated power. The baseline EFs contained in Figure 6.13 have been corrected, for the power classes involved by the NRMM used in the construction site, using the load and deterioration factors illustrated before. The final EFs are reported in Table 6.48. Finally, the emissions related to the i pollutant for the generic k activity have been computed using:

$$E_{i,k} = \sum_{m=Excavator\ 1}^{N=Trencher} E_{i,k,m} \qquad \forall\, i,k = \begin{cases} i = Pollutants \\ k = Activities \end{cases} \tag{6.4}$$

where $E_{i,k}$ [g] represents the mass value of the emission obtained using eq. 6.2 and m is the type of machine whose contribution is summed to those of the other listed in Table 6.47 for the k activity. As already specified, following this procedure it was also computed the total diesel consumption FC_k related to the single activities. The resulting $E_{i,k}$ and FC_k are shown (in kg) for each activity in Table 6.49.

Table 6.47: Total number of hours worked by each type of machine (N·H) for the specific activity groups.

Activity group / NRMM	Wind turbines and platforms (h)	Cable trenches and internal roads (h)	External roads (h)	Transformer substation (h)	Total (h)	Rated power (kW)
Excavator 1	223	784	256	0	1263	51.8
Excavator 2	381	622	20	5	1028	115.0
Excavator 3	104	320	0	0	424	40.9
Roller	49	102	41	104	296	108.7
Excavator 4	561	365	0	296	1222	89.0
Telescopic handler	14	24	0	104	142	64.0
Grader	20	75	0	0	95	152.5
Mini excavator	5	305	80	56	446	18.2
Excavator 5	0	5	0	0	5	203.7
Asphalt scraper	0	16	0	0	16	251.0
Asphalt paver	0	13	0	0	13	110.0
Excavator 6	30	157	111	6	304	33.6
Skid steer loader	34	72	0	0	106	55.4
Excavator 7	215	0	0	0	215	229.0
Pump (for concrete)	36	0	0	0	36	160.0
Crane 1	196	0	0	0	196	205.0
Crane 2	256	0	0	0	256	300.0
Trencher	0	393	0	0	393	205.1

Table 6.48: The emission factors used in eq 4.2 corrected using the load factor and deterioration factor adjustments.

Power [kW] / Technology level / Pollutant	8<=P<19 Stage V [g/kWh]	19<=P<37 Stage IIIA [g/kWh]	37<=P<56 Stage IIIB [g/kWh]	56<=P<75 Stage IV [g/kWh]	75<=P<130 Stage IV [g/kWh]	130<=P<560 Stage IV [g/kWh]
NOx	6.1043	6.3485	3.8252	0.4016	0.4016	0.4016
VOC	0.6892	0.6385	0.2838	0.2838	0.1318	0.1318
CH4	0.0160	0.0140	0.0070	0.0070	0.0030	0.0030
CO	4.2590	3.6201	2.3661	2.3661	1.6133	1.6133
N2O	0.0350	0.0350	0.0350	0.0350	0.0350	0.0350
NH3	0.0020	0.0020	0.0020	0.0020	0.0020	0.0020
PM	0.4946	0.7271	0.0309	0.0309	0.0309	0.0309
PM10	0.4000	0.4000	0.0250	0.0250	0.0250	0.0250
PM2.5	0.4000	0.4000	0.0250	0.0250	0.0250	0.0250
BC	0.3200	0.3200	0.0200	0.0200	0.0200	0.0180
FC	270.0000	264.6200	260.0000	260.0000	255.0000	250.0000

Table 6.49: Pollutant emissions and fuel consumption (in kg) related to each activity group performed in the construction site.

Activity group / Pollutant	Wind turbines and platforms [kg]	Cable trenches and internal roads [kg]	External roads [kg]	Transformer substation [kg]
NOx	123.9865	250.8796	57.6230	17.1018
VOC	28.2028	34.9368	5.3856	5.1966
CH4	0.6485	0.8161	0.1264	0.1209
CO	328.4299	353.4067	41.5262	55.2642
N2O	6.8891	6.6518	0.5910	1.0811
NH3	0.3937	0.3801	0.0338	0.0618
PM	6.5830	10.0600	2.7139	1.3655
PM10	5.1969	7.4714	1.7250	1.0789
PM2.5	5.1969	7.4714	1.7250	1.0789
BC	3.9230	5.8470	1.3800	0.8631
FC	49,675.4612	48,426.1062	4,389.0449	7,910.1275

As specified by the EMEP/EEA guidebook, the emission factors related to CO2 and SO2 are constant and rely on the data published by the Danish Energy Authority (DEA) (EEA, 2023b). If country-specific data differing from the DEA figures are present, the use of country-specific data is preferred (EEA, 2023b). The CO2 emission

factors have been retrieved directly from the Italian Greenhouse Gas Inventory 1990-2021 (ISPRA, 2023). The coefficients, reported in Table 6.50, refer to the average emissions for diesel burned in engines over the period ranging from 2017 to 2021. Country-specific values for SO2 emissions, instead, were not available. For this reason, the Danish database concerning fuel use and emissions from NRMM was used (Winther, 2023). The SO2 EFs refer in this case to the non-road machinery emissions measured in 2021. Their values are shown in Table 6.50, together with those of CO2.

Table 6.50: Emission factors related to CO2 and SO2 for diesel NRMM (ISPRA, 2023; Winther, 2023).

Emission factor / Pollutant	g/MJ	g/g_fuel	g/l_fuel
CO2	73.510	3.150	2.633
SO2	0.468	0.020	0.017

Since the fuel consumption in kg is given by the previous computations for each activity group, CO2 and SO2 emissions deriving from the machines used in the construction site can be computed using the EFs contained in the second column of Table 6.50 using:

$$E_{i,k} = FC_k \cdot EF_i \qquad \forall\, i,k = \begin{cases} i = CO2, SO2 \\ k = Activities \end{cases} \tag{6.5}$$

where $E_{i,k}$ [g] is the mass value of the emission related to the pollutant i for the activity group k, FC_k [g] is the fuel consumption for the activity group k and $EF_i \left[\frac{g}{g_{fuel}}\right]$ is the emission factor for the pollutant i. The final results (in kg) are reported in Table 6.51, 6.52.

Table 6.51: Pollutant emissions and fuel consumption (in kg) with CO2 and SO2 contributions related to each activity group performed in the construction site.

Activity group / Pollutant	Wind turbines and platforms [kg]	Cable trenches and internal roads [kg]	External roads [kg]	Transformer substation [kg]
NOx	123.9865	250.8796	57.6230	17.1018
VOC	28.2028	34.9368	5.3856	5.1966
CH4	0.6485	0.8161	0.1264	0.1209
CO	328.4299	353.4067	41.5262	55.2642
N2O	6.8891	6.6518	0.5910	1.0811
NH3	0.3937	0.3801	0.0338	0.0618
PM	6.5830	10.0600	2.7139	1.3655
PM10	5.1969	7.4714	1.7250	1.0789
PM2.5	5.1969	7.4714	1.7250	1.0789
BC	3.9230	5.8470	1.3800	0.8631
FC	49,675.4612	48,426.1062	4,389.0449	7,910.1275
CO2	156,527.3784	152,590.6606	13,829.8804	24,924.8116
SO2	996.2123	971.1572	88.0197	158.6330

Table 6.52: Pollutant emissions and fuel consumption (in kg/GWh) with CO2 and SO2 contributions related to each activity group performed in the construction site.

Activity group / Pollutant	Wind turbines and platforms [kg/GWh]	Cable trenches and internal roads [kg/GWh]	External roads [kg/GWh]	Transformer substation [kg/GWh]
NOx	0.1368	0.2767	0.0636	0.0189
VOC	0.0311	0.0385	0.0059	0.0057
CH4	0.0007	0.0009	0.0001	0.0001
CO	0.3622	0.3898	0.0458	0.0610
N2O	0.0076	0.0073	0.0007	0.0012
NH3	0.0004	0.0004	0.0000	0.0001
PM	0.0073	0.0111	0.0030	0.0015
PM10	0.0057	0.0082	0.0019	0.0012
PM2.5	0.0057	0.0082	0.0019	0.0012
BC	0.0043	0.0064	0.0015	0.0010
FC	54.7907	53.4127	4.8410	8.7247
CO2	172.6454	168.3033	15.2540	27.4914
SO2	1.0988	1.0712	0.0971	0.1750

The inventory data concerning diesel supply and the emission to air deriving from its combustion have been implemented in SimaPro as shown in Table 6.53. To account for the diesel transport requirements, the *market* dataset was used. Moreover, carbon containing substances have been selected as "fossil" since they originate from the

combustion of a fossil fuel. This setting is essential, considering that fossil and biogenic compounds can have different characterization factors when evaluating the GWP100.

Table 6.53: Implementation in SimaPro of the inventory data related to the fuel consumption and pollutant emission deriving from the NRMM activity in the construction site.

Fuel	Ecoinvent process
Diesel	Diesel {RER}| market group for diesel | Cut-off, U
Emission to air	**Ecoinvent substance**
NOx	Nitrogen oxides
VOC	VOC, volatile organic compounds as C
CH4	Methane, fossil
CO	Carbon monoxide, fossil
N2O	Dinitrogen monoxide
NH3	Ammonia
CO2	Carbon dioxide, fossil
SO2	Sulfur dioxide

One last point of discussion is related to the civil works required for the cable trenches construction and external roads adjustments. These two activities produced inert waste and waste asphalt that are supposed to be fully recovered to generate secondary raw materials. The designated locations for the recovery operations have been retrieved from the available plant documentation. 3 recovery centers were found for inert waste, while only one for waste asphalt. Since inert waste originated exclusively from the external roads adjustments, the transport requirements have been computed by estimating the mean distance between each of the 15 locations where the building works took place and the three recovery centers. On the other hand, waste asphalt was derived exclusively from the cable trenches construction, hence transport requirements have been computed estimating the mean distance between the 4 accesses to the power plant site and the dedicated recovery center. All the data necessary to model the transport inventory are shown in Table 6.54. Since both waste types are assumed to reach the end-of-waste state without needing any pre-treatment or additional transport in other recycling facilities, no further processes have been included.

Table 6.54: Inventory data related to the waste materials deriving from the external roads adjustments and cable trenches construction.

Activity	Location	Transport type	Mean distance (km)	Waste weight (t)	t*km
External roads adjustments	Location 1	Road	14.8	16	236.27
	Location 2	Road	15.2	58.52	889.50
	Location 3	Road	14.5	31.63	457.51
	Location 4	Road	13.9	119.44	1660.21
	Location 5	Road	13.8	42.84	591.19
	Location 6	Road	17.6	84.00	1481.20
	Location 7	Road	18.0	158.50	2858.28
	Location 8	Road	18.3	207.05	3782.15
	Location 9	Road	19.4	396.32	7688.61
	Location 10	Road	18.7	0	0
	Location 11	Road	19.1	83.50	1592.07
	Location 12	Road	19.3	18.82	362.52
	Location 13	Road	19.7	0.45	8.94
	Location 14	Road	31.1	0	0
	Location 15	Road	21.1	0	0
Cable trenches	Site	Road	3.5	1348.99	4721.46

6.2.5. Operation and maintenance (O&M)

The operational phase of the power plant is expected to last 25 years. During this period, both scheduled and unscheduled maintenance activities will be necessary to preserve the system availability for producing electricity. Specifically, wind turbines reliability is one of the most critical factors in achieving success of a wind power plant project (Walford, 2006). Low reliability negatively impacts the revenues by increasing the cost of the O&M phase and reducing the available time to generate power due to the system downtime (Walford, 2006). Wind turbines reliability depends on several factors, including the particular machine model, the design, the quality of the manufacture, but also on the operating conditions and on the site characteristics (Walford, 2006). Many of these represent complex statistical phenomena that are hard to predict. The scheduled maintenance, in this context, is also known as "preventive" since it's devoted to the replacement and refurbishment of those components that, based on the knowledge of failure theory and technology understanding, have defined useful life (much shorter than the expected life of the system) and usually represent the main causes of future failures (Walford, 2006).

In the Iurefalco wind power plant, the scheduled maintenance involves 2 inspections per year for each wind turbine gearbox, while 1 inspection per year is planned for the transformers and the electric systems. Inspections are carried out by the personnel using a small capacity truck, eventually also transporting spare parts to be replaced.

Once every 10 years, instead, the complete replacement of the gearboxes lubricant oil is performed.

While the replacement of mechanical parts is usually not tracked due to the modest entity of the interventions, it has been possible to retrieve from the power plant documentation that, on average, 3 kg of lubricant per gearbox are added every inspection, i.e. 6 kg per year. The demand of gearbox lubricant needed for one complete replacement has been assumed based on Schreiber et al. (2019) inventory data concerning the 3 MW geared turbine, which is equal to 1.28 tons. Overall, the total amount of lubricant required for the wind farm over 25 years of operations has been computed through[5]:

$$m_{lub} = 6\ turbines \cdot \left[\frac{6\ kg}{year \cdot turbine} \cdot 25\ years + ceil\left(\frac{25\ years}{10\ years}\right) \cdot 1280\ kg \right] \qquad (6.6)$$

equal to 23,940 kg. The inventory data related to the use of lubricant oil have been added in SimaPro as reported in Table 6.55. The *market* dataset was used to account for the transport requirements.

Table 6.55: Inventory data related to the use of lubricant oil over the entire expected life of the wind power plant.

Material	Mass per turbine (t)	Mass per wind farm (t)	Mass per wind farm/FU (t/GWh)	SimaPro Process (Ecoinvent database)
Lubricating oil	3.99	23.94	0.026405	Lubricating oil {RER}| market for lubricating oil | Cut-off, U

Considering the high number of parameters that can affect the reliability of wind turbines components and the confidentiality to which this type of data is subjected, the estimation of the impacts related to the unscheduled maintenance activities has been done starting from literature sources. The approach followed is based on the work of Schreiber et al. (2019). The authors referred to the reliability data used by McMillan et al. (2010) and Echavarria et al. (2008) based on German and Danish wind power plants, covering together more than 5000 turbines and a rated power range between tens of kW to several MW. Since the failure rates are related to machines dating back to 2007 or earlier, the improvements of the technology over the next 10 years which also include the development of the G114 – 2.5 MW (2013) have been accounted reducing

[5] In the equation it's also included the initial amount of lubricant oil needed for the 6 turbines.

the values of a factor equal to 1.26, as suggested by Reimers (2016) (Shreiber et al., 2019).

The final failure rates are reported in Table 6.56. These values are used for the estimation of the number of units of each wind turbine component that needs to be entirely replaced during the plant lifetime. In order to be conservative, results are then rounded up to the next integer. All the inventory data concerning the replaced parts are assumed to be the same as modeled before, from the raw materials acquisition to the assembly in site.

The fuel consumption and pollutants emissions deriving from the installation of the replaced components have been computed using the same approach described in the previous section, supposing that the substitution of each component will require 2 complete working days ($8\ \frac{hours}{day} \cdot 2\ days = 16$ hours) employing the same cranes used for the turbines' erection (Crane 1 and Crane 2). Results are reported in Table 6.57. Moreover, the replaced gearboxes will need an additional amount of lubricant oil equal to $8\ gearboxes \cdot 1{,}280\ \frac{kg\ oil}{gearbox} = 10{,}240\ kg$, for a total of 34,180 kg ($0.03770\ \frac{t}{GWh}$). The disposal of failed components has been modeled according to what will be described in the end-of-life section in relation to wind turbines.

Since what happens during the unscheduled maintenance activities is one of the most uncertain aspects of the power plant life cycle, in the sensitivity analysis the variation of the components failure rate will be covered to assess the reliability of the results.

Table 6.56: Failure rates and number of failures for the turbines' major components.

Component	Failure rate [units/(year*turbine)]	Number of failures (6 turbines, 25 years)	
Gearbox	0.0476	7.1429	8
Generator	0.0095	1.4286	2
Hub	0.0190	2.8571	3
blades	0.0040	0.5952	1

Table 6.57: Pollutant emissions and fuel consumption related to the installation of the replaced turbines' components.

NRMM / Pollutant	Crane 1 [kg/GWh]	Crane 2 [kg/GWh]	Total [kg/GWh]
NOx	0.01363	0.01994	0.03357
VOC	0.00447	0.00654	0.01101
CH4	0.00010	0.00015	0.00025
CO	0.05474	0.08011	0.13486
N2O	0.00119	0.00174	0.00293
NH3	0.00007	0.00010	0.00017
PM	0.00105	0.00154	0.00258
PM10	0.00085	0.00124	0.00209
PM2.5	0.00085	0.00124	0.00209
BC	0.00061	0.00089	0.00150
FC	8.48363	12.41506	20.89869
CO2	26.73190	39.11986	65.85176
SO2	0.17013	0.24898	0.41911

6.2.6. Decommissioning

After 25 years of operations, the power plant will be decommissioned in order to restore the initial conditions of the site. The main activities that will characterize the *decommissioning* phase are:

- Electrical disconnection of the power plant.
- Wind turbines disassembly. This activity is expected to be executed in the same way of the assembly. Wind turbines foundations will be left on site.
- Transformer substation removal. This includes the disassembly and removal of the electromechanical components previously installed, the ground network and the reinforced concrete walls. All the other concrete constructions will be left on site.
- MV and HV cables removal. It's also included the HV ground network.
- Platforms and cable trenches renaturation. The surface occupied by the wind turbines platforms and cable trenches will be covered with a layer of topsoil 20 cm and 15 cm thick, respectively, then sowed with various herbaceous species.

As stated before, wind turbines are expected to be disassembled using the same procedures and equipment employed during the assembly phase. The energy requirements and pollutant emissions related to this activity correspond to the inventory data computed in the *components assembly and installation* phase referring only to cranes usage, i.e. Crane 1 and Crane 2, as shown in Table 6.58.

About the transformer substation, similarly to the case of wind turbines, the disassembly efforts related to the electromechanical components and ground network in terms of energy and pollutant emissions have been assumed equal to the inventory data associated with the telescopic handlers usage for the transformer substation contained in Table 6.58. The reinforced concrete wall is expected to be demolished once the wall foundations are extracted from the ground. Based on the dimensions and the depth of the foundations, an excavated volume of 165.57 m^3 was assumed. The electromechanical components foundations, together with the other concrete works (curbs, sidewalks, ramps), will be left on site. The inventory data related to the excavation and demolition activities have been included using the Ecoinvent processes reported in Table 6.59.

Table 6.58: Pollutants emissions and fuel consumption related to the wind turbines and electromechanical components disassembly.

NRMM / Pollutant	Telescopic handler [kg/GWh]	Crane 1 [kg/GWh]	Crane 2 [kg/GWh]
NOx	0.00198	0.01192	0.02279
VOC	0.00140	0.00391	0.00748
CH4	0.00003	0.00009	0.00017
CO	0.01164	0.04790	0.09156
N2O	0.00017	0.00104	0.00199
NH3	0.00001	0.00006	0.00011
PM	0.00015	0.00092	0.00175
PM10	0.00012	0.00074	0.00142
PM2.5	0.00012	0.00074	0.00142
BC	0.00010	0.00053	0.00102
FC	1.27887	7.42317	14.18864
CO2	4.02972	23.39041	44.70841
SO2	0.02565	0.14887	0.28454

Table 6.59: Inventory data related to the transformer substation removal.

Activity	Allocation quantity	Value per wind farm	Value per wind farm/FU	SimaPro Process (Ecoinvent database)
Concrete walls demolition	Demolished mass (t)	408.81	0.45	Rock crushing {GLO}| market for rock crushing | Cut-off, U
Excavation	Excavated volume (m^3)	165.57	0.18	Excavation, hydraulic digger {GLO}| market for excavation, hydraulic digger | Cut-off, U

Since the energy requirements and pollutant emissions related to the cables and ground network extraction from the trenches couldn't be evaluated starting from the available documentation, a rough conservative estimation was conducted using literature data. The total energy output required for the extraction may be assumed as equal to:

$$E_{ex}\,[J] = E_{fr} + E_g \tag{6.7}$$

where E_{fr} $[J]$ is the energy required to win the friction force between the outer surface of the cable and the inner surface of the corrugated pipe, while E_g $[J]$ is the energy required to lift the cable from the laying depth to the ground level. Eq. 6.7 can be written as:

$$E_{ex}\,[J] = E_{fr} + E_g = F_{fr} \cdot l \; + \; F_g \Delta h = \mu m g \cdot l + m g \Delta h \tag{6.8}$$

where F_{fr} $[N]$ is the friction force, F_g $[N]$ is the gravitational force, l $[m]$ is the length of the cable, Δh $[m]$ is the elevation difference between the laying depth and the ground level, μ $[-]$ is the friction coefficient, m $[kg]$ is the mass of the cable, $g\left[\frac{m}{s^2}\right]$ is the gravitational acceleration. All the data except the friction coefficient were available from the plant documentation. The friction coefficient between two surfaces in contact normally depends on several factors, including the surfaces roughness, type of contact, types of materials, normal force and much more.

For the specific case presented, the friction coefficients were retrieved from Essential Energy (2021). In the reference document, a guide on the calculation of the pulling force for a given cable and trench configuration using the Neara software is given (Essential Energy, 2021). Neara is a tool typically used to design power line infrastructures. For the computation, Neara uses the friction coefficients shown in

Table 6.60, depending on the coupling between conduit material and cable sheath material. The coefficients are expressed for lubricated or unlubricated contact.

Table 6.60: Friction coefficients used by Neara for the calculation of the pulling force for a given cable and trench configuration (Essential Energy, 2021).

Conduit type	Cable sheath type	Unlubricated	Lubricated
PVC	PVC	0.60	0.20
PVC	HDPE	0.35	0.20
PVC	XLPE	0.45	0.20
HDPE	PVC	0.40	0.20
HDPE	HDPE	0.35	0.20
HDPE	XLPE	0.45	0.20
Metal	PVC	0.45	0.20
Metal	HDPE	0.40	0.20
Metal	XLPE	0.40	0.20

For the wind power plant case, the unlubricated contact was chosen. The specific material couplings for the cables employed in the trenches, as well as the corresponding friction factors, are contained in Table 6.61. For the copper rope, the friction factor is based on the inverted material coupling due to the lack of information.

Table 6.61: Friction coefficients used for the extraction of the cables installed in the trenches of Iurefalco power plant.

Cable	Conduit type	Cable sheath type	Friction coefficient
HV	HDPE	HDPE	0.35
MV (Wind turbines)	HDPE	XLPE	0.45
MV (Transformer substation)	HDPE	PVC	0.40
Copper rope	HDPE	Metal	0.40

Eq. 6.8 was applied in each case using Table 6.61 friction factors. The results are reported in Table 6.62.

Table 6.62: Output energy required for the extraction of each cable type.

Cable	Required energy output [MJ]
HV	18.615
MV (Wind turbines)	348.852
MV (Transformer substation)	0.206
Copper rope	0.833
All	368.506

The machinery used for cables extraction is supposed to be diesel powered. To compute the energy input to perform each extraction operation, an overall efficiency of 20% has been assumed based on the work of Schreiber et al. (2019). Hence, the total energy input resulted to be equal to $\frac{368.506\ MJ}{0.2} = 1{,}842.529\ MJ$. The inventory data related to both diesel usage and pollutant emissions due to combustion have been included using the Ecoinvent process *Diesel, burned in building machine {GLO}| market for diesel, burned in building machine | Cut-off, U*, specifying the energy input just computed. All the relevant results concerning this part are summarized in Table 6.63.

Table 6.63: Inventory data related to the extraction of the cables installed in the trenches of Iurefalco power plant.

Activity	Energy required per wind farm (MJ)	Energy required per wind farm/FU (MJ/GWh)	SimaPro Process (Ecoinvent database)
Cables extraction	1842.53	2.03	Diesel, burned in building machine {GLO}| market for diesel, burned in building machine | Cut-off, U

Platforms renaturation will involve a total surface of 16,670 m^2. The inventory data related to the energy consumption for this activity have been estimated starting from the Ecoinvent process *Recultivation, limestone mine {RoW}| recultivation, limestone mine | Cut-off, U*. The process represents the recultivation of 1 m^2 of topsoil after limestone extraction. The topsoil employed for the coverage of the surface is supposed to have an average thickness of 0.3 m and a density of 1,400 $\frac{kg}{m^3}$. Diesel powered machinery is used for land transformation. Since diesel consumption has been computed based on the mass of topsoil per square meter, in the specific case of the wind turbines' platforms the value in MJ reported in the process' inventory must be weighted for the ratio between the real thickness per m^2 (0.2 m) and the reference one (0.3 m), assuming the same topsoil density. Hence, a new process has been defined including a diesel consumption computed as follows:

$$E_{fuel} = E_{fuel,0} \cdot S_p \cdot \left(\frac{z}{z_0}\right) \tag{6.9}$$

where $E_{fuel,0} = 7.44\ \frac{MJ}{m^2}$ is the fuel consumption per m^2 related to the reference Ecoinvent process, $S_p = 16{,}670\ m^2$ is the total surface of the platforms, $\frac{z}{z_0} = \frac{0.2\ m}{0.3\ m} = 0.67$ is the correction considering the thickness difference between the real and the reference case. The resulting fuel consumption for the platforms renaturation is equal to $E_{fuel} = 82{,}683.2\ MJ$. Similarly to the case of cables extraction, the pollutant emissions inventory has been included using the Ecoinvent process *Diesel, burned in building machine {GLO}| market for diesel, burned in building machine | Cut-off, U,* specifying the energy input just computed.

The cable trenches renaturation will involve a total surface of 3843 m^2. The same approach followed for the platforms renaturation was used. This time, the correction factor $\frac{z}{z_0}$ used in eq. 6.9 has been set to $\frac{z}{z_0} = \frac{0.15\ m}{0.3\ m} = 0.5$ since the topsoil thickness is half of the reference one. The resulting fuel consumption for the cable trenches renaturation is equal to $E_{fuel} = 14{,}295.96\ MJ$. Table 6.64 summarizes the inventory data concerning this part.

Table 6.64: Inventory data related to the renaturation of platforms and cable trenches.

Activity	Energy required per wind farm (MJ)	Energy required per wind farm/FU (MJ/GWh)	SimaPro Process (Ecoinvent database)
Platforms renaturation	82683.20	91.20	Diesel, burned in building machine {GLO}| market for diesel, burned in building machine | Cut-off, U
Cable trenches renaturation	14295.96	15.77	

6.2.7. End-of-life

As previously introduced in the literature review (Chapter 5), the *end-of-life* phase of a wind power plant always represents the most uncertain phase along its entire life cycle, especially considering the temporal extension of the operational phase, which is in most of the cases equal or longer than 20 years. The typical waste management techniques that are nowadays employed when dealing with wind power plants will probably be revised, adjusted and improved, especially those concerning wind turbines blades. The power plant analyzed in the present study makes no exception: the main disposal scenario that will be discussed represents the most probable outcome based on the current technology level as suggested by the wind turbines' manufacturers, but nothing prevents future modifications.

The inventory data related to the *end-of-life* phase have been collected according to the EPD System approach, as set in the goal and scope definition. This means that, in the case of recycled or reused waste, only the environmental impacts related to those processes leading up to the end-of-waste state should be considered. These include all the transport requirements and the pre-treatments the waste undergoes prior to reach the recycling facility where the actual recycling process takes place (EPD International, 2021). The environmental burdens related to landfilling and incineration procedures, instead, should be entirely considered (EPD International, 2021). Moreover, since in this study the 100-0 waste allocation approach is adopted, no credit deriving from the recycling, reuse or energy recovery from incineration is assigned to the system analyzed.

Transport requirements

At the end of the *decommissioning* phase, each component of the power plant's physical system is broken down into its sub-assemblies ready to be delivered to the recovery centers in case of recycling, while to landfills or incinerators in case of disposal. For the calculation of the mean transport distances that sub-components and materials are expected to cover, data provided by the national register of special waste management plants published by ISPRA (Istituto Superiore per la Protezione e la Ricerca Ambientale) were used (ISPRA, 2021; ISPRA 2019).

The distances related to landfilled materials have been obtained considering a representative set of 6 landfills for non-hazardous waste and 4 landfills for inert waste located in Puglia and Basilicata, i.e. the closest regions to the wind power plant's location. Incinerated materials, either hazardous or not, are expected to be delivered to the only active incinerator located in Basilicata region. Recycled materials will be first transported to specialized recovery centers and then to the recycling facilities. Recycled metallic waste is transported to recovery centers that deal with the production of secondary raw materials for the metallurgical industry. The related distances have been obtained considering a representative set of 6 recovery centers in

Puglia region. Recycled waste concrete is supposed to be recovered in the same locations discussed when dealing with inert waste coming from the external roads adjustments. Recycled waste from electrical and electronic equipment (WEEE), e.g. cables, transformers, generators and electromechanical components is managed by separate facilities. In this case, distances have been computed considering a set of 3 recovery centers located in Puglia and Basilicata. Lastly, recycled waste lubricants are expected to be delivered to the nearest recovery center located in Campania region.

Metals and plastic materials leaving the recovery centers are delivered to the respective recycling facilities. It's important noting that, at the gate of the recovery centers, plastic materials have already reached the end-of-waste state, therefore further transport requirements will be considered only for metals. Metals are expected to be recycled through casting processes, hence the mean distance between the recovery centers and a representative foundry location was evaluated. All the computed distances just mentioned are summarized in Table 6.65. Transport will be carried out by truck. Conservatively, the same Ecoinvent process used in the previous life cycle phases has been employed to define the inventory data (*Transport, freight, lorry, unspecified {RER}| transport, freight, lorry, all sizes, EURO4 to generic market for transport, freight, lorry, unspecified | Cut-off, U)*, even if the mean efficiency of truck engines is expected to rise in the future.

Table 6.65: Mean distances covered by trucks for each waste destination.

Waste management	Waste destination	Mean distance (km)	Transport type
Landfilling	Landfills for non-hazardous waste	79	Road
	Landfills for inert waste	86.4	Road
Incineration	Incinerator for hazardous and non-hazardous waste	117.3	Road
Recycling	Recovery centers for metals	181.5	Road
	Recovery centers for WEEE	131.7	Road
	Recovery/recycling facility for waste lubricants[6]	265	Road
	Recycling/recycling facilities for waste concrete[7]	21.3	Road
	Recycling facility for metals	277.8	Road
	Recycling facility for metals, from WEEE	141.2	Road

[6] In this case the recovery center coincides with the recycling facility.
[7] In this case the recovery center coincides with the recycling facility.

Waste management

As already anticipated, the forecasted waste management scenario is based on the indications given by the wind turbines' manufacturer aimed to maximize the recycling rate of the materials derived from the decommissioned components. The destination of each type of material regarding wind turbines and the cable transmission system has been linked in first place to the specific sub-component to be disposed of, as shown in Table 6.66.

In general, wind turbine's sub-components present a high recovery and recyclability rate due to the dominant role of metals in the total mass fraction. The small fraction of inert materials found in the electrical components, i.e. the transformer and the generator, is considered non-recoverable, therefore it's expected to be disposed in landfill (for inert waste). The waste composite material originating from the blades, the nacelle's cover and cone, according to the EU dispositions will not be disposed in landfill but it will be first shredded and then incinerated, with potential recovery of the generated heat. A large fraction (80%) of the exhausted oil used in the wind turbines is expected to be regenerated to make lubricant bases, while the remaining non-recoverable part will be incinerated. Wind turbines' foundations, as already described, will be left on site. Cables deriving from the transmission system are mainly composed of metals and plastic which are easy to separate and recycle, therefore their recovery rate is typically very high. The non-recoverable waste fraction is expected to be disposed in landfill.

A more detailed recovery rate breakdown for the wind turbine's components and cable transmission system is shown in Table 6.67, 6.68. Recovery rates for each material have been computed considering the global values for the sub-components reported in Table 6.66. In particular, it's worth noting that:

- Metals recovery rates have been assumed homogeneous internally to each sub-component, as suggested by many of the reviewed LCA studies dealing with wind power plants. A similar assumption was made with the recovery rates of plastic materials used in cables.

- The tower's painted steel and the composite material used in the blades, nacelle's cover and cone have been considered as single entities, since they won't be separated prior or during the waste treatments.

Table 6.66: Total recovery rate and destinations of each type of material for the sub-components deriving from the decommissioning phase.

Component	Sub-component	Recovery (%)	Materials destination
Wind turbine	Blades, nacelle's cover and cone	88	- Composite material shredded and incinerated with energy recovery - Non-recoverable fraction disposed in landfill
	Tower	95	- Steel casting - Non-recoverable fraction disposed in landfill
	Foundations	0	- Left on site
	Cables	90	- Metals casting - Non-recoverable fraction disposed in landfill
	Mechanical parts	80	- Metals casting - Non-recoverable fraction disposed in landfill
	Waste oil	80	- Waste oil recovered to make lubricant bases - Non-recoverable fraction incinerated
	Electrical components	80	- Metals casting - Inert materials disposed in landfill
Power transmission system	HV	90	- Metals casting - Plastic granules making - Non-recoverable fraction disposed in landfill
	MV (Wind turbines)	90	- Metals casting - Plastic granules making - Non-recoverable fraction disposed in landfill
	MV (Transformer substation)	90	- Metals casting - Plastic granules making - Non-recoverable fraction disposed in landfill
	Copper rope	95	- Metal casting

Waste management for components and sub-components deriving from the transformer substation, in contrast to what was done for the wind turbines and the cable transmission system, has been expressed directly for the single materials employed, as shown in Table 6.69. This was done due to the absence of specific indications reported in the available plant documentation. Typical recovery rates for materials used in the electromechanical components have been retrieved from the EPD of the three-pole switch: metals (aluminium and steel) are expected to be recovered for the 90% of the mass, while other materials (silicone, glass fibre, porcelain) will be incinerated, possibly recovering the generated heat (Hitachi, 2021). The combustion residues, similarly to the case of the turbines' blades, will be disposed in landfill. Concrete and steel deriving from the reinforced concrete fraction that will be

decommissioned are supposed to be recovered for 90% of their total mass, according to the work of Bonou et al. (2016). Concrete will be crushed to make inert aggregates, while reinforcing steel will undergo casting processes. The non-recoverable part will be disposed in landfill.

Table 6.67: Total recovery rates breakdown for the turbines' sub-components.

Component	Sub-component	Material	Material fraction for sub-component (%)	Recovery (%)	Total recovery (%)
Tower	Painted steel	Steel	99.23	95.00	95
		Paint	0.78		
Nacelle	Frame	Iron	100.00	80.00	80
	Main shaft	Steel	100.00	80.00	80
	Transformer	Silica	4.00	0.00	
		Copper	30.00	83.33	80
		Steel	66.00	83.33	
	Generator	Silica	3.00	0.00	
		Copper	31.00	82.50	80
		Steel	66.00	82.50	
	Gearbox	Iron	50.00	90.00	80
		Steel	50.00	90.00	
	Cover	Fibre glass	40.00	88.00	88
		Epoxy	60.00		
	Brake system	Steel	100.00	80.00	80
	Cables	Aluminium	42.33	90.00	90
		Copper	57.67	90.00	
	Revolving system	Steel	100.00	80.00	80
	Crane	Steel	100.00	80.00	80
Rotor	hub	Cast iron	100.00	80.00	80
	Cone	Epoxy	60.00	88.00	88
		Fibre glass	40.00		
	blades (3)	Epoxy	60.00	88.00	88
		Fibre glass	40.00		

In Table 6.70 – 6.72 are shown all the Ecoinvent processes used to model each of the process just discussed concerning waste treatment. Due to the lack of specific data, several assumptions were made to fill the gaps in the inventory finalization:

- The disassembly phase of each turbines' sub-component preceding any type of waste treatment (landfilling, incineration or recycling) was conservatively modeled in the same way adopted for the assembly phase, hence using an electric consumption equal to 0.5 kWh per kg. The Italian mix was chosen from the Ecoinvent database to model the corresponding inventory data.

- An electric consumption of 0.075 kWh per kg of waste was assumed for the blades' shredding based on the work of Vo Dong et al. (2018).

Table 6.68: Total recovery rates breakdown for cables deriving from the decommissioning phase.

Component	Material	Material fraction per component (%)	Recovery (%)	Total recovery %
MV cables (Wind turbines)	Aluminium	49.37	90	90
	Semiconducting XLPE	11.30	90	
	XLPE	22.37	90	
	HDPE	15.70	90	
	Polyester non-woven	1.26	90	
MV cables (Transformer substation)	Copper	66.92	90	90
	Semiconducting HEPR	6.11	90	
	HEPR	16.03	90	
	PVC	10.94	90	
HV cables	Aluminium	35.83	90	90
	Semiconducting XLPE	8.92	90	
	XLPE	54.32	90	
	AL/PE[8]	-	-	
	Polyester non-woven	0.93	90	
Copper rope	Copper	100	95	95

- Metals derived from wind turbines and the transformer substation are supposed to undergo sorting and pressing treatments before the actual recycling process (melting). Pressing and sorting of iron scraps was used as proxy for each metallic material derived from wind turbines and the transformer substation.

- Inventory data related to metals landfilling have been retrieved from the iron scraps landfill disposal process in the case of every metallic material except for aluminium.

- Silica landfilling was modeled as waste glass landfilling.

[8] As discussed in the raw materials acquisition section, the AL/PE tape was excluded from the end-of-life phase.

- Epoxy resin incineration was modeled as plastic mixture incineration, according to the Ecoinvent processes that deal with composite blades incineration.

- Incineration of silicone and porcelain deriving from the electromechanical components used in the transformer substation were modeled as waste rubber and glass incineration, respectively.

- Pre-treatments concerning MV and HV cables recycling have been modeled starting from the *Used cable {GLO}| treatment of used cable | Cut-off, U* Ecoinvent process. Specifically, it was possible to retrieve the energy consumption needed for the separation of metallic and plastic materials, equal to 0.18 kWh of electricity per kg of treated cable. After the separation, plastic materials will undergo mechanical shredding to be transformed into granulate, i.e. their end-of-waste condition. For this reason, no further processes related to plastic materials have been considered. For metals, instead, a last transport process from the recovery center to the recycling facility (foundry) was considered, as already anticipated.

- HDPE landfilling was chosen as proxy for landfilling of any plastic material used in cables except for HEPR, for which it was replaced by plastic mixture landfilling.

Table 6.69: Material recovery rates and destinations for the transformer substation sub-components deriving from the decommissioning phase.

Component	Sub-component	Material	Recovery (%)	Materials destination
Transformer substation	Civil works	Concrete	54.24[9]	- Crushed to make inert aggregates - Non-recoverable fraction disposed in landfill
		Reinforcing steel (B450C)	51.48[10]	- Metals casting - Non-recoverable fraction disposed in landfill
		Asphalt	0	- Left on site
		Limestone gravel	0	- Left on site
	Electromechanical components	Copper	95	- Metals casting - Non-recoverable fraction disposed in landfill
		Steel	90	- Metals casting - Non-recoverable fraction disposed in landfill
		Aluminium	90	- Metals casting - Non-recoverable fraction disposed in landfill
		Silicone	100	- Incinerated with energy recovery
		Glass fibre	100	- Incinerated with energy recovery
		Porcelain	100	- Incinerated with energy recovery

[9] The recovery rate also includes the contribution of the non-recovered waste concrete left in site.
[10] The recovery rate also includes the contribution of the non-recovered waste reinforcing steel left in site.

Table 6.70: Ecoinvent processes used for the inventory data modeling concerning waste materials management in wind turbines.

Component	Material	Waste management	Ecoinvent process
Wind turbines	Steel	Recycling	Iron scrap, sorted, pressed {RER}| sorting and pressing of iron scrap | Cut-off, U
		Landfilling	Scrap steel {Europe without Switzerland}| treatment of scrap steel, inert material landfill | Cut-off, U
	Iron	Recycling	Iron scrap, sorted, pressed {RER}| sorting and pressing of iron scrap | Cut-off, U
		Landfilling	Scrap steel {Europe without Switzerland}| treatment of scrap steel, inert material landfill | Cut-off, U
	Cast iron	Recycling	Iron scrap, sorted, pressed {RER}| sorting and pressing of iron scrap | Cut-off, U
		Landfilling	Scrap steel {Europe without Switzerland}| treatment of scrap steel, inert material landfill | Cut-off, U
	Aluminium	Recycling	Iron scrap, sorted, pressed {RER}| sorting and pressing of iron scrap | Cut-off, U
		Landfilling	Waste aluminium {CH}| treatment of waste aluminium, sanitary landfill | Cut-off, U
	Copper	Recycling	Iron scrap, sorted, pressed {RER}| sorting and pressing of iron scrap | Cut-off, U
		Landfilling	Scrap steel {Europe without Switzerland}| treatment of scrap steel, inert material landfill | Cut-off, U
	Silica	Landfilling	Waste glass {CH}| treatment of waste glass, inert material landfill | Cut-off, U
	Epoxy resin	Incineration	Waste plastic, mixture {CH}| treatment of waste plastic, mixture, municipal incineration | Cut-off, U
		Landfilling	Waste plastic, mixture {CH}| treatment of waste plastic, mixture, sanitary landfill | Cut-off, U
	Fibre glass	Incineration	Waste glass {CH}| treatment of waste glass, municipal incineration | Cut-off, U
		Landfilling	Waste glass {CH}| treatment of waste glass, inert material landfill | Cut-off, U

Table 6.71: Ecoinvent processes used for the inventory data modeling concerning waste materials management in cables.

Component	Material	Waste management	Ecoinvent process
Power transmission system	Aluminium	Recycling	(User-defined process)
		Landfilling	Waste aluminium {CH}| treatment of waste aluminium, sanitary landfill | Cut-off, U
	Semiconducting XLPE	Recycling	(User-defined process)
		Landfilling	Waste polyethylene {CH}| treatment of waste polyethylene, sanitary landfill | Cut-off, U
	XLPE	Recycling	(User-defined process)
		Landfilling	Waste polyethylene {CH}| treatment of waste polyethylene, sanitary landfill | Cut-off, U
	HDPE	Recycling	(User-defined process)
		Landfilling	Waste polyethylene {CH}| treatment of waste polyethylene, sanitary landfill | Cut-off, U
	Polyester non-woven	Recycling	(User-defined process)
		Landfilling	Waste polyethylene {CH}| treatment of waste polyethylene, sanitary landfill | Cut-off, U
	Copper	Recycling	(User-defined process)
		Landfilling	Scrap steel {Europe without Switzerland}| treatment of scrap steel, inert material landfill | Cut-off, U
	Semiconducting HEPR	Recycling	(User-defined process)
		Landfilling	Waste plastic, mixture {CH}| treatment of waste plastic, mixture, sanitary landfill | Cut-off, U
	HEPR	Recycling	(User-defined process)
		Landfilling	Waste plastic, mixture {CH}| treatment of waste plastic, mixture, sanitary landfill | Cut-off, U
	PVC	Recycling	(User-defined process)
		Landfilling	Waste polyvinylchloride {CH}| treatment of waste polyvinylchloride, sanitary landfill | Cut-off, U

Table 6.72: Ecoinvent processes used for the inventory data modeling concerning waste materials management in the transformer substation's components.

Component	Material	Waste management	Ecoinvent process
Transformer substation	Concrete	Recycling	-[11]
		Landfilling	Waste concrete {Europe without Switzerland}| treatment of waste concrete, inert material landfill | Cut-off, U
	Reinforcing steel (B450C)	Recycling	Iron scrap, sorted, pressed {RER}| sorting and pressing of iron scrap | Cut-off, U
		Landfilling	Scrap steel {Europe without Switzerland}| treatment of scrap steel, inert material landfill | Cut-off, U
	Asphalt	-	-
	Limestone gravel	-	-
	Copper	Recycling	Iron scrap, sorted, pressed {RER}| sorting and pressing of iron scrap | Cut-off, U
		Landfilling	Scrap steel {Europe without Switzerland}| treatment of scrap steel, inert material landfill | Cut-off, U
	Steel	Recycling	Iron scrap, sorted, pressed {RER}| sorting and pressing of iron scrap | Cut-off, U
		Landfilling	Scrap steel {Europe without Switzerland}| treatment of scrap steel, inert material landfill | Cut-off, U
	Aluminium	Recycling	Iron scrap, sorted, pressed {RER}| sorting and pressing of iron scrap | Cut-off, U
		Landfilling	Waste aluminium {CH}| treatment of waste aluminium, sanitary landfill | Cut-off, U
	Silicone	Incineration	Waste rubber, unspecified {CH}| treatment of waste rubber, unspecified, municipal incineration | Cut-off, U
	Glass fibre	Incineration	Waste glass {CH}| treatment of waste glass, municipal incineration | Cut-off, U
	Porcelain	Incineration	Waste glass {CH}| treatment of waste glass, municipal incineration | Cut-off, U

[11] As pointed out when discussing the management of waste concrete resulting from the external roads adjustments, waste concrete resulting from the transformer substation is also expected to reach the end-of-waste state without needing any pre-treatment or additional transport other than the delivery to the recovery center.

7 LCIA and results interpretation

According to the ISO 14040:2006 and 14044:2006 standards, the life cycle impact assessment section of an LCA study must include (ISO 14040:2006, ISO 14044:2006):

- The identification, description and justification of the impact categories, category indicators and characterization models that will assess the environmental impact of the system.

- The attribution of the inventory data obtained in the LCI section to the selected impact categories (also known as *classification* procedure).

- The computation of the category indicator results (also known as *characterization* procedure).

As described in the goal and scope section, this study is devoted to the evaluation and interpretation of the level of sustainability which characterizes the energy balance and carbon footprint involved between the system and the environment. To meet the targets set in the scope of the analysis, the Cumulative Energy Demand (CED) and the Intergovernmental Panel on Climate Change (IPCC) impact assessment methods were selected. The impact categories related to these two methods refer, respectively, to *fossil and renewable energy resources consumption* and *fossil, biogenic and land transformation emissions* (PRé Sustainability, 2022). In the case of the IPCC method, the indicators referred to each impact category are associated with the number of kilograms of CO2 equivalent able to determine the same infrared radiative forcing (measured in $\frac{W}{m^2}$) on the atmosphere caused by the GHGs emitted during the system life cycle. The CED method, instead, uses as indicators the sum of the primary energy inputs (in MJ) coming from the specific energy source evaluated by the impact categories. The characterization factors that bring to the category indicators results are represented by the heating value of the fuels used in the case of the CED, while the global warming potential (GWP) for the IPCC method. For the CED, when dealing with renewable energy sources differing from renewable fuels, e.g. wind and solar energy sources, the related primary energy consumption is obtained considering the amount of electrical energy converted by the technologies that exploit them. Finally, the indicator results are expressed in MJ per functional unit in the case of the CED, while in kg of CO2 equivalent per functional unit in the case of the IPCC method. As

already anticipated, results concerning the energy balance will be primarily expressed using the CED standard method (i.e. based on fuels HHV), since it represents the most widely employed impact assessment method among the comparison studies. However, the CED – LHV version will be also used to justify the assumptions made regarding the use of EPD data for the inventory definition. The time horizon employed to evaluate the effects of GHGs on global warming, instead, is 100 years.

The attribution of the inventory data obtained in the LCI section to the selected impact categories and the computation of the category indicator results were performed using the SimaPro software. The main targets set in the scope of the LCA have been achieved starting from the simulation output upon further elaborations. An in-depth interpretation of the results will be given for the single life cycle phases and then for the single main items that make up the system object of the analysis to highlight the hot spots concerning the impact categories just discussed. Additional considerations will be derived by the examination of scenarios differing from the reference one through sensitivity analysis, in order to evaluate the reliability and consistency of the analysis.

7.1. LCA results: life cycle phases

The results related to the reference scenario (Table 7.1) are shown in first place for the single life cycle phases with grouped category indicators belonging to each impact assessment method. The contribution of the power plant's main components is highlighted as well.

As expected, the *raw materials acquisition* phase resulted to be the most critical for both primary energy consumption and GHGs emissions of the system, accounting for more than $\frac{2}{3}$ of the total environmental impacts. The materials required for the wind turbines alone are responsible for 43% of the overall CED and GWP, representing the hot spot of this stage. The turbines' foundations follow right after with a contribution of 15% for the CED and 21% for the GWP. The materials used for the power transmission system and its cable trenches account, instead, for 8% of the CED and 5% of the GWP. The transformer substation, most likely due to the lack of data concerning part of its sub-systems, represents in both cases less than 3% of the total impact, of which around 85% is caused by the transformer and the civil works' materials only. The remaining part of the materials used for the power plant's civil works (platforms, internal roads, external roads) has low influence on the CED and GWP, considering that it makes up 1% of the overall contribution in both cases.

The *components manufacturing* phase resulted to be the second most critical for the CED and GWP impact assessment methods, accounting, respectively, for 12% and 9% of the total. Similarly to the *row materials acquisition* phase, the contribution of the turbines is the dominant one. This time, however, the other main components are responsible for a much lower fraction of the impacts on the total and internally to the phase itself

compared to the previous case. In fact, the summation of all the contributions excluding the one of the wind turbines make up around 1% of the overall environmental damage for both CED and GWP, i.e. around 10% of the total damage deriving from the *components manufacturing* phase. These results are clearly determined by the substantial absence of any additional transformation procedure other than the preliminary raw materials processing characterizing all the items present in the plant's civil works.

The *components assembly and installation* phase represent the second least relevant phase of the plant's life cycle for both primary energy consumption and GHGs emissions, accounting for 4% of the total results. Due to the impossibility of separating the contributions belonging to each type of activity performed in the construction site, they have been grouped in the same way adopted during the definition of the related inventory data.

The *operation and maintenance* phase accounts for 8% of the CED and 7% of the GWP. As will be shown in the next paragraphs, the environmental impacts are mostly caused by the unscheduled maintenance activities, which will require the replacement of some of the turbines' components installed during the plant's construction phase. Scheduled maintenance activities, instead, are expected to determine very limited burdens. This result is closely related to one of the major points of strength of renewable power plants towards sustainability along the use phase: the exploitation of a clean and virtually unlimited source of energy using fossil-free conversion and transmission systems.

The *decommissioning* phase represents the least critical phase of the plant's life cycle concerning primary energy consumption and GHGs emissions, accounting for less than 1% of the total impacts in both cases. Wind turbines disassembly is responsible for more than 80% of the overall impacts related to this phase. All the other contributions, given the small relevance of the environmental burdens, can be considered negligible.

The *end-of-life* phase accounts for 7% of the CED and 8% of the GWP, placing itself between the *components manufacturing* and *operation and maintenance* phases. Also in this case, the wind turbines contribution is dominating the others, with more than 95% of the total impacts. Such result can be explained considering that a large fraction of the total waste mass deriving from the plant's decommissioning comes from wind turbines, whose components require, in addition to the actual waste treatment processes referred to the single material types (landfilling, incineration, recycling), the execution of several pre-treatments (disassembly, sorting, pressing) aimed to a proper prosecution of the disposal activity. This topic, together with the more relevant ones, will be further discussed in the next sections.

Table 7.1: LCA results for the reference scenario.

Life cycle phase	Component	CED (MJ)	CED %	IPCC GWP100 (KgCO2eq)	IPCC GWP100 %
Raw materials acquisition	Turbines	94,876.8	43.27	6,385.7	42.64
	Foundations	32,934.4	15.02	3,075.8	20.54
	Power transmission	7,877.0	3.59	349.8	2.34
	Transformer substation	5,618.5	2.56	375.6	2.51
	Cable trenches	8,642.2	3.94	360.7	2.41
	Platforms	623.8	0.28	46.3	0.31
	Internal roads	620.1	0.28	46.1	0.31
	External roads	767.4	0.35	83.9	0.56
	Total	151,960.3	69.30	10,723.8	71.60
Components manufacturing	Turbines	22,836.6	10.41	1,154.5	7.71
	Foundations	1,321.6	0.60	83.0	0.55
	Power transmission	639.9	0.29	28.8	0.19
	Transformer substation	497.4	0.23	27.5	0.18
	Cable trenches	70.3	0.03	4.5	0.03
	Platforms	73.3	0.03	4.7	0.03
	Internal roads	75.0	0.03	6.2	0.04
	External roads	0.0	0	0.0	0.00
	Total	25,514.1	11.63	1,309.3	8.74
Components assembly and installation	Turbines, foundations and platforms	3,770.4	1.72	268.3	1.79
	Transformer substation	486.0	0.22	35.4	0.24
	Cable trenches and internal roads	3,737.7	1.70	265.6	1.77
	External roads	601.9	0.27	41.0	0.27
	Total	8,596.0	3.92	610.2	4.07
Operation and maintenance	Turbines	17,449.3	7.96	1,076.8	7.19
Decommissioning	Turbines	1,200.5	0.55	87.0	0.58
	Transformer substation	76.2	0.03	5.5	0.04
	Power transmission and cable trenches	24.8	0.01	1.8	0.01
	Platforms	127.0	0.06	9.1	0.06
	Total	1,428.4	0.65	103.3	0.69
End-of-life	Turbines	14,181.2	6.47	1,127.6	7.53
	Transformer substation	67.9	0.03	20.8	0.14
	Power transmission	94.7	0.04	5.2	0.03
	Total	14,343.8	6.54	1,153.7	7.70
Total		219,291.9	100	14,977.1	100.00

7.1.1. Raw materials acquisition

Since the *raw materials acquisition* phase represents by far the most critical one concerning the system's primary energy consumption and GHGs emissions, an in-depth analysis covering all the main components of the power plant will be conducted in order to point out which are the drivers that lead to such result.

Wind turbines

As already specified, wind turbines' raw materials acquisition determine the highest environmental impact for the considered categories, equal to 43% of the total CED and GWP. In Figure 7.1 is reported a more detailed breakdown of these contributions for the turbines' major components, i.e. the tower, nacelle, hub[12] and blades. The largest contributors for the CED result to be the blades (35.5%), followed by the tower (31.7%), the nacelle (28.3%) and the hub (4.6%). In general, the total primary energy required for the acquisition of a material employed in a component of the system can be computed as:

$$E_p\,[MJ] = m_{i,c} \cdot f_i \tag{7.1}$$

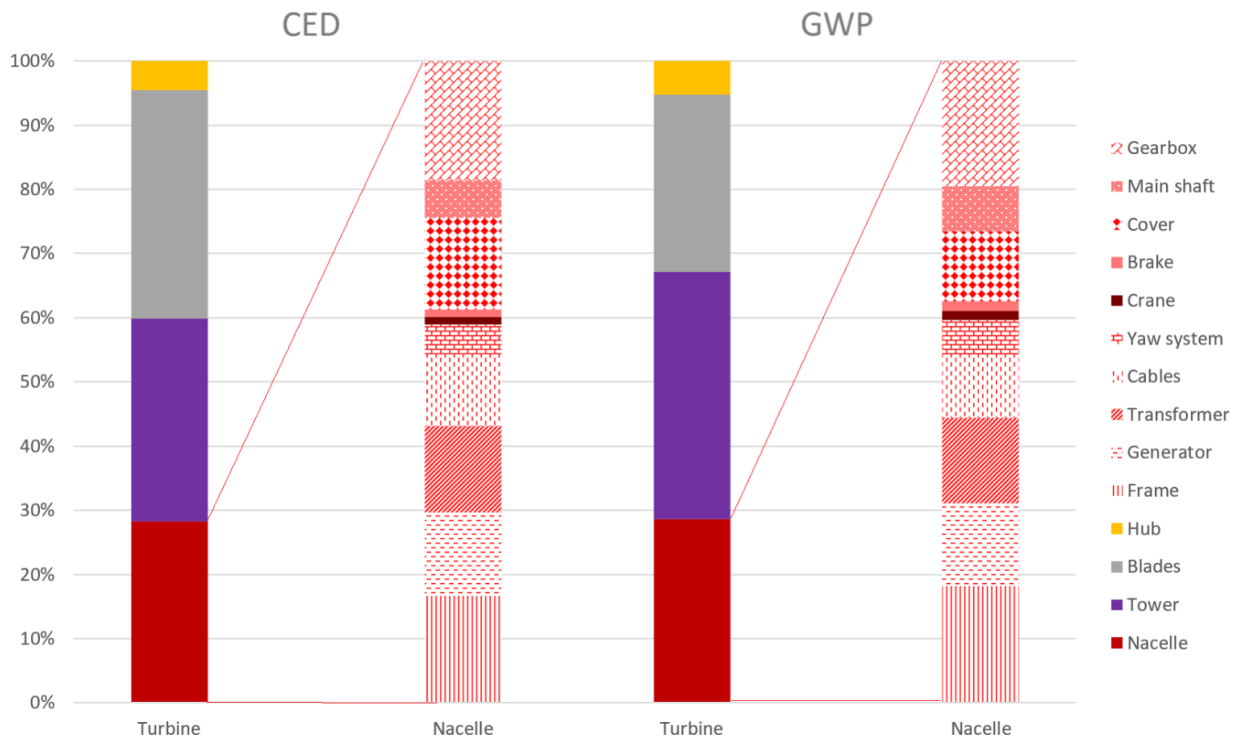

Figure 7.1: Breakdown of the wind turbines' impacts at component level.

[12] In this paragraph, the hub will always be referred as the combination of hub + cone.

where E_p is the total primary energy, $m_{i,c}$ [kg] is the mass of the material i required to manufacture the component c and $f_i \left[\frac{MJ}{kg}\right]$ is the specific energy factor expressing the primary energy required to acquire 1 kg of the material i. Applying eq. 7.1 to each major components of the turbines can put in evidence whenever the energy required for the acquisition of the material i referred to the component c is mostly influenced by its mass or by its specific energy. In Figure 7.2 is shown the total mass in kg of the single materials used for the 6 wind turbines installed in the power plant's site together with their contribution to the CED in MJ. The mean specific energy required for the acquisition of each material, reported in Table 7.2, was computed dividing the values on the vertical axis for the values on the horizontal axis.

The mass of the turbine's components, as well as their material composition, are shown in Table 6.11. From Table 6.11 data it's possible to note that the mass of the tower is clearly the highest among the other major components. Nevertheless, the influence of the tower on the CED results to be noticeably lower than the blades' contribution, even though the mass of 3 blades (40.47 t) is more than 4 times less than the mass of one tower (185.90 t). This outcome is related to the materials' specific energy effect. While the tower is almost entirely made of low-alloyed steel, the blades are made of a composite material featuring glass fiber and epoxy resin.

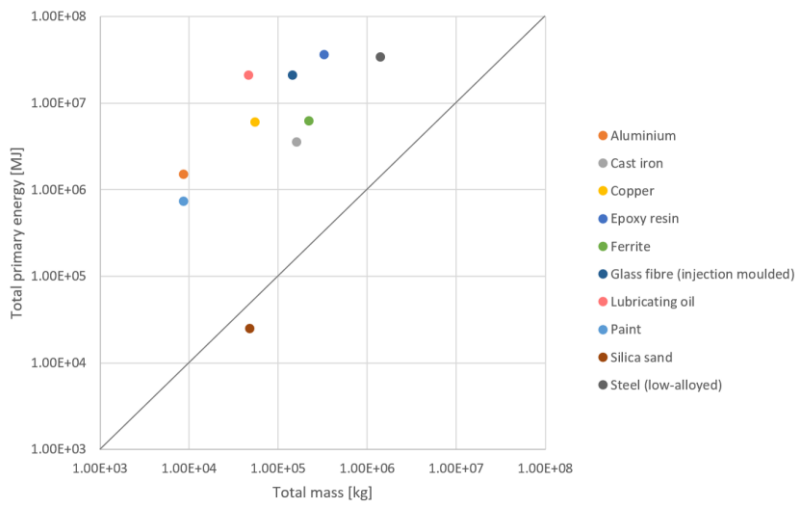

Figure 7.2: Total masses and primary energy contributions for the acquisition of the turbines' raw materials.

Table 7.2: Specific energy factors for the acquisition of the turbines' raw materials.

Material	MJ/kg
Paint	84.90
Aluminium	173.13
Cast iron	22.28
Copper	111.42
Epoxy resin	111.68
Ferrite	27.94
Glass fibre	144.98
Lubricating oil	68.31
Silica sand	0.53
Steel (low-all.)	24.26

In the case of the present study, considering the processes and datasets chosen for the turbines' assembly, the specific energy of low-alloyed steel required for its acquisition is equal to 24.26 $\frac{MJ}{kg}$ (Table 7.2), which represents a value around 5 times lower than the one associated to the composite material, computed using:

$$f_{comp} = 0.4 \cdot f_{glass} + 0.6 \cdot f_{epoxy} = 125 \ \frac{MJ}{kg} \tag{7.2}$$

thus, the superimposition of the mass and specific energy effects results in a higher primary energy consumption for the turbines' blades.

On the other hand, the nacelle's contribution to the CED is determined by numerous factors, given its complexity. The breakdown of the nacelle's energy requirement has been reported in Figure 7.1, highlighting the influence of each sub-component. Considering the material composition of the nacelle, shown in Table 6.11, 6.12, it emerges that a large fraction of the mass (85%) is made of steel (low-alloyed) and iron, whose corresponding inventory data have been referred to those of ferrite production. Since the specific energy factors related to the acquisition of these materials are quite similar (Table 7.2), it's expected that the most critical sub-components concerning the primary energy consumption will be the most massive ones. In fact, the gearbox (25.7 t) and the frame (24.2 t), representing almost one fourth of the total nacelle's mass each, place themselves on top of the list with 19% and 17% contribution, respectively. Lighter ferrous components, i.e. the main shaft, the yaw system, the service crane and the mechanical brake are on the bottom, accounting for 6%, 5%, 1% and 1% of the nacelle's total, respectively.

Nevertheless, steel-containing components with intermediate weight such as the generator and the transformer present a fraction of copper that has a strong influence on their primary energy consumption, as well as on the whole nacelle (see Figure 7.3). Copper is the most widely used material for electric wirings due to its high conductivity. However, primary copper production is an energy-intensive process that requires several thermal and electrochemical treatments due to the low ore grade normally found in the extraction sites. In the case of the present study, the computed specific energy required for primary copper acquisition is equal to 111.42 $\frac{MJ}{kg}$. Such value determines 69% of the total generator impacts (13% of the nacelle's CED) and 66% of the total transformer impacts (13% of the nacelle's CED), even if the mass fraction of copper in these two sub-components is around 30%. Copper is found together with aluminium in the nacelle's cables as well. Likewise copper, primary aluminium production requires a significant amount of energy, especially when the purity required is near 100%. As shown in Table 7.2, the computed specific energy for aluminium deriving from the selected Ecoinvent processes is even higher than the copper one, reaching a value of 173.13 $\frac{MJ}{kg}$. That's why the nacelle's cables, although representing only 3% of the nacelle's total mass, account for 11% of its total CED contribution. The nacelle's cover, instead, which features the same material composition of the blades, determines a similar effect compared to what discussed between these ones and the tower. Given that the composite material specific energy

is significantly more relevant than the one characterizing ferrous materials (i.e. the nacelle's dominant materials), even with a small mass fraction (< 5%) the cover affect the nacelle's CED in a significant way, accounting for more than 14% of its total primary energy consumption related to the materials acquisition phase. Lastly, the hub, due to its modest weight compared to the turbine's total and its average specific energy (cast iron) determines the lowest impact for the turbine's primary energy consumption, representing 5% of the total.

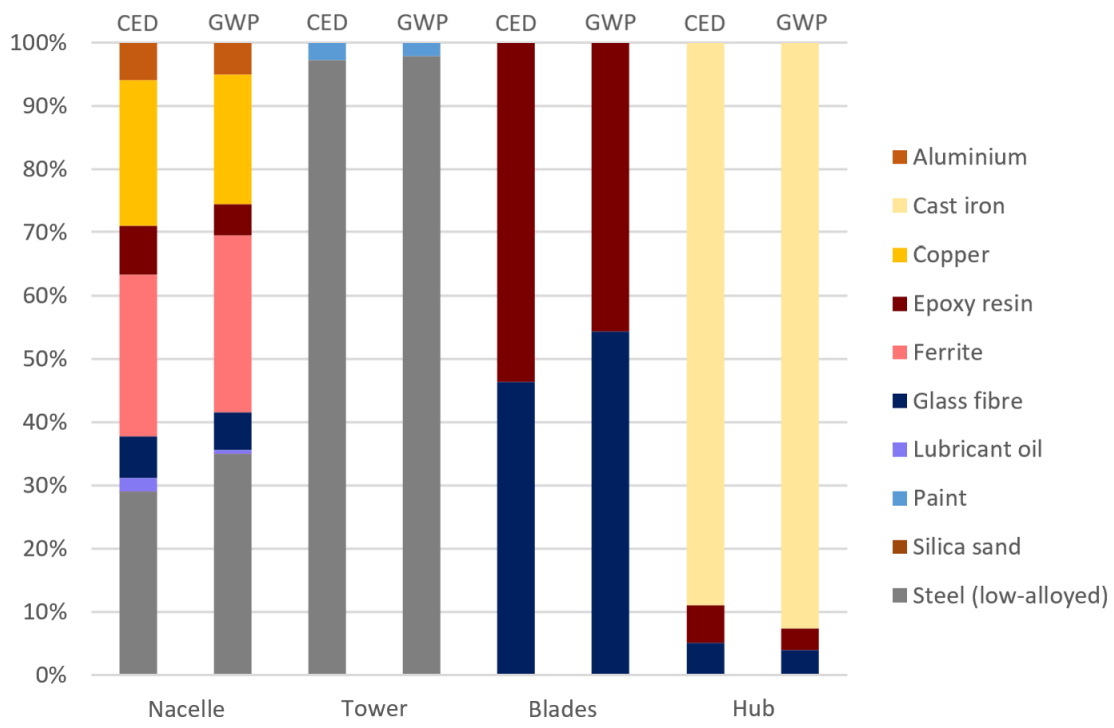

Figure 7.3: Breakdown of the wind turbines components' impacts at material level.

The impacts related to the GHGs emissions involved in the *raw materials acquisition* phase, although with some differences, present a similar trend compared to the one just illustrated for the primary energy consumption, since typically pollutants emissions are proportional to the energy required. The same approach followed by using eq. 7.1 can still be employed by replacing the specific energy with the specific emission factor (see eq. 7.3), expressed in $\frac{kgCO2eq}{kg}$.

$$e_p\ [kgCO2eq] = m_{i,c} \cdot f_i \tag{7.3}$$

The specific emission factors (Table 7.3) were computed using Figure 7.4 data. Once again, the composite material employed in the blades and the nacelle's cover resulted to determine a considerably higher damage on the environment per kg of substance ($6.51\ \frac{kgCO2eq}{kg}$) compared to the turbine's average, mainly composed of ferrous materials. Nonetheless, this time the GWP of the tower turned out to overcome the one of the blades, accounting together for 39% and 28% of the total turbine's GWP, respectively (see Figure 7.1). This difference is caused since the ratio between the two emission factors, equal to $\frac{f_{comp}}{f_{steel}} = \frac{6.51\frac{kgCO2eq}{kg}}{2.00\frac{kgCO2eq}{kg}} = 3.26$, is not able to counterbalance the ratio between the two masses, equal to $\frac{m_{tower}}{m_{blades}} = \frac{185.90\frac{kgCO2eq}{kg}}{40.47\frac{kgCO2eq}{kg}} = 4.59$, determining a clear dominance of the mass effect on the emission factor one.

Moving on to the nacelle, instead, the heaviest and the lightest ferrous sub-components are still placed on the top and on the bottom of the list, respectively. Specifically, the gearbox and the frame account for 20% and 18% of the total nacelle's GWP, while the main shaft, yaw system, service crane and the mechanical brake for 7%, 6%, 1% and 1% of the total. The lower ratio between f_{comp} and f_{steel} compared to the one that characterizes the primary energy consumption makes this time the impact of the cover less relevant than before, from 14% to 11%, allowing the transformer and the generator to rank just after the nacelle's frame, both with 13% of the total nacelle's GWP. The cables, instead, still present a relatively high influence (10% of the total) despite their minor weight considering that, as already mentioned, pollutant emissions are typically proportional to primary energy consumption.

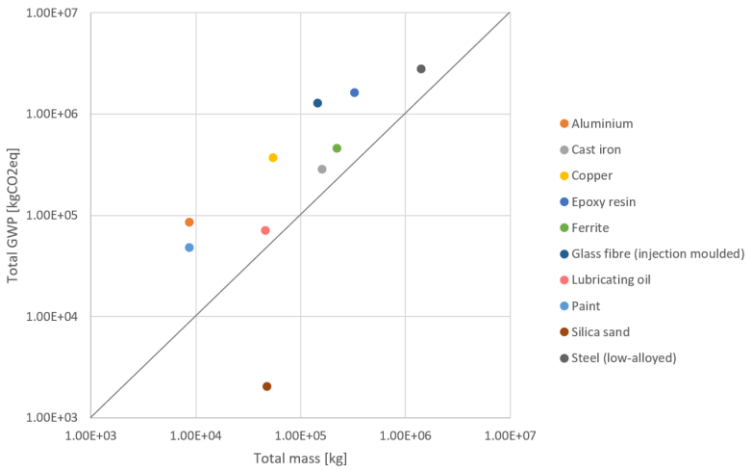

Figure 7.4: Total masses and GWP for the acquisition of the turbines' raw materials.

Table 7.3: Specific emission factors for the acquisition of the turbines' raw materials.

Material	kgCO2eq/kg
Paint	5.55
Aluminium	9.89
Cast iron	1.79
Copper	6.79
Epoxy resin	4.97
Ferrite	2.07
Glass fibre	8.81
Lubricating oil	1.54
Silica sand	0.04
Steel (low-all.)	2.00

Civil works

The acquisition of the raw materials required for the civil works involved in the plant's construction site determines a contribution equal to 21% of the total CED and 25% of the total GWP. In Figure 7.5 is reported a more detailed breakdown of the impacts for each main activity performed.

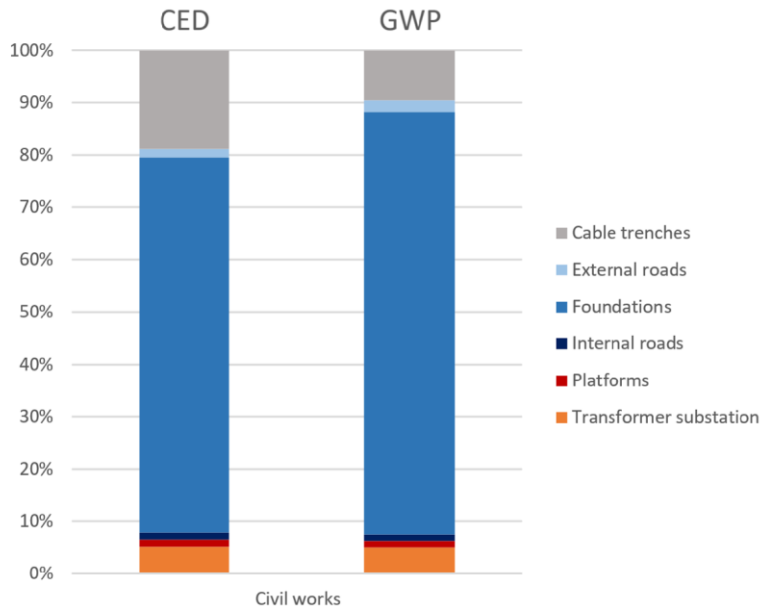

Figure 7.5: Breakdown of the civil works' impacts at component level.

Starting from the CED, the turbines' foundations resulted to influence for the most part the primary consumption required for the acquisition, accounting for 72% of the civil works total. The cable trenches and the transformer substation construction follow right after with 19% and 5% of the CED, respectively. The remaining fraction is covered by the external roads, platforms and internal roads construction, which represent 2%, 1% and 1% of the total. As seen with the wind turbines, eq. 7.1 can be used also in this case to highlight whenever the energy required for the acquisition of a certain material is determined primarily by its mass or by its specific energy. The specific energy factors (Table 7.4) were computed using Figure 7.6 data, which contains the total mass in kg of the single materials used for each construction activity performed during the installation phase. How each material affects the CED of the construction activities is shown, instead, in Figure 7.7.

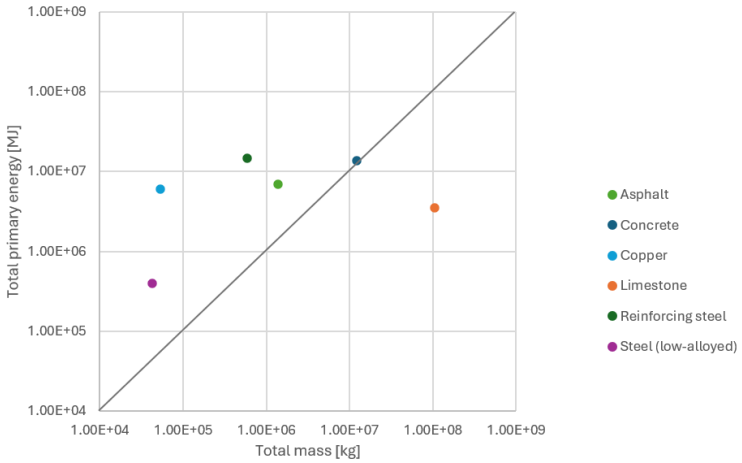

Figure 7.6: Total masses and primary energy consumption for the acquisition of the civil works' raw materials.

Table 7.4: Specific energy factors for the acquisition of the civil works' raw materials.

Material	MJ/kg
Asphalt	5.08
Concrete	1.10
Limestone	0.03
Copper	111.42
Reinforcing steel	24.72
Steel (low-all.)	9.43[13]

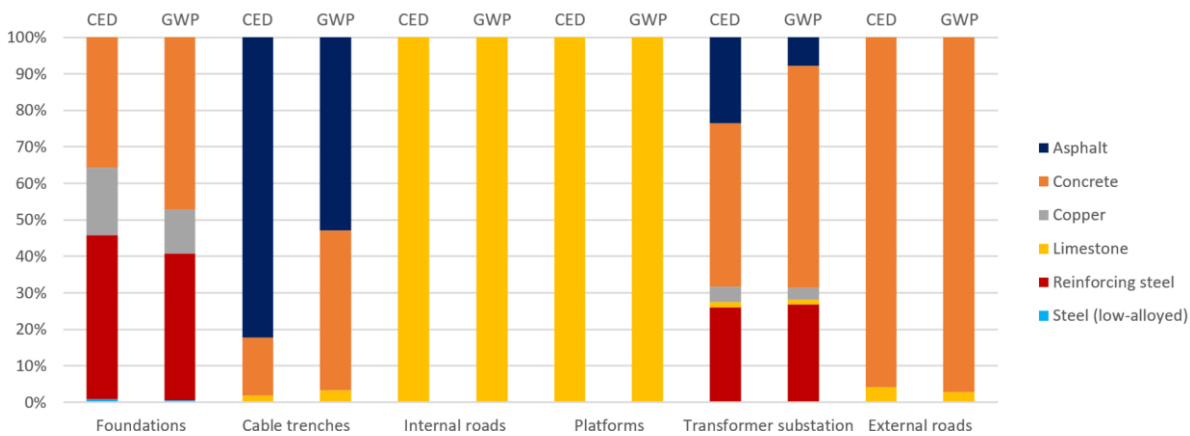

Figure 7.7: Breakdown of the civil works components' impacts at material level.

The turbines' foundations are generally designed to be bulky and heavy. Concrete is the material that clearly dominates the mass composition of both the types of foundation used in the site, representing more than 90% of the total mass, as shown in Table 6.13. Reinforcing steel and low-alloyed steel accounts together for 5%, while the copper used for the grounding of the electrical system for less than 1%. Despite such

[13] In the context of the power plant civil works, low-alloyed steel was included in the inventory data of the turbines' foundations only (grouting components). Since this was the only case in which the steel maker, together with the production method, were known from the power plant documentation, the Ecoinvent process referring to its acquisition has been selected differently from the generic global acquisition of steel (see Table 6.13). The resulting impacts turned out to be lower, mostly because the production of steel using electric arc furnaces is often characterized by the use of steel scraps, whose environmental burdens are supposed to be equal to 0 with the cut-off end-of-life approach.

prevalence of concrete against other materials, reinforcing steel has yet the major influence on the foundations' CED, since it requires a way higher specific energy to be produced (24.72 $\frac{MJ}{kg}$ vs 1.10 $\frac{MJ}{kg}$). This effect is even more pronounced for copper, which represents almost 19% of the foundation's CED although only 0.4% of its total mass.

Moving on to the cable trenches, limestone and concrete were used as filling material in both the HV and MV trench, while asphalt was used for the public roads reconstruction after the excavation activities. All these materials, especially limestone, have been employed in significative amounts, as already reported in Table 6.17. Nonetheless, despite its high mass fraction, the impact of limestone turned out to be practically insignificant compared to the other materials due to its minimum specific energy. Between asphalt and concrete, instead, the former prevails on the latter due to its higher specific energy (5.08 $\frac{MJ}{kg}$ vs 1.10 $\frac{MJ}{kg}$), since both are used in similar amounts for the trenches construction (see Table 6.17). Given the importance of the ratio between the two specific energy factors, which is close to 5, asphalt alone covers more than 80% of the cable trenches' total primary energy consumption, while concrete only 16%.

The civil works involved in the construction of the transformer substation required the acquisition of the materials reported in Table 6.27. Reinforced concrete building works resulted in the most critical item impacting on the substation's CED, with more than 70% of the total contribution, followed by the asphalt's 24%. Limestone, instead, according to what has just been discussed concerning the cable trenches, determines negligible burdens despite its consistent mass fraction. On the other hand, the copper required for the grounding of the electrical system is too limited to cause significant effect on the CED, although having a high specific energy.

External roads derive their energy requirements almost completely from concrete building works. This happens again due to the marginal role of limestone acquisition. Lastly, since both internal roads and platforms are made of crushed limestone only, their entire CED is related to this material.

The trend that characterizes the GWP of each activity involved in the plant's civil works turned out to be consistent with what discussed for the CED, but with some differences in the materials contributions. The emission factors used for the analysis (Table 7.5) have been computed using Figure 7.8 data. The turbines' foundations produce even in this case the highest environmental damage, determining 81% of the total GWP. Compared to the previous situation, concrete is impacting slightly more due to a small increase of the ratio between its emission factor and the ones involved with both reinforcing steel and copper production. A similar conclusion can be made for the cable trenches as well, now representing 9% of the total GWP. In fact, the ratio between the concrete emission factor and the asphalt one increases in such a way that in this condition concrete now covers almost 45% of the trenches' impact, while the asphalt only 53%. In the transformer substation, which accounts for 5% of the civil

works' GWP, a similar effect reduces the asphalt contribution to 8% while increases the concrete one to 61%. External roads, platforms and internal roads are characterized, instead, by the same conditions described in the CED section, representing also in this case 2%, 1% and 1% of the total, respectively.

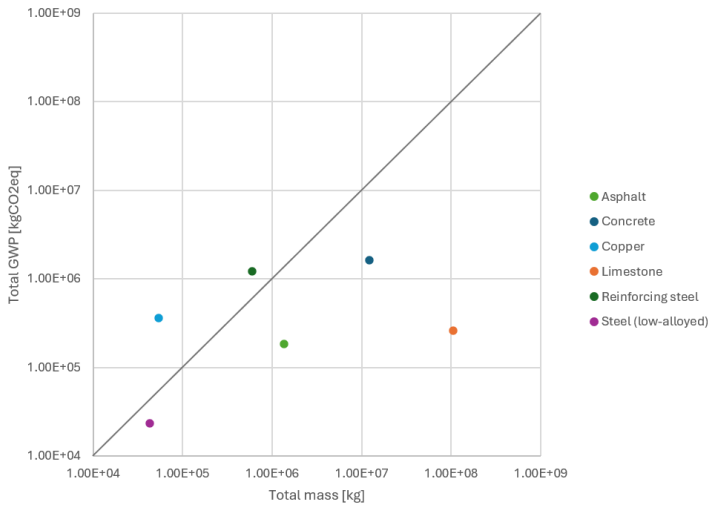

Figure 7.8: Total masses and GWP for the acquisition of the civil works' raw materials.

Table 7.5: Specific emission factors for the acquisition of the civil works' raw materials.

Material	KgCO2eq/kg
Asphalt	0.14
Concrete	0.13
Limestone	0.003
Copper	6.79
Reinforcing steel	2.07
Steel (low-all.)	0.55

Power transmission cables

Raw materials acquisition concerning the power transmission cables will be examined in this section including the effects of the grounding system, the optic fiber and corrugated pipes, given that all these elements are buried together in the cable trenches. The overall contribution determines 4% of the total CED impacts and 2% of the total GWP impacts. A more detailed breakdown of the impacts concerning each item is reported in Figure 7.9.

Starting from the CED, the aluminium stranded MV cables require the highest fraction of the total primary energy, accounting for 66% of the overall impacts. The HV cables follow right after with 15% of the total, while the copper stranded MV cables affect only 1% of it. Among the remaining components installed in the trenches, the corrugated pipes clearly contribute the most with 17% of the total impacts, while the copper rope and the optic fiber account for less than 1% each. The materials' burdens on each contribution are shown in Figure 7.10 for the power cables only, since the other components are assumed to be made of a single material, as shown in Table 6.20. The specific energy factors (Table 7.6) were computed using Figure 7.11 data.

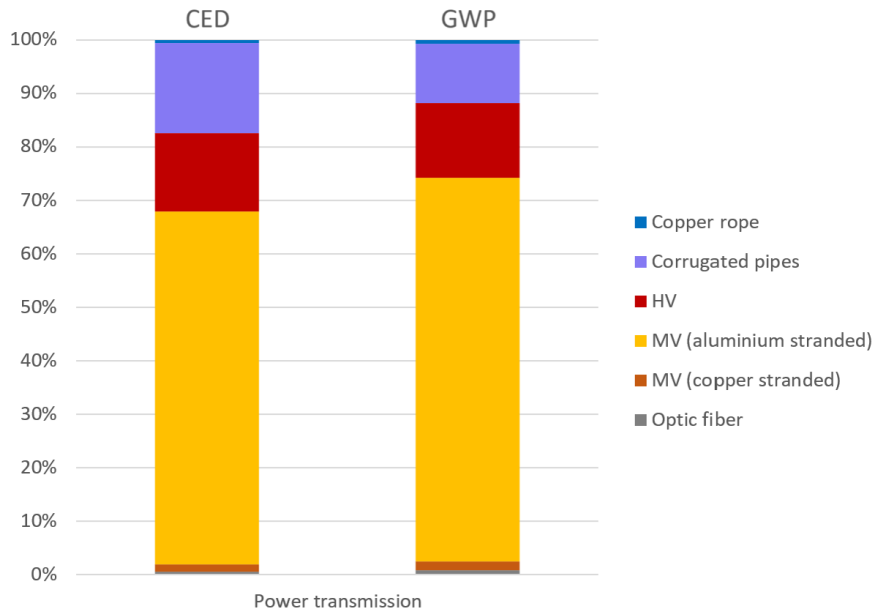

Figure 7.9: Breakdown of the power transmission's impacts at component level.

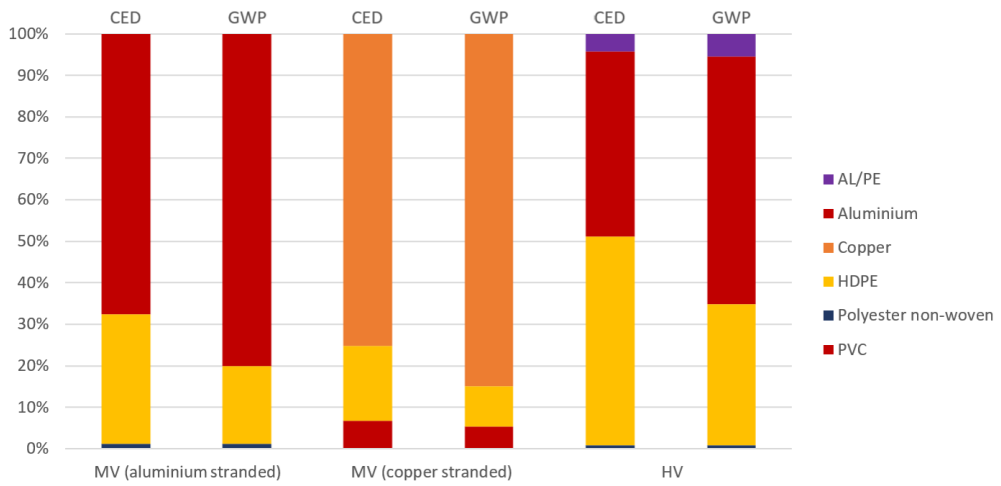

Figure 7.10: Breakdown of the power cables' impacts at material level.

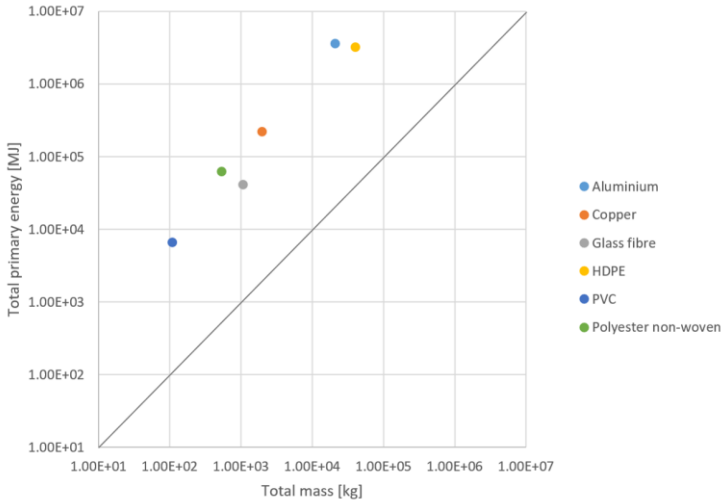

Figure 7.11: Total masses and primary energy consumption for the acquisition of the power transmission's raw materials.

Table 7.6: Specific energy factors for the acquisition of the power transmission's raw materials.

Material	MJ/kg
Aluminium	173.13
Copper	111.41
Glass fibre	38.15
HDPE	80.37
PVC	61.66
Polyester non-woven	117.04

Focusing on the power cables, the main drivers that affect the environmental damage from primary energy resource depletion resulted to be dependent mainly on the conductors' materials and size, the nominal voltage and the cable length. The MV cables used in the power plant employ aluminium conductors in the case of the connection between wind turbines and the transformer substation, while copper conductors in the case of the transmission of power internally to the substation itself. The choice of the conductor material is usually a trade-off between several properties, including conductivity, density, mechanical resistance, corrosion resistance, but also cost. Typically, MV cables internal to the transformer substation that connect the production meter and the exchange meter employ copper conductors due to their higher electrical conductivity, considering that lower power losses compared to the rest of the power line are wanted between these two elements. Power cables connecting wind turbines and the transformer substation are instead made of aluminium conductors to reduce the total investment cost, considering the relatively high distance between the generation and the transformation units. Moreover, aluminium stranded cables are characterized by an easier installation procedure due to their considerably lower density compared to copper stranded cables. Aluminium in fact, while presenting an electrical conductivity which is 61% the one of a copper conductor with the same size, is able to grant the same conductivity of copper with less than half the weight thanks to its 70% lower density. From an environmental point of view, this feature positively affects the primary energy consumption of aluminium stranded cables when compared to the equivalent copper stranded for the same type of application. The ratio between the specific energy factors characterizing the acquisition of primary aluminium and copper for the power cables used in the system

($\frac{173.13\,\frac{MJ}{kg}}{111.42\,\frac{MJ}{kg}}$ = 1.55) is in fact not able to counterbalance the ratio between the aluminium and copper mass required to obtain the same electrical conductivity, hence using eq. 7.1 it's possible to conclude that the conductor material of aluminium stranded cables requires less primary energy than the copper stranded cables one for a given application.

Since the cables' conductor section depends, once the voltage is fixed, on the electric power that is required to deliver, the MV cables connecting the wind turbines and the transformer substation usually present different size in function of the actual framework of the power line. Considering that only a fraction of the power line is required to carry the entire production coming from the wind turbines, all the other power cables that deliver only a part of this production are designed to be thinner and with smaller conductors. For this reason, the aluminium stranded MV cables employed in the plant have on average an even lower primary energy demand per unit length compared to copper stranded MV cables, given that these ones are designed to carry up to the plant's nominal electric energy production. Specifically, the superimposition of these two effects determines a primary consumption per meter of cable produced that is almost double for the MV copper stranded cables.

The nominal voltage of power cables, as already anticipated in the LCI section, usually affects the number and the thickness of all the conductive, semiconductive and insulant layers present in the cables themselves. The HV aluminium stranded cable used in the analyzed system presents the same conductor section of the MV aluminium stranded cable connecting the power block with the transformer substation, but its insulation layer and semiconducting layers are more than twice as thick than before, while also using the same materials. Moreover, 3 water blocking layers are present instead of 1, as well as 2 metallic sheaths. Typically, the biggest impact among all the possible changes that can happen after the voltage increase is determined by the thicker insulation and semiconducting layers. In fact, while in the MV cables these two layers account for less than 30% of the total cable weight, in the HV cables they represent more than 50% of the total weight. On top of this, the increased thickness of the above-mentioned layers determines a cable size that is almost double, while the mass per meter is around 2.5 times the previous one. This explains why HV cables are the most demanding in terms of primary energy consumption per unit length, requiring 3.5 times the energy of the MV aluminium stranded cables, and the XLPE (modeled as HDPE in SimaPro) presents such a high share in the HV cables' CED.

Nevertheless, the overall impacts of the power transmission cables are highly influenced in the case of the present study by the total length of the cables used, since the extension of the MV network connecting wind turbines and the transformer substation is way bigger than the other two segments. This driver can of course vary a lot its effect depending on the plant and site's characteristics, e.g. wind turbines'

disposition and number, terrain morphology, distance from the transmission grid and many others.

The power cables' GWP is characterized by a similar distribution compared to the CED one. Small differences are mainly related to the lower ratio between the HDPE emission factor and the one of the other materials. MV aluminium stranded cables are still on top with 72% of the total impacts, followed by the HV cables with 14% and the MV copper stranded cables with 2%. The corrugated pipes, for the reason just mentioned, reduced their contribution from 17% to 11%, while the optic fiber and the copper rope still holds around 1% each. The emission factors (Table 7.7) were computed using Figure 7.12 data. The same drivers discussed for the CED are those that primarily affect the impacts per unit length of each power cable and their material related burdens. In this case, the conductor material of aluminium stranded cables produces a lower global warming compared to the copper stranded cables one for a given application since the ratio between the emission factors characterizing the acquisition of primary aluminium and copper ($\frac{9.89\,\frac{kgCO2eq}{kg}}{6.79\,\frac{kgCO2eq}{kg}}$ = 1.46) is not able to counterbalance the ratio between the aluminium and copper mass required to obtain the same electrical conductivity. Moreover, the smaller mean size caused by the network architecture contributes to further reducing the aluminium stranded MV cables emissions per unit length, resulting in an impact more than 2 times lower than the one of copper stranded MV cables. Nevertheless, HV cables still cause the highest specific damage due to their bigger size and complexity despite having the same layers composition of MV aluminium stranded cables, accounting for more than 3 times the mass of its CO2-equivalent emissions. This time, the influence of XLPE (HDPE) is a bit reduced due to the previously mentioned lower ratio between its emission factor and the other materials' one (see Figure 7.10).

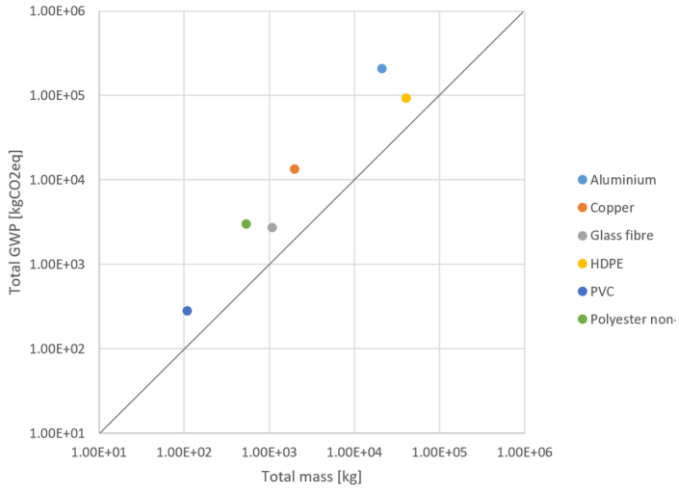

Figure 7.12: Total masses and GWP for the acquisition of the power transmission's raw materials.

Table 7.7: Specific emission factors for the acquisition of the power transmissions' raw materials.

Material	kgCO2eq/kg
Aluminium	9.89
Copper	6.79
Glass fibre	2.54
HDPE	2.33
PVC	2.61
Polyester non-woven	5.62

7.1.2. Components manufacturing

The *components manufacturing* phase represents the second most relevant concerning the impact categories included in the assessment, accounting for 12% of the total CED and 9% of the total GWP. As already anticipated, compared to the *raw materials acquisition* phase, the turbines' manufacturing has a more central role due to the very limited presence of additional transformation activities other than the preliminary raw materials processing characterizing all the items present in the plant's civil works. Focusing on the wind turbines, a more detailed breakdown of the impacts is shown in Figure 7.13, which includes the contributions of the single manufacturing processes selected during the inventory definition (Table 6.29, 6.30).

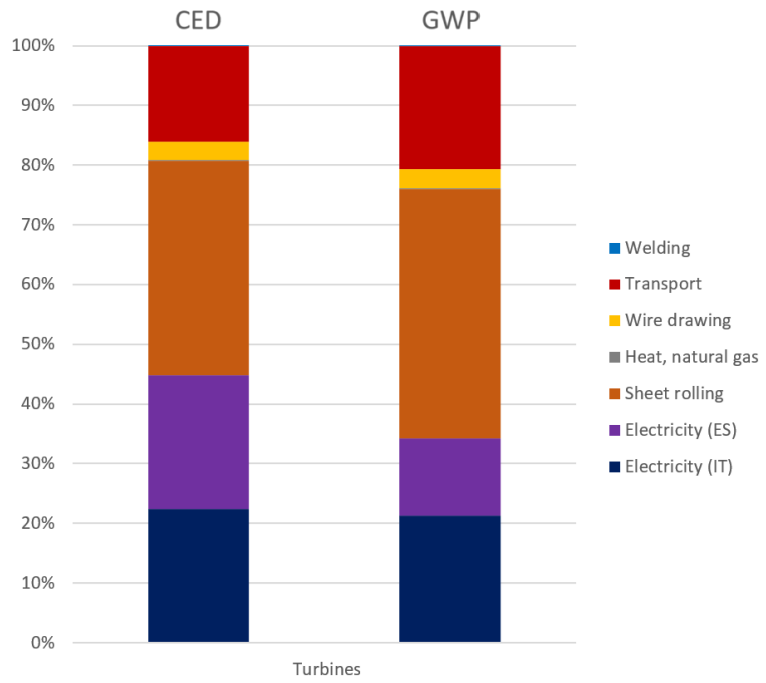

Figure 7.13: Breakdown of the turbines manufacturing's impacts at process level.

The electricity used for moving parts turned out to be the most critical element for the primary energy consumption used in the components manufacturing, representing 44% of the CED. Sheet rolling used for steel and aluminium parts, instead, follows right after with 36%.

Road and sea transport involved between the manufacturing facilities and the site's location produce fairly different results. Based on Table 6.31 data, it's possible to compute the total transport requirements related to both, equal to 1384.17 $\frac{t*km}{GWh}$ and 2059.64 $\frac{t*km}{GWh}$, respectively. Road transport was assumed to be carried out using EURO 4 lorries, while sea transport using container ships. According to the selected Ecoinvent processes, the primary energy required for transport totalizes 16% of the overall wind turbines' manufacturing consumption (see Figure 7.13), of which 8% is represented by sea transport and 92% by road transport. This means that sea transport is much more efficient than road transport, considering that to fulfil a duty 49% higher it requires 11.5 times less energy. Hence, especially for longer trips, transport by ship should be preferred, when possible, on lorries.

Wire drawing, while requiring twice the primary energy per kg compared to sheet rolling, has still a small influence on the CED - equal to 3% of the total - due to the limited mass fraction interested by the process itself. The remaining manufacturing processes, i.e. silica melting in the turbines' generator and transformer (heat, natural gas) and the tower segments welding account all together for less than 0.5% of the total primary energy consumed, therefore they can be considered negligible.

Since pollutant emissions are proportional to energy consumption, the GWP of the previous manufacturing processes is affected by similar contributions compared to the CED ones. However, considering that each of them employs different sources of energy, results are still influenced by the type of fuel used and the energy conversion processes involved.

Electricity used for moving parts, for example, is supposed to be generated using different primary resources depending on the location of the manufacturing facilities. As specified in the inventory definition (see Table 6.30), all the turbines' parts besides the tower are made and assembled in Spain, while the tower itself is produced in Italy. Therefore, the Spanish and the Italian electricity mix were selected in SimaPro to include the amount of electricity required for the manufacturing of these components. While the CED referring to the overall energy used in the two locations turned out to be identical, each accounting for 22% of the total, their GWP resulted to determine 13% of the total GHGs damage for the Spanish mix, while 21% for the Italian mix. The outcome is twofold: first, the electric energy used for moving parts has a GWP lower than the mean value coming from every manufacturing process concerning the wind turbines, given the lower total contribution compared to the CED one (44% vs 34%); second, the Spanish electricity mix is cleaner in terms of CO2-equivalent emissions compared to the Italian one, since the former, with the same primary energy consumption, determines almost half the damage of the latter. It's worth noting that the Ecoinvent dataset dealing with electric energy consumption (*market for electricity*) includes, for a given energy input in kWh, not only the impacts deriving from the national production of electricity, but also the ones associated with the electricity imported from other nations, as well as the those concerning the transmission network.

On the other hand, sheet rolling of steel and aluminium, accounting for 36% of the turbines' manufacturing CED, present a GWP per MJ of primary energy higher than the average, determining 42% of the overall GWP. This is caused by the need to use power coming from both electricity and natural gas, which brings towards higher emissions compared to using only electricity.

Similar considerations can be made for the road and sea transport activities involved in the turbines' manufacturing, since lorries and container ships are powered by diesel and heavy fuel oil, respectively. In fact, their contribution to the GWP is equal to 21% while representing 16% of the CED. Nevertheless, the higher efficiency of sea transport still holds even in the case of the GWP, since the total transport CO2-equivalent emissions originate for 9% from container ships, while the remaining 91% from lorries.

Wire drawing, instead, keeps accounting for 3% of the total GWP given that its impacts derive from a small fraction of the turbine's mass, as well as the remaining manufacturing processes (silica melting, tower welding) still determine less than 0.5% of the overall CO2-equivalent emissions.

7.1.3. Operation and Maintenance

The system's *operation and maintenance* phase accounts for 8% of the life cycle CED and 7% of the life cycle GWP. Since the effect of the electric consumption related to the supervisory control and data acquisition system (i.e. SCADA system) and all the other auxiliary systems required during the plant's operation is already included in the net production delivered to the transmission grid, the environmental burdens concerning the O&M phase derive by the maintenance activities only. A detailed breakdown of the contributions of scheduled and unscheduled maintenance activities is shown in Figure 7.14 for both CED and GWP.

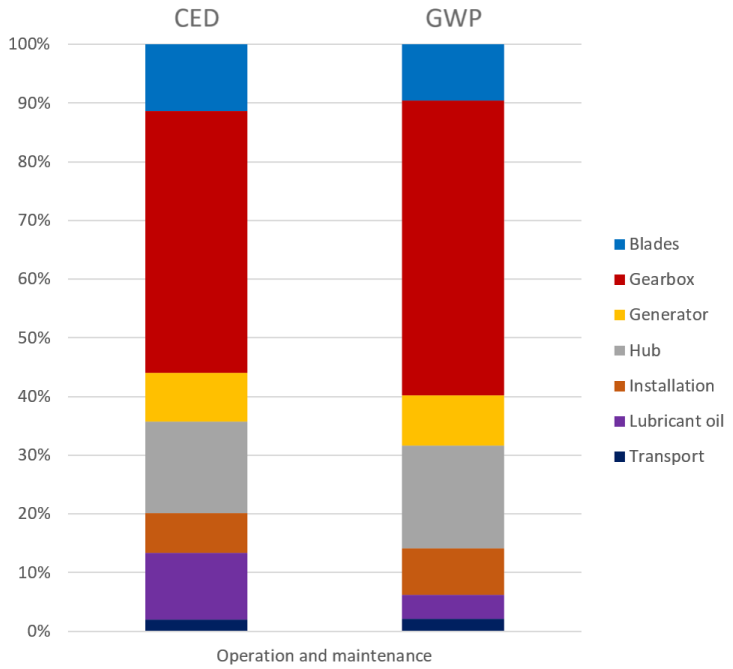

Figure 7.14: Breakdown of the O&M's impacts.

As discussed in the inventory definition, the only relevant activity characterizing the scheduled maintenance is related to the turbines' gearboxes lubricant oil refilling and substitution, which turned out to represent 11% of the total primary energy consumption and 4% of the total GWP involved in the O&M phase. The remaining impacts are determined instead by the replacement of those turbines' components that are expected to fail in a critical way during the plant's useful life. Given the statistical nature of these types of phenomena, they are typically classified as unscheduled maintenance activities.

For the baseline scenario, the approach followed by Schreiber et al. (2019) was used to predict which components and how many times they will fail over 25 years of operation. The resulting data (Table 6.56) were implemented in SimaPro assuming that production (raw materials acquisition + components manufacturing) and installation

of each replaced component would have been defined by the same datasets and processes selected for the initial plant's configuration. Overall, the replaced components' production accounts for 80% of the total O&M CED and 86% of its GWP. The contribution of the single components mainly depends on two factors: number of units replaced and primary consumption/CO2-equivalent emissions per unit produced. These items have been reported in Table 7.8, expressing the environmental impacts in terms of percentage on the life cycle's total. It's evident that, given the high number of components replaced, the gearbox represents the most critical element, determining 45% of the total O&M CED and 50% of its GWP. The hub replacements follow right after with 16% and 18% of the O&M impacts. The blades, instead, despite requiring only one replacement over 25 years, affect the results more than what the generator does, since their production, as discussed in the *raw materials acquisition* section, is quite energy intensive. Their contribution to the O&M impacts is in fact 11% for the CED and 10% for the GWP, compared to the 8% and 9% coming from the generator. The remaining items, i.e. the installation of the replaced components and their transport[14], determine together 9% of the O&M CED and 10% of its GWP.

Table 7.8: Number of units replaced and primary consumption/CO2-equivalent emissions per unit produced compared to the system's total.

Component	N. replaced	% CED/unit	% GWP/unit
Blades	1	0.90	0.69
Gearbox	8	0.44	0.45
Generator	2	0.33	0.31
Hub	3	0.41	0.42

7.1.4. End-of-life

The system's *end-of-life* phase accounts for 8% of the overall CED and 9% of the overall GWP. The analyzed scenario is based on the components and materials destinations assumed during the design phase of the power plant with the only exclusion of the transformer substation's electromechanical components, whose end-of-life has been modelled instead using the data retrieved from the EPD of the three-pole switch. As already specified, the largest contribution to the end-of-life environmental impacts (~98%) comes from the wind turbines' components disposal, not only considering their high mass fraction on the total waste amount deriving from the *decommissioning* phase, but also since these components require several pre-treatments in addition to the disposal activities themselves that enhance even more the burdens generated.

[14] In this case, transport refers only to those trips belonging to the replaced parts' manufacturing phase that were modelled using the *market for transport* dataset.

How the single turbines' components affect the primary energy consumption and carbon footprint of the system is substantially dependent on three factors: waste treatment process, waste material composition and waste mass. In Figure 7.15 are shown the contributions to the CED and GWP coming from the turbines' major components and the nacelle's sub-components. Focusing on the primary energy consumption, the tower determines the highest burdens with 46% of the total CED, followed by the nacelle with 34%, the blades with 11% and the hub with 10%.

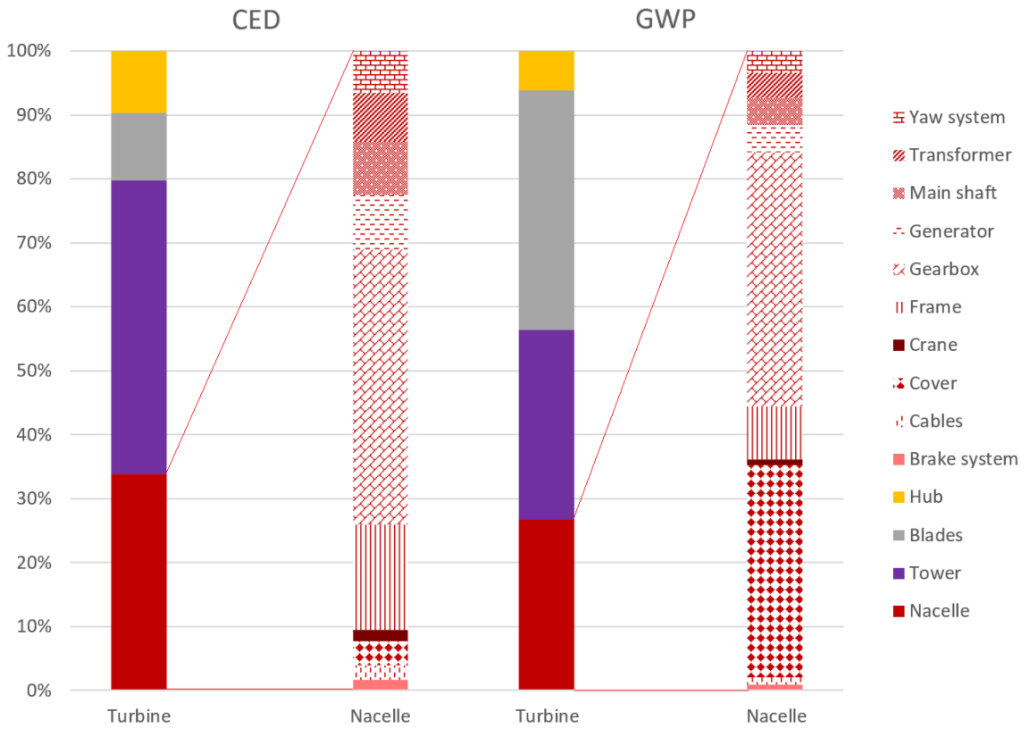

Figure 7.15: Breakdown of the wind turbines' end-of-life impacts at component level.

In general, the components' disassembly phase required to separate each material type and prepare the waste to the disposal/recycling procedures resulted to be the most demanding activity, typically accounting for around 80% of the total primary consumption of the single turbine's major components, as reported in Figure 7.16.

The incineration process involving the composite material found in the blades, the cone and the nacelle's cover, is expected to require a limited amount of energy (< 1% of the process' CED) to perform the combustion, since combustion is typically fed by the reaction itself and only requires to be triggered using a small amount of fuel. Nonetheless, the whole process is characterized by the addition of several chemicals and auxiliary materials that are needed to purify the flue gases whose production determines a specific primary energy consumption comparable with the other disposal/recycling processes (see Figure 7.16). The transport requirements for

incinerated components are the least demanding from the CED point of view, since the mean distance covered by lorries is the lowest, even more considering that the pre-treatments are supposed to be carried out in the same facility. As described in the inventory definition, the composite material is expected to be shredded before the incineration itself. Shredding turned out to be more energy intensive than the subsequent disposal procedure. Taking the blades as example, shredding accounts for 10% of the total blades' CED, while the actual incineration process only 7%. Given the small mass fraction of the blades compared to the other turbine's major components and the average specific impacts concerning their disposal scenario, they result not to be able to cover much more than $\frac{1}{10}$ of the turbines' end-of-life CED.

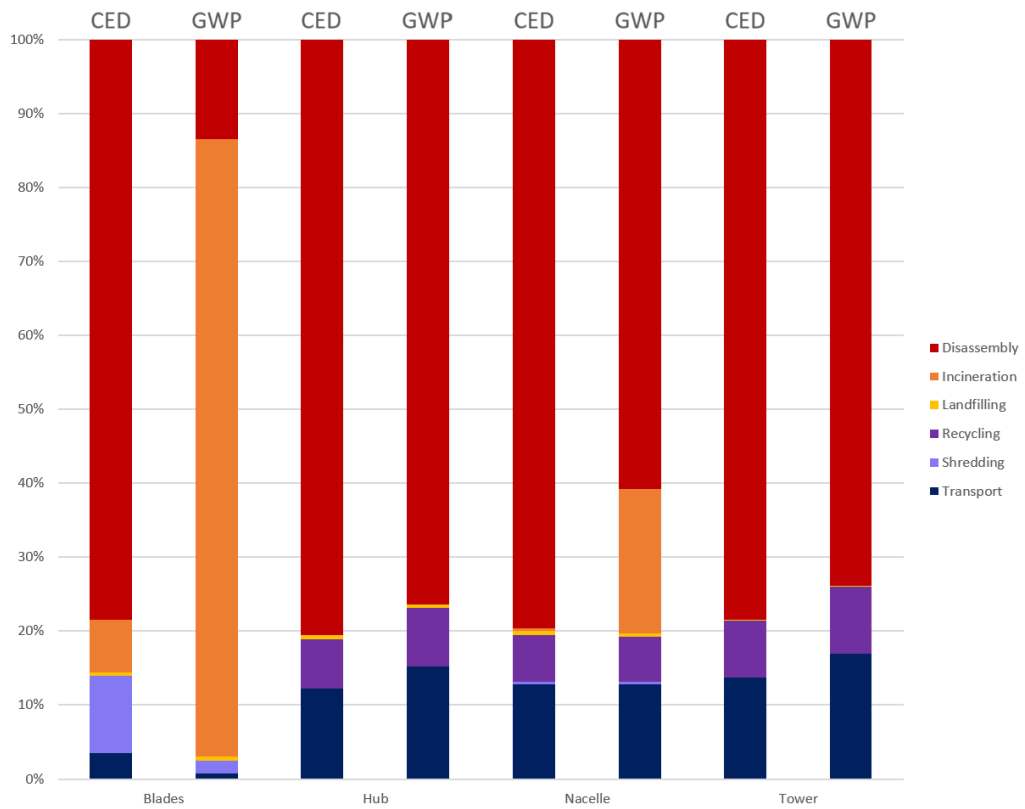

Figure 7.16: Breakdown of the wind turbines components' end-of-life impacts at process level.

The tower and the nacelle, instead, which represent the heaviest turbine's components, clearly define the most energy demanding items. Considering that a large mass fraction of these two components is composed of ferrous materials, they are expected to undergo similar disposal processes, as well as recycling procedures. After the disassembly, recycled metallic components will be sorted and then pressed. Since the recycling facility does not coincide with the recovery center, these components will need additional road transport compared to the incinerated ones. Moreover, the distances involved between the site, the recovery centers and the recycling facilities

are way higher on average than the distance between the site and the incinerator (see Table 6.65), hence, the superimposition of these two effects determines that transport primary energy has a relevance around 5 times higher for the nacelle and the tower compared to the blades' one, even higher than the sorting and pressing contributions, which are represented by half of these values (see Figure 7.16).

Focusing on the nacelle's sub-components, since all of them besides the cover are expected to undergo similar disposal scenarios, the relative environmental impacts tend to be proportional to the sub-components weight. An important factor in this case is also the amount of waste deriving from the unscheduled maintenance activities, considering that, according to the baseline maintenance scenario previously described, 10 out of 14 replaced components during the 25 years of operation will belong to the nacelle's assembly. Specifically, wind turbines will require the replacement of 8 gearboxes and 2 generators (see Table 6.56). Given that the gearbox production is the most critical among the other nacelle's sub-component both in terms of primary energy consumption and carbon footprint, its replacements can significantly affect the impacts of the nacelle itself, especially since the total number of units required is more than double the initial amount installed during the first turbines' erection. That's why the gearbox alone is responsible for almost half the impacts coming from the nacelle's sub-components disposal (see Figure 7.15). It's worth noting that the burdens deriving from the lubricant oil end-of-life have been included in those of the gearbox, but their effect on its CED are quite limited (~ 5% of the gearbox total).

Lastly, while the waste management of the hub results to be identical to the one of the tower but with slightly lower recycling rate, its impacts are the lowest among the other turbine's major components due to its small mass fraction, even by adding the contribution of the replaced components during the useful life, which in the case of the hub are equal to 3.

Moving on to the GWP, major changes to the distribution of the environmental impacts are caused by the GHGs emissions deriving from the incineration processes. The impacts related to the blades now cover 37% of the total burdens, while the tower and the nacelle 30% and 27%, respectively. The hub still holds the lowest damage with 6% of the total.

As introduced before, when a waste material is incinerated, the flue gases originating from the combustion are typically treated using various chemicals and auxiliary materials to cleanse the stream of toxic and hazardous compounds, such as sulfur oxides, nitrogen oxides and heavy metals. For this reason, the outlet stream at the stack of the facility mainly consists in a CO2-rich gas later dispersed in the atmosphere, while the solid unburnt residues are landfilled. Among the components decommissioned from the wind power plant, the turbine's blades, the nacelle's cover and the lubricant oil used in the gearbox are expected to be disposed through incineration. The composite material found in the blades and the cover is composed of

epoxy resin (60%) and glass fibre (40%). After the shredding pre-treatment, this material is supposed to be incinerated as a whole. Since glass fibre is an inert material and can't be burned, the entire emissions generated from the combustion are provided by epoxy resin, which is instead a synthetic organic compound. The environmental damage caused by such emissions, together with those coming from the life cycle of the other auxiliary materials and the residues landfilling, turned out to be remarkably higher than the ones derived from the remaining processes, disassembly included (see Figure 7.16). In fact, while the incineration process resulted in accounting for only 7% of the blades' end-of-life CED and the disassembly for 79%, in this case the former determines 84% of their total GWP, while the latter only 13%. In absolute terms, the GHGs emissions originated from the blades' disposal overcome the amount generated by any other component due to the significantly higher emission factor of epoxy resin incineration compared to the one of the other processes.

A similar outcome also characterizes the nacelle's cover: despite representing only less than 1% of the nacelle's end-of-life CED, now it accounts for 13% of its GWP. Moreover, the gearbox emissions still define a considerable fraction of the damage thanks to the effect of the lubricant oil incineration, which alone determines 19% of the total nacelle's impacts, for a total of 40% considering also the waste management of the metallic parts.

All the other components, i.e. the tower, the hub and the remaining nacelle's sub-components, since they present similar disposal procedures involving mainly metallic parts, determine a GWP share that is proportional to their mass, which reflects the contributions shown in Figure 7.15.

7.2. Environmental indexes calculation and comparisons with other studies

Environmental indexes are typically used to give a synthetic but effective interpretation of the level of sustainability related to power plants' primary energy consumption and carbon footprint. Based on the goal and scope of the present assessment, 3 environmental indexes have been selected to assist the fulfilment of the targets previously set:

- Energy payback time (EPBT): EPBT (see eq. 5.1) is defined as the ratio between the primary energy used by the system along its entire life cycle and the net electrical energy delivered from the power plant to the national grid in one year of service. Considering the meaning of the cumulative energy demand impact assessment method and how its category indicators are defined, the EPBT can be expressed as:

$$EPBT\ [year] = \frac{E_{prim,tot}\ [GWh]}{AEY\ \left[\frac{GWh}{year}\right]} = \frac{CED\ [GWh]}{AEY\ \left[\frac{GWh}{year}\right]} \tag{7.4}$$

where the CED category indicator result, expressed in GWh, is equal to the sum of all the results concerning the impact categories included in the assessment, i.e. non-renewable, fossil; non-renewable, nuclear; renewable, biomass; renewable, wind, solar, geothermal; renewable, water.

- Energy return on investment (EROI): EROI (see eq. 5.2) is defined as the ratio between the net electrical energy delivered from the power plant to the national grid over its useful life and the primary energy used by the system along its entire life cycle. Again, the cumulative energy demand impact assessment method can be used to express the EROI through:

$$EROI\ [-] = \frac{AEY\left[\frac{GWh}{year}\right] \cdot plant\ lifetime\ [years]}{E_{prim,tot}\ [GWh]} = \frac{OEY\ [GWh]}{CED\ [GWh]} \tag{7.5}$$

where OEY is the overall electric energy yield and the CED indicator result is defined using the sum of all the results concerning the impact categories included in the assessment.

- Carbon Payback Time (CPBT): CPBT (see eq. 5.3) is defined as the ratio between the carbon dioxide emissions generated over the entire life cycle of the system and the emissions saved per year with respect to a reference non-renewable electricity generation technology. If the CPBT is used to compare the impact on the global warming caused by all the greenhouse gases instead of only CO2, the IPCC GWP100 impact assessment method can be used in the equation as follows:

$$CPBT\ [year] = \frac{GWP100\ [KgCO2eq]}{GWP100_{saved,year}\ \left[\frac{KgCO2eq}{year}\right]} \tag{7.6}$$

where the category indicator result, expressed in kgCO2eq, is equal to the sum of all the results concerning the impact categories included in the assessment,

i.e. fossil emissions, biogenic emissions and land transformation emissions. Electricity generation from natural gas was chosen as reference technology for the CPBT computation since gas-fired power plants produce the highest fraction of the total electric energy consumed in Europe. A mean GWP of 0.434 $\frac{kgCO2eq}{kWh}$ (2020) for European gas-fired power plants was retrieved from the work of Guidi et al. (2023).

Using Table 7.1 data and the information on the power plant's annual net production, an EPBT of 1.52 years and an EROI of 16.42 were computed, together with a CPBT of 0.86 years. Considering that the plant's useful life is expected to extend for 25 years, the primary energy required by the system life cycle and its emission generated are going to be repaid after 6% and 4% of its operational period, respectively, which proves the high level of renewability and sustainability of this type of technology. These values can be compared with those concerning the LCA studies previously reviewed. In Table 7.9[15] are reported the maximum, minimum and average values for the selected environmental indexes taken from the comparison studies which dealt with onshore wind power plants.

Table 7.9: Environmental indexes comparison between the reviewed and the present study.

Environmental index	Min	Avg	Max	This study
EPBT [y]	0.40	0.79	2.14	1.52
EROI [-]	9.35	30.57	50.00	16.42
CPBT [y]	0.21	0.42	0.83	0.86

The wind power plant object of the present study appears to perform worse than the average for both primary energy consumption and carbon footprint. Nevertheless, this outcome can be justified in several ways:

- The mass of the whole turbine, as well as the one of its major components, is significantly higher than the average characterizing wind turbines with similar nominal power retrieved from the comparison studies. Table 7.10 shows the minimum, maximum and average mass values concerning wind turbines parts with nominal power included between 2 MW and 3 MW ($\pm$0.5 MW compared to the G114 – 2.5 MW) for which explicit data were available in the reviewed LCA. All the major components, foundations included, resulted to be above average, especially the rotor, which exceeds the maximum value. The G114 – 2.5 MW wind turbines, in fact, feature a wide rotor with a diameter 112 m long, whose size is comparable with turbines having 4.5 MW (Tremeac and Meunier,

[15] Crawford (2009) environmental indexes have been excluded from the comparison, since the methodological approach used to define the life cycle inventory differs from the one used by the present and the reviewed studies, as remarked in Chapter 5.

2009) and 3 MW (Gomaa et al., 2019) nominal power, equipped with 113 m and 112 m rotors, respectively. The turbine's blades represent an important fraction of the rotor weight, accounting for 60% of its total mass. As previously discussed, the blades are composed of a composite material whose production requires a considerable amount of primary energy, which determines itself just as high GHGs emissions. The necessity of using turbines with bigger sizes is mainly related to the site's wind resource. Since Iurefalco's site location is characterized by a mean wind speed for a given hub height that is sensibly lower than the average involved in the comparison studies, to achieve a certain power (see eq. 3.4) it's required a bigger rotor and/or a taller turbine, causing the turbine's weight to rise. This is particularly critical due to the fact that the turbines' raw materials acquisition always represents a very significant fraction of the impacts concerning the system's primary energy consumption and carbon footprint, as also confirmed by the present study. Moreover, a higher turbine's weight typically reflects in a bigger foundation that has to sustain the stresses coming from the base of the tower. The turbines foundations' production, according to all the reviewed LCA, always determines the highest burdens after the turbines' contribution, and Iurefalco's power plant makes no exception, as reported in Table 7.1. For these reasons, having bigger and heavier components concerning wind turbines and their civil works considerably worsens the system's environmental impacts.

Table 7.10: Wind turbines components' mass comparison (in tons) between the reviewed and the present study.

Component	Min	Avg	Max	This study
Rotor	33.81	42.39	56.50	67.27
Nacelle	46.10	72.82	120.00	101.35
Tower	108.00	176.97	245.72	185.90
Foundation	740.00	1222.44	1924.23	1618.08[16]

- The plant's capacity factor is lower than the average reported in the comparison studies (Table 7.11). As already specified in the literature review, the capacity factor (CF) is equal to the ratio between the net electric energy delivered to the grid in a given period and the electric energy that the power plant would have produced if running constantly at its rated power in the same period. CF is one of the most critical parameter for both the revenues and the sustainability of a wind power plant, considering that it's proportional to the annual energy yield. Among the multitude of parameters that can affect the CF, it's widely acknowledged that the quality of the wind resource in terms of

[16] The foundation mass was calculated as weighted average of all the types of foundation present in the power plant using the concrete densities proposed by the SimaPro datasets.

mean wind speed and turbulence intensity is the main contributor to its final value. Specifically, a more limited wind resource generally determines a lower mean power generated by the turbines, causing a smaller energy yield along the useful life. Hence, the lower mean wind speed characterizing the site involved in the present work, in addition to increasing the size of the turbines, also generates a smaller electricity output delivered to the grid, which negatively impacts on the environmental indexes considered.

Table 7.11: CF comparison between the reviewed and the present study.

Min	Avg	Max	This study
0.190	0.340	0.554	0.276

- In this study, it was possible to evaluate the environmental burdens related to the life cycle of those civil works that are generally neglected in the reviewed assessments, i.e. the construction of the MV and HV cable trenches, the site's internal roads, the turbines' platforms, the transformer substation and the external roads adjustments required for the components transportation. These elements turned out to determine together 14% of the system's primary energy consumption and 11% of its global warming potential. Such values are in line with the results reported by the few studies that included in their inventory data information regarding the whole civil works activities involved in the power plant construction. Bonou et al. (2016) assessed the carbon footprint of two onshore wind power plants using 20 turbines with 2.3 MW and 3.2 MW nominal power, respectively. The carbon footprint environmental impacts were evaluated using the IPCC method. In both cases, the total burdens deriving from the plant's civil works excluding the building of the turbines' foundations over the entire life cycle accounted for 11% of the overall damage. Ardente et al. (2008) assessed the primary energy consumption of an onshore wind power plant using 11 turbines with 0.66 MW nominal power. In this case, the above-mentioned construction activities resulted to require 16% of the total primary energy, also including the contribution of the power cables production. It's worth noting, however, that a more accurate estimation of the impacts associated with the transformer substation construction involved in the present study, i.e. including the inventory data concerning all the auxiliary systems and control units, will probably lead to a slightly higher environmental damage compared to what has been shown up to now.

- The *end-of-life* phase doesn't generate any recycling credit for the system. This is a direct consequence of choosing the 100-0 approach as modeling method for recycled or reused waste materials. The 100-0 approach was used primarily to

give a conservative estimation of the end-of-life environmental impacts, considering that the boundaries of the system have been defined excluding the actual recycling/reusing processes that should be employed for the waste deriving from the *decommissioning* phase. Nevertheless, this methodology always provides an overestimation of the impacts compared to the 0-100 approach. The entity of the credit that is assigned to the system depends on several factors, among them the recycling/reusing rate, the type of recycling/reusing processes and the avoided products that the recycled/reused items are assumed to replace. More in general, in fact, when a material/component is recovered, its recovery process could also determine a net environmental damage that penalizes the total eco-profile of the system after the product substitution, for example due to being very energy intensive. In the case of wind power plants' end-of-life, the 100-0 credit system generally produces a highly positive effect for the impacts related to primary energy consumption and GHGs emissions. This is possible especially thanks to the remarkable recyclability of metals, which often represent the highest waste mass fraction to dispose and whose recovery processes require significantly less energy and GHGs emissions compared to their raw materials extraction and refining. Moreover, as emphasized many times, the *raw material acquisition* phase represents by far the most critical phase of the power plant's life cycle, hence decreasing its burdens is an effective way to improve the system's energy balance and carbon footprint. Table 7.12 summarizes the spectrum of reduction of the environmental impacts concerning the CED and the IPCC GWP assessment methods generated by the application of the credit system for those studies among the reviewed ones in which it was possible to retrieve explicit data about the end-of-life effects on the plant's eco-profile. The width of the spectrum mainly originates from the different assumptions regarding the materials' recycling rates and how the non-recovered fraction is disposed. On average, the credit system provides a reduction of the impacts close to 50% of the total, which demonstrates that wind power plants circularity already has a great potential in the mitigation of the burdens related to the life cycle of this technology. It is expected, for this reason, that accounting for the benefits of recycled materials could potentially lead to much lower EPBT and CPBT than what has been reported for the present study in Table 7.9, as well as higher EROI.

Table 7.12: Reductions of the CED and GWP values in response to the end-of-life credit.

Impact assessment method	Min %	Avg %	Max %
CED	43.4	51.7	63.6
IPCC GWP100	15.7	36.0	65.8

Further investigations have been conducted by comparing the environmental damage caused by the system's carbon footprint with other electricity generation technologies. The comparison is based on the results obtained by Guidi et al. (2023) in their literature review concerning cradle-to-grave LCAs of both conventional and low carbon technologies (Guidi et al., 2023). The research involved studies published from 2013 to 2022 consistent with the ISO 14040 and 14044 standards (Guidi et al., 2023). In Table 7.13 is shown the GHG intensity characterizing all the plant types for which it was explicit the minimum and maximum value among the respective classes. Based on Table 7.1 results, the GHG intensity of the wind power plant object of the study resulted to be equal to 14.98 $\frac{gCO2eq}{kWh}$. Comparing this value with Table 7.13 intervals, it turns out to be close to the lower end of the most sustainable technologies, i.e. nuclear and run-of-river (hydro) power plants. Moreover, it's worth noting that the most widespread solar PV technologies relying on silicon modules result to generate in the best case almost double the damage of the assessed wind power plant. Since the EU environmental and energetic policies are going towards consistent investments on wind and solar plants to overcome energy dependance and meet the climate targets, this is an aspect that has to be taken into consideration. More in general, in fact, as reported by Guidi et al. (2023), wind technology determines an average GWP of 16.4 $\frac{gCO2eq}{kWh}$, one of the lowest among low carbon technologies (Guidi et al., 2023). Nevertheless, it's clear that both wind and solar technologies, compared to fossil ones, provides massive improvements and will surely play a fundamental role in the future energy scenario.

Table 7.13: GHG intensity of conventional and low carbon technologies (Guidi et al., 2023).

Technology	Plant type	gCO2eq/kWh
Fossil	Coal-fired	753.9 – 1215.4
	Gas-fired	379.0 – 678.3
Hydropower	Reservoir	31.1 – 74.4
	Run-of-river	12.3 – 19.2
Photovoltaics	Mono-Si	31.1 – 74.3
	Multi-Si	30.8 – 71.2
	Mono and multi-Si	25.1 – 61.5
Concentrated solar power	Parabolic trough with storage	26.0 – 60.0
Geothermal	Single flash	18.0 – 24.0
	Double flash	15.0 – 23.0
Nuclear	LWR	5.1 – 6.4
	PWR	8.0 – 13.1
	SMR	5.1 – 10.3
	EPR	8.0 – 64.0
	GT-MHR	9.6 – 9.9

7.3. Interpretation of CED category indicators' results

The share of renewable energy sources in the primary consumption required by the system over its life cycle was evaluated with the aim of giving an insight on the resource depletion severity characterizing the exploitation of each input. Renewable energies, by definition, are in fact considered as naturally replenishing and virtually inexhaustible, although with limited amount available per unit time (EIA, 2023). Non-renewables, instead, are not able to regenerate themselves in a human timescale, hence their consumption results in a permanent loss.

As already mentioned, the CED impact categories indicators provide the subdivision of the total primary energy consumption associated with execution of a generic process in renewable and non-renewable energy sources. Non-renewable energy sources are classified as *fossil*, *nuclear* and *biomass*, while renewables in *solar*, *wind*, *geothermal*, *biomass* and *hydro*. In Table 7.14 are shown the shares of the indicators' results for the main components production + installation and the remaining life cycle phases of the system. In general, renewable energies represent no more than 15% of the total primary energy consumed in any stage considered. The highest shares are found in those stages that involve more than the others the use of electricity.

The *end-of-life* phase, which is supposed to require a significant amount of electricity for the components' disassembly and pre-treatments before recycling, represents for this reason the most sustainable one, with 15% of its primary energy coming from renewable sources. The production and installation of the wind turbines follows right after with 8% of renewables. Steel making, likewise the other ferrous materials, typically involves the use of electric arc furnaces that smelt iron scraps using electricity as a fraction of their energy demand. The remaining fraction is covered by natural gas and/or hard coal. Depending on the material's final carbon content, a higher or lower amount of coal may be necessary to obtain the desired chemical composition of the alloy. The production of low-alloyed steel and ferrite (used as proxy for iron components), which require limited amount of carbon, turned out to be more sustainable than cast-iron production, which instead presents this element in higher quantities. Copper and aluminium production, instead, although being very energy intensive, are characterized by a consistent fraction of renewables equal to 21% and 25%, respectively, due to the use of electrochemical processes needed to obtain high purity materials. The two main manufacturing processes employed for metals working, i.e. sheet rolling and wire drawing, require both heat from natural gas and electricity. In general, the amount of electricity is able to increase a bit the share of renewables in the production of metallic parts, since in this case natural gas is used in smaller quantities.

Epoxy resin and glass fibre found in the blades and the nacelle's cover are characterized by several chemical processes which require heating usually provided by natural gas and, in smaller part, by steam. While also electricity is used in the

manufacturing process, the overall energy mix has a higher fraction of fossil resources compared to the metals' one which makes less sustainable the turbines' production, given that the blades alone are responsible for more than 35% of the total CED.

The turbines' foundations are composed of concrete and reinforcing steel. Concrete energy requirements are mainly related to those of the cement since the inert aggregates, as previously demonstrated, present a very small specific energy factor. Electricity is used in cement production to mill the raw materials and allow the rotation of the rotary furnace needed to burn them. After the burning process, milling is also required to crush the products. Nevertheless, the amount of energy spent to perform these activities is quite low compared to the fossil resources fed to the furnace to reach its working temperatures, hence more than 90% of the concrete CED is on average determined by non-renewable fossil resources, with renewable ones accounting for less than 5%. Reinforcing steel production is expected to use an energy mix that contains fewer renewables compared to other low-alloyed steel components, since the raw materials employed are processed for the most part through the converter technology. This technology uses blast furnaces to produce cast iron which will then oxidized in order to produce low-alloyed or unalloyed steel. As mentioned before, cast iron production is characterized by a higher fossil consumption, hence by a lower share of renewables. Considering the contributions of concrete and reinforcing steel, the turbines' foundations are quite problematic from the sustainability side, even more given that they represent alone almost 13% of the total life cycle CED (excluding the copper rope burdens).

Similarly to the wind turbines, the transformer substation construction required 8% of renewable energies. In this case, 85% of the environmental impacts are determined by the transformer life cycle and the civil works materials production. According to the data contained in the transformer's EPD, more than 70% of the transformer's mass is composed of metals, such as steel, copper and aluminium, while 20% of lubricant oil, whose production energy mix was found to be similar to the one of epoxy resin by comparing the datasets present in the Ecoinvent database. Given the similarities characterizing the material composition of the wind turbines and the transformer, the share between renewable and non-renewable energies resulted to be approximately the same[17]. The civil works materials, instead, are mainly affected by the reinforced concrete energy requirements that, as explained before, reduce the average renewable share.

The O&M phase, again, turned out to behave not so differently from the wind turbines since its primary energy consumption is essentially related only to the supply of

[17] Since renewable and non-renewable primary energy consumption are usually not subdivided per energy source in EPDs, for the sake of the present study in which the interest is placed only on the resource depletion severity, the whole transformer's non-renewable consumption was considered as fossil energy, while the renewable one as wind energy.

turbines' parts. Conduits and internal roads construction still have a comparable renewable share (7%) due to the influence of the power cables, representing almost 40% of its environmental impacts. The materials used for the civil works, i.e. concrete, limestone and asphalt, are instead highly non-renewable reliant, especially the asphalt, which accounts for more than 80% of the civil works CED, as explained before. For the same reason, the platforms and the external roads construction are characterized by the lowest fractions of renewable energies among all the components and life cycle stages considered.

Table 7.14: CED indicators' results for the main components production and life cycle phases.

Impact category	Turbines[18]	Conduits + int. roads[19]	Platforms	External roads	Transformer substation	O&M	Decommissioning and end-of-life	Weighted average
CED %	69.1	9.9	2.0	0.6	3.0	8.2	7.2	-
N-R, fossil	82.8	88.6	97.8	93.4	89.7	82.3	76.1	83.4
N-R, nuclear	8.7	4.3	1.1	2.5	2.1	9.7	9.2	8.0
N-R, biomass	0.0	0.0	0.0	0.0	0.0	0.0	0.0	0.0
R, biomass	1.7	1.3	0.2	2.2	1.1	1.3	2.0	1.6
R, wind, solar, geot.	1.5	0.3	0.2	0.4	4.9	1.9	4.2	1.7
R, water	5.3	5.5	0.8	1.4	2.2	4.9	8.6	5.3

A last clarification concerns the assumptions made on the HV/MV transformer and the three-pole switch primary resources consumption. Since in both EPDs used to derive the related inventory data the energy values are reported using the fuels LHV, in order to evaluate the CED standard these values were conservatively increased by a 10% factor based on the work of Frischknecht et al. (2015). This assumption was justified by computing again the CED of the system but using its LHV version and excluding the contributions of the transformer and the three-pole switch. The output was then compared with the result given by applying the CED standard, also in this case excluding the above-mentioned contributions. Since $\frac{CED_{std}}{CED_{LHV}} - 1 = 0.094 = 9.4\%$, the assumption was considered consistent with the scope of the present study.

[18] The turbines' foundations are included.
[19] The power cables are included.

7.4. Sensitivity analyzes

7.4.1. Wind power plant useful life

Wind power plant useful life is one of the most critical parameters concerning its environmental performance. Likewise the capacity factor, the useful life is closely related to the plant's net electric production: if the operating period is extended, wind turbines are allowed to convert more wind kinetic energy in electric energy, increasing the revenues at the cost of more maintenance. Given that the system's primary energy consumption and its GHGs emissions are weighted for the overall GWhel generated during its life cycle, it's clear that a longer useful life could potentially greatly improve the associated environmental impacts, as well as a shorter one could sensibly make them worse.

In general, the extension of the useful life is related to both technical and economic/decisional aspects (Wiser and Bolinger, 2019). The technical aspects are primarily associated with the turbines' design certifications, which mainly depend on the specific turbine model and wind class (Wiser and Bolinger, 2019). Turbines' certifications often grant at least 20 years of operation, but recently many manufacturers are moving towards periods of 25, 30 or even more (Wiser and Bolinger, 2019). Technology maturity is also an important factor: more recent wind turbines' models present increased robustness, better performance and resistance to intensive wear conditions compared to older ones, which are able to extend its average lifetime (Wiser and Bolinger, 2019). Moreover, O&M practices also play a crucial role in the preservation of the turbines' integrity since they involve actions devoted to delay the ageing effects progression (Wiser and Bolinger, 2019). The economic and decisional aspects mainly focus on the type of energy market in which the power plant is involved and the end-of-life strategy planned for the project: after the last year of operation, either decommissioning or repowering can be expected, depending on the cases (Wiser and Bolinger, 2019).

In the design phase of the plant object of the study, a useful life of 25 years was estimated with subsequent decommissioning. Since the useful life depends on several uncertain factors, the variation of the impacts associated with a higher and lower useful life has been investigated. Given that 20 years is by far the most common extension of the plant's useful life among the reviewed studies and 30 years are considered the average value for the state-of-the-art technology (Wiser and Bolinger, 2019), the analysis was conducted for these two values. Compared to the baseline scenario, a variation of the plant's useful life mainly affects three aspects of the LCI:

- The net electric energy delivered to the grid. Assuming the same annual energy yield, in 20 years of operation the plant's production is expected to reduce of 20% in respect to the main case, while in 30 years of operation it's expected to increase of the same quantity. For this reason, all the values present in the LCI

defined in the previous sections have been recomputed by dividing the amounts per plant for the new electricity productions in order to obtain the updated values per FU. This applies also to the modifications that will be described in the next points.

- The use of primary resources and the global warming potential (expressed in kg CO2eq) of the HV/MV transformer. These quantities were in fact computed starting from the values reported per functional unit in the EPD published by Tamini (2020) (see Table 6.21). Since the functional unit is represented by a nominal transformer power of 25 MVA for 1 year of operation, in the two alternative scenarios these inventory data have to be multiplied for a factor equal to $\frac{16\ MVA \cdot 20\ y}{25\ MVA \cdot 1\ y} = 12.8$ and $\frac{16\ MVA \cdot 30\ y}{25\ MVA \cdot 1\ y} = 19.2$, respectively, for the case of 20 and 30 years of useful life.

- The number of components replaced during the O&M phase. It's expected that, for a shorter useful life, the total number of critical failures concerning the wind turbines' components is going to be lower than the baseline case, while higher for a longer one. The failure rates used for the baseline case have been assumed as unchanged in both the alternative scenarios. This assumption is based on the fact that each component that replace the old one is supposed to present the same initial conditions in terms of physical and geometrical properties and the evolution of its integrity over time (i.e. its damage mechanism) is negligibly affected by the ageing of the other components that have never been replaced. Table 7.15 shows the amount of replaced components for the 3 compared scenarios using the above-mentioned hypothesis. The inventory data related to each replacement have been obtained by using the same assumptions employed for the baseline case, waste management included.

Table 7.15: Number of components replaced over different useful life durations.

Replaced components / Scenario type	Gearbox	Generator	Hub	Blades
25 years (baseline)	8	2	3	1
20 years	6	2	3	1
30 years	9	2	4	1

Overall, extending and reducing the useful life of the power plant turned out to be quite impactful on the system primary energy consumption and carbon footprint (Figure 7.17). In both cases, a useful life of 30 years was able to reduce the total impacts by 16%, which also means a reduction of the same amount for the EPBT and CPBT of

the system, now attesting to 1.29 and 0.73 years, respectively. On the other hand, a useful life of 20 years determined an increase of the CED and GWP by 23%, bringing the EPBT and CPBT to 1.88 and 1.06 years, respectively. This outcome demonstrates that the Iurefalco wind power plant significantly benefits from having 5 more expected years of operations compared to the reviewed studies. Moreover, it can be foreseen that future wind power plants that will present for technological reasons a useful life equal or greater than 30 years are going to have way better eco-profiles compared to the older ones.

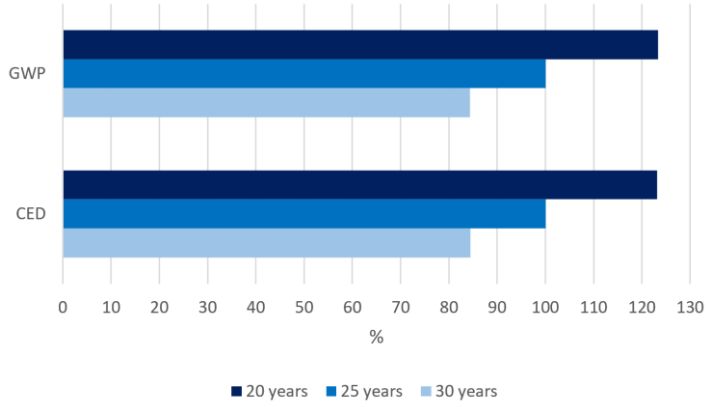

Figure 7.17: CED and GWP variations for the selected useful life durations compared to the baseline scenario.

7.4.2. Wind turbine's components replacement rates

As already remarked many times, wind turbines' components reliability is affected by multiple uncertainty factors that make difficult its determination and evolution over time. Moreover, wind turbines' manufacturers hardly ever disclose to the public such kind of information due to confidentiality reasons. For the estimation of the environmental impacts deriving from the components replacement over the plant's useful life the approach used by Schreiber et al. (2019) was followed, which based the replacement rates of each major component on the reliability data computed by McMillan et al. (2010) and Echavarria et al. (2008). These data have been consequently corrected with the reduction factor suggested by Reimers (2016) to account for the technological improvements including the development of the G114 – 2.5MW (2013) wind turbine. Given the potential uncertainty of the results obtained with this methodology and the relatively high influence of the unscheduled maintenance activities on both the CED and GWP of the system, a sensitivity analysis on the replacement rates of the turbines' components was performed to highlight how much the environmental impacts are affected in response to their sensible variation. The new scenarios were defined, this time, using the approach employed by Razdan and Garrett (2015) for Vestas Wind Systems. In their LCA concerning an onshore power plant featuring 25 wind turbines with 2 MW nominal power, the sensitivity analysis

on the parts replacements was conducted by doubling and halving the replacement frequencies (Razdan and Garrett, 2015). Table 7.16 reports the variation of the number of components replaced in the case of the present study by applying the above-mentioned methodology. The inventory data related to each replacement have been obtained using the same assumptions employed for the baseline case, waste management included.

Table 7.16: Number of components replaced with modified failure rates.

Replaced components / Scenario type	Gearbox	Generator	Hub	Blades
Baseline	8	2	3	1
X2 failure rates	15	3	6	2
X0.5 failure rates	4	1	2	1

The computation of the CED and the GWP of the system for the possible scenarios brought to the results shown in Figure 7.18. In the worst case (X2), the system's primary energy consumption and carbon footprint increase for 7% of the baseline values, while in the best case (X0.5) they decrease for 4% of the baseline values. Although a 7% increase of the impacts can't be considered as negligible, it's also true that the worst scenario is very unlikely to happen since the failure rates differ a lot from the average ones and Razdan and Garrett themselves claimed that this estimate is very conservative. At the same time, even if they are halved, the possible reduction of the impacts is not particularly significative. Therefore, it can be stated that the results obtained with the baseline scenario present poor sensitivity towards the turbines' components replacement rates.

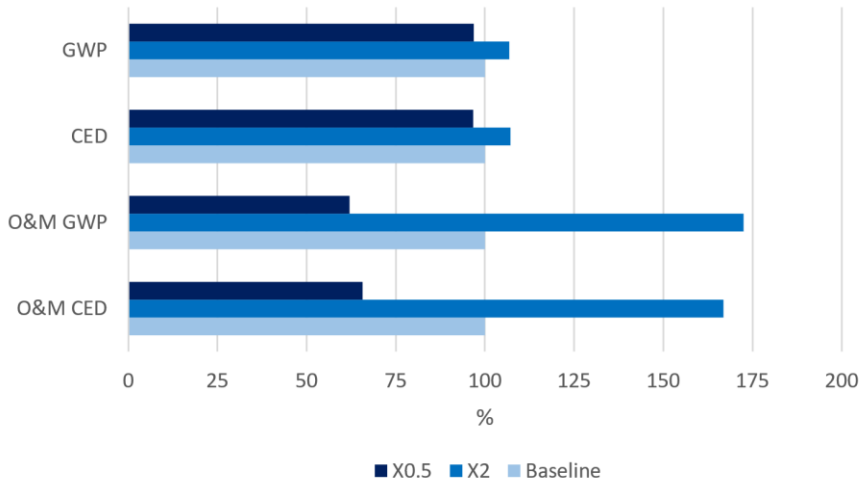

Figure 7.18: CED and GWP variations with modified failure rates compared to the baseline scenario.

7.4.3. Annual energy yield

In the baseline case, the indicators' results have been computed assuming that the net electric production of the power plant related to its first year of operation would be equal to the mean annual energy yield over the entire useful life. This assumption, although based on real data, may be considered quite limiting given that normally the wind resource can significantly change year by year depending on the behavior of meteorological phenomena that affect not only the site's region but also the whole continent or even the global hemisphere to which it belongs. Many of these phenomena occur on a periodical basis, e.g. daily, seasonal, yearly and so on, but they are not easy to predict since the impacts developed on the wind currents always have a random component to deal with.

The energy yield assessment (EYA) is the mean through which wind currents properties are used in order to obtain the mean energy production of a wind farm installed on a given site. Generally, the potential site selection is based on preliminary consultation of the data reported in wind atlases. These data are accessible in the public domain, but due to their relatively low spatial and temporal resolution they allow at most to make rough estimates of the power plant production, since the uncertainties involved are quite high. For this reason, when a potential site location is selected, it's common practice to set up a detailed site characterization aimed to obtain wind measurements with better accuracy. The duration of the measurement campaign can depend on several factors, including the expected size of the power plant, its CAPEX and the availability of data obtained by previous assessments in the same region. Nonetheless, according to the international standard, a minimum temporal extension of one year is recommended to consider at least seasonal wind behaviors (NREL, 1997). For more complex and expensive projects, several years of measurements are suggested to account for phenomena recurring with lower frequency.

In the case of the present study, an EYA has been conducted starting from the wind measurements acquired during the feasibility study of the power plant, with the aim of obtaining a new value of the annual energy yield (AEY) that accounts, as far as possible, for all the meteorological phenomena that should take place over the plant's useful life. The extension of the campaign represents in this case quite an exception compared to the average (1-2 years), given that the period under investigation goes from 2007 to 2015. The advantage of this condition is that the effects deriving from meteorological phenomena with periodicity equal or higher than one year can be integrated with higher accuracy compared to assessments with lower duration. Since the temporal extension of the wind power plant's useful life is typically much higher than the one characterizing the wind resource assessment (WRA), the data obtained with the measurement campaign should always be correlated to long-term mesoscale reference data. The uncertainty of the correlation, however, is expected to be sensibly higher in case the initial measured (and more accurate) data throughout the campaign refer to a shorter period.

The anemometric station whose data have been used in the present assessment was installed directly in the internal area of the power plant's site, represented in Figure 3.1. The site occupies a surface approximately 4 km long from W to E and 2 km long from N to S, while presenting a mean altitude of 307 m. The orography of the terrain is rather simple, since the mean slope is lower than 2%. Nevertheless, the wind's vertical profile is affected by the presence of many olive and almond trees planted around the wind turbines. In general, the number and the position of the measuring towers required to obtain sufficient data to reach the goal of the assessment within the admissible range of uncertainty is highly dependent on the site complexity, both in terms of orography and presence of obstacles. Met masts should not be built too close to stream obstructors (e.g. buildings) due to the formation of turbulent structures (NREL, 1997). Moreover, complex orographies imply the necessity of using more masts to elaborate a reliable wind profile across the site, since the extrapolation of the data would otherwise be affected by a higher uncertainty (NREL, 1997). Given the extension of the site and the low complexity of its orography, the use of a single measuring tower was considered sufficient to obtain an accurate wind profile over the field.

The main characteristics concerning the met mast sensors are reported in Table 7.17. The mast tower is 66 m high and it's made of a lattice structure supported by 6 steel guys. For the wind speed measurements, 2 calibrated cup anemometers model NRG #40C were used, mounted 65 m and 40 m above the tower base, respectively. The 65 m high anemometer is oriented at 240° in respect to the azimuth direction, while the 40 m high one at 120° in respect to the same direction. The anemometers' height can influence a lot the evaluation of the wind profile. In general, for larger wind projects whose nominal power is greater than 100 MW, it's recommended that at least one in three meteorological towers shall be equipped with anemometers mounted at the turbines' hub height, since measuring the wind without vertically extrapolating the data from lower heights to obtain the generated power reduces the total uncertainty of the estimation (Brower, 2012). At the same time, using taller towers also increases the cost of the measurement campaign. For this reason, smaller projects including the case of the present study employ shorter measuring towers with several anemometers in order to obtain, after further elaborations of the data, the wind speeds at increased height. Typically, this choice can be cost-effective when the vertical profile of the wind is well understood (hence, predictable), but in the other cases, especially when the orography and the roughness of the site are difficult to characterize, taller and multiple measurement towers may be required to improve the accuracy of the assessment (Brower, 2012).

Table 7.17: Characteristics of the met mast sensors.

Sensor	Height [m]	Direction [deg]
Anemometer NRG #40C	65	Azimuth 240°
Anemometer NRG #40C	40	Azimuth 120°
Wind vane NRG #200P	65	Azimuth 0°
Wind vane NRG #200P	40	Azimuth 0°

For the wind direction measurements, instead, 2 wind vanes model NRG #200P were used, mounted at the same height of the anemometers to couple the respective data. Their orientation is in both cases at 0° in respect to the azimuth direction. The measurement plan focused on the acquisition of the following parameters per given height and time interval:

- Mean wind speed,
- Wind speed standard deviation,
- Mean wind direction,
- Wind direction standard deviation.

The wind monitoring campaign lasted from 17/10/2007 to 17/3/2015, for a total duration of 7 years and 5 months. The above-mentioned parameters have been computed every 10 minutes using wind data sampled every 2 seconds. Data validation was performed by first converting the measurements provided by the control unit in time series using Symphonie Data Retriever ver. 7.08.18. Symphonie Data Retriever is a software that allows to export the original .raw file format containing the measured data in a .txt file that enables their readability. The .txt file has been subsequently imported in Python prior copying the data in a Microsoft Excel sheet. Python libraries represented the only tools used for all the elaborations and calculations concerning the input data up to the obtainment of the power plant's AEY. The validation of the data derived from the wind monitoring campaign mainly consisted in 3 phases:

1. Visual inspection of the plotted time series referring to the mean wind speed and direction for both the anemometers. This phase is aimed to give a first look on the principal features of the measured parameters, including the presence of malfunctioning periods and abnormal values (e.g. mean wind speeds > 50 $\frac{m}{s}$).

2. Wind data filtering. Based on the pieces of information obtained in the previous phase, invalid data were removed using range test criteria involving either the measured parameters or their standard deviation.

3. Tower shadowing correction. Tower shadowing occurs when the measured wind current presents a direction such that the anemometer is located downwind in respect to the mast (Brower, 2012). As a result, the anemometer may sample a wind speed that is sensibly lower compared to the one upwind due to the effects of the turbulence generated by the presence of the mast's tower. Tower shadowing was detected for the anemometer oriented at 240°, i.e. the one located at 65 m above the base of the tower. The correction of the data involved the substitution of the mean wind speed values for the wind rose sector that is defined by the opposite direction of the anemometer's orientation: since anemometer was installed coherently with the WSW sector, the substitution interested the ENE sector. Given that no additional anemometers were coupled at the same height of the shadowed one, the replacement data were obtained by vertically extrapolating the wind speed data of the 40 m anemometer. The extrapolation process will be outlined in the next sections.

The data validation procedure just described provided a recovery rate equal to 94.3% of the time series' initial size. After the validation, the mean wind speed and mean wind direction measurements have been averaged on an hourly basis. The resulting time series were analyzed through the representation of statistical plots, including the wind speed frequency and the wind rose[20]. Focusing on the 65 m anemometric time series, from the wind rose plots it was possible to point out that the WNW, S and SSE sectors are characterized by the highest presence of wind. Nevertheless, by combining the results of the wind speed frequency for these sectors with the wind rose data, the SSE and the S sectors resulted to generate by far the highest amount of energy since they present a much greater mean wind speed. The layout of the power plant, as shown in Figure 3.1, appears to fit quite well with this outcome, since the incident wind on the turbines' rotor is expected to be poorly influenced by the wake effects when the wind itself is coming from South.

When anemometric data are not available at the turbines' hub height, the associated time series is typically computed through vertical extrapolation using the measurements referring to the lower heights. The aim of the extrapolation is deriving the shear coefficient α of the power law defining the wind's vertical profile in a given position for a given wind direction and time period, which is equal to:

$$v_2 = v_1 \left(\frac{h_2}{h_1}\right)^{\alpha} \tag{7.7}$$

[20] The plots are not shown due to confidentiality.

where $v_2 \left[\frac{m}{s}\right]$ is the mean wind speed over the set time period and wind direction at height h_2 [m], while $v_1 \left[\frac{m}{s}\right]$ is the mean wind speed over the set time period and wind direction at height h_1 [m]. Considering that, in the case of the present study, the turbines' hub is located at 93 m from the base of the tower, the time series at 93 m should be obtained starting from the anemometric data at 65 m and 40m. When α is known, $v(h = h_2 = 93\ m) = v_2$ can be calculated through eq. 7.7 using as v_1, h_1 the mean wind speed and the height referred to the anemometer installed at 65 m above the mast's base. More in general, the reference height (hence, the reference mean wind speed) should always be the nearest to the one for which the wind speed is wanted to be extrapolated, since in this way the uncertainty is lower. The accuracy of the vertical extrapolation strongly depends on the number of heights at which the time series are available. Normally, it's recommended to use at least 3 heights with the respective mean wind speeds in order to determine the shear coefficient, otherwise the accuracy would be quite poor. Since for the present work anemometric data were available only for 2 heights, the shear coefficient was computed using mesoscale data instead of measured data.

Mesoscale data, as suggested by their name, are wind data mapped at a coarse scale for a given region, usually with a resolution included between 2 and 10 km. Wind data are obtained in this case through the application of detailed climatology models that are able to describe for very long periods the wind behavior across the world, covering - although in a more approximated way compared to direct wind measurements - all the possible meteorological phenomena that could affect the wind stream over the plant's lifetime. Mesoscale data can't be used to predict wind flows at the microscale level, since even by using very detailed orography maps and local surface roughness data errors can exceed 25% (ESMAP, 2010). However, especially when the site is characterized by a simple and uniform terrain as seen with the wind power plant object of the analysis, such data are often employed to obtain the shear coefficient needed for the wind vertical extrapolation when anemometric data are not sufficient to make an accurate estimation.

Specifically, for the present EYA, mesoscale data were retrieved from the EMD-WRF Europe+ dataset for the closest location where the met mast was installed in the site. Wind data were available at 4 heights: 25 m, 50 m, 75 m and 100 m. The time series referring to each height are defined on an hourly basis from 01/01/2000 to 01/01/2023, covering 23 out of 25 years of expected power plant operation. The mean wind speeds associated with the above-mentioned heights were computed over the entire time span for the 12 directional sectors defined by the wind rose, in order to obtain 4 points per each sector. These points have been consequently fit using Python by defining the power law as shown in eq. 7.7, leaving α as free parameter. At the end of the process, the shear coefficients were employed first to correct the shadowed data by extrapolating the time series at 65 m using the data at 40 m as reference, and then to

perform the extrapolation of the 93 m time series over the entire anemological campaign period using the 65 m data as reference. The mean wind speed at 93 m for the anemometer was found equal to 6.2 $\frac{m}{s}$, value that compared to the reviewed studies resulted to be quite limited.

The time series just obtained, as previously mentioned, refers to a period extending from 17/10/2007 to 17/3/2015, hence it's representative of only a fraction of the total power plant's useful life. To account for the variability of the wind concerning 25 years of operation, the mesoscale data can be rescaled - for the periods in which the anemological campaign does not provide any measurement - by correlating the mean wind speeds per direction sector with those concerning the anemological campaign itself but in case of concurrent timestamps. Clearly, the mesoscale data must be first extrapolated to 93 m using the same shear coefficients used in the case of the anemometer measurements before applying such procedure. This methodology is also known as *measure, correlate, predict* (MCP). MCP approaches are multiple, but they all share the key assumption that the future wind resource will behave in a similar way compared to the past, hence the wind climate results to be stable (Brower, 2012). For the case of the present EYA, given the lack of more sophisticated tools that allow to obtain very accurate correlations (e.g. neural networks), a simple sectorial linear regression was chosen as MCP approach. The idea is representing the extrapolated mesoscale data in a 2D plot with the concurrent anemometric data for a given sector in order to define the points that will be interested by the regression. As an example, the results are shown in Figure 7.19 for the SSE sector.

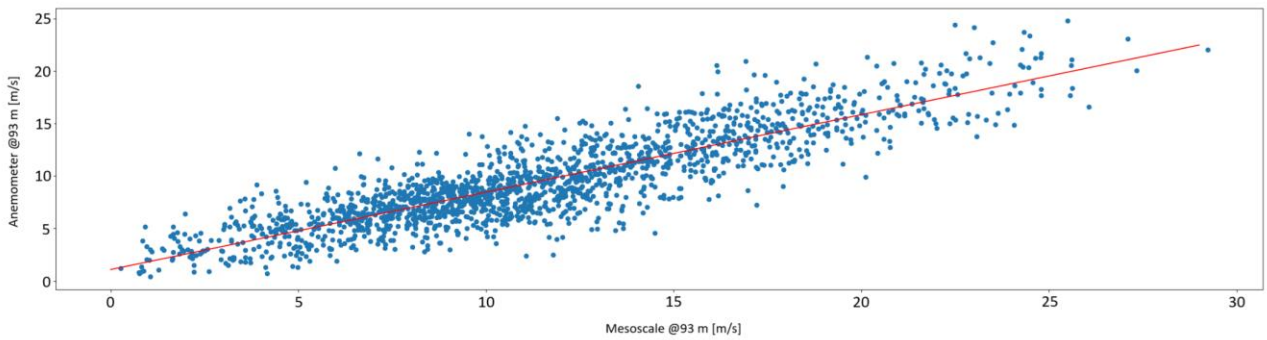

Figure 7.19: Regression line for the SSE sector.

The slope and the intercept of the regression line for each sector were used to transform the extrapolated mesoscale data for the non-concurrent timestamps using the linear relation:

$$v_2 = v_1 \cdot s_{regr,i} + q_{regr,i} \tag{7.8}$$

where $v_2 \left[\frac{m}{s}\right]$ is the predicted wind speed value, $v_1 \left[\frac{m}{s}\right]$ is the initial mesoscale value, $s_{regr,i}$ [-] is the slope of the regression line related to the *i* sector and $q_{regr,i} \left[\frac{m}{s}\right]$ is the intercept of the regression line related to the *i* sector. The resulting time series accounts for 23 out of 25 years of meteorological phenomena, hence almost all the events that should characterize the plant's useful life. The mean wind speed over 23 years resulted to be slightly higher than the value calculated for the anemometric time series through 7.5 years of measurements: specifically, while $v_{7.5y} = 6.2\ \frac{m}{s}$, a $v_{23y} = 6.7\ \frac{m}{s}$ was obtained. This is expected to determine a greater AEY compared to the previous case. Moreover, the most relevant contributions to the total energy production turned out again to arrive from the southern sectors.

The time series just computed through the long-term correlation refers to the wind behavior over time in the position of the met mast, which coincides exactly with the location of the WTG 20 (see Figure 3.1). As already mentioned, wind measurements are usually taken only in a few site's locations mainly for reasons of cost. Since to obtain the AEY it's necessary to know the wind time series in correspondence of all the turbines installed in the power plant, horizontal wind flow modeling must be pursued in order to extrapolate the remaining data. Several kinds of approaches exist to solve this problem, including (Brower, 2012):

- *Conceptual* models, which describe the variation of the wind resource over the site's surface based on a combination of experience and theoretical understanding of the boundary layer evolution (Brower, 2012).

- *Experimental* models, which involve the testing of a scaled model of the site's surface in a wind tunnel (Brower, 2012).

- *Statistical* models, based on correlations relying for the most part on measurements carried out directly on site (Brower, 2012).

- *Numerical* models, which aim to solve at least part of the flow equations governing the motion of the wind in the atmosphere (Brower, 2012).

Given the complexity and the significant amount of computational resources required to apply almost all the above-mentioned methodologies without using any commercial software dealing with wind flow modeling or expensive equipment, for the present EYA the horizontal wind extrapolation was conducted in a simpler way by referring to a resource map characterizing the area of the power plant's site. The resource map considered was retrieved from the Global Wind Atlas and it defines the variation of mean wind speed at 100 m height across the whole site with a spatial resolution of 250 m. The speed gradient at 100 m has been assumed as representative for the one at 93 m. The coordinates of the wind turbines were used to determine their positions on the resource map, as shown in Figure 7.20. A mean wind speed value at

100 m is associated to each pixel composing the map, including those in which wind turbines are located. By comparing the values related to each turbine's pixel to the one of the anemometric station, it was possible to rescale the previous time series to extrapolate the new ones for the remaining turbines. The scaling factors used for the extrapolation are shown in Table 7.18.

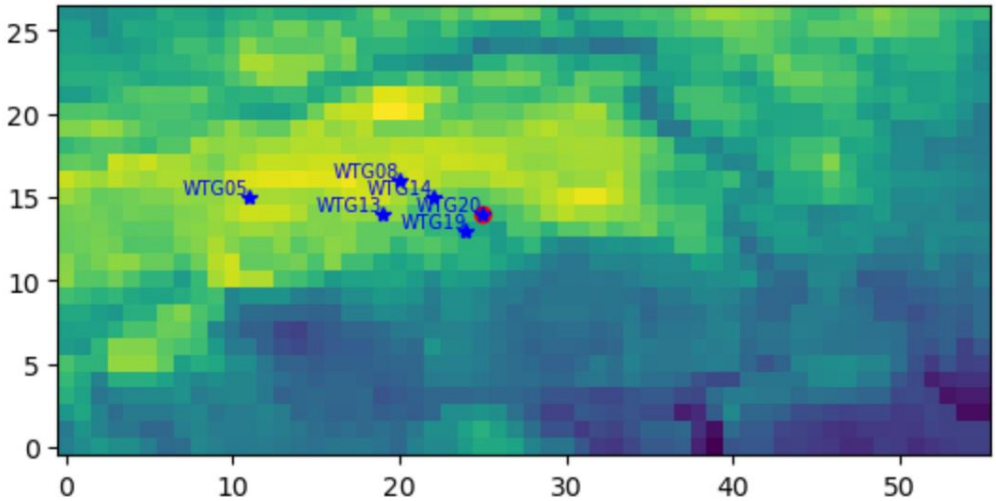

Figure 7.20: Resource map of the site at 100 m. Axis labels refer to the number of pixels.

Table 7.18: Scaling factors used for the horizontal extrapolation.

WTG 05	WTG 08	WTG 13	WTG 14	WTG 19	WTG 20
0.9944	1.0115	1.0079	0.9882	0.9964	1

Overall, the new time series were determined by a positive or negative variation of the long-term data not higher than 1.2%. Such result can be explained considering that, as already mentioned before, the orography of the site is very simple and it's roughness is quite uniform.

An aspect that hasn't been accounted yet in the wind flow model is the influence of the interaction between the turbines' blades and the incident stream, i.e. the wake effect. When the wind impacts on the rotor, the progressive detachment of the boundary layer generated on the blades' surface determines a strong turbulent flow downstream, which is typically much slower than the upstream one and is characterized by a significantly more complex motion. Although the wind stream gradually recovers its original undisturbed speed, if the downstream flow encounters another turbine's rotor its production may be negatively affected depending on the distance in respect to the first turbine and the evolution of the wake itself. In this context, the direction of the wind and the disposition of the turbines in the park are fundamental in order to limit the impacts of this phenomenon. As already seen, the location of the turbines involved

in the plant object of the study is expected to mitigate quite well the wake effects, since most of the energy is produced by wind arriving from South. However, a more precise calculation using wake models is always needed in an EYA.

In general, wake models are able to solve the fluid-dynamic problem using empirical approaches or fully numerical approaches. Numerical approaches are often the most used ones, but they differ in terms of complexity. Specifically, although all of them are designed to solve Navier – Stokes equations, the main differences are related on how the problem is defined (linear, steady or unsteady…) and the turbulence scale for which the equations are solved. In fact, depending on these parameters, Navier – Stokes equations can be highly simplified at the cost of a more inaccurate flow physics modeling. More complex physics modeling require not only more computational resources, but also dedicated software that contain the specific code that allows to execute the calculations. For the present EYA, which was carried out only using Python, the wake effect has been integrated in the calculation of the AEY using the FLORIS library. FLORIS wake modeling is based on control-focused simulations incorporating steady-state wake models that focus on the resolution of simplified linearized Navier – Stokes equations (NREL, 2023). The physics behind each available model is quite simple compared to many other CFD codes usable through licensed software, but the advantage of FLORIS is that simulations runs in fraction of seconds even with large wind systems using personal computers.

The FLORIS library was imported in Python together with the time series obtained after the horizontal extrapolation. In order to allow the calculation of the AEY accounting for the wake effects, it was necessary the definition of the following items:

- The wind turbines' power curve, i.e. the link between the wind speed crossing the rotor and the electric power produced. The required values for the turbines' operative range were retrieved from the G112 – 2.5 MW documentation.

- The power weights vector, i.e. an array containing the ratios between the AEY produced by the single turbines and the one of the reference turbine, assumed as WTG 20 (whose position is coincident with that of the met mast). The evaluation of the AEY was carried out without wake effects and applying the power curve data to the 6 time series previously computed. The resulting vector is shown in Table 7.19.

Table 7.19: Power weights vector.

WTG 05	WTG 08	WTG 13	WTG 14	WTG 19	WTG 20
0.9912	1.0173	1.0119	0.9812	0.9944	1

- The turbines' wind speed density matrices. A wind speed density matrix is a matrix that contains, for a given direction sector, the frequency with which the wind assumes a mean wind speed included between a maximum and minimum value. This matrix was computed starting from the 6 time series for every turbine with a directional step of 2 degrees and a speed step of 1 $\frac{m}{s}$.

- The position of each wind turbine, which was obtained from the power plant documentation.

- The wake model. For the present assessment, the Gauss model was chosen. This model describes the wind speed reduction in response to the interaction between the wind and the rotor blades using a gaussian distribution along the span of the rotor itself.

- The air density. Since the mean pressure of the site was not available, the air density has been estimated as a function of the site temperature and elevation, using (Brower, 2012):

$$\rho\left[\frac{kg}{m^3}\right] = \left(\frac{P_0}{RT}\right) e^{\left(\frac{-gz}{RT}\right)} \tag{7.9}$$

  where P_0 [Pa] is the atmospheric pressure at sea-level, T [K] is the mean air temperature of the site over the useful life, g is the gravitational constant, R $\left[\frac{j}{mol \cdot K}\right]$ is the gas constant and z [m] is the mean hub elevation. The mean air temperature was computed starting from the mesoscale data and it was found equal to 288.96 K, while the mean site elevation was retrieved from the plant documentation and it's equal to 307 m. Since the mean slope of the site is very small, the hub elevation was computed by directly adding the hub height to the previous value, for a total of 400 m. Using eq. 7.9, the air density resulted to be 1.165 $\frac{kg}{m^3}$.

The remaining parameters, including the turbulence intensity and the wake model coefficients, have been kept as default. After giving the above-mentioned inputs to the FLORIS interface, the simulation provided an AEY equal to 51.142 GWh. The wake effect turned out to reduce the Gross AEY of about 3.2% of its initial value, i.e. 52.846 GWh. In order to obtain the Net AEY, in addition to the wake effect it's required to also consider the other sources of loss that can affect the power plant production over its entire useful life. The typology and the entity of these losses are summarized in Table 7.20 as suggested by the power plant's EPC Contractor. Consequently, the power plant's Net AEY will be equal to:

$$P_{net} = P_{50} = P_{gross} \cdot \prod_i (1 - l_i) \tag{7.10}$$

Table 7.20: Estimated power losses.

Loss typology	Loss %
WTG availability	3
Balance of plant availability	0.2
Grid availability	0.5
Power curve performance	1
High-wind hysteresis	0.1
Self-consumption	~ 0
Grid losses	1.5
Performance degradation	0.5

Where $P_{gross} = 52.846$ GWh is the Gross AEY, while l_i are the power losses shown in Table 7.20 plus the wake effect. Eq. 7.10 provided a P_{net} equal to 47.749 GWh. P_{net} is also known as P_{50}, since the real AEY is expected to exceed this value with a probability of 50%. The capacity factor associated with P_{net} is 0.363, which is 31.7% higher than the one observed by considering as AEY the production concerning the first year of the plant's operation.

To assess the sensitivity of this result, it's required to compute the uncertainty related to the wind measurements, data elaboration and power conversion. Since it's common practice to assume that the probability density of the AEY follows a Gaussian distribution, the calculation of the standard deviation of each uncertainty source turns out to be very useful in the estimation of the confidence intervals[21]. The methodology employed to obtain the standard deviations is reported in Table 7.21 together with their estimated values. It's worth noting that not all the values are computed directly with respect to the AEY, since some of them refers to the wind measurements. In order to relate these standard deviations to the AEY, the combined uncertainty (11.18%) was used as a positive mean wind speed variation for the time series associated with the 6 turbines, aiming to evaluate the AEY sensitivity resulting from such wind condition. By using the same parameters and models described for the P_{50} computation, the new value of AEY turned out to be 55.973 GWh, i.e. 17.22% more than the previous P_{50} value. For this reason, the standard deviation referring to the wind speed variations was set to be equal to 17.22%. The final combined standard deviation on the AEY, at

[21] The standard deviation represents the confidence interval in which the AEY is supposed to occur with a probability of 68.27%, i.e. with an 84% probability of exceedance (Solargis, 2018).

the end of the process, was found to be equal to 19.18%. The confidence intervals have been consequently calculated by applying the well-known Gaussian formulae from the statistical analysis, reported in Table 7.22.

The value of P_{75} resulted to be 13% lower than P_{50}, while P_{90} and P_{99} turned out to be 25% and 45% lower, respectively. The AEY registered after the first year of operation, equal to 36.266 GWh, lies very close to the P_{90} value, indicating a clear lack of wind resource in the region during 2023. A more precise evaluation of the environmental impacts concerning the energy balance and carbon footprint of the power plant can be done using the P_{50} as average AEY over the plant's useful life, since by definition it represents the mean value of the Gaussian distribution. Given that the CED and the GWP of the system are normalized through the total net production, which is a multiple of the AEY, their value results to be inversely proportional in respect to the AEY itself. Hence, it is expected that by considering the complete climatology characterizing 25 years of operations instead of one, the indicators' results will differ compared to the previous case by a factor equal to the ratio between the old and the new capacity factor, i.e. 0.76. Therefore, the environmental impacts computed in the baseline case could be at least 24% lower, although the definitive eco-profile will depend by the real behavior of the wind resource.

Table 7.21: Uncertainty factors and standard deviations' calculation methods.

Uncertainty factor		STD % on wind	STD % on AEY	Calculation method
Wind measurements	Anemometer type	1.88	-	From anemometer datasheet
	Anemometer calibration	0.74	-	From anemometer datasheet
	Met mast installation	2.5	-	EPC Contractor suggestion based on experience
Data elaborations	Wind vertical extrapolation	0.9	-	EPC Contractor suggestion based on WindPro analysis
	Wind long-term extrapolation	8.34	-	Combined weighted standard deviation of sectorial regression slopes and intercepts
	Wind horizontal extrapolation	0.58	-	EPC Contractor suggestion based on WindPro analysis
	Yearly wind speed variability	6.63	-	Standard deviation of the long-term anemometric yearly mean wind speed
Total		11.18	17.22	Standard deviation on AEY based on the AEY sensitivity to a 11.18% wind speed variation
Power conversion	Wake model		0.24	Standard deviation of the Net AEY obtained using 5 different wake models
	Power curve		5	EPC Contractor suggestion based on experience
	Losses		6.8	EPC Contractor suggestion based on experience
Total			19.18	-

Table 7.22: Gaussian formulae for the confidence intervals evaluation (Solargis, 2018).

	Probability of exceedance	Uncertainty	Formula	Value [GWh]
P75	75%	0.675σ	$P50\cdot(1-0.675\sigma)$	41.567
P90	90%	1.282σ	$P50\cdot(1-1.282\sigma)$	36.008
P99	99%	2.326σ	$P50\cdot(1-2.326\sigma)$	26.447

8 Conclusions, limitations, and recommendations

The present study has been devoted to the evaluation of the environmental sustainability of an onshore Italian wind farm featuring 6 G114 – 2.5 MW wind turbines, with a focus on its effects towards the global energy balance and carbon footprint. The analysis was conducted by applying the LCA methodology "from-cradle-to-grave" according to the ISO 14040:2006 and 14044:2006 regulating framework, aiming to give a complete insight on the most critical stages over system's life cycle and comparing the entity of the burdens with those characterizing other electricity generation technologies, either renewable or not. The Cumulative Energy Demand (CED) and the IPCC Global Warming Potential were selected as impacts assessment methods in order to estimate, respectively, the primary energy consumption associated with the processes included in the system's boundaries and the environmental damage caused by the GHGs emissions from them generated. This choice was made not only to fulfil the goal of the analysis, but also to grant the maximum compatibility with other LCA studies dealing with wind power plants. The functional unit to which input and output flows have been normalized was set as "the delivery of 1 GWh of electricity to the national grid", since electricity represents the only product of the system. The attribution of the impacts related to the *end-of-life* phase has been done according to the 100-0 approach (also known as "cut-off" approach). This choice was mainly driven for conservative reasons by the fact that the system's boundaries were defined following the prescriptions given by the General Programme Instructions (GPI) for the International EPD system, therefore excluding those processes aimed at reaching the *end-of-waste* state.

For the LCI definition, the main data source employed comprises the available documentation dealing with the design phase of the power plant provided by the EPC Contractor. The system under analysis has been investigated from the *raw materials acquisition* phase to the *end-of-life* phase. According to all the reviewed studies, the *raw materials acquisition* phase represents the most critical one over the entire life cycle, accounting for 69% of the total CED and 72% of the total GWP. Wind turbines and their foundations are responsible alone for more than 80% of these contributions, while the remaining impacts derive from the acquisition of the materials required for the plant's civil works and the power transmission system. Ferrous materials including

steel, cast iron and iron, make up almost 85% of the total wind turbines' mass (foundations excluded) and represent at the same time 50% of the total primary energy consumption and 61% of the GHGs emissions' GWP concerning this phase. Since metals can be recycled very easily and the recycling process itself requires less energy compared to the production obtained using virgin raw materials, it's widely believed that a large portion of the total volume of metals involved in the global market is generated starting from recycled content (Tagliabue, 2015), hence it's expected that the real influence on the energy balance and carbon footprint of the system coming from these materials could be significantly lower than what has been discussed in the baseline scenario.

On the other hand, the composite material found in the rotor blades turned out to determine more than 35% of the CED and 28% of the GWP generated by the *raw materials acquisition* phase, while only accounting for 11% of the turbines' total mass. Such composite material, in fact, resulted to be the one of the most energy intensive employed in the entire power plant. Unlike metals, composites are typically much harder to recycle due to the high variability of the recycled products' quality that current recycling processes generate and the cost of the processes themselves (Mishnaevsky, 2021). Moreover, some of them are considered to require more energy and/or GHGs emissions than what the replaced product would demand otherwise when produced using primary raw materials (Gennitsaris et al., 2023). For these reasons, improvements should be made not only from a process point of view but also from the material one, by manufacturing components with suitable mechanical properties but at the same time easy to recycle.

The materials required for the turbines foundations' construction turned out to represent almost 13% of the total system's CED and 18% of its GWP. Reinforced concrete represents nowadays an unreplaceable standard in supporting large and heavy structures like wind turbines. Although waste concrete can be recovered and recycled, the size and weight of the foundations often limit the benefits of the process, since this material is typically used to replace the production of primary inert aggregates which often requires so low amount of energy and GHGs emissions that is not able to counterbalance what required by the transport of the waste and its processing. However, in more recent times, concrete production is gradually shifting towards new regulating frameworks aimed to reduce the overall environmental burdens, especially against its carbon footprint (Federbeton, 2023). Major changes involve the replacement of a fraction of the raw materials required by the default process with several by-products or waste product derived from different industrial processes, allowing not only the recovery of materials that would be alternatively disposed, but also the implementation of thermal and chemical transformations that demand fewer primary resources and generate reduced emissions (Federbeton, 2023).

With the present study, in addition to the wind turbines' foundations, it was possible to evaluate the impacts associated with all the other activities concerning the power

plant's civil works, i.e. the platforms, cable trenches, transformer substation, internal and external roads. Such activities are generally neglected by many authors due to the lack of sufficient primary data able to define a proper LCI for the assessment. According to the reviewed studies that included these elements, their impacts turned out to determine together 14% of the system's CED and 11% of its GWP. Concrete, reinforced concrete and asphalt resulted to be the most critical materials for every impact category, while limestone gravel – although being used in much higher amount compared to the above-mentioned – proved to generate almost insignificant burdens.

The acquisition of the raw materials concerning the power cables installed in the trenches was also investigated. The interpretation of the results led to the conclusion that aluminium stranded cables, besides costing significantly less than copper stranded ones, are also more environmentally sustainable for a given application compared to the latter. In fact, despite its lower electrical conductivity and higher specific primary energy consumption, aluminium is 70% less dense than copper, which allows to obtain the same resistance with lower weight while counterbalancing the effect of the higher energy demand.

The *components manufacturing* phase resulted to be the second most relevant concerning the two impact assessment methods included in the analysis, accounting for 12% of the total CED and 9% of the total GWP. Wind turbines turned out to determine by far the highest fraction of the burdens (~ 90% in both cases). Electricity and sheet rolling used, respectively, for the components assembly and working metals, represent alone around 80% of the primary energy consumption and global warming potential related to this contribution. The transport activities required to deliver the turbines' parts to the manufacturers and then to the site's location generated overall almost 2% of the system's GHGs environmental damage. According to the reviewed studies, transport by ship revealed to be much more efficient than transport by truck.

The final assembly in site and the execution of the civil works generated limited burdens, equal to 4% of the total for both the assessment methods. During the useful life, the impacts deriving from maintenance activities turned out to depend almost entirely on the actual behavior of the turbines components' reliability. The production of such components is in fact the most demanding in terms of primary energy consumption and GHGs emissions, hence, even the replacement of a few of them can imply a non-negligible deterioration of the plant's eco-profile. This topic remains quite uncertain, given that the components' failure rates are based on statistical phenomena that can be partially mitigated but not predicted. In the present study, mean failure rates for the turbines' major components were obtained starting from literature data related to existing wind power plants. Based on the scenarios discussed through the sensitivity analysis, it's expected that the CED and GWP fraction on the total associated to this phase will not exceed 10%.

Since most of the structures and the roads built during the installation phase will be left almost unchanged after the plant's decommissioning, the decommissioning itself resulted to determine the lowest fraction of the burdens with less than 1% of the system's CED and its GWP.

The *end-of-life* phase, considering the temporal uncertainty caused by the extension of the plant's useful life, still remains a point of debate. For the baseline scenario, the data relying on the indications given by the wind turbines' manufacturer during the plant's design phase concerning the waste management were considered. Further pieces of information on typical recovery rates for the materials used in the electromechanical components employed in the transformer substation have been retrieved from literature. The waste deriving from the *decommissioning* phase is expected to include the wind turbines' parts, the power cables and part of the transformer substation. Once again, wind turbines' contribution resulted to dominate on the others, this time with more than 95% of the total impacts, which attest to 7% of the system's CED and 8% of its GWP. In general, the components disassembly phase required to separate the different kinds of materials prior to their specific disposal process resulted to determine the highest fraction of the burdens. Focusing on the waste management, recycling and landfilling procedures turned out to affect roughly equally the primary energy consumption and the carbon footprint of the system. Interestingly, waste transport in the case of recycling showed almost double the environmental impacts of the waste treatment itself. This outcome is caused by the fact that recycling facilities for metallic components, which make up almost the entire mass of the turbines, do not coincide with the recovery centers where pre-treatments take place, hence lorries are expected to cover a higher mean distance compared to the other cases. Incinerated components, on the other hand, revealed to influence way more the carbon footprint of the system compared to its primary consumption. The incineration of the turbines' blades represents the most critical aspect of this disposal method, since the GWP associated with the process resulted to account alone for 3% of the system's total. While the heat generated from the combustion might be recovered for secondary uses, the flue gases must be in any case released in the atmosphere although cleansed from hazardous compounds. This condition further increases the need of finding ways to reuse or recycle the component in order to limit the environmental impacts associated with its disposal.

The primary resources employed over the system's life cycle turned out to be heavily reliant on non-renewable fuels. Specifically, renewable energies represent only 8.6% of the total primary consumption, which indicates that almost the entire contribution has a direct effect on the global resources depletion. It was possible to put in evidence that processes characterized by the utilization of a relevant share of electricity on their overall energy demand are able to increase more than the others the total renewable fraction. Electricity is in fact the main energy vector used for the conversion of

renewable energies, thus it's expected that increasing the level of electrification concerning each process will potentially lead to a higher share.

Environmental indexes have been computed to give a synthetic but effective interpretation of the impacts related to the primary energy consumption and carbon footprint of the system, including the Energy Payback Time (EPBT) and the Carbon Payback Time (CPBT). The former indicates the time expressed in years required by the power plant in order to deliver to the national grid an amount of electric energy equal to the primary energy that has been used over its entire life cycle, while the latter is related to the time that is necessary for the power plant to compensate its GHG emissions generated during its entire lifetime. For the CPBT calculation, electricity generation from natural gas was chosen as reference technology to account for the saved pollutant emissions resulting from the power plant's energy production. In the present work, the EPBT resulted to be equal to 1.52 years, while the CPBT to 0.86 years. Compared to the reviewed studies, these values attest that the wind power plant performs worse than average in both the categories analyzed. The main reason that led to such conclusion was found to be the *end-of-life* phase modeling, since the 100-0 approach doesn't generate any recycling credit for the system in response to the recovery or recycling of an item. Many authors, instead, while giving recycling credits to the system, claimed that the impacts associated with the primary energy consumption and carbon footprint of the system were able to reduce, on average, of almost 50% of their initial values.

Wind energy, together with solar energy, has the advantage of being a much more distributed energy source all over the world, but the choice of the site's location remains a crucial factor in obtaining a successful project, both in terms of profitability and sustainability. With the present work, it was possible to point out that sites that are characterized by an irregular and/or mediocre wind resource show significantly worse environmental performances compared to the others. This is caused by the superimposition of two effects:

- Lower capacity factor (CF). The wind resource quality is the main driver that affects the CF, which is directly related to the average annual energy yield of the power plant. For the baseline scenario, the net electrical production measured in the first year of the plant's operation was considered as mean value along its entire useful life. The corresponding capacity factor, equal to 0.276, resulted to be 24% lower than the one obtained from the energy yield assessment. Since the environmental impacts are evaluated per unit of electric energy delivered to the grid, the two production values just mentioned are able to determine fairly different results. In fact, it was demonstrated that the baseline scenario generates 31.7% more environmental burdens per GWhel compared to the other using the estimated production, attesting the importance of the actual behavior of the wind resource over time.

- Bigger wind turbines. For a given power output, wind turbines' size is required to grow either in terms of rotor diameter or hub height to counterbalance the detrimental influence of a lower mean wind speed intercepting the swept area. In the wind power plant under investigation, due to the presence of a limited wind resource compared to the reviewed studies, the size of the turbines' rotor resulted to be similar to those concerning wind turbines with higher rated power, determining a considerably higher rotor weight than average. Moreover, since the design of the G114 – 2.5 MW wind turbine also requires the use of heavier mechanical and electrical components in the nacelle, the additional weight has to be supported by bigger foundations, which contribute in worsening the overall environmental impacts.

It's already clear that wind energy will play a fundamental role in the future to reduce energy dependance and meet climate targets. Many studies have confirmed that wind power plants are able to drastically reduce the life cycle primary resources consumption and GHGs emissions compared to modern technologies that are still reliant on fossil fuels, even while using carbon capture and storage systems. Moreover, it's widely acknowledged that wind power plants present, on average, one of the lowest payback indexes among the other renewable technologies, while also offering a great potential of scalability. The present study provides a further evidence to the statements just mentioned. Through the LCA methodology, it was possible to demonstrate that the assessed wind power plant is able to compensate the emission generated over its entire life cycle in less than a year compared to the modern gas-fired power plants, which are expected to represent the future of fossil-generated electricity in Europe. The effects related to waste recycling or reusing could potentially improve this result even more, shifting the break-even point towards values below 6 months and. Nevertheless, the goals set by the environmental policies are very challenging: to meet carbon neutrality within 2050, serious investments and careful designs procedures are still required, since the sustainability of wind power plants - similarly to the other renewable technologies - strongly depends on both technological and decisional aspects, especially the site selection and the end-of-life waste management.

References

Articles

Al-Behadili and El-Osta, 2015

Al-Behadili, S. H. and W. B. El-Osta. "Life Cycle Assessment of Dernah (Libya) wind farm" in Renewable Energy 83, (2015): 1227-1233.

Alsaleh and Sattler, 2019

Alsaleh, A. and M. Sattler. "Comprehensive life cycle assessment of large wind turbines in the US" in Clean Technologies and Environmental Policy 21, (2019): 887–903.

Ardente et al., 2008

Ardente, F., M. Beccali, M. Cellura, V. Lo Brano. "Energy performances and life cycle assessment of an Italian wind farm" in Renewable and Sustainable Energy Reviews 12, (2008): 200–217.

Bhandari et al., 2020

Bhandari, R., B. Kumar and F. Mayer. "Life cycle greenhouse gas emission from wind farms in reference to turbine sizes and capacity factors" in Journal of Cleaner Production 277, (2020): 123385

Bonou et al., 2016

Bonou, A., A. Laurent and S. I. Olsen. "Life cycle assessment of onshore and offshore wind energy-from theory to application" in Applied Energy 180, (2016): 327–337.

Chipindula et al., 2018

Chipindula, J., V. S. V. Botlaguduru, H. Du, R. R. Kommalapati and Z. Huque. "Life Cycle Environmental Impact of Onshore and Offshore Wind Farms in Texas" in Sustainability 10(6), (2018): 2022.

Crawford, 2009

Crawford, R.H. "Life cycle energy and greenhouse emissions analysis of wind turbines and the effect of size on energy yield" in Renewable and Sustainable Energy Reviews 13, (2009): 2653–2660.

Davidsson et al., 2012

Davidsson, S., M. Höök, G. Wall. "A review of life cycle assessments on wind energy systems" in The International Journal of Life Cycle Assessment 17, (2012): 729-742.

Dolan and Heath, 2012

Dolan, S. L. and Garvin A. Heath. "Life Cycle Greenhouse Gas Emissions of Utility-Scale Wind Power" in Journal of Industrial Ecology 16, (2012): S136-S154.

Echavarria et al., 2008

Echavarria, E., B. Hahn, G. J. W. van Bussel and T. Tomiyama. "Reliability of Wind Turbine Technology Through Time" in Journal of Solar Energy Engineering 130, (2008): 031005-1 – 031005-8.

Frischknecht et al., 2015

Frischknecht, R., F. Wyss, S. Büsser Knöpfel, T. Lützkendorf, M. Balouktsi. "Cumulative energy demand in LCA: the energy harvested approach" in International Journal of Life Cycle Assessment 20, (2015): 957–969.

Gennitsaris et al., 2023

Gennitsaris, S., A. Sagani, S. Sofianopoulou and V. Dedoussis. "Integrated LCA and DEA approach for circular economy-driven performance evaluation of wind turbine end-of-life treatment options" in Applied Energy 339, (2023): 120951.

Gomaa et al., 2019

Gomaa, M. R., H. Rezk, R. J. Mustafa and M. Al-Dhaifallah. "Evaluating the Environmental Impacts and Energy Performance of a Wind Farm System Utilizing the Life-Cycle Assessment Method: A Practical Case Study" in Energies 12, (2019): 3263.

Guezuraga et al., 2012

Guezuraga, B., R. Zauner and W. Pölz. "Life cycle assessment of two different 2 MW class wind turbines" in Renewable Energy 37, (2012): 37-44.

Guidi et al., 2023

Guidi, G., A. C. Violante and S. De Iuliis. "Environmental Impact of Electricity Generation Technologies: A Comparison Between Conventional, Nuclear, and Renewable Technologies" in Energies 16, (2023): 7847.

Kaldellis and Apostolou, 2017

Kaldellis, J.K. and D. Apostolou. "Life cycle energy and carbon footprint of offshore wind energy. Comparison with onshore counterpart" in Renewable Energy 108, (2017): 72-84.

Köck et al., 2023

Köck, B., A. Friedl, S. Serna Loaiza, W. Wukovits and B. Mihalyi-Schneider. "Automation of Life Cycle Assessment - A Critical Review of Developments in the Field of Life Cycle Inventory Analysis" in Sustainability 15(6), (2023): 5531.

Lichtenegger et al., 2020

Lichtenegger, G., A. A. Rentizelas, N. Trivyza and S. Siegl. "Offshore and onshore wind turbine blade waste material forecast at a regional level in Europe until 2050" in Waste Management 106, (2020): 120-131.

Martínez et al., 2009

Martínez, E., F. Sanz, S. Pellegrini, E. Jiménez, J. Blanco. "Life cycle assessment of a multi-megawatt wind turbine" in Renewable Energy 34, (2009): 667–673.

McMillan et al., 2010

McMillan, D. and G. W. Ault. "Techno-Economic Comparison of Operational Aspects for Direct Drive and Gearbox-Driven Wind Turbines" in IEEE Transactions on Energy Conversion 25(1), (2010): 191-198.

Mishnaevsky, 2021

Mishnaevsky, L., Jr. "Sustainable End-of-Life Management of Wind Turbine Blades: Overview of Current and Coming Solutions" in Materials 14, (2021): 1124.

Oebels and Pacca, 2013

Oebels, K. B. and S. Pacca. "Life cycle assessment of an onshore wind farm located at the northeastern coast of Brazil" in Renewable Energy 53, (2013): 60-70.

Schreiber et al., 2019

Schreiber, A., J. Marx and P. Zapp. "Comparative life cycle assessment of electricity generation by different wind turbine types" in Journal of Cleaner Production 233, (2019): 561-572.

Tagliabue, 2015

Tagliabue, L. "Modellazione di Riciclo, Riuso e Recupero Energetico nelle analisi del ciclo di vita dei prodotti: un confronto fra le equazioni disponibili nella Normativa Tecnica" in Ingegneria dell'Ambiente 2-3, (2015): 45-63 (in Italian).

Tchakoua et al., 2013

Tchakoua, P., R. Wamkeue, T. A. theubou Tameghe and G. Ekemb. "A review of concepts and methods for wind turbines condition monitoring" in 2013 World Congress on Computer and Information Technology (WCCIT), (2013): 1-9.

Tremeac and Meunier, 2009

Tremeac, B. and F. Meunier. "Life cycle analysis of 4.5 MW and 250 W wind turbines" in Renewable and Sustainable Energy Reviews 13, (2009): 2104–2110.

Turconi et al., 2013

Turconi, R., A. Boldrin, T. Astrup. "Life cycle assessment (LCA) of electricity generation technologies: Overview, comparability and limitations" in Renewable and Sustainable Energy Reviews 28, (2013): 555–565.

Vo Dong et al., 2018

Vo Dong, P. A., C. Azzaro-Pantel, A. Cadene. "Economic and environmental assessment of recovery and disposal pathways for CFRP waste management" in Resources, Conservation & Recycling 133, (2018): 63–75.

White, 2007

White, S. W. "Net Energy Payback and CO2 Emissions from Three Midwestern Wind Farms: An Update" in Natural Resources Research 15(4), (2007): 271-281.

Xu et al., 2018

Xu, L., M. Pang, L. Zhang, W. R. Poganietz and S. D. Marathe. "Life cycle assessment of onshore wind power systems in China" in Resources, Conservation & Recycling 132, (2018): 361–368.

Zhuo et al., 2023

Zhuo, Z., M. Chen, X. Li. "A comparative analysis of carbon reduction potential for directly driven permanent magnet and doubly fed asynchronous wind turbines" in Energy Science & Engineering 11, (2023): 978–988.

Reports

EEA, 2023a

"Trends and projections in Europe", Report from European Environmental Agency (EEA), Kongens Nytorv 6, Copenhagen, Denmark, 2023.

EEA, 2023b

"EMEP/EEA air pollutant emission inventory guidebook 2023 - Technical guidance to prepare national emission inventories", Report from European Environmental Agency (EEA), Kongens Nytorv 6, Copenhagen, Denmark, 2023.

Ekvall et al., 2020

Ekvall, T., A. Björklund, G. Sandin, K. Jelse, J. Lagergren and M. Rydberg. "Modeling recycling in life cycle assessment", Report No C551 from IVL Swedish Environmental Research Institute, Gothenburg, Sweden, 2020.

IEA, 2023

"Renewables 2023 Analysis and forecast to 2028", Report from the International Energy Agency (IEA), 2023.

IPCC, 2021

Intergovernmental Panel on Climate Change (IPCC): "IPCC Sixth Assessment Report", WGI, Technical Summary, 2021.

ISPRA, 2023

"Italian Greenhouse Gas Inventory 1990-2021 National Inventory Report 2023", Report from Istituto Superiore per la Protezione e la Ricerca Ambientale (ISPRA), Via Vitaliano Brancati 48, Rome, Italy, 2023.

Razdan and Garrett, 2015

Razdan, P. and P. Garrett. "Life Cycle Assessment of Electricity Production from an onshore V110-2.0 MW Wind Plant", Report from Vestas Wind Systems A/S, Hedeager 42, Aarhus N, 8200, Denmark, 2015.

SPE, 2023

"EU Market Outlook for Solar Power 2023-2027", Report from SolarPower Europe (SPE), 2023.

Walford, 2006

Walford, C. A. "Wind Turbine Reliability: Understanding and Minimizing Wind Turbine Operation and Maintenance Costs", Report from Sandia National Laboratories, 2006.

WindEurope, 2023

"Wind energy in Europe: 2022 Statistics and the outlook for 2023-2027", Report from WindEurope, 2023.

Winther, 2023

Winther, M. "Energy consumption and emissions from non-road machinery in Denmark. Time series from 1980-2040", Scientific Report from DCE – Danish Centre for Environment and Energy, 2023.

Wiser and Bolinger, 2019

Wiser, R. and M. Bolinger. "Benchmarking Anticipated Wind Project Lifetimes: Results from a Survey of U.S. Wind Industry Professionals", Summary Report from Berkeley Lab Electricity Markets and Policy Department, 2019.

Websites

EIA, 2023

U.S. Energy Information Administration (EIA): "Renewable energy explained", 2023. Available online at:

https://www.eia.gov/energyexplained/renewable-sources/. Last accessed: 17/6/2024

ISPRA, 2019

Istituto Superiore per la Protezione e la Ricerca Ambientale (ISPRA): "Catasto Rifiuti Sezione Nazionale – Ricerca Comunicazioni Attività di Recupero", 2019 (in Italian). Available online at:

https://www.catasto-rifiuti.isprambiente.it/index.php?pg=comautc03. Last accessed 16/06/2024

ISPRA, 2021

Istituto Superiore per la Protezione e la Ricerca Ambientale (ISPRA): "Catasto Rifiuti Sezione Nazionale – Gestione nazionale dei rifiuti speciali – elenco impianti", 2021 (in Italian). Available online at:

https://www.catasto-rifiuti.isprambiente.it/index.php?pg=gestrsnazioneimp&aa=2021&regid=&mappa=0#p. Last accessed 16/6/2024

NREL, 2020

National Renewable Energy Laboratory (NREL): "The Leading Edge: April 2020 Wind Energy Newsletter", 2020. Available online at:

https://www.nrel.gov/wind/newsletter-202004.html. Last accessed 15/6/2024

NREL, 2023

National Renewable Energy Laboratory (NREL): "FLORIS Wake Modeling & Wind Farm Controls", 2023. Available online at:

https://nrel.github.io/floris/. Last accessed: 17/6/2024

PRé Sustainability, 2023

PRé Sustainability: "SimaPro Help Center - What is the difference between ecoinvent market and transformation processes?", 2023. Available online at:

https://support.simapro.com/s/article/What-is-the-difference-between-ecoinvent-market-and-transformation-processes. Last accessed 16/6/2024

Solargis, 2018

Solargis: "How to calculate P90 (or other Pxx) PV energy yield estimates", 2018. Available online at:

https://solargis.com/blog/best-practices/how-to-calculate-p90-or-other-pxx-pv-energy-yield-estimates. Last accessed: 17/6/2024

Documents from websites

EPD International, 2021

EPD International: "General Programme Instructions for the International EPD System", version 4.0, 2021. Available online at:

https://www.datocms-assets.com/37502/1617181375-general-programme-instructions-v-4.pdf. Last accessed 16/6/2024

ESMAP, 2010

The World Bank's Energy Sector Management Assistance Program (ESMAP): "Best Practice Guidelines for Mesoscale Wind Mapping Projects for the World Bank", 2010. Available online at:

https://pubdocs.worldbank.org/en/781171541803329105/WB-ESMAP-Guidelines-Mesoscale-Wind-Mapping-Oct2010-ARCHIVE.pdf. Last accessed: 17/6/2024

Essential Energy, 2021

Essential Energy: "How to Set the Coefficient of Friction in Neara", 2021. Available online at:

https://engage.essentialenergy.com.au/32707/widgets/298151/documents/222515**.** Last accessed: 16/6/2024

Federbeton, 2023

Federbeton: "Rapporto di Sostenibilità 2022", 2023. Available online at:

https://blog.federbeton.it/wp-content/uploads/2023/10/Rapporto_di_Sostenibilita%CC%80_Federbeton_2022.pdf. Last accessed: 17/6/2024

Hyundai Welding, 2023

Hyundai Welding: "Wind tower welding solutions", Hyundai Welding wind brochure, 2023. Available online at:

https://www.hyundaiwelding.com/data/file/download/brochures/Hyundai_Welding_Wind_Brochure_2023_eng.pdf. Last accessed 16/6/2024

NREL, 1997

National Renewable Energy Laboratory (NREL): "Wind Resource Assessment Handbook - Fundamentals for Conducting a Successful Monitoring Program", 1997. Available online at:

https://www.nrel.gov/docs/legosti/fy97/22223.pdf. Last accessed: 17/6/2024

PRé Sustainability, 2022

PRé Sustainability: "SimaPro database manual – Methods library", 2022. Available online at:

https://simapro.com/wp-content/uploads/2022/07/DatabaseManualMethods.pdf. Last accessed 16/6/2024

Saveri, 2010

Saveri, G.: "I cavi in media tensione", Voltimum Italia s.r.l., 2010 (in Italian). Available online at:

https://www.voltimum.it/sites/www.voltimum.it/files/it/attachments/pdi/f/1003guida_cavi_mt.pdf. Last accessed 16/6/2024

Theses

Gode, 2020

Gode, P. R. "How to design future wind farms to best mitigate their disturbance effects on birds?", MSc Thesis, University of Strathclyde, Department of Civil & Environmental Engineering, 2020.

Reimers, 2016

Reimers, B., "Heutige und zukünftige Konzepte einer Offshore-Windstromerzeugung: technische, ökonomische und ökologische Analyse", Doctoral Thesis, Technische Universität Hamburg, Department of Environmental Technologies & Energy Industry, 2016.

Environmental Product Declarations

Hitachi, 2021

Environmental Product Declaration: "COMPASS I – Interruttore di alta tensione con TA incorporati unipolare/tripolare", Hitachi Energy Italy S.p.A., 2021 (available at: https://www.epditaly.it/wp-content/uploads/2016/12/EPD_COMPASS-I_Hitachi-ABB_def.pdf).

Siemens Gamesa Renewable Energy, 2017

Environmental Product Declaration: "Electricity from European G114-2.5 MW On-shore Wind Farm", Siemens Gamesa Renewable Energy S.A., 2017 (available at: https://www.environdec.com/library/epd1097).

Tamini, 2020

Environmental Product Declaration: "Three-phase transformer in mineral oil (Mod. INS MT S 07 25MVA)", Tamini Trasformatori s.r.l., 2020 (available at: https://www.environdec.com/library/epd2161).

Standards

IEC 61400-1:2019

BS EN IEC 61400-1:2019 "Wind energy generation systems – Part 1: Design requirements".

ISO 14040:2006

BS EN ISO 14040:2006+A1:2020 "Environmental management – Life cycle assessment – Principles and framework".

ISO 14044:2006

BS EN ISO 14044:2006+A2:2020 "Environmental management – Life cycle assessment – Requirements and guidelines".

Books

Brower, 2012

Brower, M. C. "Wind Resource Assessment – A Practical Guide to Developing a Wind Project", Jhon Wiley & Sons, 2012.

De Brito and Agrela, 2019

De Brito, J. and F. Agrela. "New Trends in Eco-efficient and Recycled Concrete", Woodhead Publishing, 2019.

A Appendix A

A.1. Tables

Table A.1: Plant, turbine and eco-profile characteristics concerning the reviewed studies. Legend: WF=wind farm; ST=single turbine; ON=onshore; OFF=offshore; CF=capacity factor; AEY=annual energy yield; EPBT=energy payback time; EROI=energy return on investment.

Source	Config.	Type	N. WTGs	Expected life (Y)	Rated power (MW)	Rotor Ø (m)	hub height (m)	Mean wind speed (m/s)	CF (%)	AEY (GWh)	Energy intensity (kWhp/kWhel)	GHG intensity (gCO2eq/kWhel)	EPBT (months)	EROI
Bonou et al. (2016)	WF	ON	20	20	2.3	108	99.5	8.5	0.55	223.4	0.026	6	6.2	38.7
	WF	ON	20	20	3.2	113	92.5	8.5	0.51	288.1	0.022	5	5.2	46.2
	WF	OFF	80	20	4	130	68.25	9.5	0.59	1642.2	0.046	10.9	11.1	21.6
	WF	OFF	80	25	6	154	87.72	10	0.59	2483.6	0.033	7.8	10	30
Xu et al. (2018)	WF	ON	18	20	1.5	77	65	8.3 @ 70 m	0.3	130	0.026	8.6	6.2	38.5
			30	20	0.75	50	50	8.3 @ 70 m	0.3					
Guezuraga et al. (2012)	ST	ON	1	20	1.8	70	65	6	0.21	3.3	0.032	8.82	7.7	31.3
	ST	ON	1	20	2	90	105	7.4	0.34	6	0.033	9.73	7.8	30.8
Oebels and Pacca (2013)	WF	ON	14	20	1.5	-	80	7.8	0.34	63	-	7.1	-	-
Tremeac and Meunier (2009)	ST	ON	1	20	4.5	113	124	-	0.3	11.7	0.08	15.8	20.4	11.8
Crawford (2009)	ST	ON	1	20	3	90	80	7.75	0.33	29.7	0.147	9.3	35.4	6.8
	ST	ON	1	20	0.85	52	60	7.75	0.34	8.6	0.162	10.28	38.8	6.2
Ardente et al. (2008)	WF	ON	11	20	0.66	50	55	-	0.19	12.1	0.052	14.8	12.5	19.2
Al-Behadili and El-Osta (2015)	WF	ON	37	20	1.65	82	71	-	0.42	226.7	0.024	4.65	5.7	42.1
Schreiber et al. (2019)	ST	ON	1	20	3	-	84	6.8	0.3	8	0.026	7.25	6.2	38.3
	ST	ON	1	20	3	-	84	6.8	0.31	8.2	0.044	12.43	10.4	22.9
	ST	ON	1	20	3	-	84	6.8	0.31	8.3	0.025	7.25	6	40.2
Zhuo et al. (2023)	ST	ON	1	20	2.5	-	80	-	0.3	6.6	0.04	10.43	9.6	25
	ST	ON	1	20	2.5	-	80	-	0.3	6.6	0.033	8.48	7.9	30.3
Chipindula et al. (2018)	WF	ON	-	20	1	-	-	7.5	0.35	-	-	7.35	-	-
	WF	ON	-	20	2	-	-	7.5	0.35	-	-	7.09	-	-
	WF	ON	-	20	2.3	-	-	7.5	0.35	-	-	5.84	-	-
	WF	OFF	-	20	2	-	-	8-8.5	0.45	-	-	9.49	-	-
	WF	OFF	-	20	2.3	-	-	8-8.5	0.45	-	-	6.49	-	-
	WF	OFF	-	20	2.3	-	-	8-8.5	0.47	-	0.046	7.89	11	21.8
	WF	OFF	-	20	5	-	-	8-8.5	0.47	-	0.04	7.28	9.6	25
Gomaa et al. (2019)	WF	ON	38	20	3	112	119	-	0.37	371	0.035	9.11	8.3	29
Martı´nez et al. (2009)	ST	ON	1	20	2	80	67	-	0.23	4	0.02	6.58	4.8	50
Alsaleh and Sattler (2019)	WF	ON	100	20	2	83	78	-	0.17	665.8	0.107	18	25.68	9.35
			100	20	2	87	78	-	0.17					

Table A.2: Impact evaluation methods and software/database used by each study.

Source	Software/database used	Method	End of life	Credits to the system
Bonou et al. (2016)	SimaPro	ReCiPe	✓	✓
Xu et al. (2018)	GaBi 6	CLM 2001	✓	✓
Guezuraga et al. (2012)	GEMIS	CED	×	-
Oebels and Pacca (2013)	Own calculations based on national and international databases	GHG emissions	×	-
Tremeac and Meunier (2009)	SimaPro	Impact 2002+	✓	✓
Crawford (2009)	SimaPro Australian database (Process) + I–O model of Australian energy use (Prof. Lenzen)	Embodied energy	×	-
Ardente et al. (2008)	Own calculations based on national and international databases	Global energy requirement	✓	×
Al-Behadili and El-Osta (2015)	Energy: own calculations using literature references. Emissions: IPCC for the national Greenhouse gas Inventories 2006	Global energy requirement and IPCC 2006	✓	✓
Schreiber et al. (2019)	GaBi 8.7	ILCD/PEF impact categories (v. 1.09)	✓	×
Zhuo et al. (2023)	Ecoinvent 3.1 + national and international databases	IPCC 2013 and CED	✓	✓
Chipindula et al. (2018)	SimaPro	Impact 2002+	✓	✓
Gomaa et al. (2019)	SimaPro	TRACI 2 V3.01	×	-
Martı´nez et al. (2009)	SimaPro	Eco-Indicator 99	✓	✓
Alsaleh and Sattler (2019)	SimaPro	TRACI	✓	✓

Table A.3: Assumption related to scheduled and unscheduled maintenance activities in the reviewed studies.

Source	Scheduled maintenance	Unscheduled maintenance
Bonou et al. (2016)	Not included	Not included
Xu et al. (2018)	Not included	Substitution of 1 blade per turbine and 15% of generator's components
Guezuraga et al. (2012)	Substitution of lubricants and oils 3 times/y. Distance covered = 100 Km per trip	Geared turbine: 1 gearbox replacement every 7 years. Gearless turbine: minor generator parts replacement
Oebels and Pacca (2013)	Not included	Not included
Tremeac and Meunier (2009)	3 inspections per year. Distance covered = 300 Km/y	Substitution of 1 blade per turbine and 15% of nacelle's components
Crawford (2009)	Substitution of lubricants and oils once every 5 years	Replacement of half gearbox over the lifetime
Ardente et al. (2008)	Daily inspection during the first operation period and successively one inspection every 2-3 weeks. Substitution of lubricants and spare parts + painting	Substitution of 1 blade per turbine and 15% of generator's components
Al-Behadili and El-Osta (2015)	Not included	Not included
Schreiber et al. (2019)	DFIG: 2 maintenance activities per year (consumables: lubricating oil and coolants). DDSG and DDPMSG: 5 maintenance activity per year (consumables not specified). Distance covered = 150 Km per maintenance activity (for all the turbines)	Only DFIG: 4 maintenance activities per year. All the turbines: replacement rate of 0.024 units/y for rotor and 0.005 units/y for the blades, both reduced by a factor of 1.26
Zhuo et al. (2023)	Daily wind turbine inspection + eventual adding/replacing lubricating oil	DFIG: blades replaced once in the lifetime, gearbox replaced for 95%, generator for 19%. DDPMSG: blades replaced once in the lifetime, generator replaced for 25% and nacelle components for 15%
Chipindula et al. (2018)	Routine inspection once every year, oils change once every 3 years	Half of the gearbox replaced every 5 years
Gomaa et al. (2019)	Routine inspection every year, oils change every 5 years	Not specified
Martínez et al. (2009)	Regular lubrication of gearboxes. Substitution of lubricants and coolants once in the plant's lifetime	Substitution of 1 generator per turbine
Alsaleh and Sattler (2019)	2 inspections per year. Distance covered = 400 Km/y	Substitution of the brake system every 5 years and the control system every 10 years.

List of Figures

Figure 1.1: GHG emissions reduction over time by sector (EEA, 2023a). 4

Figure 2.1: Rooftop and utility-scale solar capacity trend forecast in Europe up to 2027 (SPE, 2023). 9

Figure 2.2: Total installed wind capacity trend forecast in EU up to 2030 (WindEurope, 2023). 10

Figure 2.3: Evolution of wind turbines' size and nominal power over time (NREL, 2020). .. 10

Figure 3.1: layout of the wind power plant. In blue the location of the 6 WTGs; in purple hatched lines the path followed by the MV and HV cables. The filled regions in purple and red represent respectively the transformer substation and primary substation (adapted from Project documentation). 12

Figure 3.2: Wind turbine's main components (Gode, 2020). 14

Figure 3.3: Overview of Nacelle's main components (Tchakoua et al., 2013). 16

Figure 3.4: G114-2.5 MW power and cp curve (adapted from Project documentation). 18

Figure 4.1: LCA framework (modified from ISO 14040:2006) 24

Figure 4.2: Schematic representation of a generic system interested by input and output flows (Köck et al., 2023). 26

Figure 4.3: Definition of the mandatory elements concerning the evaluation of the system's carbon footprint (ISO 14044:2006). 28

Figure 5.1: Specific embodied energy evolution with turbine rated power (Kaldellis and Apostolou, 2017). 38

Figure 6.1: Product system of the LCA. 53

F*igure 6.2: Wind classes definition according to the IEC 61400-1 standard (IEC 61400-1:2019).* 62

Figure 6.3: Wind turbines' foundations design details (adapted from Project documentation). 73

Figure 6.4: Wind turbines' platforms design details (adapted from Project documentation). 77

Figure 6.5: Longitudinal section of a typical internal road (adapted from Project documentation). 79

Figure 6.6: MV trench design details (adapted from Project documentation). 82

Figure 6.7: HV trench design details (adapted from Project documentation). 84

Figure 6.8: graphical representation of the 6 main layers of a single core MV cable (adapted from Saveri, 2010). 85

Figure 6.9: Transformer substation design details (adapted from Project documentation). ... 92

Figure 6.10: Manufacturing processes for the steel tower (Hyundai Welding, 2023). 102

Figure 6.11: Procedure used to select the most appropriate method for the estimation of the pollutant emissions from NRMM (EEA, 2023b). 113

Figure 6.12: Overview of the Stages concerning the limitations on pollutants emissions for NRMM imposed by the European Commission (EEA, 2023b). 115

Figure 6.13: Emission factors for diesel NRMM (EEA, 2023b). 116

Figure 6.14*: Load factor adjustments for the affected pollutants. Note: TSP = Total Suspended Particles = PM (Particulate matter with diameter > 10 μm) (EEA, 2023b).* 117

Figure 6.15: Maximum deterioration factors corresponding to the average engine lifetime for diesel NRMM (EEA, 2023b). 118

Figure 7.1: Breakdown of the wind turbines' impacts at component level. 149

Figure 7.2: Total masses and primary energy contributions for the acquisition of the turbines' raw materials. 150

Figure 7.3: Breakdown of the wind turbines components' impacts at material level. 152

Figure 7.4: Total masses and GWP for the acquisition of the turbines' raw materials. 153

Figure 7.5: Breakdown of the civil works' impacts at component level. 154

Figure 7.6: Total masses and primary energy consumption for the acquisition of the civil works' raw materials. 155

Figure 7.7: Breakdown of the civil works components' impacts at material level. 155

Figure 7.8: Total masses and GWP for the acquisition of the civil works' raw materials. 157

Figure 7.9: Breakdown of the power transmission's impacts at component level. 158

Figure 7.10: Breakdown of the power cables' impacts at material level. 158

Figure 7.11: Total masses and primary energy consumption for the acquisition of the power transmission's raw materials. 159

Figure 7.12: Total masses and GWP for the acquisition of the power transmission's raw materials. 162

Figure 7.13: Breakdown of the turbines manufacturing's impacts at process level. 163

Figure 7.14: Breakdown of the O&M's impacts. 165

Figure 7.15: Breakdown of the wind turbines' end-of-life impacts at component level. 167

Figure 7.16: Breakdown of the wind turbines components' end-of-life impacts at process level. 168

Figure 7.17: CED and GWP variations for the selected useful life durations compared to the baseline scenario. 182

Figure 7.18: CED and GWP variations with modified failure rates compared to the baseline scenario. 183

Figure 7.19: Regression line for the SSE sector. 189

Figure 7.20: Resource map of the site at 100 m. Axis labels refer to the number of pixels. 191

List of Tables

Table 3.1: Main features of the power plant. 13

Table 5.1: Main characteristics and environmental impacts concerning the 7 wind farm analyzed by Chipindula et al. (2018). 37

Table 5.2: Main characteristics and environmental impacts concerning the 3 single turbine wind power plants analyzed by Schreiber et al. (2019). 40

Table 6.1: Weight of the major turbine's components. 63

Table 6.2: Nacelle sub-components of the G114 – 2.5 MW wind turbine. 63

Table 6.3: Weight of the G114 – 2.5 MW rotor's sub-components. 64

Table 6.4: Main materials of all the turbine's sub-components retrieved from the G114 – 2.5 MW technical report. 65

Table 6.5: Weights and mass fractions and material fractions of sub-components for the G8X – 2 MW wind turbine (Martínez et al., 2009). 66

Table 6.6: Inventory data for the 3MW wind turbine reported by Crawford (2009). 67

Table 6.7: Mass fraction of the missing nacelle's sub-components (Crawford, 2009). 68

Table 6.8: Mass fraction of the drive train's components (Martínez et al., 2009). 68

Table 6.9: Mass fraction of the remaining sub-components making up 85 % of the nacelle's mass (Martínez et al., 2009). 68

Table 6.10: Mass fractions hub (Martínez et al., 2009). 69

Table 6.11: Inventory data for the raw materials used in a single G114 – 2.5 MW turbine... 70

Table 6.12: Definition of the Ecoinvent processes for each material used in the wind turbine. 71

Table 6.13: Inventory data concerning the raw materials employed in the two types of foundations. 75

Table 6.14: Inventory data related to the raw materials used for the platforms construction. 78

Table 6.15: Inventory data related to the raw materials used for the internal roads construction. 79

Table 6.16: Inventory data related to the raw materials used for the external roads adjustments. 81

Table 6.17: Inventory data related to the raw materials used for the MV and HV trench construction..... 85

Table 6.18: Inventory data related to the raw materials used for the HV cables. 88

Table 6.19: Inventory data related to the raw materials used for the MV cables...... 89

Table 6.20: Inventory data related to the raw materials used for the copper rope, optic fiber and corrugated pipes. 90

Table 6.21: LCIA output for Tamini's transformer. FU=25 MVA, 1 year. Numbers in parenthesis refer to the real contributions used in the present study with the neglection of the use phase (Tamini, 2020). 95

Table 6.22: LCIA output for Tamini's transformer referred to the Iurefalco's 16 MVA transformer...... 95

Table 6.23: Life cycle impacts for the 16 MVA transformer. 96

Table 6.24: LCIA output for Hitachi's three-pole switch. Numbers in parenthesis refer to the real contributions used in the present study with the neglection of the electric losses (Hitachi, 2021)...... 97

Table 6.25: LCIA output for Hitachi's three-pole switch referred to the one used in the Iurefalco power plant...... 97

Table 6.26: Life cycle impacts for the three-pole switch. 98

Table 6.27: Inventory data referred to the raw materials used for the transformer substation civil works and electromechanical components (Shelters included). 99

Table 6.28: Manufacturing processes used in the wind energy section of the Ecoinvent database. 101

Table 6.29: Inventory data concerning the material manufacturing processes used for the production of the turbines' components...... 103

Table 6.30: Inventory data concerning the turbine's components manufacturing processes. 103

Table 6.31: Inventory data related to the wind turbines' components and sub-components transport requirements from the suppliers to the site's location. Note: Trip ^{r} *= road trip. Trip* ^{s} *= sea trip.* 105

Table 6.32: Inventory data related to the wind turbines' components and sub-components transport requirements from the suppliers to the site's location (grouped)...... 106

Table 6.33: Inventory data concerning the manufacturing processes used for the production of the copper rope and grouting components used in the turbines' foundations. 106

Table 6.34: Inventory data related to the transport requirements characterizing the concrete, reinforcing steel and grouting components used in the turbines' foundations, from the suppliers to the site's location. 107

Table 6.35: Inventory data related to the transport requirements characterizing each material used in the turbines' platforms, from the suppliers to the site's location. 107

Table 6.36: Inventory data related to the transport requirements characterizing each material used in the internal roads, from the suppliers to the site's location. 108

Table 6.37: Inventory data related to the transport requirements characterizing each material used in the cable trenches, from the suppliers to the site's location. 109

Table 6.38: Inventory data concerning the manufacturing processes used for the production of the MV and HV cables. 110

Table 6.39: Inventory data related to the transport requirements characterizing the MV and HV cables used in the power transmission system, from the suppliers to the site's location. 110

Table 6.40: Inventory data concerning the manufacturing processes used for the production of the corrugated pipes and the copper rope used in the power transmission system. 111

Table 6.41: Inventory data related to the transport requirements characterizing the corrugated pipes used in the power transmission system, from the suppliers to the site's location. 111

Table 6.42: Inventory data related to the transport requirements characterizing the limestone gravel used in the transformer substation, from the suppliers to the site's location. 112

Table 6.43: Inventory data concerning the manufacturing processes used for the production of the electromechanical components employed in the transformer substation. 112

Table 6.44: Inventory data related to the transport requirements characterizing the electromechanical components employed in the transformer substation, from the suppliers to the site's location. 112

Table 6.45: Technology levels chosen for the power classes involved in the construction site. 115

Table 6.46: Deterioration factors related to an intermediate engine age. 118

Table 6.47: Total number of hours worked by each type of machine (N·H) for the specific activity groups. 119

Table 6.48: The emission factors used in eq 4.2 corrected using the load factor and deterioration factor adjustments. 120

Table 6.49: Pollutant emissions and fuel consumption (in kg) related to each activity group performed in the construction site. 120

Table 6.50: Emission factors related to CO2 and SO2 for diesel NRMM (ISPRA, 2023; Winther, 2023). 121

Table 6.51: Pollutant emissions and fuel consumption (in kg) with CO2 and SO2 contributions related to each activity group performed in the construction site. 122

Table 6.52: Pollutant emissions and fuel consumption (in kg/GWh) with CO2 and SO2 contributions related to each activity group performed in the construction site. 122

Table 6.53: Implementation in SimaPro of the inventory data related to the fuel consumption and pollutant emission deriving from the NRMM activity in the construction site. 123

Table 6.54: Inventory data related to the waste materials deriving from the external roads adjustments and cable trenches construction. 124

Table 6.55: Inventory data related to the use of lubricant oil over the entire expected life of the wind power plant. 125

Table 6.56: Failure rates and number of failures for the turbines' major components. 126

Table 6.57: Pollutant emissions and fuel consumption related to the installation of the replaced turbines' components. 127

Table 6.58: Pollutants emissions and fuel consumption related to the wind turbines and electromechanical components disassembly. 128

Table 6.59: Inventory data related to the transformer substation removal. 129

Table 6.60: Friction coefficients used by Neara for the calculation of the pulling force for a given cable and trench configuration (Essential Energy, 2021). 130

Table 6.61: Friction coefficients used for the extraction of the cables installed in the trenches of Iurefalco power plant. 130

Table 6.62: Output energy required for the extraction of each cable type. 131

Table 6.63: Inventory data related to the extraction of the cables installed in the trenches of Iurefalco power plant. 131

Table 6.64: Inventory data related to the renaturation of platforms and cable trenches. 132

Table 6.65: Mean distances covered by trucks for each waste destination. 134

Table 6.66: Total recovery rate and destinations of each type of material for the sub-components deriving from the decommissioning phase. 136

Table 6.67: Total recovery rates breakdown for the turbines' sub-components. 137

Table 6.68: Total recovery rates breakdown for cables deriving from the decommissioning phase. 138

Table 6.69: Material recovery rates and destinations for the transformer substation sub-components deriving from the decommissioning phase. 140

Table 6.70: Ecoinvent processes used for the inventory data modeling concerning waste materials management in wind turbines. 141

Table 6.71: Ecoinvent processes used for the inventory data modeling concerning waste materials management in cables. 142

Table 6.72: Ecoinvent processes used for the inventory data modeling concerning waste materials management in the transformer substation's components. 143

Table 7.1: LCA results for the reference scenario. 148

Table 7.2: Specific energy factors for the acquisition of the turbines' raw materials. 150

Table 7.3: Specific emission factors for the acquisition of the turbines' raw materials. 153

Table 7.4: Specific energy factors for the acquisition of the civil works' raw materials. 155

Table 7.5: Specific emission factors for the acquisition of the civil works' raw materials. 157

Table 7.6: Specific energy factors for the acquisition of the power transmission's raw materials. 159

Table 7.7: Specific emission factors for the acquisition of the power transmissions' raw materials. 162

Table 7.8: Number of units replaced and primary consumption/CO2-equivalent emissions per unit produced compared to the system's total. 166

Table 7.9: Environmental indexes comparison between the reviewed and the present study. 172

Table 7.10: Wind turbines components' mass comparison (in tons) between the reviewed and the present study. 173

Table 7.11: CF comparison between the reviewed and the present study. 174

Table 7.12: Reductions of the CED and GWP values in response to the end-of-life credit. .. 175

Table 7.13: GHG intensity of conventional and low carbon technologies (Guidi et al., 2023). 176

T*able 7.14: CED indicators' results for the main components production and life cycle phases.* 179

Table 7.15: Number of components replaced over different useful life durations. 181

Table 7.16: Number of components replaced with modified failure rates. 183

Table 7.17: Characteristics of the met mast sensors. 186

Table 7.18: Scaling factors used for the horizontal extrapolation. 191

Table 7.19: Power weights vector. 192

Table 7.20: Estimated power losses. 194

Table 7.21: Uncertainty factors and standard deviations' calculation methods. 196

Table 7.22: Gaussian formulae for the confidence intervals evaluation (Solargis, 2018). 196

Table A.1: Plant, turbine and eco-profile characteristics concerning the reviewed studies. Legend: WF=wind farm; ST=single turbine; ON=onshore; OFF=offshore; CF=capacity factor; AEY=annual energy yield; EPBT=energy payback time; EROI=energy return on investment. 214

Table A.2: Impact evaluation methods and software/database used by each study. 215

Table A.3: Assumption related to scheduled and unscheduled maintenance activities in the reviewed studies. 216

Acknowledgements

I would like to thank my Advisor Prof. Paolo Silva for giving me the opportunity to carry out this thesis work and providing useful suggestion for its drafting.

I acknowledge Ing. Francesca Pippione and Dott. Luca Bortolotti for supporting and guiding me during the long data research required for the Life Cycle Assessment and for sharing their knowledge on the wind technology.

I thank Ing. Gaia Brussa and Prof. Mario Grosso, whose experience concerning wind power plants sustainability gave me precious insights on the methodology followed in the thesis and the end-of-life of the system.

I would like to also thank Giuseppe (Peppe) Manzi for its valuable help in understanding the technical documentation of the power plant.
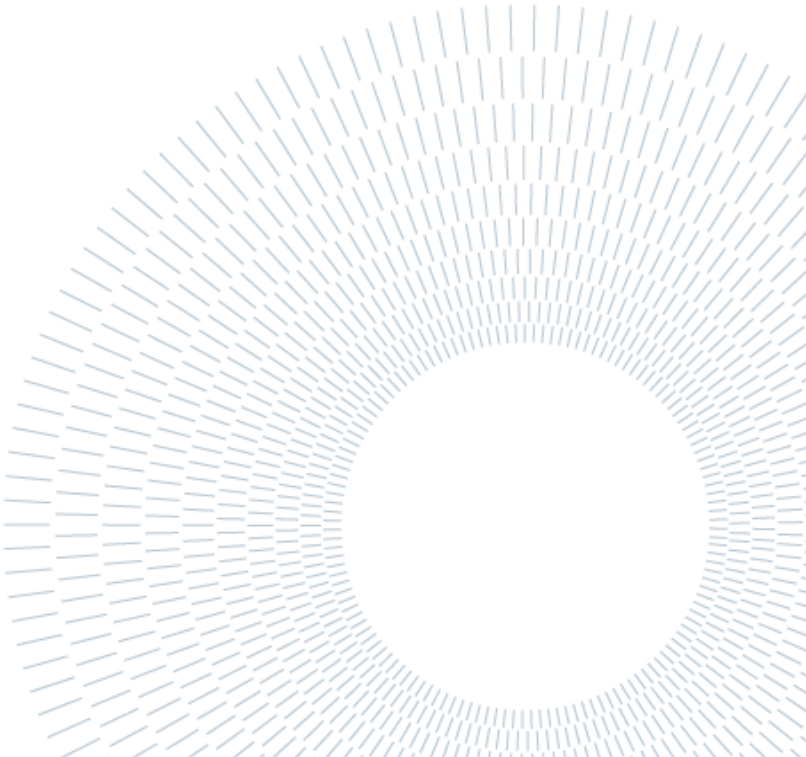
Lastly, I thank my family and all my friends for supporting my journey at PoliMI and for never leaving me alone, especially in the most difficult times. Without you, all of this wouldn't be possible.